Geological Survey of Wyoming • Gary B. Glass, State Geologist

Geologic field tours of western Wyoming

and parts of adjacent Idaho, Montana, and Utah

Edited by Sheila Roberts

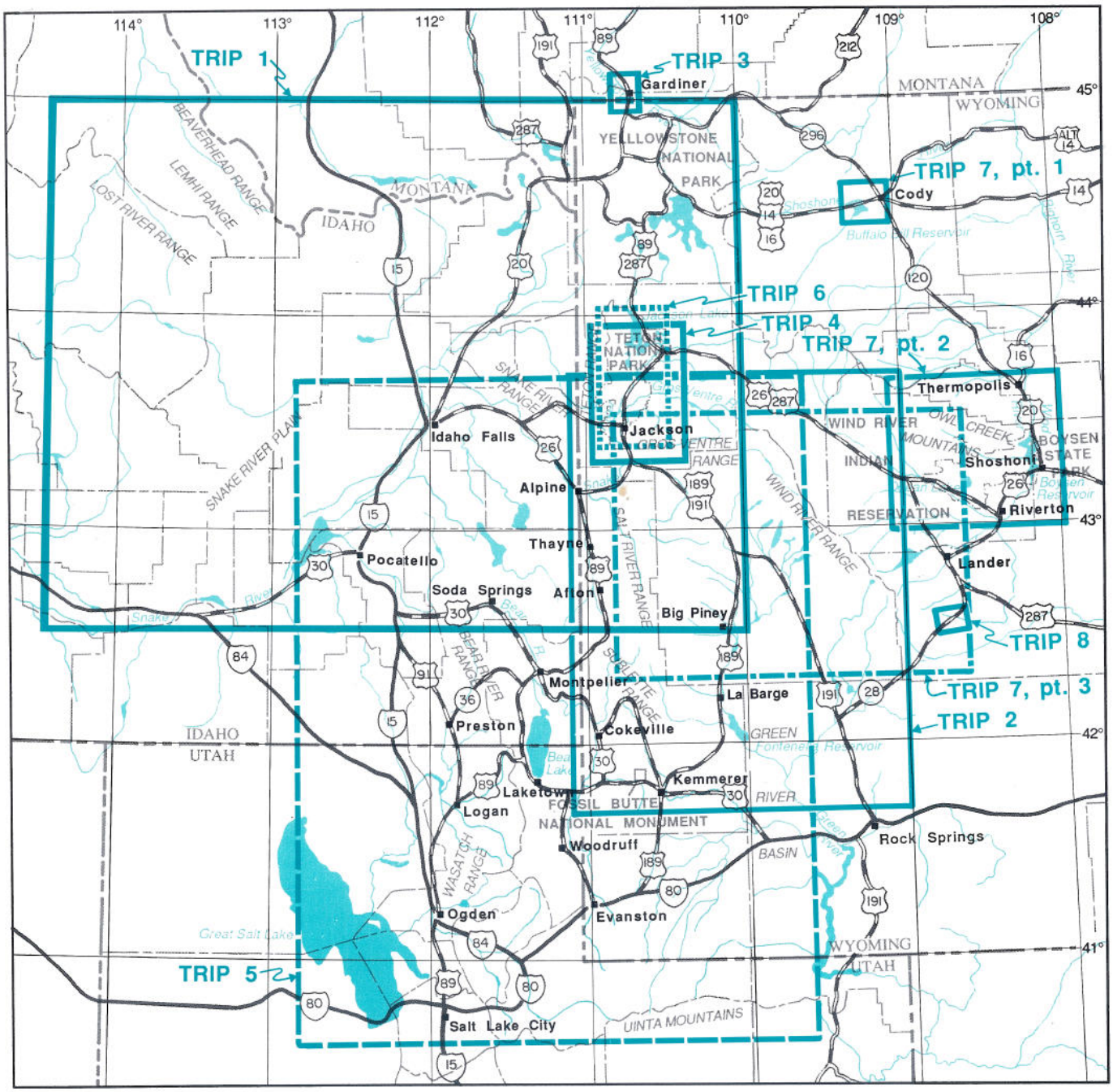

Public Information Circular No. 29
Laramie, Wyoming
1990

First printing of 600 copies by Frontier Printing, Cheyenne, Wyoming.

This and other publications available from:

The Geological Survey of Wyoming
P.O. Box 3008, University Station
Laramie, Wyoming 82071-3008
(307) 766-2286

Front cover: Map showing general geographic locations of the eight geologic tours included in this book.

Back cover: Side Looking Radar mosaic of the region surrounding Jackson, Wyoming, starting point for most of the field trips (scale 1:1,500,000; from U.S. Geological Survey data).

THE GEOLOGICAL SURVEY OF WYOMING
Gary B. Glass, State Geologist

Public Information Circular No. 29

GEOLOGIC FIELD TOURS OF WESTERN WYOMING
AND PARTS OF ADJACENT IDAHO, MONTANA, AND UTAH

EDITED BY

SHEILA ROBERTS

LARAMIE, WYOMING
1990

These geologic field trip guides were prepared for the **Rocky Mountain Section, Geological Society of America 43rd Annual Meeting** in Jackson, Wyoming, May, 1990.

Meeting Chairman
Ronald W. Marrs
Department of Geology and Geophysics, University of Wyoming
Field Trip Coordinator
James C. Case
Geological Survey of Wyoming
Transportation Coordinator
Richard J. Weiland, Jr.
Department of Geology and Geophysics, University of Wyoming
Reviewers
Jason L. Lillegraven
Department of Geology and Geophysics, University of Wyoming
J. David Love
U.S. Geological Survey, Laramie, Wyoming, retired
Gary B. Glass
Geological Survey of Wyoming

Table of contents

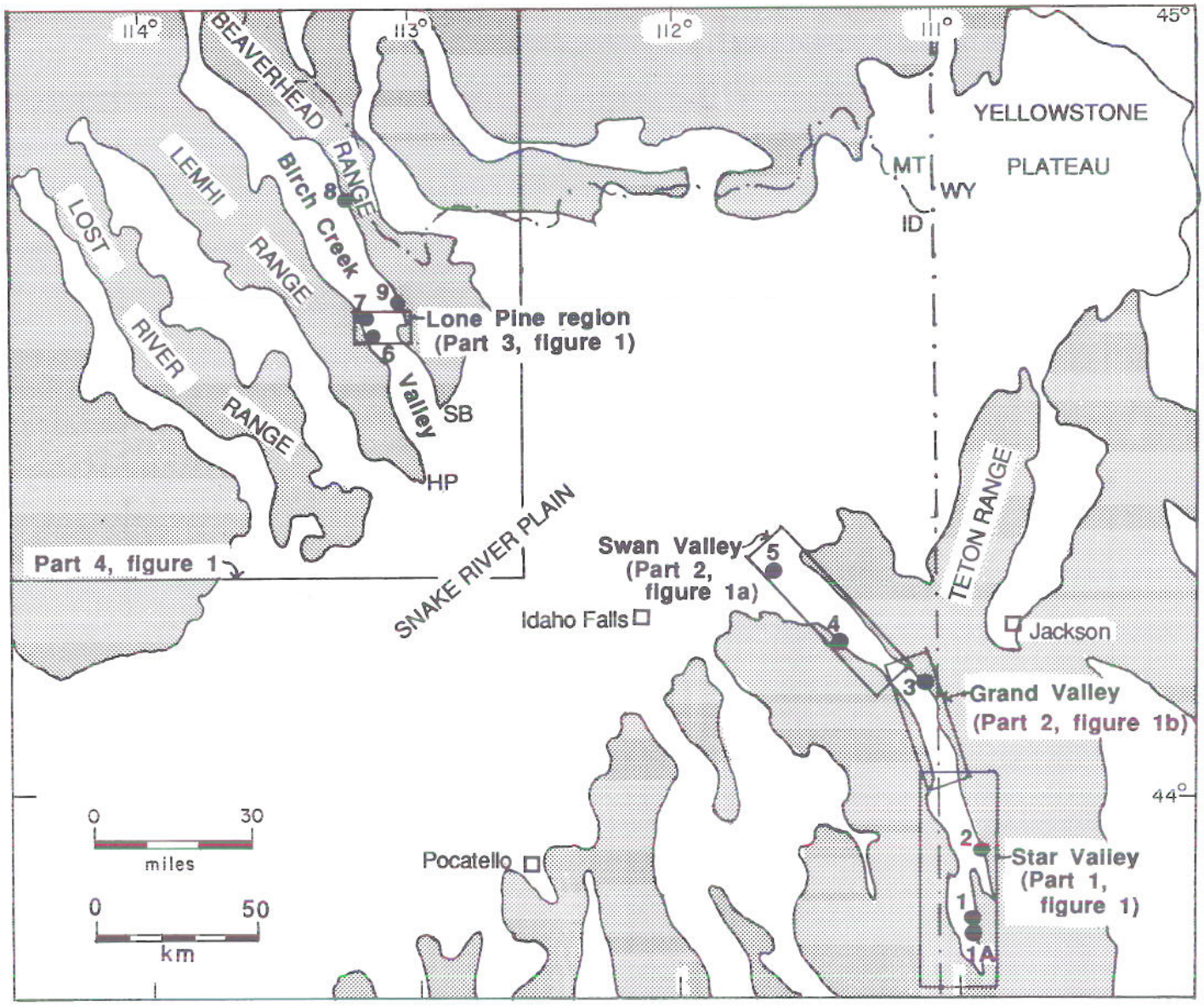

Figure 1. Generalized map of the circum-Snake River Plain, showing the areas covered by maps in parts 1 through 4 of field trip no. 1 and field trip stops. Shaded areas indicate pre-Cenozoic rocks. (HP = Howe Point sampling area; SB = southernmost Beaverhead Mountains sampling area.)

Field trip no. 1, Introduction

LATE TERTIARY AND QUATERNARY FAULTING NORTH AND SOUTH OF THE EASTERN SNAKE RIVER PLAIN

Mark H. Anders[1]
David W. Rodgers[2]
James P. McCalpin[3]
Kathleen M. Haller[4]

[1] Lamont-Doherty Geological Observatory of Columbia University, Palisades, New York 10964
[2] Department of Geology, Idaho State University, Pocatello, Idaho 83209
[3] Department of Geology, Utah State University, Logan, Utah 84322
[4] U.S. Geological Survey, Denver, Colorado 80225

Overview

North and south of the Snake River Plain there are a number of northwest trending basins that have been actively subsiding during the late Cenozoic. These basins are mostly half-grabens that result from extension on northwest trending normal faults. Our field trip will examine the structure and stratigraphy of basin-fill deposits in some of these basins in order to interpret the styles and temporal patterns of late Cenozoic normal faulting in the northeastern Basin and Range province. The field trip consists of two traverses along these major fault-bounded basins, one to the south of the Snake River Plain and one to the north. The southern traverse (parts 1 and 2) starts 60 miles (100 km) southeast of the Snake River Plain in Star Valley, Wyoming (**Figure 1**) and continues northeastward into Grand and Swan valleys, Idaho. Each of these three southern basins is formed by extension on a single continuous 85-mile-long (140-km) fault, which is called the Star Valley fault in Star Valley and the Grand Valley fault in Grand and Swan valleys. We will often refer to these two faults together as the Grand Valley/Star Valley fault.

The second day (parts 3 and 4) begins north of the Snake River Plain at the southern end of Birch Creek Valley, stopping at four locations in the valley. Birch Creek Valley is the southernmost of two basins that are formed by late Cenozoic extension along the 90-mile-long (150 km) Beaverhead fault. Birch Creek Valley extends about 36 miles (60 km) northwest from the Snake River Plain and can be divided into two distinct physiographic sub-basins. Birch Creek Valley, like the basins south of the Snake River Plain, is filled with alluvium, colluvium, loess, and lake sediments, all interbedded with Snake River Plain volcanic rocks.

Displacement history of the Grand Valley/Star Valley fault in Star, Swan, and Grand valleys

Seismic reflection data indicates that the Grand Valley/Star Valley fault, as well as other basin-bounding faults south of the Snake River Plain, are listric (Royse and others, 1975; Dixon, 1982). The maximum thickness of Cenozoic sediment in the basin formed by extension on the Grand Valley/Star Valley fault is from 6,500 to 13,000 feet (2-4 km) (Dixon, 1982). The hanging wall of the listric fault is cut by the antithetic Snake River fault, which bounds the southwestern side of Swan and Grand Valley; however, this fault does not

extend south into Star Valley. Displacement on the Snake River fault is minor compared to that on the Grand Valley/Star Valley fault.

In Star Valley, the southernmost basin, there are Miocene through Quaternary basin-fill deposits of alluvium and colluvium with a veneer of latest Quaternary loess and recent stream deposits. Star Valley can be divided into two distinct physiographic and geologic sub-basins. The Star Valley fault in southern Star Valley is the most active segment of the entire Grand Valley/Star Valley fault. Fault scarps in some locations on the southern Star Valley fault have over 36 feet (11 m) of offset (Piety and others, 1986; Anders and others, 1989; this field trip, part 1). Piety and others (1986) estimated latest Quaternary displacement rates on this segment to be between 0.02 and 0.04 inches per year (0.6 and 1.1 mm). To the north, only the southernmost part of the Star Valley fault in northern Star Valley has been active in the latest Quaternary. Between this active portion of the Star Valley fault and the Snake River Plain there are no fault scarps on deposits of latest Quaternary age. We will make two stops in Star Valley to examine latest Quaternary fault scarps.

Although latest Quaternary displacement rates in Star Valley can be accurately estimated based on offset deposits of known age, displacement rates over longer intervals cannot presently be estimated for this fault. This is due to the limited exposures of older basin-fill deposits in Star Valley. Northwest of Star Valley, in Grand and Swan valleys, this problem is mitigated by exposures of late Miocene and younger volcanic and sedimentary rocks. In Grand Valley and Swan Valley, the late Miocene and younger basin-fill deposits are moderately tilted to the northeast, suggesting that there has been significant pre-latest Quaternary movement on the Grand Valley fault. Although there must have been significant tectonic activity in these valleys, almost none has occurred during the Quaternary. There has been only minor offset (91 ft/28 m) since deposition of a 1.5 Ma basalt across the Grand Valley fault (Piety and others, 1986). Furthermore, the 2.0 Ma Huckleberry Ridge Tuff in Swan Valley is not tilted (Anders and others, 1989). This field trip provides an opportunity to examine a variety of volcanic rocks used to assess the movement history of the Grand Valley fault.

Displacement history of the Beaverhead fault in Birch Creek Valley

Birch Creek Valley is bounded on the northeast by the Beaverhead fault, a southwest dipping normal fault with several miles (kilometers) of displacement (Garmezy, 1981). Based on range-front and fault-scarp morphology patterns, two segments of the Beaverhead fault are recognized in Birch Creek Valley, the Blue Dome segment in southern Birch Creek Valley and the Nicholia segment in northern Birch Creek Valley (this field trip, part 4). At the southern end of Birch Creek Valley (Howe Point, **Figure 1**), basin fill accumulated and was progressively tilted northeastward from middle Miocene to late Pliocene/early Quaternary time (Rodgers and Zentner, 1988). In central Birch Creek Valley, near Lone Pine (**Figure 1**), middle Miocene to early Quaternary basin fill accumulated without tilting, then was subsequently tilted to the northeast during the Quaternary (this field trip, part 3). Along southern Birch Creek Valley, the Blue Dome segment of the Beaverhead fault does not cut latest Quaternary (< 15 ka) deposits, and pediment surfaces estimated to be about middle to lower (?) Pleistocene (Scott, 1982) are roughly symmetric about the axis of southern Birch Creek Valley. In contrast, the Nicholia fault segment in northern Birch Creek Valley consists of fault scarps cutting latest Quaternary deposits, and pediment surfaces have steeper slopes on the west side of the valley than the east. These data suggest that Quaternary tilting and fault displacement rates increase to the north in Birch Creek Valley. This conclusion is further supported by the surficial geology of both subbasins: Neogene basin fill is commonly exposed in the southern valley, whereas Quaternary basin fill covers most of the northern valley. A more quantitative evaluation of fault displacement rates through the late Cenozoic will be made in the future.

The southern part of the Nicholia segment in northern Birch Creek Valley is characterized by a discontinuous sequence of prominent fault scarps. Fault scarps on latest Quaternary sediments are 16 to 32 feet (5-10 m) high, yet Holocene alluvium within the canyons are not faulted. This suggests that the most recent rupture on this segment occurred approximately 15 ka. The range-front along the Nicholia segment is also more linear than the range front along the Blue Dome segment, with well-defined facets.

North of the Snake River Plain, there are limited seismic reflection data suitable for interpreting the geometry of the basin-bounding late Cenozoic faults. Despite the lack of reflection data, structural analyses (Scott and others, 1985), aftershock data from the Borah Peak earthquake (M_s = 7.3) (Richins and others, 1987), and paleomagnetic data (this field trip, part 3)

all suggest late Cenozoic tectonics in the northern circum-Snake River Plain are dominated by large horizontal block rotations on planar normal faults. Birch Creek Valley is located between two of these large blocks, the southern Beaverhead and Lemhi Ranges, both of which have rotated about 10°NE since 6.5 Ma (Anders and others, 1988).

Apart from the difference between "domino" style faulting of the Beaverhead fault and listric faulting of the Grand Valley/Star Valley faults, there are broad similarities in the timing of faulting relative to their distances from the Snake River Plain. Close to the Snake River Plain, neither fault shows latest Quaternary fault scarps. The southern Birch Creek Valley, like the Grand and Swan valleys, has numerous exposures of middle Miocene to Quaternary basin fill. In these basins, most of the deposits are exposed on the southwest margins of the basins and are tectonically tilted to the northeast. Farther from the Snake River Plain, latest Quaternary fault scarps characterize both the Beaverhead and the Star Valley faults. Scarps on both faults exceed 30 feet (10 m) in places, indicating high displacement rates during the latest Quaternary. In the basins adjacent to these active faults, surficial deposits are almost exclusively latest Quaternary, most likely due to latest Quaternary subsidence and burial of older basin fill. Although the subsidence relations are not symmetric about the axis of the Snake River Plain (i.e. northern Birch Creek Valley is closer to the axis than Star Valley), the timing of late Cenozoic faulting is remarkably similar north and south of the Snake River Plain. For a further discussion of this pattern of faulting, we refer the reader to Scott and others (1985) for faults north of the Snake River Plain, and to Anders and others (1989) for faults south of the Snake River Plain.

References cited

Anders, M.H., Geissman, J.W., Piety, L.A., and Sullivan, J.T., 1989, Parabolic distribution of circum-eastern Snake River Plain seismicity and latest Quaternary faulting: migratory pattern and association with the Yellowstone hotspot: Journal of Geophysical Research, v. 94, no. B2, p. 1589-1621.

Anders, M.H., Hagstrum, J.T., and Rodgers, D.W., 1988, Late Cenozoic structural development of the southern Beaverhead and Lemhi Ranges, Idaho: Geological Society of America Abstracts With Programs, v. 20, no. 7, p. A63.

Dixon, J.S., 1982, Regional structural synthesis, Wyoming salient of western Overthrust Belt: American Association of Petroleum Geologists Bulletin, v. 66, n.o 10, p. 1560-1580.

Garmezy, L., 1981, Geology and tectonic evolution of the southern Beaverhead Range, east-central Idaho: M. S. thesis, Pennsylvania State University, 155 p.

Piety, L.A., Wood, C.K., Gilbert, J.D., Sullivan, J.T., and Anders, M.H., 1986, Seismotectonic study for Palisades Dam and Reservoir, Palisades Project, Idaho: U.S. Bureau of Reclamation Pacific and Northwest Regional Office and Engineering and Research Center, Seismotectonic Report 86-3, p. 355.

Richins, R.D., Pechmann, J.C., Smith, R.B., Langer, C.J., Goter, S.K., Zwollweg, J.E., and King, J.J., 1987, The 1983 Borah Peak, Idaho earthquake and its aftershocks: Bulletin of the Seismological Society of America, v. 77, no 3, p. 694-723.

Rodgers, D.W., and Zentner, N.C., 1988, Fault geometries along the northern margin of the eastern Snake River Plain, Idaho: Geological Society of America Abstracts with Programs, v. 20, no. 6, p. 465.

Royse, F., Jr., Warner, M.A., and Reese, D.L., 1975, Thrust belt structural geometry and related stratigraphic problems, Wyoming-Idaho-northern Utah, *in* Boyard, D.W., editor, Deep drilling frontiers of the Central Rocky Mountains: Rocky Mountain Association of Geologists Symposium, p. 41-54.

Scott, W.E., 1982, Surficial geologic map of the eastern Snake River Plain and adjacent areas, 111° to 115° W, Idaho and Wyoming: U.S. Geological Survey Miscellaneous Investigations Map I-1372, scale 1:250,000.

Scott, W.E., Pierce, K.L., and Hait, M.H., Jr., 1985, Quaternary tectonic setting of the 1983 Borah Peak earthquake, central Idaho: Bulletin of the Seismological Society of America, v. 75, no. 4, p. 1053-1066.

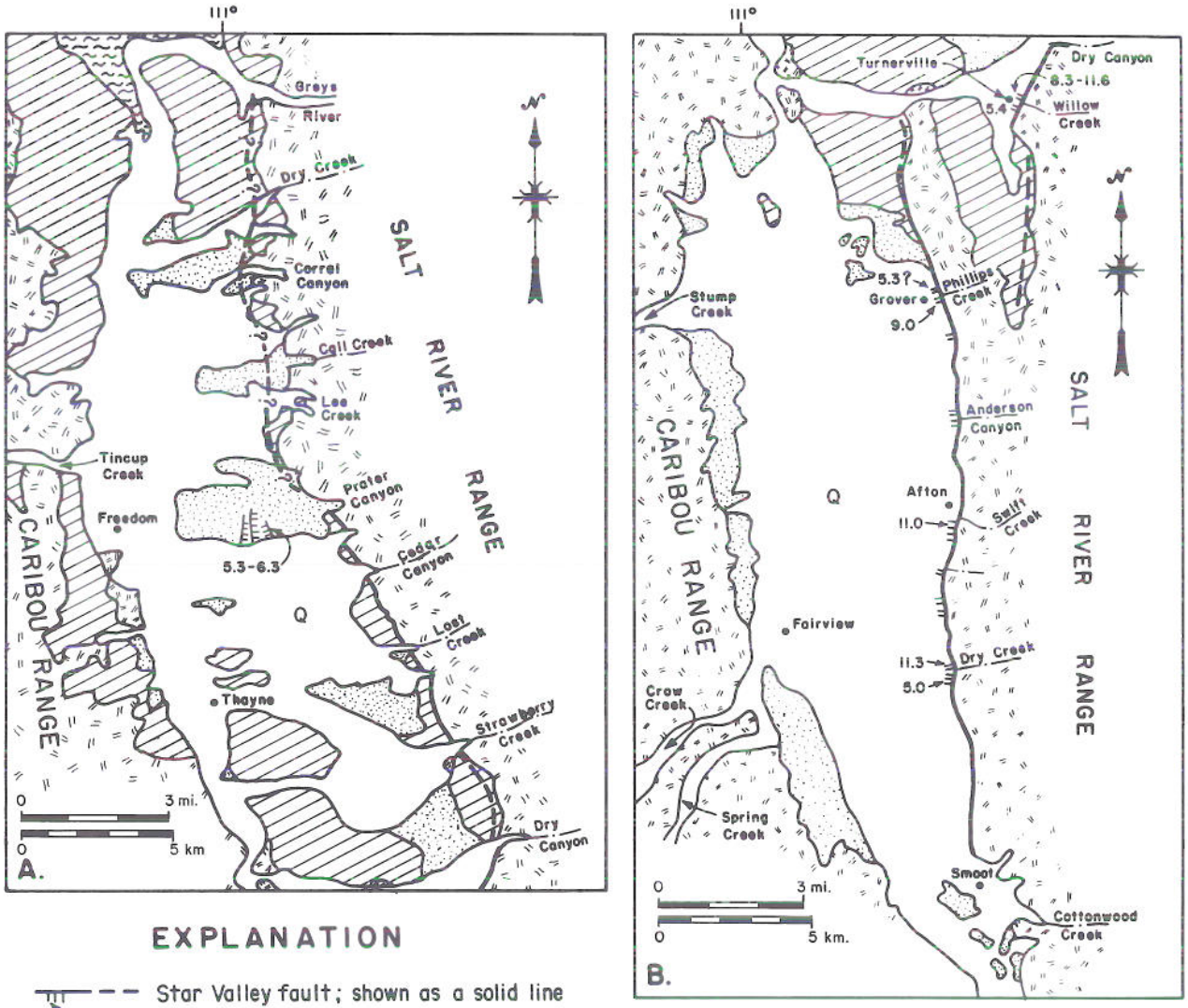

EXPLANATION

9.0 — Star Valley fault; shown as a solid line where the range front is straight and faceted spurs are preserved; shown as dashed where the range front is more sinuous, and queried where the fault is concealed; bars show the locations of scarps in younger upper Quaternary (≤ 15 ka) alluvial fan deposits; numbers show vertical surface displacements (in meters) taken from topographic profiles measured across scarps at the locations indicated.

5.3 — Scarps in older upper Quaternary (> 15 ka) deposits; numbers show vertical surface displacements (in meters) taken from topographic profiles measured across the scarp near the location indicated.

Upstream end of Palisades Reservoir.

Generalized geology:

Q — Younger upper Quaternary alluvium and colluvium.

Older upper Quaternary alluvium and colluvium; usually covered by loess ≥ 1.5 m thick.

Upper Tertiary and (or) lower Quaternary basin-fill deposits; commonly covered by loess ≥ 1.5 m thick.

Paleozoic and Mesozoic rocks, undifferentiated.

Geology generalized from Jobin (1972), Rubey (1973), Albee and Cullins (1975), and Oriel and Platt (1980), or geology inferred from Ravenholt and others (1976).

Figure 1. Generalized geologic maps of (A) northern Star Valley and (B) southern Star Valley, showing locations of the Star Valley fault and the Quaternary fault scarps. The two maps overlap about 1.2 miles (2 km). (From Anders and others, 1989.)

Field trip no. 1, part 1

LATEST QUATERNARY FAULTING AND STRUCTURAL EVOLUTION OF STAR VALLEY, WYOMING

James P. McCalpin[1]
Lucille A. Piety[2]
Mark H. Anders[3]

[1] Department of Geology, Utah State University, Logan, Utah 84322
[2] Seismotectonics and Geophysics Section, U.S. Bureau of Reclamation, Denver, Colorado 80225
[3] Lamont-Doherty Geological Observatory of Columbia University, Palisades, New York 10964

Trip summary (see Figure 1, Introduction to field trip no. 1)

Stop 1. Holocene Star Valley fault scarp
Stop 1A. (optional) Dry Creek fault scarps
Stop 2. Strawberry Creek landslide and fault scarp

Introduction

Star Valley is composed of two half-graben structures that are the result of Neogene extension on the Grand Valley/Star Valley fault. Star Valley fault is the southernmost portion of the Grand Valley/Star Valley fault and trends approximately north-south, parallel to the trend of Mesozoic thrust faults within the Salt River Range to the east and the Caribou Range to the west. Physiographically, Star Valley is divided into two basins of approximately equal areas but with fundamental differences in sediment type exposed and in latest Quaternary displacement rates on their respective segments of the Star Valley fault (**Figure 1**). In southern Star Valley, the range front is a sharp linear escarpment between the valley-fill sediments and the deformed Mesozoic/Paleozoic rocks of the Salt River Range. Steep-walled canyon tributaries, diamond-shaped range-front facets, and numerous scarps on young range-front alluvial fans all suggest rapid basin subsidence associated with extension on the southern Star Valley fault. Sediments exposed in the southern basin are alluvium and loess deposits younger than about 15 ka. Basin-fill deposits older than 15 ka are exposed only in a small area north of Grover, Wyoming. In northern Star Valley, the front of the Salt River Range is more sinuous than in the southern basin. Range-front facets are more dissected, tributaries more sinuous, valley walls less steep, and most significantly, there are no fault scarps north of Freedom, Wyoming (**Figure 1**). These geomorphic features indicate lower displacement rates on the northern segment than on the southern segment of the Star Valley fault. Valley-floor deposits include early to middle Pleistocene alluvial fans and extensive outcrops of the late Tertiary Salt Lake and Long Springs formations, the latter of which are also extensively exposed in Grand Valley and Swan Valley to the northwest. Presence of these older valley-fill deposits at the surface also suggest that Quaternary subsidence of northern Star Valley has been considerably less than that of southern Star Valley. Between Grover and Turnerville, Wyoming (**Figure 1B**), there is overlap of the northern and southern Star Valley fault segments.

This curious feature results in east-west extension being partitioned between two parallel north-south fault segments. The region of overlap includes the only late Quaternary fault scarps on the northern segment of the fault and the only pre-latest Quaternary sediments found in the southern basin. Within the overlap area, there is a northward extending peninsula of Mesozoic and Paleozoic rocks. This overlap region may be the result of fault segments propagating northward and southward.

Acknowledgments

We thank J. D. Gilbert and J. T. Sullivan for important insights into the regional geology and neotectonics of Star Valley; the U.S. Bureau of Reclamation for funding the earlier work done by L.A. Piety and M.H. Anders for a seismic hazards study of the Palisades Dam; and A. Holmes, P. Olsen and M. Levy for helpful reviews.

Latest Quaternary fault scarps on the southern Star Valley fault segment

In southern Star Valley, no fault scarps are observed south of Cottonwood Creek or north of about 1.8 miles (3 km) north of Grover. The portion of the southern segment that is most active is the middle portion between Phillips Creek and Dry Creek (**Figure 1B**). Latest Quaternary displacement rates on the southern segment are summarized in **Table 1**. These data are based on offset geomorphic surfaces. Ages of respective surfaces are based on soil development, carbonate rind thickness, and concomitant correlations to deposits of known age. The number of displacement events on each scarp is inferred from abrupt changes in scarp profiles that may reflect multiple events, following Wallace (1977). Slope angles were measured using the techniques developed by Bucknam and Anderson (1984) and Machette (1982). A more complete compilation of slope profiles and dating of geomorphic surfaces is found in Piety and others (1986).

The largest measured vertical surface displacement on the southern Star Valley fault is 38 feet (11.6 m), located in an alluvial fan at the mouth of Dry Creek. Along the southern Star Valley fault, the number of late Quaternary scarp-forming events is estimated between 2 and 4 with a maximum single event at 17.7 feet (5.4 m). The number of events is not well constrained, but planned trenching may better delineate the number of events as well as the magnitude of each event. Anders and others (1989) have estimated that the maximum displacement rate on the Star Valley fault is .046 inches/year (0.6 to 1.2 mm) during the latest Quaternary. This is comparable to fault displacement rates determined for the Teton fault (Gilbert and others, 1983) and the Wasatch fault (Schwartz and Coppersmith, 1984), thus making the southern Star Valley fault one of the most active faults in the northeastern Basin and Range province. At Stop 1, we will

Table 1. Latest Pleistocene-Holocene displacement on Star Valley fault (modified from Anders and others, 1989).

Location of scarp used to determine displacement of fault segment	Vertical surface displacements across scarp m(ft)	Age of displaced surface (10^3 yrs)	Estimated number of events	Estimated single-event surface displacement m(ft)	Latest Pleistocene-Holocene displacement rate (mm(in)/yr)[a]
Dry Creek	11.5 (37.7)	10-14	2	5.0 (16.4)	0.8-1.1 (.03-.04)
	5.0 (16.4)	9-11	1		
Swift Creek	11.0 (36.1)	10-14	2?	6.3[b](20.6)	0.8-1.1 (.03-.04)
Phillips Creek	9.0 (29.5)	10-14	2	5.3 (17.4)	0.6-0.9 (.02-.035)
	5.3 (17.4)	9-11	1		
Willow Creek	11.6 (38.0)	10-14	2-4	3.5 (11.5)-5.4 (17.7)	0.8-1.2 (.03-.046)
	9.5 (31.1)		2-3		
	7.5 (24.6)		2?		
	5.4 (17.7)	9-11	1?		
	3.3 (10.8)		1		
Prater Canyon	5.3 (17.4)-6.3 (20.6)	>10-14 <70	1?	5.3 (17.4)-6.3 (20.6)	
Corral Canyon	0.0	10(70)[c]	0		0.0

[a] Displacement rate since 10 to 14 ka.
[b] Single-event displacement estimated from possible multiple-event scarp profile.
[c] Age of unfaulted loess is estimated to be at least 10 ka, and probably 70 ka.

examine an 36-foot (11-m) scarp in an alluvial fan at the mouth of Swift Creek (**Figure 2**). Slope profiles (**Figure 3**) across the scarp exhibit a maximum slope angle of 34°. As discussed in Piety and others (1986), two events are estimated for this scarp using slope angles. We expect that future trenching may identify more events.

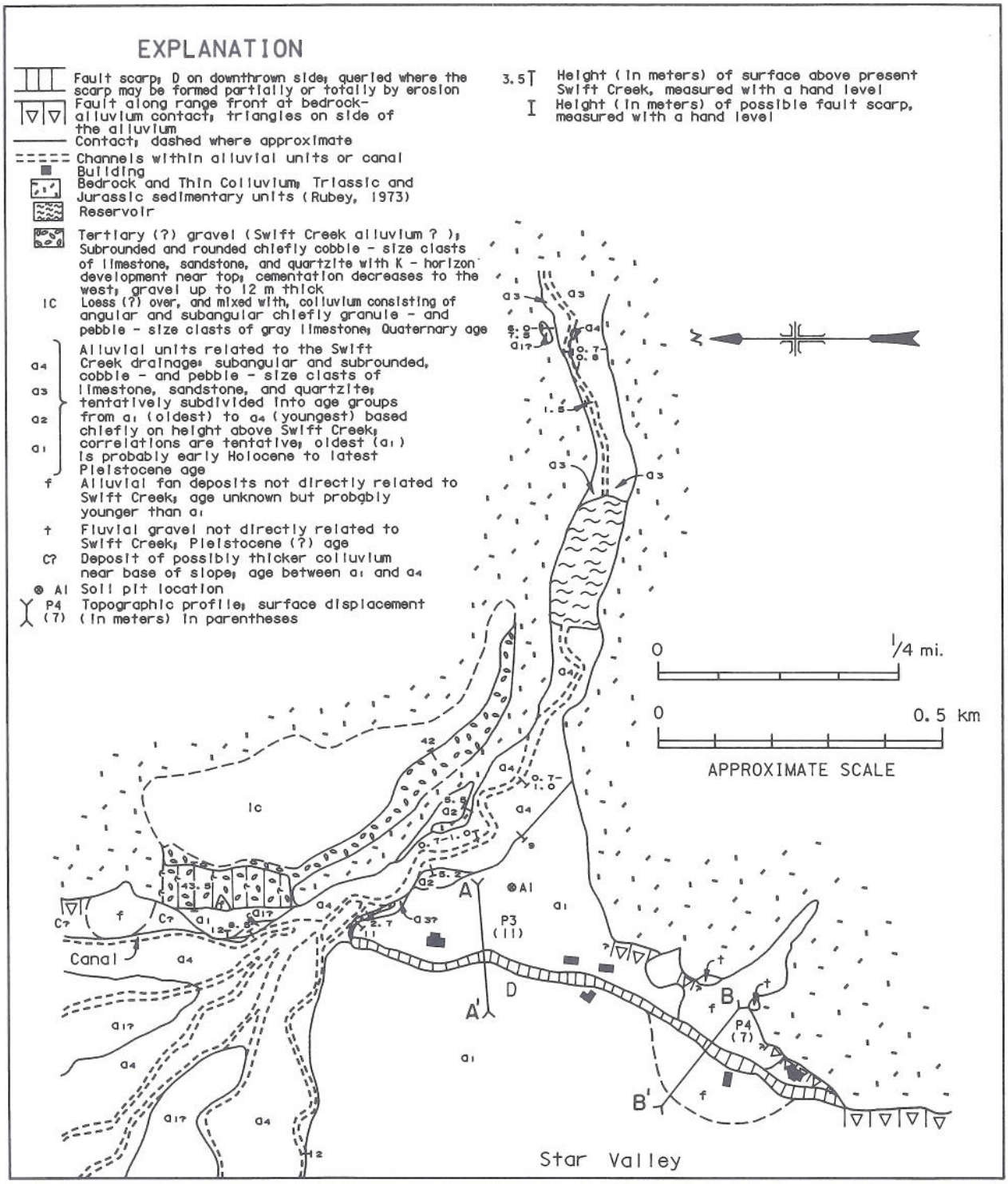

Figure 2. Sketch map of alluvial deposits and fault scarps at the mouth of Swift Creek in southern Star Valley from Piety and others (1986). Location of Swift Creek is shown in Figure 1 and is described as Stop 1 in the text.

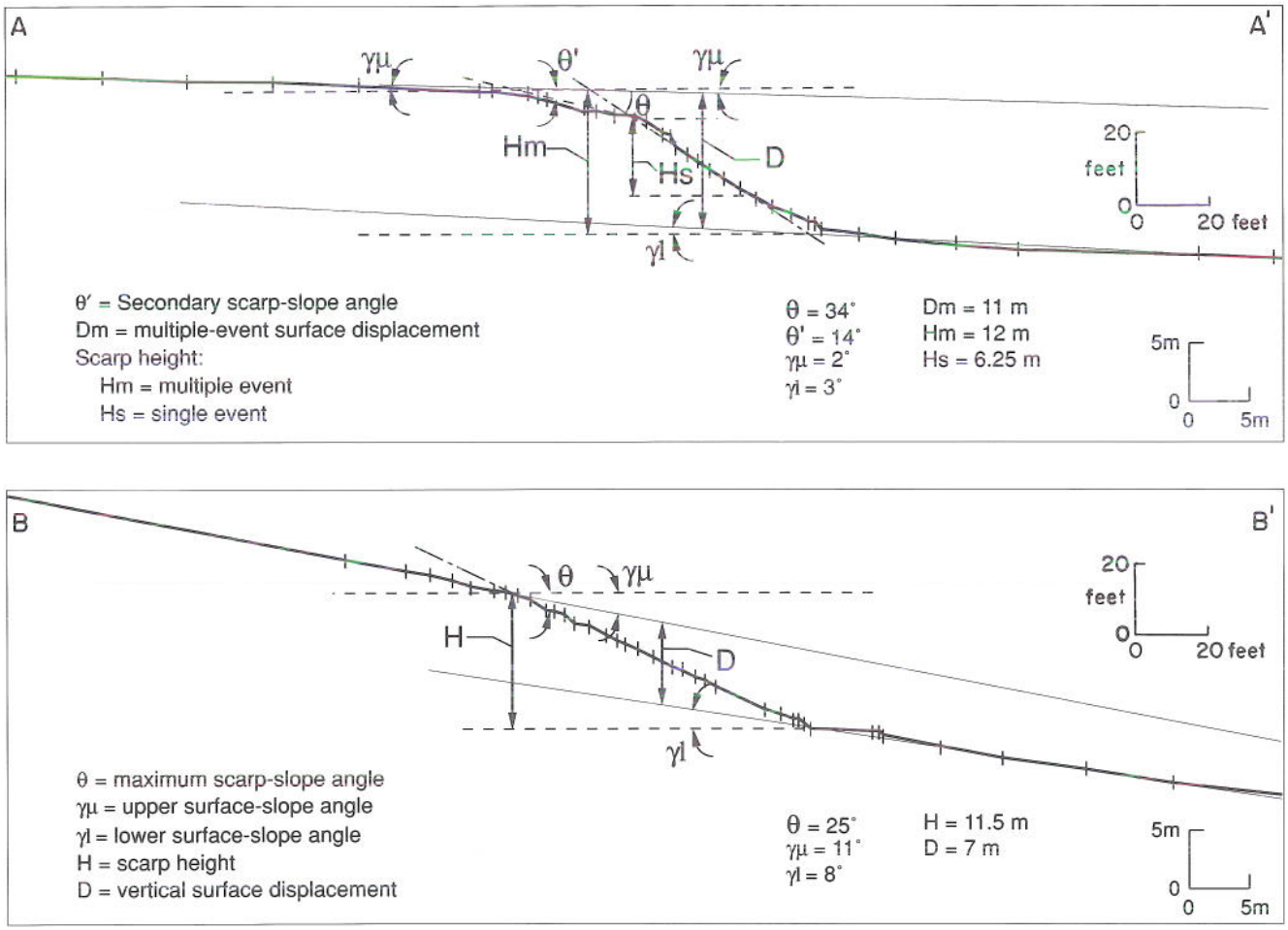

Figure 3. Topographic scarp profiles measured at Swift Creek along the Holocene southern Star Valley fault. Surface-slope angles, scarp-slope angles, scarp heights, and vertical surface displacements were measured using the methods of Bucknam and Anderson (1979) and Machette (1982). Locations of profiles are shown in Figure 2. (Diagram from Piety and others, 1986.)

Latest Quaternary fault scarps on the northern Star Valley fault segment

The northern Star Valley fault segment can be divided into three portions representing a progressive, southward-younging of rupture events. The southernmost portion, between Dry Canyon and Willow Creek (**Figure 1B**), has fault scarps on latest Quaternary alluvial fans at the mouth of Willow Creek and a straight-faceted range front between the two canyons. Along the middle portion, between Dry Canyon and Prater Canyon to the north, there are no Quaternary sediments along the range-front that are offset by the Star Valley fault. Each of the canyons have latest Quaternary alluvial fans at their mouths, yet the fans have no scarps. Scarps are present along the contact between the Miocene-Pliocene Salt Lake Formation and Paleozoic bedrock (such as at Strawberry Canyon, Stop 2) and have a maximum slope angle of 35°. About 1.2 miles (2 km) west of Prater Canyon, three scarps in alluvium are estimated to be late Pleistocene age. These synthetic and antithetic scarps are likely related to the rupture on a largely buried splay of the Prater Canyon/Dry Canyon segment.

Along the third portion of the northern Star Valley fault segment, from Prater Canyon north to Grand Valley, there are no observable fault scarps in Quaternary deposits. Loess-covered alluvial surfaces with an estimated age of 70 ka (Piety and others, 1986) cross the fault without displacement. Range-front sinuosity is significantly greater, canyons are broader, and faceted spurs are less distinct than on the southernmost

portion of the northern Star Valley fault. In contrast, Tertiary deposits are exposed only along the western valley margin in northern Star Valley, and do not surface anywhere within southern Star Valley. Each of the above lines of evidence suggest that the northernmost portion of the northern Star Valley fault has the lowest Quaternary slip rate of all segments of the Star Valley fault.

Basin-fill slide blocks

About 0.6 mile (1 km) south of Freedom, Wyoming, there are several slide blocks of Mesozoic/Paleozoic rock in the Salt Lake Formation (Hait and others, 1977). These blocks dip about 30°E and are probably gravity slides that came from the Salt River Range and slid across Star Valley to their present position. They were subsequently tilted to their present eastward dips by movement on the Star Valley fault. Near Strawberry Creek (Stop 2), is a middle (?) Pleistocene slide block derived from the Salt River Range that has been subsequently partly buried by middle to late Pleistocene fans. From the random orientations of large blocks of Madison Group limestone (up to 49 ft/15 m long) we infer that this slide block was transported in a fluidized rockslide. Two factors could have contributed to the failure: (1) the successive oversteepening of the range front and "daylighting" of bedding planes in the Madison Group during Quaternary uplift on the Star Valley fault and (2) shaking during a surface-faulting earthquake event. East of this stop, we see a tectonic graben that offsets the landslide deposit and its source area on the faceted spur. Surface faulting following landsliding has created a valley-facing scarp up to 164 feet (50 m) high on the east side of the graben, although net vertical tectonic displacement across the graben is less than 164 feet (50 m). Unfortunately, no middle or late Quaternary deposits cross the fault trace here, so it is difficult to estimate the number of paleoseismic events or to constrain their timing.

These slide blocks are important indicators of rates of basin subsidence. The blocks record times during which the rate of basin subsidence exceeded erosional denudation in the Salt River Range. The presence of the older blocks on the west side of the valley suggests that there was enough relief on the Salt Range to provide sufficient energy to propel the blocks across the valley. The slide blocks are tilted 30°E, suggesting the slide event predates a significant amount of the basin's subsidence history. The slide block near Strawberry Creek is a stratigraphically higher analogue for the older slide blocks farther west. Unfortunately, insufficient stratigraphic data exist to date the slides in Star Valley. As discussed in Anders (this field trip, part 2), there are datable interbedded ashes that constrain slide block activity in Grand Valley to the northwest.

Late Tertiary faulting in Star Valley

Limited exposures of datable units older than Quaternary make the reconstruction of basin initiation and subsequent development difficult. Volcanic units used to assess rates of basin formation in Grand and Swan valleys, and in Birch Creek Valley north of the Snake River Plain (Anders and others, 1989; this field trip, part 2) are absent in Star Valley. The only volcanic unit known in this basin is an ash deposit within the Salt Lake Formation, located in the northwestern portion of northern Star Valley. Interpretations of seismic reflection data suggest that the total depth of basin fill is similar in Star, Grand, and Swan valleys. Because those segments of the graben to the northwest in Grand and Swan valleys have been essentially inactive during the last 2 million years and the Star Valley fault has been active through the Quaternary, faulting on the Star Valley fault is thought to have begun about 2 million years after initiation of faulting in Grand and Swan valleys. This, of course, makes a speculative assumption of equivalent displacement rates on each segment of the Grand Valley/Star Valley fault.

Road log and stop descriptions

0.0 Depart from the town square in Jackson, Wyoming and proceed south on U.S. Highway 89 for 12 miles to Hoback Junction; turn right (west) and continue for 11 miles through the Snake River gorge to Alpine Junction. The descriptive part of this road log begins in Alpine Junction. For an explanation of features exposed along the first 23 miles of the field trip route between Jackson and Alpine Junction, refer to previously published road logs of Albee and others (1977) and Miller (1987).

Mileage

23.0 Alpine Junction (separation of U.S. Highways 26 and 89). Turn left (south) onto U.S. Highway 89. The valley floor surrounding Alpine Junction is a glacial outwash plain probably correlative with the maximum Pinedale (Burned Ridge) ice advance in Jackson Hole (about 30 ka). A lower terrace 59 feet (18 m) above river level is visible from the bridge crossing, and probably correlates with the later Pinedale (Jackson Lake) advance (about 15 ka).

For the next 13 miles, travel south down the center of the northern Star Valley. Star Valley is a half-graben bounded on the east by the Star Valley fault. Piety and others (1986) noted that the fault bounding northern Star Valley has a more subdued range-front morphology than does the same fault farther south in southern Star Valley. They term this northern part of the fault the "older Star Valley fault". Continue west, then south on U.S. 89.

32.0 Etna. The front of the Salt River Range makes an abrupt change in strike roughly 1.8 miles (3 km) east-southeast of Etna. North of that point, the front strikes nearly north-south, is relatively sinuous, and lacks steep-faceted spurs. Outcrops of Tertiary and lower Quaternary deposits are common on the valley floor, indicating that valley subsidence and filling is not rapid. No fault scarps have been observed in Pleistocene deposits (younger than about 150 ka) in this north trending segment.

South of the bend, the mountain front trends approximately N30°W for 9 miles (15 km), is linear, and has faceted spurs and small fault scarps in early to middle Pleistocene deposits. This 9-mile (15-km) stretch is probably part of a single seismogenic segment but the segment boundaries are not known at present. Continue south on U.S. 89.

36.0 Entering the "Narrows" between northern and southern Star Valley. The Narrows are formed where the Salt River incised pre-Cenozoic bedrock on the western side of the valley. This is the region of the two overlapping fault segments. Proprietary seismic reflection lines trending roughly east-west show that there are two east dipping wedge-shaped basins, one with a tilt axis on the western margin of Star Valley. The tilt axis for the easternmost basin is in the Narrows. To the east, large hills are underlain by Tertiary Salt Lake Formation. Continue south on U.S. 89.

40.0 Entering southern Star Valley. The young intermontane basin before you is bounded on the east by the Holocene Star Valley fault (after Piety and others, 1986). Geophysical data suggest that the Star Valley fault is listric and merges with a ramp of the Absaroka thrust at a depth of 1.2 to 2.4 miles (2 to 4 km) (Dixon, 1982). For the next 13 miles (22 km), the range front trends nearly north-south, has steep-faceted spurs, and has fault scarps in late Pleistocene and Holocene alluvial deposits. Continue south on U.S. 89.

45.0 Afton. One of the most prominent fault scarps on the Holocene Star Valley fault crosses the mouth of Swift Creek on the eastern side of Afton. Scarp surface offset ranges from 36 feet (11 m) across the main stream alluvium (age 10-15 ka?) to 23 feet (7 m) across a Holocene (?) alluvial fan. Younger terraces, up to 8.8 feet (2.7 m) above Swift Creek, cross the fault without disturbance, indicating that the latest faulting event is pre-late Holocene. Enter town, turn left (east) on 2nd Avenue.

Stop 1. Holocene Star Valley fault scarp

46.0 The northern section of this fault scarp across Swift Creek has a scarp height of 40 feet (12.0 m) and a net vertical surface offset of 36.1 feet (11.0 m) (Piety and others, 1986). Abundant vegetation on the scarp face and a spring at the scarp base indicate that ground water traveling westward through the alluvium is somehow dammed and brought to the surface.

South of the road, the scarp displaces a small alluvial fan at the mouth of an unnamed tributary. Here, the surface offset (from scarp profiling) decreases to 23 feet (7 m), 63 percent of that measured farther north. The fan shape suggests that the fan overlies Pleistocene (late Pinedale?) alluvial gravels of Swift Creek. The 13-foot (4-m) difference in surface offsets suggests that the scarp across the valley mouth alluvium has experienced a single 13-foot (4-m) displacement, which predated the deposition of the tributary fan. If 13 feet (4 m) of displacement per event is typical, then the scarp with a 23-foot (7-m) offset may represent two paleoseismic events, and the 36-foot (11 m) scarp may represent three events. Presently, we can only surmise that three faulting events have probably occurred here since 10 to 15 ka, the latest of which predates the low (4.9-8.8 ft/1.5-2.7 m) alluvial terraces of Swift Creek, which are assumed to be several thousand years old (Piety and others, 1986). Return to U.S. 89 (Main Street).

Stop 1A (optional). Dry Creek fault scarps

Time permitting and depending on location of trenches, an optional stop may be made at the mouth of Dry Creek, 4 miles south of Afton on U.S. 89. Here scarps of different vertical displacements occur north (37.7 ft/11.5 m) and south (16.4/5.0 m) of the creek. The higher scarp has a similar surface offset to the higher scarp at Swift Creek, but the lower scarp is considerably smaller than the smaller scarp at Swift Creek (16.4 vs 23 ft/5 vs. 7 m). Piety and others (1986) suggested that the 16.4-foot (5-m) scarp may represent a single event, and the 37.7-foot (11.5-m) scarp represents two events. If true, the displacement per event (16.4, 21.3 feet/5.0 m, 6.5 m) would imply M_s = 7.4 to 7.5 earthquakes (Slemmons, 1982). The 17.4-mile (29-km) length of the Holocene Star Valley fault segment, however, suggests smaller paleoevents (M_s = 7.1). Piety and others (1986) suggested that the Holocene Star Valley fault (17.4 miles/29 km long) and the southern (linear) portion of the older Star Valley fault (9.6 miles/16 km long) might have ruptured together, producing a maximum length of surface rupture of 27 miles (45 km). This length corresponds to M_s 7.2 earthquakes of historic record (Slemmons, 1982).

An alternative hypothesis is that even the smaller scarp at Dry Creek is a multiple-event scarp, and that single-event displacements on the Star Valley fault are on the order of 8.2 feet (2.5 m) rather than 16.4 feet (5 m). An 8.2-foot (2.5-m) displacement correlates with an M_s 7.2 rupture length of 27.6 miles (46 km), which is similar to the maximum rupture length hypothesized by Piety and others (1986). In this scenario, the 36-foot (11 m) scarps at Swift Creek and Dry Creek would represent four, not two, paleoevents. Hopefully, backhoe trenches across these scarps will help determine which hypothesis is correct. Return to U.S. 89, turn right (north), and continue through Afton northward.

52.0 Grover; turn right (east) onto small paved road.

52.5 Road enters mouth of Phillips Creek drainage. On the south side of the road at the range front, a scarp with 29.5 feet (9 m) of vertical surface offset has been disturbed by man. Piety and others (1986) proposed that a much-modified 17.4-foot (5.3 m) scarp also exists on the north side of the road, and they assume this to be a single-event scarp.

Continue up Phillips Creek; road turns to dirt. For the next 5 miles ascend and then descend a large salient of pre-Cenozoic bedrock that protrudes into the Star Valley graben. The basin-bounding fault occurs in the thick forest to the east and has not been traced out on foot.

57.5 Enter Turnerville. At the mouth of Willow Creek, 1,300 feet (400 m) to the east, Piety and others (1986) described multiple scarp heights of 10.8,17.7, 24.6, 31.1, and 38 feet (3.3 m, 5.4 m, 7.5 m, 9.5 m, and 11.6 m) across terraces of various ages. However, surfaces here have been modified extensively by man and the area was the site of a sawmill and related structures as well as a pipeline. The 38-foot (11.6-m) offset of the late Pleistocene aggradation surface is similar to that observed at Dry Creek and Swift Creek, and the 17.7-foot (5.4-m) offset is similar to that seen at the smaller scarp at Dry Creek. Intermediate scarp heights seen here raise the possibility that individual paleoseismic displacements occurred on the order of 8.2-11.4 ft/2.5-3.5 m) rather than nearly 16.4-19.6 ft/5-6 m).

59.1 Intersection with Willow Creek Road; continue northwest.

62.0 Enter Bedford; turn right (east) on a paved road and continue toward the mouth of Strawberry Creek.

62.7 Turn left (north) onto a dirt road leading across Strawberry Creek. Continue 1.1 miles, turn northeast through subdivision, and then north to the crest of a hill in the Bridger Lakes subdivision.

Stop 2. Strawberry Creek landslide and fault scarp

63.8 During landslide mapping for the U.S. Forest Service in 1985, McCalpin (unpublished) interpreted the irregular topography west of this stop to be a giant landslide. Rubey (1973) mapped portions of the area as Salt Lake Formation (Tertiary) and Madison Group (Mississippian), although he did not speculate how these rocks came to be exposed on the downthrown side of the Star Valley fault. Blocks of limestone up to 49 feet (15 m) long are common in the deposit, but all have different bedding orientations. McCalpin inferred that the faceted spur east of this stop, a dip slope of the Madison Group limestone, failed as a catastrophic rockslide and became a fluidized rockfall avalanche, which spread 1 mile (1.7 km) out onto the valley floor. Retrace route to Bedford, Wyoming.

65.6 Bedford; turn right (north) in center of town and proceed north.

70.4 Enter Thayne; turn right (north) onto U.S. 89. Proceed north and retrace route to Alpine Junction.

References cited

Albee, H.F., and Cullins, H.L., 1975, Geologic map of the Alpine Quadrangle, Bonneville County, Idaho, and Lincoln County, Wyoming: U.S. Geological Survey Geologic Quadrangle Map GQ-1259, scale 1:24,000.

Albee, H.P., Lingley, W.S., and Love, J.D., 1977, Geology of the Snake River Range and adjacent areas: Wyoming Geological Association 29th Annual Field Conference Guidebook, p. 769-783.

Anders, M.H., Geissman, J.W., Piety, L.A., and Sullivan, J.T., 1989, Parabolic distribution of circumeastern Snake River Plain seismicity and latest Quaternary faulting: migratory pattern and association with the Yellowstone hotspot: Journal of Geophysical Research, v. 94, no. B2, p. 1589-1621.

Bonilla, M.G., Mark, R.K., and Lienkaemper, J.J., 1984, Statistical relations among earthquake magnitude, surface rupture length, and surface fault displacement: Bulletin of the Seismological Society of America, v. 74, no. 6, p. 2379-2411.

Bucknam, R.C., and Anderson, R.E., 1979, Estimation of fault-scarp ages from a scarp-height-slope-angle relationship: Geology, v. 7, p. 11-14.

Dixon, J.S., 1982, Regional structural synthesis, Wyoming salient of western Overthrust Belt: American Association of Petroleum Geologists Bulletin, v. 66, no. 10, p. 1560-1580.

Gilbert, J.D., Ostenaa, D.A., and Wood, C.K., 1983, Seismotectonic study for Jackson Lake Dam and Reservoir, Minidoka Project, Idaho-Wyoming: U.S. Bureau of Reclamation Pacific Northwest Regional Office and Engineering and Research Center, Seismotectonic Report 83-8, 123 p.

Hait, M.H., Prostka, H.J., and Oriel, S.S., 1977, Geologic relations of late Cenozoic rockslide masses near Palisades Reservoir, Idaho and Wyoming: U.S. Geological Survey report for the U.S. Bureau of Reclamation (unpublished), p. 21.

Jobin, D.A., 1972, Geology map of the Ferry Peak Quadrangle, Lincoln County, Wyoming: U.S. Geological Survey Geologic Quadrangle Map GQ-1027, scale 1:24,000.

Machette, M.N., 1982, Quaternary and Pliocene faults in the La Jencia and southern part of the Albuquerque-Belen basins, New Mexico: Evidence of fault history from fault-scarp morphology and Quaternary geology: New Mexico Geological Society 33rd Field Conference Guidebook, p. 161-169.

Miller, W.R., 1987, Road log, geology of the Snake River Range and adjacent areas: Wyoming Geological Association 38th Annual Field Conference Guidebook, p. 359-384.

Oriel, S.S., and Platt, L.B., 1980, Geological map of the Preston 1° x 2° Quadrangle, southeastern Idaho and western Wyoming: U.S. Geological Survey Miscellaneous Investigations Map I-1127, scale 1:250,000.

Piety, L.A., Wood, C.K., Gilbert, J.D., Sullivan, J.T., and Anders, M.H., 1986, Seismotectonic study for Palisades Dam and Reservoir, Palisades Project, Idaho: U.S. Bureau of Reclamation Pacific and Northwest Regional Office and Engineering and Research Center, Seismotectonic Report 86-3, p. 355.

Ravenholt, H.B., Glenn, W.R. and Larson, K.N., 1976, Soil survey of Star Valley area, Wyoming-Idaho, parts of Lincoln County, Wyoming, and Bonneville and Caribou counties, Idaho: U.S. Department of Agriculture Soil Conservation Service and Forest Service, 74 p.

Rubey, W.W., 1973, Geologic map of the Afton Quadrangle and part of the Big Piney Quadrangle, Lincoln and Sublette counties, Wyoming,: U.S. Geological Survey Miscellaneous Investigations Map I-686, scale 1:62,500.

Schwartz, D.P., and Coppersmith, K.J., 1984, Fault behavior and characteristic earthquakes—examples from the Wasatch and San Andreas fault zones: Journal of Geophysical Research, v. 89, p. 5681-5698.

Slemmons, D.B., 1982, Determination of design earthquake magnitudes for microzonation: Proceedings of the Third International Earthquake Microzonation Conference, Seattle, Washington, p. 119-130.

Wallace, R.E., 1977, Profiles and ages of young fault scarps, north-central Nevada: Geological Society of America Bulletin, v. 88, p. 1267-1281.

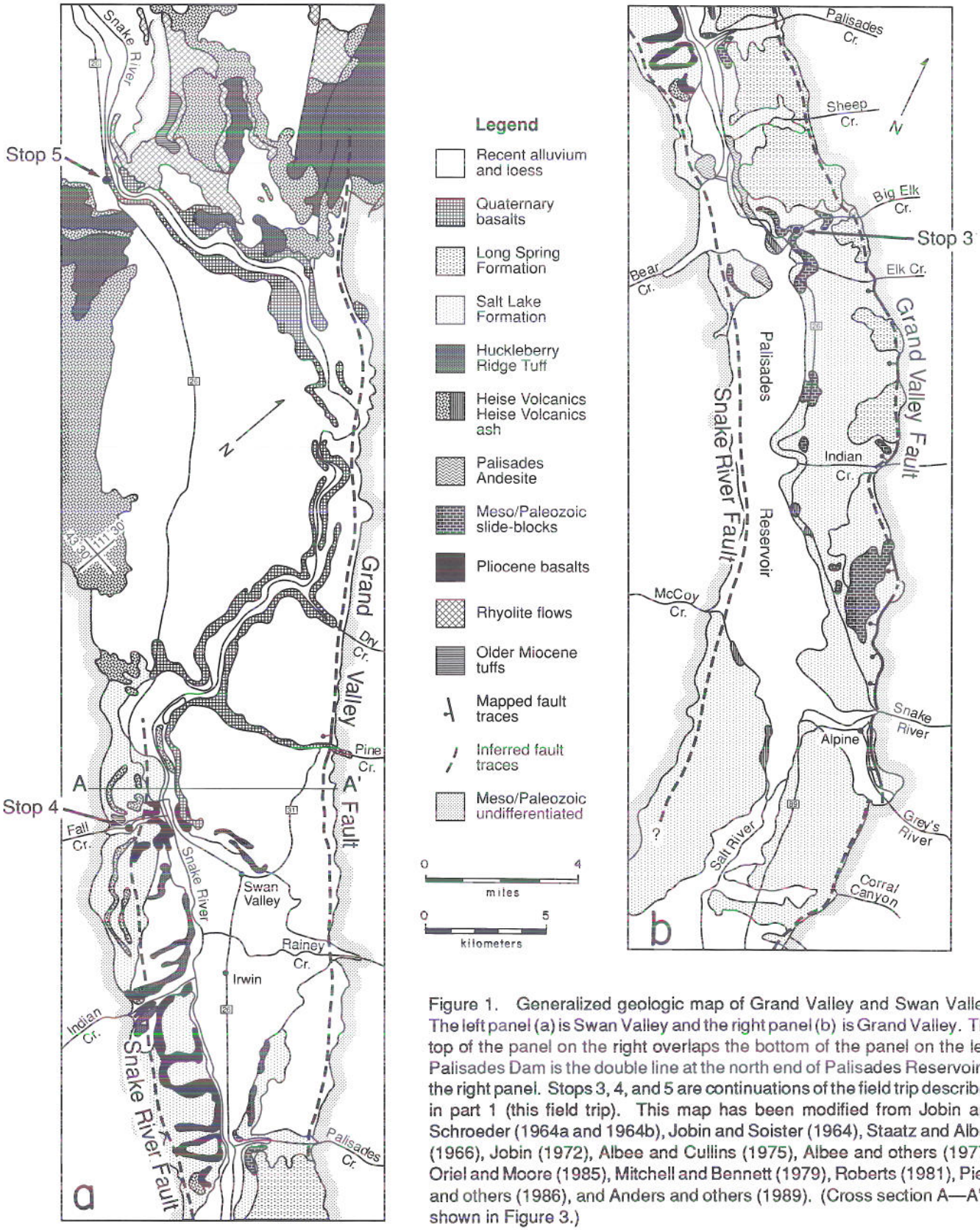

Figure 1. Generalized geologic map of Grand Valley and Swan Valley. The left panel (a) is Swan Valley and the right panel (b) is Grand Valley. The top of the panel on the right overlaps the bottom of the panel on the left. Palisades Dam is the double line at the north end of Palisades Reservoir in the right panel. Stops 3, 4, and 5 are continuations of the field trip described in part 1 (this field trip). This map has been modified from Jobin and Schroeder (1964a and 1964b), Jobin and Soister (1964), Staatz and Albee (1966), Jobin (1972), Albee and Cullins (1975), Albee and others (1977), Oriel and Moore (1985), Mitchell and Bennett (1979), Roberts (1981), Piety and others (1986), and Anders and others (1989). (Cross section A—A' is shown in Figure 3.)

Field trip no. 1, part 2

LATE CENOZOIC EVOLUTION OF GRAND AND SWAN VALLEYS, IDAHO

Mark H. Anders

Department of Geological Sciences and
Lamont-Doherty Geological Observatory
Columbia University
Palisades, New York 10964

Trip summary (see Figure 1, opposite, and Figure 1, Introduction to field trip no. 1)

Stop 3. Pliocene volcanic ash deposit, Big Elk Creek
Stop 4. Exposures of tilted Neogene sediments and interbedded volcanic rocks
Stop 4A. (optional) Quaternary basalts in Conant Valley
Stop 5. Overview of late Cenozoic volcanics, northern Swan Valley

Introduction

Grand Valley and Swan Valley are two interconnected northwest trending valleys that are 55 miles (90 km) in total length and 3 to 6 miles (5-10 km) wide (**Figure 1**). Paralleling the valleys are Paleozoic and Mesozoic rocks of the Caribou Range to the southwest and the Snake River Range to the northeast. Both Grand and Swan valleys are half-grabens that resulted from extension on the listric Grand Valley fault (Royse and others, 1975; Dixon, 1982). Parallel to the Grand Valley fault along the southwestern side of these valleys is the Snake River fault (**Figure 1**). Interpretations of seismic reflection data (Dixon, 1982) suggest that this fault is antithetic and experienced only minor displacement. Based on interpretations of seismic reflection profiles, Royse and others (1975) suggested that extension on the Grand Valley fault was the result of back-sliding down a Mesozoic thrust ramp following a regional shift from compression to extension. Basin-fill sediments in the half-graben form a succession of wedge-shaped reflecting surfaces (Royse and others, 1975). These reflectors represent a successive southwestward migration of onlapping surfaces. The basin-fill sediments are predominantly alluvial, colluvial, lacustrine, and ash units that were deposited throughout southern Idaho and northern Utah. Collectively, these deposits are referred to as the Miocene to Pliocene Salt Lake Formation.

The divide between Grand Valley and Swan Valley is marked by both structural and stratigraphic changes that occur north of the Palisades Reservoir Dam in the area between Sheep Creek and Palisades Creek (**Figure 1**). North of Sheep Creek in Swan Valley, there are a large number of volcanic units, primarily ash-flow tuffs, basalts, and rhyolite flows. These volcanic units are not found southeast of Sheep Creek. Conversely, south of Palisades Creek there are numerous deposits of the late Pliocene to Quaternary Long Spring Formation alluvium and colluvium of Merritt (1958); these are not found north of Palisades Creek. Furthermore, in the area between the two creeks there is a 1,300-foot (400-m) drop in the elevation of the basin-fill deposits from southeast to northwest. The elevation of basin-fill deposits in Swan Valley remains low until just north of Stop 5, where it rises again to an elevation equivalent to the north end of Grand Valley.

Swan Valley can be divided into three distinct sections based on geology and physiography. These are the northwestern, southeastern, and central sections, whose boundaries are near Stops 4 and 5 in **Figure 1**. In the southeastern section, Neogene units are exposed on the southwestern side of the valley and have been tilted to the northeast by movement on the Grand Valley fault. Volcanic rocks in this section are superbly

exposed along the southwest side of the valley and range in age from 1.5 Ma to 10 Ma. The youngest of these rocks, the 1.5 Ma Pine Creek Basalt, flowed up the Snake River drainage to Fall Creek as well as up the Pine Creek drainage and across the Grand Valley fault. Other than the Pine Creek Basalt, the only volcanic unit found on the northeastern side of the valley is the 2.0 Ma Huckleberry Ridge Tuff. All older volcanic rocks are restricted to the southwestern side of the valley. These units are interbedded with gravels of the Salt Lake Formation and tilted up to 30°NE.

The central section of Swan Valley is mostly covered by late Pleistocene loesses, on which there is intensive agricultural development. In this section, Neogene rocks that record the movement of the Grand Valley fault are buried beneath younger rocks. Along the southwestern side of the central section, the Caribou Mountains are covered by the tuff of Kilgore and the tuff of Blacktail (referred to as Heise Volcanics in **Figure 1**). The Snake River cuts a deep canyon through this section and exposes Quaternary basalts. The northernmost section of Swan Valley is characterized by thick sequences of Neogene volcanic rocks. Quaternary Snake River Plain basalts, and late Pleistocene loesses, which cover only a small percentage of Neogene rocks. In this section of the valley, basin-fill deposits form a topographic high that diverts the Snake River to the southwest. The topographic high is composed of Huckleberry Ridge Tuff, Heise Volcanics, several rhyolite flows, and older ash-flow tuffs (**Figure 1**). This topographic high forms Lookout and Kelly Mountains. Exposures of these volcanic rocks on cliffs at Kelly Mountain are discussed at Stop 5. Northwest of these mountains, there is an elevation drop onto the Snake River Plain.

Grand Valley is both shorter and narrower than Swan Valley, and presently it is partially filled by the Palisades Reservoir. Although the measured distance between the Grand Valley fault and the Caribou Range is comparable for both Grand Valley and Swan Valley, the width of Grand Valley is much less. This is because the northeastern side of Grand Valley exposes thick basin-fill sections of alluvium and colluvium of the Miocene to Pliocene Salt Lake Formation as well as latest Pliocene to Quaternary Long Spring Formation. Interbedded within these formations are large slide blocks of Paleozoic and Mesozoic rocks (**Figure 1**). These slide blocks are up to 1,600 feet (500 m) thick and cover several square miles (km). Farther to the northwest near the dam, the valley becomes narrower than at any other location within Star, Swan, and Grand valleys. Thick sections of the Salt Lake and Long Spring formations as well as thick ash deposits are found at several locations in this part of Grand Valley, though they rarely occur in Swan Valley to the northwest.

Acknowledgments

The author thanks J. D. Gilbert and J. T. Sullivan for important insights into the regional geology and neotectonics of Star Valley and J. T. Hagstrum for his help in paleomagnetic analysis of the ashes in Grand Valley. Funding was provided by the U.S. Bureau of Reclamation for earlier work done by M.H. Anders and J.W. Geissman for a seismic hazards study of the Palisades Dam. The author also thanks Alexis B. Dudden, Robin Barber, and Yutaka Komatsu for field assistance, and Maureen T. McAuliffe for help with the graphics. Helpful reviews were contributed by M. Levy, A. Holmes, R. Schlische and P.E. Olsen.

Oldest basin deposits and the age of basin formation

The age of the oldest fill sediments is not known precisely but is considered to be mid-Miocene because the oldest volcanic units (**Figure 2**) are underlain by older gravels thought to be Salt Lake Formation (called the Teewinot Formation by Merritt, 1958). The oldest volcanic unit described in Swan and Grand valleys is the 10 Ma (Kellogg and others, 1989) tuff of Cosgrove Road at Fall Creek (Anders and others, 1989). This tuff is exposed in Swan Valley below the tuff of Blacktail in a sequence of gravels of the Salt Lake Formation. As discussed in Kellogg and others (1989), the tuff of Cosgrove Road may correlate with the tuff of Arbon Valley. Presently, more work is needed to correlate this reworked tuffaceous unit at Fall Creek to other Snake River Plain volcanic units. For example, this unit could correlate with the tuff of Newby Ranch of Hackett and Morgan (1988), making the oldest dated basin-fill deposit 8.6 Ma.

Valley formation is likely to have been initiated before 10 Ma (or 8.6 Ma), as evidenced by the basinward fining of underlying Salt Lake Formation gravels; however, the exact time of valley formation is not known. Whereas Barnosky and Labar (1989) suggested that the Jackson Hole basin north of the Snake River Range was actively subsiding at 17 Ma, there is little evidence to support a similar early Miocene age of incipient basin development for Grand and Swan valleys.

Faulting history of Grand Valley and Swan Valley

Late Cenozoic slide blocks

Exposed on the northeastern side of Grand Valley are a number of large slide blocks that are interbedded with the Salt Lake Formation hanging-wall deposits (Moore and others, 1987). These deposits are likely single-event slides caused by oversteepening of the footwall during intervals when fault displacement rates exceeded the rate at which erosion could maintain a slope equilibrium. Thus, these slide blocks define likely intervals of rapid subsidence. Moore and others (1987) suggested that slide blocks in Grand Valley were emplaced between 8 and 4 Ma. The lower limit, 8 Ma, is not well constrained and is at best only an estimate. On the southwestern side of the reservoir across from Elk Creek, a slide block is located stratigraphically

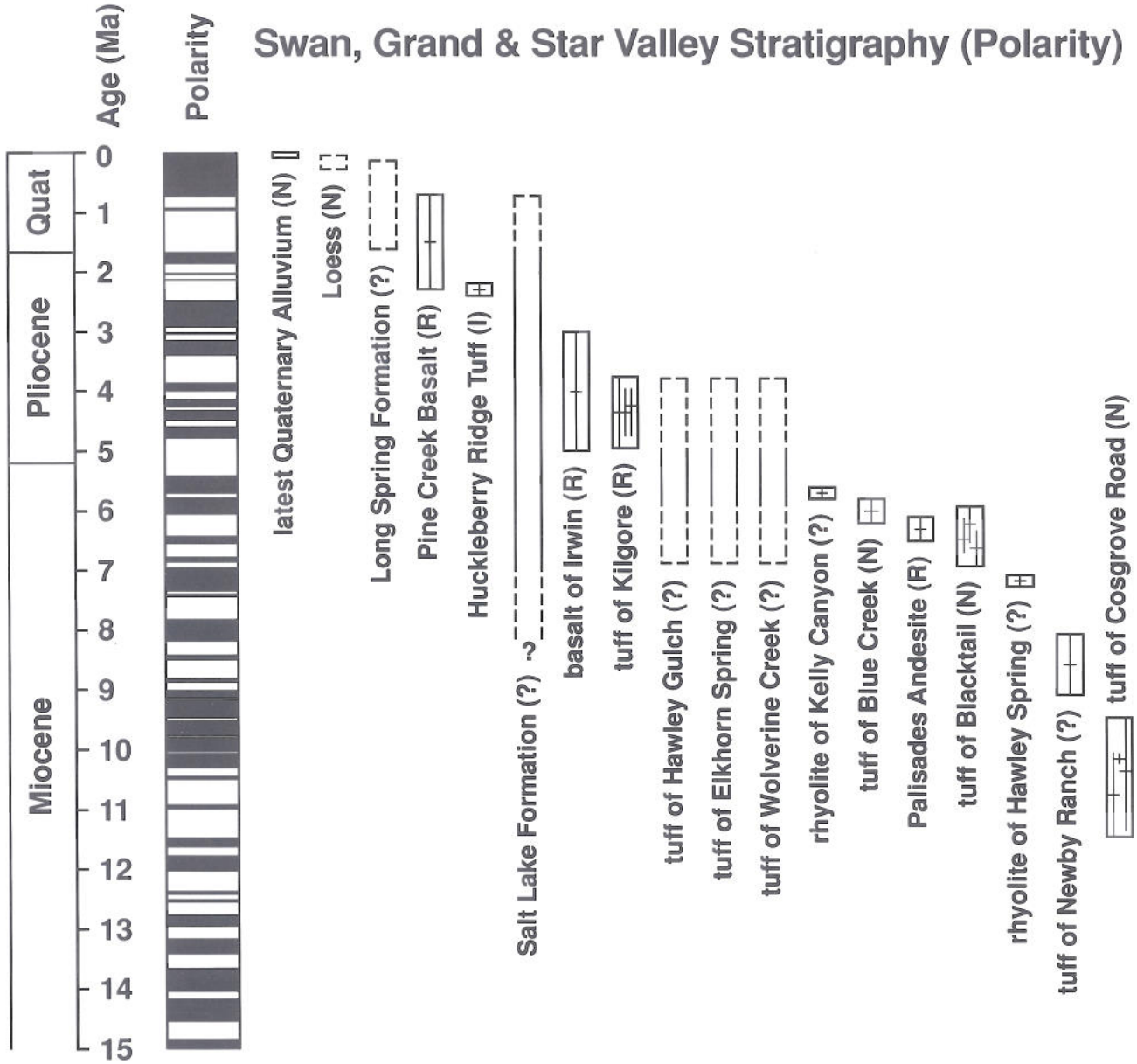

Figure 2. Diagram of the age relationships of geologic units found in Grand Valley and Swan Valley. Letter following the unit name is the magnetic polarity: (N) = normal polarity, (R) = reversed polarity, (I) = intermediate polarity, and (?) = unknown polarity. Crosses represent published isotopic ages. Queries indicate lack of confidence of stratigraphic range. Dashed upper end of boxes indicates range of ages associated with isotopic error bars for overlying unit. Dashed lines are estimates of the age range of a unit. Isotopic data from Armstrong and others (1975), Armstrong and others (1980), McBroome (1981), Morgan and others (1984), Piety and others (1986), Hackett and Morgan (1988), Kellogg and Marvin (1988), Morgan and Hackett (1989), Anders and others (1989), and Kellogg and others (1989).

below the 6.3 Ma Palisades Andesite. To the north and stratigraphically above the Palisades Andesite at Big Elk Creek (**Figure 1**), a large slide block is restricted to the interval between 6.5 and 4.4 Ma [the 6.3 Ma age of the Palisades Andesite by Armstrong and others (1980) is probably too young because ash correlated to the tuff of Blacktail overlies the andesite at several locations]. In Swan Valley, the Huckleberry Ridge Tuff overlies a slide block at Palisades Creek. and in Grand Valley, there are no slide blocks in the latest Pliocene to Quaternary Long Spring Formation (Oriel and Moore, 1985; Moore and others, 1987). This limits slide-block emplacement at Big Elk Creek to an interval several millions of years before 6.5 Ma to about 2.0 Ma.

Latest Quaternary faulting history of the Grand Valley fault in Grand Valley and Swan Valley

Witkind (1975) indicated the Grand Valley fault has been active during the Holocene. A subsequent study by Piety and others (1986) found no latest Quaternary sediments displaced by the Grand Valley fault in either Grand Valley or Swan Valley. About 1 mile (2 km) south of Rainy Creek in Swan Valley (**Figure 1**), there are several scarps up to 65 feet (20 m) high that parallel the trace of the Grand Valley fault (Piety and others, 1986). These scarps are partially filled with unfaulted loess that is latest Quaternary in age (Pierce and others, 1982).

At the mouth of the Snake River near Alpine, Wyoming, there is a terrace estimated to be latest Pleistocene (15 to 30 ka) that extends undisturbed across the Grand Valley fault (Piety and others, 1986). A scarp paralleling the trend of the Grand Valley fault on this terrace was trenched by Piety and others (1986) and found to be an erosional feature. Furthermore, a contact between this terrace and the Mississippian Lodgepole Limestone is depositional (Piety and others, 1986).

Late Cenozoic displacement history of the Grand Valley fault

An extensive study of alluvial units that were deposited over the Grand Valley fault in Swan Valley found only the fault scarps south of Rainy Creek that are discussed above. Other scarps and linear features were found on deposits of the latest Pliocene to Quaternary Long Spring Formation at several range-front locations in Grand Valley (Piety and others, 1986). These features are likely Quaternary fault scarps, but since none have been trenched, it is not known for certain that they are due to faulting. The only volcanic unit offset by the Grand Valley fault is the 1.5 Ma Pine Creek Basalt, which is displaced by 91 feet (28 m) at Pine Creek (Piety and others, 1986).

Although Quaternary units have not been offset substantially by the Grand Valley fault, the northeastward tectonic tilt of older units suggests there were significantly greater displacements during the Pliocene and Miocene. This is evidenced in Grand Valley by the 30° dips seen in seismic reflection lines across the valley (Royse and others, 1975) and by similar dips in the exposed Salt Lake Formation northeast of Palisades Reservoir. Slide blocks in these sediments show a tectonic tilt of about 30°. Paleomagnetic analysis of a 4.3 Ma ash deposit at Big Elk Creek (Stop 3) indicates the Salt Lake Formation is tilted about 25°NE. Underlying slide blocks and ash deposits are also tilted about 30°NE. Several 6.5 Ma ash deposits near Indian Creek are tilted 30°NE, as revealed by paleomagnetic analysis. On the southwestern side of Palisades Reservoir across from Big Elk Creek, the 6.3 Ma Palisades Andesite is also tilted to the northeast by about 30°.

In Swan Valley, there are several volcanic units that dip to the northeast. Anders and others (1989) used these units to establish the displacement rate on the Grand Valley fault since about 10 Ma by determining the amount of northeastward dip each volcanic unit experienced since its emplacement. For basalts, this is done simply by measuring the dip of each unit and determining its respective isotopic age. More work is required for the ash-flow tuffs because the present dip measured in the field does not represent the amount of tectonic tilt (see Anders and others, 1989). Tectonic tilt is assessed by first establishing the thermoremanent magnetization (TRM) direction of each unit in an undeformed area and comparing it to the direction at a site that has been tectonically tilted. This comparison assumes that the TRM is faithfully recorded throughout each unit at the time of emplacement. Using this technique, Anders and others (1989) found that the Huckleberry Ridge Tuff was not tectonically tilted even though it dips as much as 15°NW. The same technique was applied to several units, including the 4.3 Ma tuff of Kilgore and the 6.5 Ma tuff of Blacktail. A proprietary seismic reflection line shot parallel to the A-A' cross-section near Fall Creek (**Figure 1**) shows several straight reflectors that converge to form a wedge-shaped pattern that suggests tilted surface exposures can be projected to the Grand Valley fault as is done in **Figure 3**. Although the fault shape is not well constrained, seismic lines (Dixon, 1982) and gravity studies (Stott, 1974) indicate a basin depocenter at about the location shown on **Figure 3.** Therefore, if the

approximate depth of the depocenter is known, a good assumption can be made as to the location of the fault at depth. Using the relationships shown in **Figure 3**, displacement rates can be calculated once the age of the unit is known, as is done in **Figure 4**. A steeper slope corresponds to a greater displacement rate on the fault. **Figure 4** indicates there was a period between 2.0 and 4.3 Ma when the displacement rate was over 100 times greater than during the 2.0 million years that followed. During the Quaternary, the displacement rate on the Grand Valley fault was about 0.0005 inches/year (0.014 mm/yr). During the interval of 2.0 to 4.3 Ma, the rate was 0.07 inches/year (1.8 mm/yr). This compares closely to the displacement rate on the Teton fault—0.06 to 0.08 inches/year ((1.7 to 2.2 mm/yr) (Gilbert and others, 1983)—and the Star Valley fault—0.05 inches/year ((1.2 mm/yr) (Anders and others, 1989). This type of fault displacement behavior is similar to that observed on the Beaverhead fault in Birch Creek Valley during the Quaternary (Scott and others, 1985) and during the Neogene (this field trip, part 3). This pattern of faulting is closely tied to the passage of the Yellowstone hotspot as first suggested by Anders and Geissman (1983).

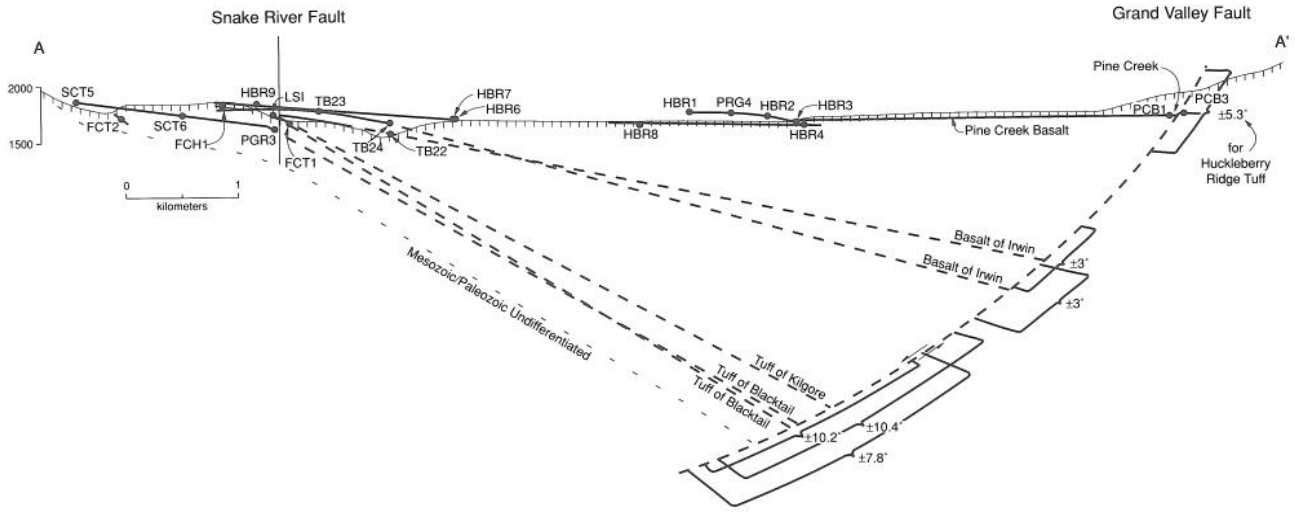

Figure 3. Cross section A-A' from Figure 1. Orientations of all volcanic units and paleomagnetic sampling sites are superimposed onto one section. Solid lines are based on surface mapping and the dashed lines are based on surface outcrops projected into the subsurface using dips determined from paleomagnetic analyses of tuffaceous units and projections based on dip measurements for basalt units. Error bars for the tuffs are the root-mean square (rms) error between the site-mean direction and the unit-mean direction; error bars for the basalts are the errors in determining attitudes in the field. Horizontal scale equals vertical scale. (Modified from Anders and others , 1989.)

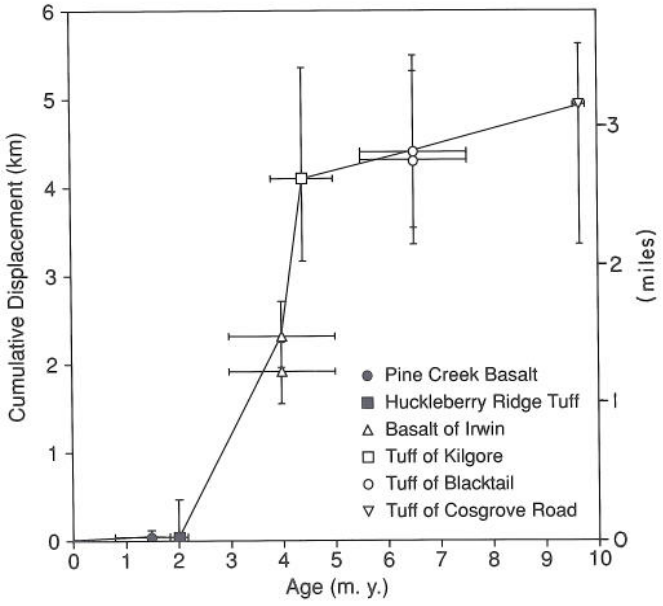

Figure 4. Apparent cumulative displacement versus age for the Grand Valley fault in southeastern Swan Valley. Horizontal error bars represent one standard deviation and values for isotopic ages. Vertical error bars are the root-mean square for angles between the site-mean and the unit-mean directions. The error for the Basalt of Irwin is based on field-measured attitudes. Error bars on the tuff of Cosgrove Road are based on errors in calculating the depth of the depocenter. (Modified from Anders and others, 1989.)

Road log and stop descriptions

Mileage continued from field trip no. 1, part 1.

87.4 Continue north on U.S. 89 and cross the bridge over the Snake River. Travel northwest on a glacial outwash plain of maximum Pinedale (Burned Ridge) advance (30 ka). A lower terrace of the later Pinedale (Jackson Lake) advance (15 ka) is visible from the bridge looking upstream.

88.2 Take U.S. 26 northwest toward Idaho Falls. The prominent 245-foot-high (75 m) terrace to the north is Pleistocene (150-200 ka) and is capped by a younger loess thought to correlate with loess unit A (10-70 ka) of Pierce and others (1982). This terrace does not cross the Grand Valley fault; the 30 ka terrace does cross the fault, but is not faulted.

90.1 U.S. Forest Service sign "4-H Camp" marks a small dirt road that leads to the 4-H Camp and the Idaho State University summer field camp. Looking north from the road, the hills in the immediate foreground are Salt Lake Formation strata dipping northeast. The outcrops of sedimentary rocks that cap some of the hills are Cambrian to Mississippian rocks that make up the largest slide-block mass exposed in Grand Valley (**Figure 1**). A more complete discussion of this location is provided in Moore and others (1987). Look southwest to white ash beds exposed on the opposite shore of Palisades Reservoir. This is one of several uncorrelated ashes exposed along the opposite shore and seen as you travel along the northeastern side of the reservoir. Continue northwest on U.S. 26.

93.8 On the northeast (right) side of the road there is a 10- to 13-foot-high (3- to 4-m) exposure of white rhyolitic ash. The ash is interbedded with fluvial pebbly-clay layers. This site, along with several others in Grand Valley, was sampled for paleomagnetic analysis. Although some horizons have been reworked, others horizons have not and are, therefore, suitable for paleomagnetic analysis. Preliminary paleomagnetic results suggest that this ash and another located 1 mile farther to the northwest are correlated to the tuff of Blacktail. This correlation is further supported by a fission-track age of 6.68 Ma on this ash reported in Moore and others (1987).

94.8 A 13-foot-thick (4-m) white ash deposit exposed here is correlated to the tuff of Blacktail. The close correlation in site-mean directions between the two deposits suggests that the horizons sampled were not reworked, although some horizons show clear indications of reworking.

95.9 A 32- to 48-foot-long (10- to 15-m) road cut exposes a chaotic assemblage of ash, Salt Lake Formation alluvium, and Paleozoic rocks. This deposit is a large slide block or debris flow.

99.4 To the northeast is Blowout Canyon, which was the 4.8-mile-long (8 km) pathway of a Holocene-aged fluidized debris flow (Thompson, 1978).

Stop 3. Pliocene volcanic ash deposit, Big Elk Creek

102.8 Turn right off U.S. 26 onto a dirt road cut into the northwest side of the reservoir inlet formed by the drainage of Big Elk Creek. Stop at wide turnout in road near white ash deposit.

This thick sequence of ashes has been described by Hait and others (1977) as a pumicite deposit. The ashes rest directly on a large slide block of Mississippian Madison Group limestone. The slide block is also exposed on the opposite side of the reservoir inlet. The ash deposits consist of several layers of coarse-grained ash shards of millimeter size, with minor amounts of pyroxene and quartz. Several layers have a salt-and-pepper appearance caused by black obsidian spherules. The shard morphology and large shard size separate this unit from the other ash deposits cropping out along U.S. 26. Results of the paleomagnetic analysis of this deposit suggest that two distinct polarities are present. The upper horizons have a reversed polarity corresponding to tuff of Kilgore unit-mean direction that has subsequently been tilted 25°NE. This agrees with the measured northeast-directed tilt of 21°. Below this horizon is a normal-polarity horizon that is unlike any previously sampled Neogene ash-flow tuff unit in the eastern Snake River Plain. This unit could come from a smaller unidentified eruption associated with the Rexburg caldera. It is unlikely that it correlates with the tuff of Elkhorn Spring because the tuff of Elkhorn Spring has a polarity similar to the tuff of Kilgore (Morgan, 1988). The tuff of Hawley Gulch is a possible correlation only because its polarity is unknown and it directly underlies the tuff of Kilgore. More work is necessary on this unit before such correlations can be made with confidence. To the southwest on the other side of the reservoir, an outcrop of the 6.3

Ma Palisades Andesite dips 30°NE, and to the southwest of the andesite is the oldest slide block exposed in Grand Valley. Located 1.4 miles due east from this stop is an exposure of Palisades Andesite on the shore of the reservoir. Overlying this unit is an ash deposit that dips 27°NE and is similar in mineralogy to the ashes sampled southeast of Indian Creek. These ashes are indistinguishable from another deposit, which also overlies the andesite, located near the town of Palisades, Idaho. All these ashes have normal site-mean directions similar to the tuff of Blacktail. This suggests that the 6.3 Ma isotopic age of Armstrong and others (1980) is too young since it underlies the well-constrained 6.5 Ma age of the tuff of Blacktail.

Farther up Big Elk Creek, is another slide block interbedded with Salt Lake Formation alluvium. Above this is the unconformity of the southwest dipping Long Spring Formation. Within Big Elk Creek drainage are variously aged units whose tectonic tilting patterns record the displacement history of the Grand Valley fault. The latest Pliocene to Quaternary Long Spring Formation (Merritt, 1958) is essentially untilted, yet the underlying 4.3 Ma ash, correlated to the tuff of Kilgore, has been tilted 25°NE. Furthermore, within the same stratigraphic section, ash correlated with the 6.5 Ma tuff of Blacktail is tilted 27°NE. This pattern of tilting suggests that there was a rapid tilting episode sometime after 4.3 Ma and before the deposition of the latest Pliocene to Quaternary Long Spring Formation. Since deposition of the Long Spring Formation there has been a dramatic reduction in tilting rate. This pattern of tectonic tilting will be observed at Stop 4 in Swan Valley.

103.8 Along the north (right) side of the road are boulder-sized gravels of the Salt Lake Formation underlying the large Madison Group limestone slide block. To the south (left), a small road leads down about 325 feet (100 m) to the reservoir. Here, the Palisades Andesite is overlain by a small mudflow that is in turn overlain by the ash deposit discussed above. Continue to Palisades Dam.

106.3 Arrive at the dam after travelling 2.5 miles along exposures of columnar-jointed Palisades Andesite. The dam abuts a large stock of the hypabyssal andesite. Continue down into Swan Valley.

107.9 Beyond the town of Palisades, an outcrop of reversed-polarity Palisade Andesite is overlain by a normal-polarity ash equivalent to the tuff of Blacktail (referred to as PTH1 in Fig. 6 of Anders and others, 1989).

108.9 In the hills in the foreground to the southwest (left) is a basalt flow that is tilted 11°NE, forming several prominent flatirons. This basalt is composed of three or four flows, each about 13 feet (4 m) thick, and is called the basalt of Irwin (Piety and others, 1986). An isotopic age of 4.0 Ma is reported for this unit (referred to as basalt TB2 in Anders and others, 1989).

109.9 Turn right on the road to Palisades Creek for an optional stop. Less than 325 feet (100 m) after turning off U.S. 26 is a fork in the road. At this location a large slide block of bedding-disrupted Gros Ventre Formation limestone is in contact with Salt Lake Formation gravels. This slide block is a continuation of the slide block that forms the large cliff of limestone to the east. Climb up 6.5 to 10 feet (2-3 m) to the base of the block. The basal contact of the slide block and the gravels is exposed here. Note that layering of the gravel cobbles suggests a fluidized flow. Return to U.S. 26 heading northwest toward Idaho Falls

111.0 To the northeast (right) is a cliff on the Palisades Bench. Midway up the cliff is an outcrop of Huckleberry Ridge Tuff. Witkind (1975) mapped a fault at the base of the cliff. A proprietary seismic line shot across the trace of this fault does not show offset. Furthermore, up to 15° of northeast tilt of the Huckleberry Ridge Tuff at this location was shown by Anders and others (1989) to be nontectonic in origin.

115.0 To the southwest, are smooth planar surfaces tilting about 10°- 15°NE. These surfaces are on the Huckleberry Ridge Tuff. Anders and others (1989) determined that the northeast dips of the Huckleberry Ridge Tuff in Swan Valley are not tectonic in origin, but are the result of emplacement of the Huckleberry Ridge Tuff over preexisting northeast dipping surfaces.

132.4 Town of Swan Valley; continue on U.S. 26 toward Idaho Falls.

134.4 On the north (right) side of the road are excellent exposures of columnar-jointed basalts that once extended across to Fall Creek on the opposite side of the Snake River. Piety and others (1986) dated this flow at 5.1 Ma. The reported isotopic age of this basalt (basalt of Fall Creek) is probably too old because the basalt directly overlies the 4.3 Ma tuff of Kilgore. This units dips 14°NE and is correlated with the basalt of Irwin.

135.0 Cross the bridge over the Snake River. Take an immediate left toward Fall Creek Campground. Continue for 1 mile on a dirt road situated between the Snake River and an outcrop of the basalt of Fall Creek.

136.1 Turn right heading southwest on another dirt road and continue 2 miles up Fall Creek.

Stop 4. Exposures of tilted Neogene sediments and interbedded volcanic rocks

138.1 Travertine deposits are actively forming at the contact between the Cenozoic and Paleozoic rocks. These deposits are carbonate precipitated from spring waters originating in Paleozoic limestones. Looking up to the southeast along the contact, observe an active travertine mine at the top of the basin-fill deposits.

Fall Creek deeply incises the Cenozoic basin fill, exposing many of the older volcanic units found in Swan Valley. Near the Echo Canyon Road fork is a deposit of the oldest volcanic unit found in Swan Valley. This normal-polarity tuffaceous unit (discussed above) is exposed along a small ridge to the northwest of the fork. It is probably the tuff of Cosgrove Road, which is dated at about 10 Ma, although it could be related to the younger 8.6 Ma tuff of Newby Ranch. Once the polarity of the tuff of Arbon Valley (thought to be equivalent to the tuff of Cosgrove Road by Kellogg and others, 1989) and the tuff of Newby Ranch are determined, correlation of these units will be greatly enhanced.

The prominent exposure on the high ridge to the northwest is the tuff of Blacktail. The tuff of Blacktail in Fall Creek is an 81-foot-thick (25 m) welded tuff that contains abundant pumice fragments that have been flattened into a prominent foliation. No basal vitrophyre is present in the tuff of Blacktail at Fall Creek. This unit is referred to in Anders and others (1989) as the tuff of Spring Creek. Morgan and others (1984) successfully correlated this unit with the tuff of Edie Ranch to the north of the Snake River Plain and named it the tuff of Blacktail. This unit tilts 10°NE for most of the length of its exposure in Fall Creek, but rocks exposed within 325 feet (100 m) of the Snake River fault dramatically increase in dip to over 30°. Paleomagnetic analysis of these units within Fall Creek confirm these field-measured tilts as tectonic. Along the same side of Fall Creek, but on the northeastern side of the Snake River fault, there is a small 2-foot-thick (.5-m) outcrop of welded orange and black tuff of Kilgore (referred to as the tuff of Heise in Anders and others, 1989) that has been tilted 28°NE. An exposure of the tuff of Kilgore in Fall Creek located to the southwest of the Snake River fault has been tilted only 9°NE. This implies that the Snake River fault was a tilt axis in Swan Valley for movement on the Grand Valley fault.

The ability to calculate tectonic tilts on units of different age within Fall Creek makes it possible to reconstruct the movement history of the Grand Valley fault. This is done by projecting surface dips into a subsurface intersection with the Grand Valley fault. For this technique to work properly, two assumptions about basin geometry are made: (1) buried surfaces must be planar (or undeformed since deposition), and (2) the shape of the fault surface must be able to be reasonably estimated. The errors associated with these assumptions are discussed in Anders and others (1989).

Figure 3 shows a compilation of tectonic tilts that are projected into the subsurface. Using the cumulative displacement from **Figure 3** and the known age of tilted units, **Figure 4** can be constructed. As seen in **Figure 4**, there has been a significant change in the displacement rate during various intervals of time. During the interval between 2 and 4.3 Ma, the displacement rate was greater than the interval before or after. Although there has not been a similar quantitative assessment of displacement rates in Grand Valley, the pattern of tilting in Grand Valley is similar to that in the southeastern section of Swan Valley.

Return to U.S. 26, travel northwest toward Idaho Falls up a small hill and then descend into Conant Valley. After 6 miles, look to the west (left) at a small hill near a ranch in the center of Conant Valley. This hill is capped with the 6.0 Ma tuff of Blue Creek (Morgan, 1988). Underlying the tuff of Blue Creek at this location is the tuff of Blacktail, which is tilted to the northeast.

Stop 4A. (optional) Quaternary basalts in Conant Valley

145.0 Just after ascending Conant Valley on U.S. 26, pull into a large area on the left side of the road created by road construction. The large (100 ft/30 m) cliff directly to the west is an outcrop of palagonite and lapilli tuffs. Hackett and Morgan (1988) refer to the basaltic units here as the Conant Valley volcanics and divide it into three units: Unit 1—matrix-supported tuff beccias with palagonite matrix, scoria clasts, and pillow basalt fragments; Unit 2—fine-grained, yellow-brown palagonite and lapilli tuffs; Unit 3—pahoehoe and pillow basalt flow. The presence of both pillows and pahoehoe suggests the basalt flowed into impounded shallow waters, probably from the Snake River. This basalt may correlate with the 1.5 Ma Pine Creek Basalt. For further details, see Jobin and Schroeder (1964a), Roberts (1981), and Hackett and Morgan (1988). Travel northwest along U.S. 26 toward Idaho Falls.

148.0 Antelope Flat is intensively farmed for wheat and potatoes owing to the thick deposits of loess. Underlying the loess, is a thin layer of Huckleberry Ridge Tuff that crops out at various locations on Antelope Flat. Basalt is assumed to underlie the Huckleberry Ridge Tuff.

151.0 Descend from Antelope Flat through a road cut that exposes a 16-foot-(5-m) section of the Huckleberry Ridge Tuff.

Stop 5. Overview of late Cenozoic volcanics, northern Swan Valley

Turn off at rest area. Stop 5 is the last stop of the day and affords an excellent view of the late Cenozoic volcanics that dominate the basin fill in the northern section of Swan Valley. Directly across the Snake River and directly below the parking lot are several Quaternary basalt flows. These basalts probably flowed upstream and filled the canyons cut by the Snake River. Across from the rest area, is a tan rhyolite flow that the basalt apparently flowed around. Exposed on the cliffs to the northwest are numerous ash-flow tuffs and rhyolite flows ranging in age from 8.6 to 2.0 Ma. From the top to the bottom of the cliff, these units are described by Morgan and Bonnichsen (1989) as the tuff of Kilgore, the tuff of Hawley Gulch, the tuff of Elkhorn Spring, the tuff of Wolverine Creek, the tuff of Blacktail, the rhyolite of Hawley Spring, and the tuff of Newby Ranch. An analysis of tectonic tilting has not been done on these basin-fill deposits but is planned for the future.

References cited

Albee, H.F., and Cullins, H.L., 1975, Geologic map of the Alpine Quadrangle, Bonneville County, Idaho, and Lincoln County, Wyoming: U.S. Geological Survey Geologic Quadrangle Map GQ-1259, scale 1:24,000.

Albee, H.P., Lingley, W.S., and Love, J.D., 1977, Geology of the Snake River Range and adjacent areas: Wyoming Geological Association 29th Annual Field Conference Guidebook, p. 769-783.

Anders, M.H., and Geissman, J.W., 1983, Late Cenozoic evolution of Swan Valley, Idaho: EOS Transactions of the American Geophysical Union, v. 64, no. 45, p. 858.

Anders, M.H., Geissman, J.W., Piety, L.A., and Sullivan, J.T., 1989, Parabolic distribution of circumeastern Snake River Plain seismicity and latest Quaternary faulting: migratory pattern and association with the Yellowstone hotspot: Journal of Geophysical Research, v. 94, no. B2, p. 1589-1621.

Armstrong, R.L., Harakal, J.E., and Neill, W.M., 1980, K-Ar dating of Snake River Plain (Idaho) volcanic rocks—new results: Isochron West, v. 27, p. 5-10.

Armstrong, R.L., Leeman, W.P., and Malde, H.E., 1975, K-Ar dating, Quaternary and Neogene volcanic rocks of the Snake River Plain, Idaho: American Journal of Science, v. 275, p. 225-251.

Barnosky, A.D., and Labar, W.J., 1989, Mid-Miocene (Barstovian) environmental and tectonic setting near Yellowstone Park, Wyoming and Montana: Geological Society of America Bulletin, v. 101, no. 11, p. 1448-1456.

Dixon, J.S., 1982, Regional structural synthesis, Wyoming salient of western Overthrust Belt: American Association of Petroleum Geologists Bulletin, v. 66, no. 10, p. 1560-1580.

Gilbert, J.D., Ostenaa, D.A., and Wood, C.K., 1983, Seismotectonic study for Jackson Lake Dam and Reservoir, Minidoka Project, Idaho-Wyoming: U.S. Bureau of Reclamation Pacific Northwest Regional Office and Engineering and Research Center, Seismotectonic Report 83-8, 123 p.

Hackett, W.R., and Morgan, L.A., 1988, Explosive basaltic and rhyolitic volcanism of the eastern Snake River Plain, Idaho: Guidebook to the geology of central and southern Idaho: Idaho Geological Survey Bulletin 27, p. 283-301.

Hait, M.H., Prostka, H.J., and Oriel, S.S., 1977, Geologic relations of late Cenozoic rockslide masses near Palisades Reservoir, Idaho and Wyoming: U.S. Geological Survey report for the U.S. Bureau of Reclamation (unpublished), p. 21.

Jobin, D.A., 1972, Geology map of the Ferry Peak Quadrangle, Lincoln County, Wyoming: U.S. Geological Survey Geologic Quadrangle Map GQ-1027, scale 1:24,000.

Jobin, D.A., and Schroeder, M.L., 1964a, Geology of the Conant Valley Quadrangle, Bonneville County, Idaho: U.S. Geological Survey Miscellaneous Field Studies Map MF-277, scale 1:24,000.

Jobin, D.A., and Schroeder, M.L., 1964b, Geology of the Irwin Quadrangle, Bonneville County, Idaho: U.S. Geological Survey Miscellaneous Field Studies Map MF-287, scale 1:24,000.

Jobin, D.A., and Soister, P.E., 1964, Geologic map of the Thompson Peak Quadrangle, Bonneville County, Idaho: U.S. Geological Survey Miscellaneous Field Studies Map MF-284, scale 1:24,000.

Kellogg, K.S., and Marvin, R.F., 1988, New potassium-argon ages, geochemistry, and tectonic setting of upper Cenozoic volcanic rocks near Blackfoot, Idaho: U.S. Geological Survey Bulletin 1806, p. 19.

Kellogg, K.S., Pierce, K.L., Mehnert, H.H., Hackett, W.R., Rodgers, D.W., and Hladky, F.R., 1989, New ages on biotite-bearing tuffs of the eastern Snake River Plain, Idaho: stratigraphic and mantle-plume implications: Geological Society of America Cordilleran and Rocky Mountain Section Abstracts with Programs, v. 21, no. 5, p. 101.

McBroome, L.A., 1981, Stratigraphy and origin of Neogene ash-flow tuffs on the north-central margin of the eastern Snake River Plain, Idaho: M.S. thesis, University of Colorado, Boulder, 74 p.

Merritt, Z.S., 1958, Tertiary stratigraphy and general geology of the Alpine, Idaho-Wyoming area: M.S. thesis, University of Wyoming, Laramie, 94 p.

Mitchell, V.E., and Bennett, E.H., 1979, Geologic map of the Driggs Quadrangle, Idaho: Idaho Bureau of Mines and Geology, Geologic Map Series, scale 1:250,000.

Moore, D.W., Oriel, S.S., and Mabey, D.R., 1987, A Neogene (?) gravity-slide block and associated slide phenomena in Swan Valley graben, Wyoming and Idaho: Geological Society of America Rocky Mountain Section Centennial Field Guide, v. 2, p. 113-116.

Morgan, L.A., 1988, Explosive rhyolitic volcanism on the eastern Snake River Plain: Ph.D thesis, University of Hawaii, Manoa, p. 191.

Morgan, L.A., and Bonnichsen, B., 1989, Heise volcanic field, Excursion 4A: Silicic volcanic rocks in the Snake River Plain-Yellowstone Plateau province, *in* Chapin, C.E., and Zidek, J., editors, Field excursions to volcanic terranes in the western U.S., v. II, Cascades and intermountain west: New Mexico Bureau of Mines and Mineral Resources Memoir 47, p. 153-160.

Morgan, L.A., Doherty, D.J., and Leeman, W.P., 1984, Ignimbrites of the eastern Snake River Plain: evidence for major caldera-forming eruptions: Journal of Geophysical Research, v. 89, p. 8665-8678.

Morgan, L.A., and Hackett, W.R., 1989, Explosive basaltic and rhyolitic volcanism of the eastern Snake River Plain, *in* Ruebelmann, K.L., editor, Field Trip Guidebook T305, Jackson, Wyoming to Boise, Idaho, July 21-29, 1989: 28th International Geological Congress, Washington D.C., 1989, p. 39-46.

Oriel, S.S., and Moore, D.W., 1985, Geologic map of the West and East Palisades roadless areas, Idaho and Wyoming: U.S. Geological Survey Miscellaneous Field Studies Map MF-1619-B, scale 1:50,000.

Pierce, K.L., Fosberg, M.A., Scott, W.E., Lewis, G.C., and Colman, S.M., 1982, Loess deposits of southern Idaho-age correlation of the upper two loess units, *in* Bonnichsen, B., and Breckenridge, R.M., editors, Cenozoic geology of Idaho: Idaho Bureau of Mines and geology Bulletin 26, p. 717-725.

Piety, L.A., Wood, C.K., Gilbert, J.D., Sullivan, J.T., and Anders, M.H., 1986, Seismotectonic study for Palisades Dam and Reservoir, Palisades Project, Idaho: U.S. Bureau of Reclamation Pacific and Northwest Regional Office and Engineering and Research Center, Seismotectonic Report 86-3, 355 p.

Roberts, J.C., 1981, Late Cenozoic volcanic stratigraphy of the Swan Valley graben between Palisades Dam and Pine Creek, Bonneville County, Idaho: M.S. thesis, Idaho State University, Pocatello, 58 p.

Royse, F., Jr., Warner, M.A., and Reese, D.L., 1975, Thrust belt structural geometry and related stratigraphic problems, Wyoming-Idaho-northern Utah, *in* Bolyard, D.W., editor, Deep drilling frontiers of the Central Rocky Mountains: Rocky Mountain Association of Geologists Symposium, p. 41-54.

Scott, W.E., Pierce, K.L., and Hait, M.H., Jr., 1985, Quaternary tectonic setting of the 1983 Borah Peak earthquake, central Idaho: Bulletin of the Seismological Society of America, v. 75, no. 4, p. 1053-1066.

Staatz, M.H., and Albee, H.F., 1966, Geology of Garns Mountain Quadrangle, Bonneville, Madison and Teton Counties, Idaho: U.S. Geological Survey Bulletin 1205, p. 122.

Stott, L.W., 1974, A gravity survey of a Late Cenozoic graben in the Wyoming-Idaho Thrust Belt: M.S. thesis, University of Michigan, Ann Arbor, 28 p.

Witkind, I.J., 1975, Preliminary map showing known and suspected active faults in Idaho: U.S. Geological Survey Open File Report 75-278, p. 71, scale 1:500,000.

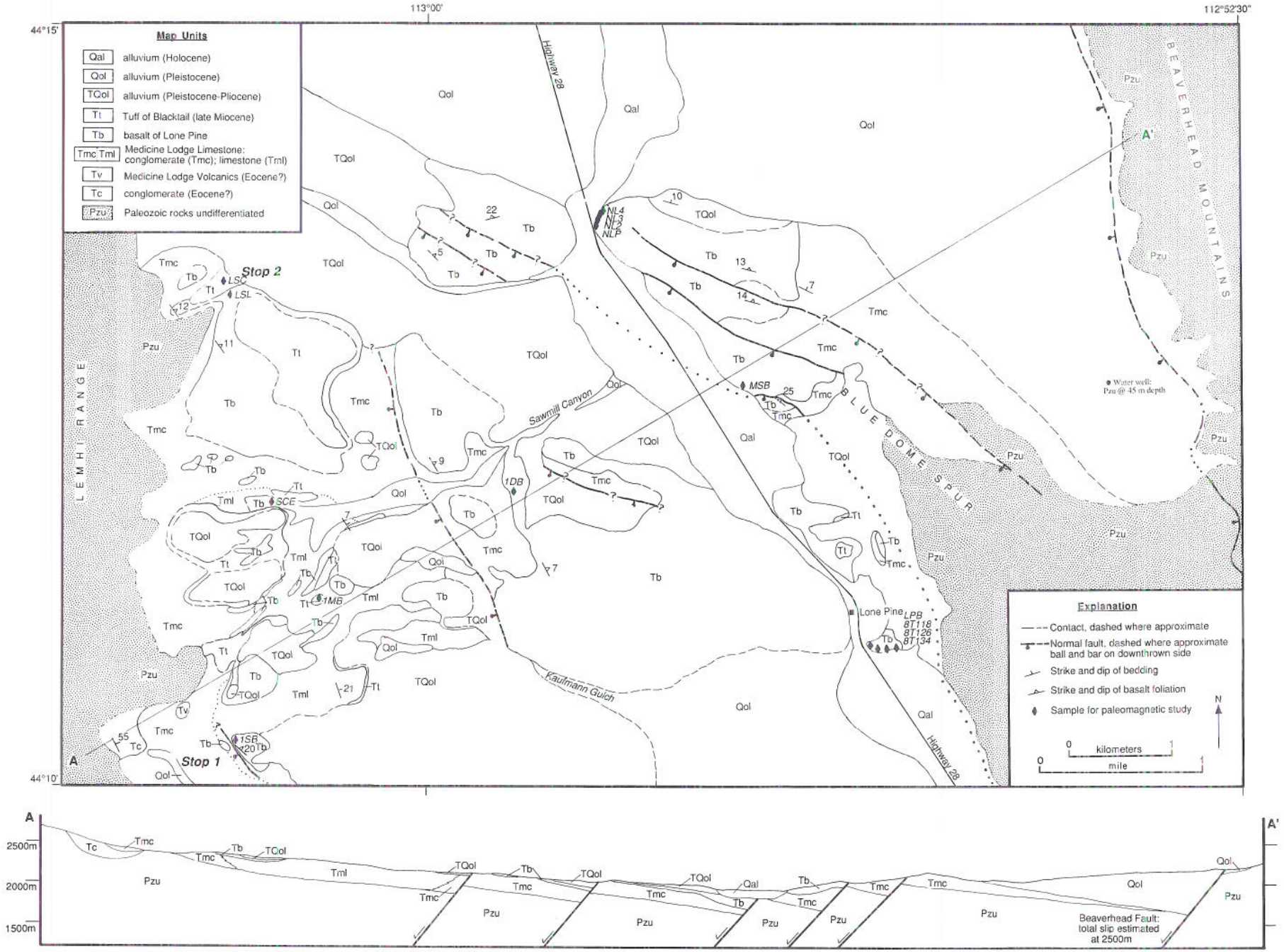

Figure 1. Geologic map and cross section of Birch Creek Valley near Lone Pine, Idaho. Field trip stops are located along the western side of the valley. Location of the Beaverhead fault is from Garmezy (1981) and Pleistocene alluvium contacts are modified from Scott (1982).

Field trip no. 1, part 3

NEOGENE EVOLUTION OF BIRCH CREEK VALLEY NEAR LONE PINE, IDAHO

David W. Rodgers[1]
Mark H. Anders[2]

[1] Department of Geology, Idaho State University, Pocatello, Idaho 83209
[2] Lamont-Doherty Geological Observatory of Columbia University, Palisades, New York 10964

Trip summary (See Figure 1, opposite, and Figure 1, Introduction to field trip no. 1)

Stop 6. Birch Creek Valley overview
Stop 7. Tilted Neogene sediments with interbedded volcanic rocks

Introduction

The Basin and Range province extends north of the Snake River Plain, throughout central Idaho and southwestern Montana. Nowhere is the classic topography and geology of the Basin and Range better developed than in east-central Idaho, where the rugged Lost River Range, Lemhi Range, and Beaverhead Mountains are flanked by late Cenozoic basins. The sediments in these basins provide an excellent record of Basin and Range tectonism, allowing us to interpret fault geometries and rates of extension. This part of the field trip concerns the basin fill in Birch Creek Valley, the southern Beaverhead Mountains, and the Lemhi Range.

Bounded on its eastern edge by the Beaverhead normal fault, Birch Creek Valley is the result of Neogene and Quaternary subsidence and basin filling. The valley can be divided into two basins, north and south of the town of Lone Pine. Northern Birch Creek Valley is bounded by the Nicholia segment of the Beaverhead fault, which Haller (this field trip, part 4) describes in detail. Southern Birch Creek Valley is bounded by the Blue Dome segment of the Birch Creek fault. The two fault segments overlap in the Lone Pine vicinity, where Blue Dome Spur marks a right step in the topographic range-front (Figure 1, introduction to field trip no. 1).

Much of Birch Creek Valley is covered by Pleistocene gravels. In places, however, underlying Neogene sediments and volcanic rocks have been uplifted and exposed. Near Lone Pine, Neogene rocks form a nearly continuous exposure from east to west across the valley, making it a natural locality to study the early evolution of the basin. Here, Paleozoic bedrock is overlain by interbedded conglomerate, limestone, basalt, and rhyolite tuff. We have mapped the distribution of Neogene rocks in the Lone Pine vicinity, and show this map and a cross section in **Figure 1**. We have also used paleomagnetic techniques on volcanic rocks to correlate units within the valley (**Figure 2**) and to assess the amount and direction of tectonic tilting subsequent to their emplacement. A total of 15 sites of basalt and 8 sites of the tuff of Blacktail were analyzed. The paleomagnetic results are shown in **Figure 3**. Overall, the distribution of Neogene units, their thickness variations, the nature of unconformities between them, their offset relationships, tectonic tilting patterns, and published radiometric ages have been used to reconstruct the early basin history of Birch Creek Valley, and to compare it to other basins in the northeastern Basin and Range.

Acknowledgments

The authors thank Alexis B. Dudden, Robin Barber, and Yutaka Komatsu for field assistance, and Maureen T. McAuliffe for help with the graphics. We especially thank John Hagstrum of the U.S. Geological

Survey for help in all aspects of the paleomagnetic study. Helpful reviews were contributed by M. Levy, A. Holmes, P.E. Olsen, and J. Hagstrum. Financial support was received from the Idaho State Board of Education.

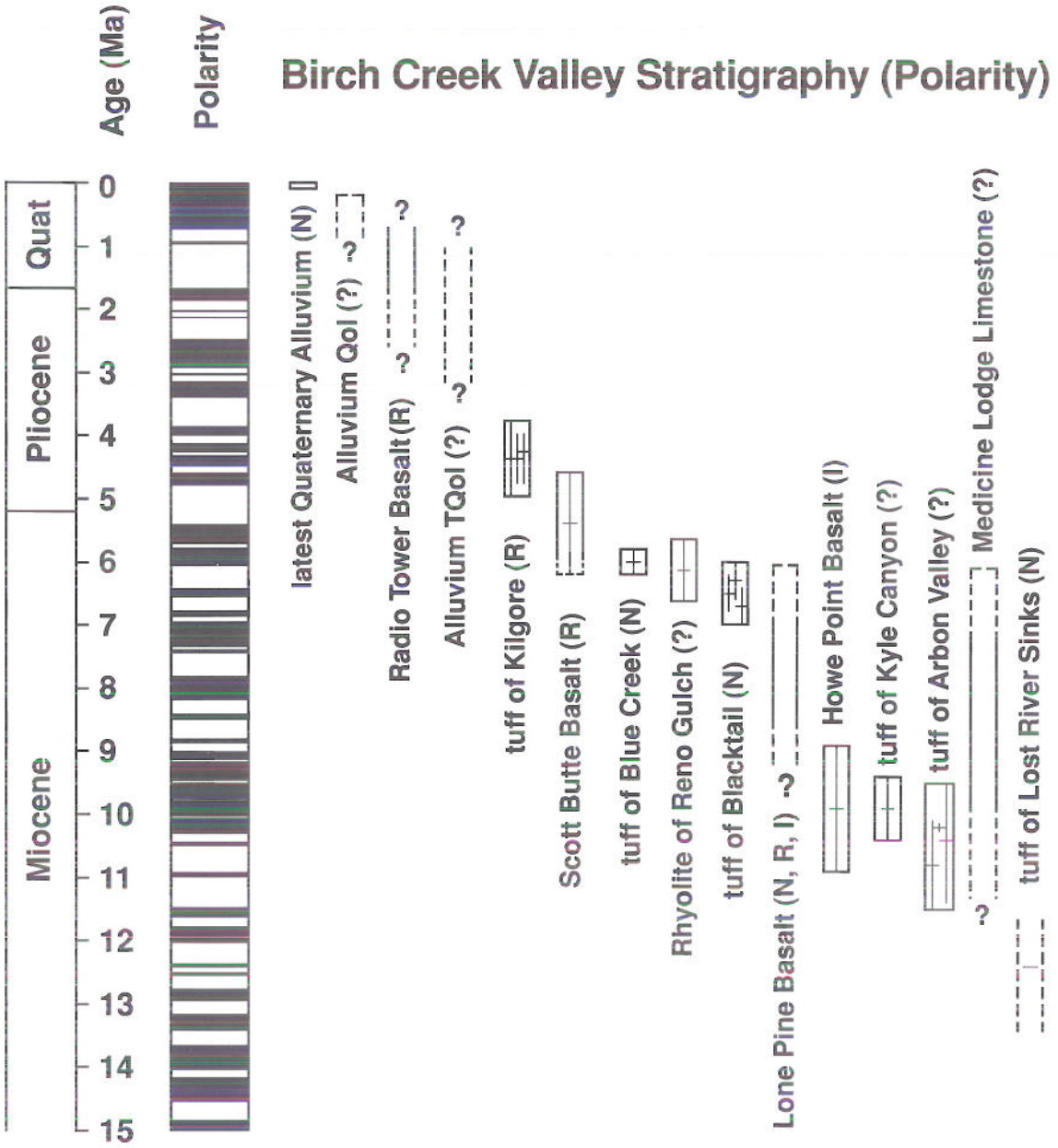

Figure 2. Diagram of the age relationships of geologic units found in Birch Creek Valley. Eocene (?) gravels and Eocene Medicine Lodge Volcanics (in Figure 1) are not shown. Letter following the unit name is the magnetic polarity: (N) = normal polarity, (R) = reversed polarity, (I) = intermediate polarity, and (?) = unknown polarity. Crosses represent published isotopic ages. Queries indicate lack of confidence of stratigraphic range. Dashed upper end of boxes indicate range of age associated with isotopic error bars for overlying unit. Dashed lines are estimates of age range of a unit. Isotopic data from Armstrong and others (1975), Armstrong and others (1980), Anders and others (1989), Chase (1972), McBroome (1981), Kellogg and Marvin (1988), Kellogg and others (1989), Morgan and others (1984), and Morgan and Hackett (1989).

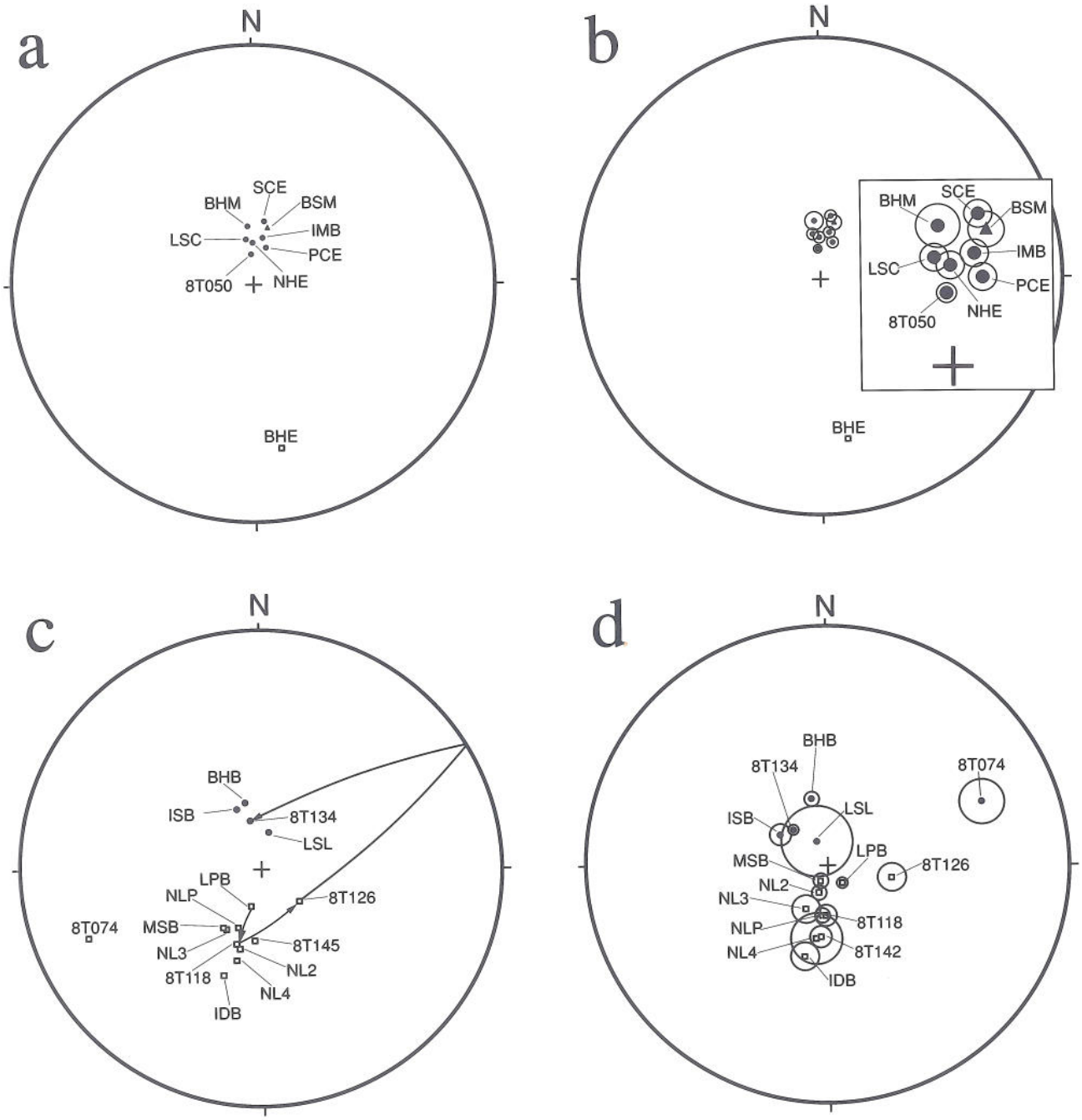

Figure 3. Equal-angle stereographic projection showing the site-mean thermoremanent magnetization direction for the tuff of Blacktail (a and b) and for basalts (c and d) found in Birch Creek Valley. Figures a, b, and d are *in situ* data, whereas c is structurally corrected data. The arrows on c indicate successively higher flows in the same stack of flows. Open circles represent the 95 percent confidence limit; solid circles are lower hemisphere; and open boxes are upper hemisphere directions. Solid triangles in a and b are the unit-means for the tuff of Blacktail sampled from the Ririe Reservoir area in the southern circum-Snake River Plain.

Basin stratigraphy near Lone Pine

The stratigraphic position, radiometric ages, and magnetic polarity of Neogene and Quaternary rocks in Birch Creek Valley is shown in **Figure 2**. We describe the rock units in more detail below.

Medicine Lodge Volcanics

At the base of the Tertiary section, along the western edge of southern Birch Valley, is pebble to cobble conglomerate overlain by altered volcanic and volcaniclastic rocks of intermediate composition (**Figure 1**). An east dipping angular unconformity of about 30° separates these rocks from overlying rocks. Previously mapped as the Medicine Lodge Volcanics, the conglomerate and volcanics are undated but lithologically similar to rocks of the Challis Volcanic Group, suggesting that they are Eocene. The overlying angular unconformity supports the interpretation that these rocks record a basin subsidence event distinct from that recorded by overlying rocks.

Medicine Lodge Limestone

Overlying the volcanic rocks or Paleozoic bedrock are intercalated conglomerate and limestone of the Medicine Lodge Limestone. Limestone is thin to medium bedded, silty, tuffaceous, and rarely fossiliferous with freshwater gastropods, pelycypods, and fish scales. The limestone is thickest in the west-central portion of the study area (**Figure 1**); to the west, north, and east it thins and interfingers with conglomerate. The conglomerate is clast supported, medium bedded to (apparently) massive, and laterally extensive. Along the west side of the modern valley, the conglomerate contains clasts of quartzite, limestone, and rare andesite porphyry. The conglomerate is also present east of the highway in the Blue Dome Spur, but here it is entirely composed of limestone clasts. In the study area, the Medicine Lodge Limestone underlies the 6.5 Ma tuff of Blacktail, and 12.4 miles (20 km) to the south it underlies a 10.3 Ma tuff (Rodgers and Zentner, 1988).

Lone Pine Basalt

The undated Lone Pine Basalt occurs along Highway 28 as a thick sequence of multiple basalt flows, farther to the west as thin single flows that dip gently toward the valley, and along the western edge of the study area as sinuous outcrops (**Figure 1**). Eastward from Highway 28, the thick basalt abruptly thins to zero. We interpret these relations to reflect the basin morphology at the time of eruption: an incised central valley with gently east dipping terraces to the west, and rather steeply dipping terraces to the east. The western terraces were incised by streams from the Lemhi Range, and basalt filled the stream channels to produce a sinuous outcrop pattern.

Paleomagnetic analyses of four flows exposed on a cliff 0.2 mile south of Lone Pine show that these flows have distinct directions of magnetization. The lowest flow (LPB), second flow (8T118), and third flow (8T126) show reversed polarity directions, whereas the 4th or topmost flow (8T134) records a normal polarity (**Figure 3c**). After correcting for tectonic tilts (method described below), each site-mean direction for these flows is statistically distinct from the others (see **Table 1**). If tectonic tilts have been properly removed, the unique site-mean directions may be used to correlate flows in the Lone Pine vicinity. For instance, the second flow (8T118) south of Lone Pine is correlative with the upper of two flows (samples NL2 and NL4) north of Lone Pine, and with a single basalt flow at site 1DB, west of Lone Pine (see **Figure 1** for sample locations, **Table 1** and **Figure 3** for paleomagnetic results). In addition, the uppermost flow (8T134) south of Lone Pine has a normal mean-site direction close to that of single basalt flows at sites 1SB and LSL, located west of Highway 28 (**Figure 1**). The lack of other normal polarity flows in the area around Lone Pine and the overlap of α_{95}'s leads us to conclude that sampling sites 1SB, LSL, and 8T134 are from the same flow. These tentative correlations will require more work to confirm.

Basalts in southern Birch Creek Valley

The Howe Point Basalt (8T074), deposited on Howe Point at the southern tip of the Lemhi Range (see Figure 1, introduction to field trip no. 1), was analyzed for paleomagnetic remanence and radiometrically dated. The whole-rock, $^{40}Ar/^{39}Ar$ age is 9.9 ± 0.7 (L.W. Snee, personal communication) and the basalt lies directly beneath the 6.5 Ma tuff of Blacktail and over the 10.3 ± 0.04 tuff of Arbon Valley (date by F.J. Moye and L.W. Snee, in Kellogg and others, 1989). The stratigraphic position of the Howe Point Basalt suggests that it may correlate with the Lone Pine Basalt, but because the site-mean directions of the two are dissimilar, more work is necessary before such a correlation can be made with confidence.

Table 1. Paleomagnetic results from basalts in Birch Creek Valley.

Sample designation	Location	*in situ*		Structurally corrected		Flow Structure orientation		N[1]	R[2]	k[3]	α_{95}[4]
		Decl.	Incl.	Decl.	Incl.	Strike	Dip				
LPB	Fig. 1	140	-78.8	194	-71	325	15	16	15.95324	321	2.1
8T118	Fig. 1	181.1	-65.4	198	-53	325	15	8	7.94082	118	5.1
8T126	Fig. 1	101.7	-58.8	131	-66	325	15	8	7.89067	64	7.0
8T134	Fig. 1	315.0	67.0	348	67	325	15	8	7.98985	690	2.1
NLP	Fig. 1	185.6	-65.8	201	-60	295	15	7	6.97498	246	3.9
NL2	Fig. 1	195.6	-75.7	195	-51	295	15	7	6.97072	205	4.2
NL3	Fig. 1	205.4	-66.6	210	-57	315	10	7	6.91678	72	7.2
NL4	Fig. 1	188.3	-55.0	195	-46	315	10	4	3.95338	64	11.4
LSL	Fig. 1	337.3	77.9	13	72	325	11	7	6.55186	13	17.1
8T142	SE SBCV[6]	185.3	-56.1	185	-56	0	0	8	7.94418	125	5.0
8T074	Howe Pt.[5]	68.4	20.4	248	-14	325	35	7	6.91141	68	7.4
1SB	Fig. 1	302.1	63.6	339	60	310	20	7	6.96098	154	4.9
1DB	Fig. 1	194.3	-46.5	200	-39	330	9	6	5.95760	118	6.2
MSB	Fig. 1	202.3	-81.7	213	-57	305	25	7	6.97841	278	3.6
BHB	Scott Butte[5]	347.9	57.9	357	52	300	10	10	9.93875	347	57.9

[1] Number of samples collected
[2] Magnetization Vector Sum
[3] Precision Parameter
[4] Radius of circle of 95% confidence
[5] Located on Fig. 1 of Anders and others (1990)
[6] Southeastern southern Birch Creek Valley - near radio tower

Two other basalts in Birch Creek Valley were sampled. The Scott Butte Basalt (sample 8T142, location shown in Figure 1, introduction to field trip no. 1) comprises several flows that are sub-horizontal and tilt 9°NE. Chase (1972) obtained a K-Ar whole-rock age of 5.4 ± 0.8 for this basalt, which compares well with the basalt's stratigraphic position above the 6.5 Ma tuff of Blacktail. Another basalt (sample BHB, located near a radio tower just south of Scott Butte) is older than 730 ka due to its reversed polarity, and is likely Quaternary owing to its stratigraphic position above Pleistocene conglomerate and its lack of measurable tectonic tilt.

Tuff of Blacktail

The tuff of Blacktail is a crystal-rich ash-flow tuff that erupted on the Snake River Plain 6.5 Ma (Morgan and others, 1984). The age of the tuff of Blacktail is assumed to be 6.5 Ma based on numerous isotopic dates (Morgan and others, 1984; Anders and others, 1989). An older date of 6.7 Ma (Kellogg and Marvin, 1988) is not used because it is not in agreement with the Harland and others (1982) polarity time scale. The unit is the result of a catastrophic eruption on the eastern Snake River Plain that covered an area over 8 X 10^3 miles^2 (2 X 10^4 km^2) with ash-flow tuff. The tuff of Blacktail is present in southern Birch Creek Valley and in southernmost northern Birch Creek Valley.

Near Lone Pine, the tuff of Blacktail is typically a thin (less than .3 ft/1 m), extensive rhyolite tuff overlying the Lone Pine Basalt. Along the western edge of the study area, its thickness locally increases to as much as 6 feet (20 m) and it overlies the Medicine Lodge Limestone, which we believe reflects preservation in incised stream channels.

Pliocene-Pleistocene conglomerate

Near Lone Pine, conglomerate (map unit TQol) overlies the tuff of Blacktail, Lone Pine Basalt, and locally the Medicine Lodge Limestone. The conglomerate is similar to conglomerate of the Medicine Lodge Limestone but can be distinguished by its stratigraphic position and by clasts of basalt and rhyolite tuff. Scott (1982) assigned a Pliocene to early Pleistocene age to this unit. The conglomerate forms thin to thick, extensive sheets between Highway 28 and the Lemhi Range to the west. Abrupt thickness changes are not evident, and the lower contact of the unit appears relatively planar. This suggests that emplacement of the underlying volcanic rocks effectively filled the previously

incised stream channels, and that little dissection occurred between the time of volcanism and deposition of the conglomerate.

North of Lone Pine in northern Birch Creek Valley, the conglomerate underlies a large fan complex that dominates the western side of the valley. On the eastern side of the valley it is generally buried, except in deeply incised canyons near the Beaverhead range front, where it is observed beneath younger alluvium.

North of Birch Creek Valley, the conglomerate is exposed extensively along the eastern side of the Lemhi Valley.

Pleistocene conglomerate

In southern Birch Creek Valley, the Pliocene to early Pleistocene conglomerate is overlain in angular unconformity by another conglomerate (map unit Qol). Scott (1982) assigned it a middle to late Pleistocene age. This unit is extensively exposed on both sides of southern Birch Creek Valley, where it forms terraces 10 to 40 feet (10-40 m) below the top of map unit TQol; it is exposed east of Blue Dome Spur (**Figure 1**), where it underlies a triangular basin between Blue Dome Spur and the Beaverhead Mountains.

Pleistocene-Holocene conglomerate

The youngest map unit in **Figure 1** is latest Quaternary (< 15 ka) alluvium, which underlies the modern Birch Creek floodplain (map unit Qal). The floodplain is incised as much as 82 feet (25 m) into Pleistocene conglomerate.

Basin structure near Lone Pine

The technique used to assess tectonic tilt of volcanic rocks is discussed in detail in Anders and others (1989). In brief, volcanic rocks are assumed to have an initial uniform magnetization at the time of cooling. To determine tectonic tilt, we determine the thermoremanent magnetization (TRM) direction at undeformed locations and then assess the angular divergence between the TRM directions at these localities and at the deformed sites. The use of paleomagnetic techniques is necessary because eutaxitic structures in ash-flow tuffs often do not faithfully record the original horizontal. The results of the paleomagnetic analysis of the tuff of Blacktail are shown in **Figure 3a** and **b** and summarized in **Table 2**. The main carrier of remanence is

Table 2. Paleomagnetic results from the tuff of Blacktail in Birch Creek Valley

Sample designation	Location	*in situ* Decl.	*in situ* Incl.	N[1]	R	k	α_{95}	Tectonic tilt
SCE	Fig. 1	10.3	60.0	17	16.87202	125	3.2	4 ± 4.3
PCE[3]	Pass Creek[3]	20.5	71.4	14	13.88766	116	2.9	9 ± 4.1
1MB	Fig. 1	12.1	67.9	9	8.97190	285	3.1	5 ± 4.2
BHM	Scott Butte[4]	355.6	62.8	12	11.88536	96	4.5	9 ± 5.3
LSC	Fig. 1	351.4	68.7	14	13.93487	200	2.8	12 ± 4.0
8T050	Howe Pt.[4]	355.9	76.0	11	10.98184	551	2.0	14 ± 3.5
NHE	N. Howe Pt.[5]	359.9	70.4	15	14.89391	132	3.3	9 ± 4.3
BHE[1]	INEL[6]	171.1	-20	13	12.61658	31	7.5	95 ± 8.0
BSM	Blacktail Res.[2]	16.0	63.5	25	24.76946	104	2.9	-

[1] Unit designation unknown - most likely not tuft at Blacktail
[2] Site mean for tuff of Blacktail at Ririe Reservoir (See Anders and others, 1989)
[3] Located on Pass Creek about 5 km south of site SCE in Fig. 1
[4] Location on Fig. 1 in Anders and others (1990, this volume)
[5] Located in Kyle Canyon 7 km north of Howe Point in Fig. 1 Anders and others (1990, this volume)
[6] Located 10 km south of Scott Butte about 100 m from northernmost boundary of the Idaho National Engineering Laboratory

magnetite, with less than 1 percent hematite present in most samples. The α_{95} values for the tuff of Blacktail are typically between 3° and 4°, indicating they are excellent for assessing tectonic tilt (for a further discussion of the magnetic properties of the tuff of Blacktail, see Anders and others, 1989).

Neogene rocks near Lone Pine (map units Tmc/Tml, Tb, Tt, and TQol) are separated everywhere by disconformities, suggesting that no significant tilting of the Neogene section occurred until after they accumulated. Presently, all Neogene rocks in the region dip to the east or northeast (**Figure 1**). Measured dips on bedding in conglomerate and limestone, and on foliation in basalt, are typically 5° to 15° and in places as much as 25°. We interpret the tilting of units to uniform eastward dips to be due to half-graben faulting, with major offset along the Beaverhead fault and minor offset along other faults within the valley (**Figure 1**).

The Beaverhead fault, located along the eastern edge of Birch Creek Valley, has accommodated the most offset. East of the Blue Dome Spur, the southern portion of the Nicholia segment cuts middle- to late-Pleistocene conglomerate (map unit Qol). Using the cross sections of Garmezy (1981), we estimate the fault has accommodated approximately 1.5 miles (2.5 km) of slip.

East and west of Highway 28 in the Lone Pine vicinity (**Figure 1**), WNW- to NW-striking normal faults offset Neogene rocks. The faults are particularly evident at the north end of Blue Dome Spur, where the Lone Pine Basalt is progressively downdropped to the southwest. The dip of NW-striking faults is poorly constrained, but assumed to be about 50° by comparison to other Basin and Range faults in east central Idaho. Maximum offset along each fault is small, about 164 to 1,150 feet (50-350 m).

Basin evolution

Lone Pine vicinity

At some time before 10.3 Ma, the Medicine Lodge Limestone was deposited in a basin characterized by internal drainage. The distribution of coeval conglomerate and limestone indicates that during deposition the Lemhi Range and Beaverhead Mountains were uplifted. Whether the boundaries of the basin corresponded to modern basin boundaries or extended farther east and west is unclear. For example, it is possible that deposits of the Medicine Lodge Limestone extended farther to the west on what is now the Lemhi Range. Subsequent northeast tilting of the Lemhi Range could have tilted the limestone to its present 10°E dip, thus uplifting and allowing erosion of the limestone originally deposited to the west. Presently, there is not enough evidence for us to suggest the modern distribution of the Medicine Lodge Limestone defines the original geographic boundaries of Birch Creek Valley. Careful basin analysis, involving a study of facies changes in the basin and/or documentation of slide blocks or other gravity-driven events, is needed.

Emplacement of the Lone Pine Basalt and the 6.5 Ma tuff of Blacktail filled stream incisions that were several tens of feet (tens of m) deep into the Medicine Lodge Limestone. The thickest accumulation of basalt is about 2 miles (3 km) west of limestone of the Medicine Lodge Limestone, indicating a westward shift in the basin depocenter. The location of the inferred stream channels is similar to their location today, suggesting that, at this locality, the modern drainage system of the Lemhi Range was established more than 6 million years ago. Extensive dissection of the Medicine Lodge Limestone may reflect uplift of the valley, or, more likely, external drainage of the valley to a lower base level.

The tuff of Blacktail erupted from a vent about 30 miles (50 km) south of the study area (Morgan and others, 1984; Hackett and Morgan, 1988). Now covered by several miles (km) of basalt, this locality at the time of eruption may have been a rhyolite plateau like the modern Yellowstone Plateau. We envision that, like the modern Yellowstone system, a north flowing river drained the ancient plateau and flowed through Birch Creek Valley. We need to test this hypothesis by finding and measuring paleocurrents in late Miocene gravels. We propose, but have not yet proved, that the change from internal to external drainage in Birch Creek Valley was influenced by northward tilting of the valley due to uplift on the Snake River Plain.

After deposition of Pliocene to lower Pleistocene conglomerate, the basin fill near Lone Pine was tilted 10° to 15°E to NE. Tilting presumably resulted from movement along west dipping normal faults, especially the Nicholia segment of the Beaverhead fault.

In the Lone Pine region, two segments of the Beaverhead fault are distributed en echelon. The Nicholia segment is exposed to the northeast, and the

Blue Dome segment is concealed beneath Quaternary gravels to the southeast. We attribute three unusual geologic features of the Lone Pine vicinity to en echelon faulting. First, in contrast to the N10°W strike of the Nicholia fault, minor normal faults in Blue Dome Spur strike about N60°W (**Figure 1**). The direction of extension and tilting evident in Blue Dome Spur is compatible with a block between right-stepping en echelon normal faults. Second, the amount of tectonic tilting near Lone Pine is relatively small. At 15 sites north of the Snake River Plain, tectonic tilts of the tuff of Blacktail are typically between 9° and 15°NE, whereas from south to north in Birch Creek Valley, the tectonic tilt is 9°±4°, 5°±4°, 4°±4°, and 12°±4° (sites BHM, 1MB, SCE, and LSC, respectively). Tilts of 5° and 4° are from the region of en echelon overlap. Third, the Lone Pine area contains relatively small volumes of Quaternary rocks. Neogene rocks are exposed in the Lone Pine vicinity, whereas to the north and south, Quaternary gravels are commonly exposed. East of Blue Dome Spur (**Figure 1**), a well drilled in the center of a triangular Quaternary basin encountered only 148 feet (45 m) of conglomerate above Paleozoic bedrock, even though the basin is bounded by the active Nicholia segment of the Beaverhead fault. The paucity of Quaternary gravels could be due to partitioning of extension on the two en echelon segments of the Beaverhead fault. The cumulative extension is the same as along single fault segments, but the area available for sediment fill is less. As described by Leeder and Gawthorpe (1987), all of these features are common near en echelon normal faults.

Birch Creek Valley

As discussed above, the style and timing of normal faulting can be interpreted from the tilting history of the basin fill. The absence in northern Birch Creek Valley of many of the units present in southern Birch Creek Valley strongly argues for a difference in the timing of faulting and subsidence between the southern and northern Birch Creek Valley. In northern Birch Creek Valley, only latest Pliocene to Holocene gravels and conglomerates are exposed. We suggest that this is due to significant Quaternary subsidence of the basin. This is most clearly shown by the relative position of the Pliocene to early Pleistocene conglomerate (TQol), which crops out about 1,000 feet (300 m) higher on the west side of the valley than the east side. In addition, thick ash deposits (called Middle Ridge) of the tuff of Blacktail in the middle of Lemhi Valley and ash-flow deposits of the tuff of Blacktail near Lone Pine indicate that this unit was once deposited in the intervening northern Birch Creek Valley but has either been eroded or buried due to subsidence in the valley. If a latest Quaternary (<15 ka) displacement rate of over .04 inch (1 mm)/yr persisted through the Quaternary, .6 mile (1 km) or more displacement could be easily achieved on the Beaverhead fault, which in turn would lead to burial of the tuff of Blacktail.

In southern Birch Creek Valley, more units of different ages are exposed, permitting better temporal control on basin subsidence. Near Lone Pine, the 6.5 Ma tuff of Blacktail and the older Lone Pine Basalt were tilted together sometime after deposition of the tuff of Blacktail. This interpretation is based on the lack of an angular unconformity between the basalt and the tuff of Blacktail and the close agreement between the tectonic tilt of the tuff of Blacktail (12°±4°) and the dip of the basalt (11°) (sites LSC and LSL in **Figure 1**). South of Lone Pine in the central portion of southern Birch Creek Valley, tandem tilting of late Miocene units is also seen at Scott Butte where the tectonic tilt of the tuff of Blacktail (9°±5°) matches that of a 5.4 Ma basalt (10°) (samples BHM and BHB, **Tables 1** and **2**). Tandem tilting of these units implies movement on the Beaverhead fault occurred after deposition of the youngest of these units. This constrains the time of tilting to between about 5.4 and 1.6 Ma. Once the age of the untilted Radio Tower Basalt is determined, a better estimate of the age of cessation of faulting in central portions of the valley can be made.

At Kyle Canyon, 3 miles (5 km) north of Howe Point in the Lemhi Range, tectonic tilts determined from the tuff of Blacktail (sample NHE, **Table 2**) are 9°±4°NE, evidence that the Miocene tilting history is the same as farther to the north. Farther south at Howe Point, a 14°±4°NE tectonic tilt was measured on the tuff of Blacktail (sample 8T050, **Table 2**), and a 35°NE tilt was measured on the intermediate direction Howe Point Basalt (sample 8T074, **Table 1**). These data suggest initial tilting at Howe Point occurred before emplacement of the 6.5 Ma tuff of Blacktail.

If the ages and patterns of tectonic tilting discussed above are correct, we have recognized a gradual northward shift in the initiation of tilting in southern Birch Creek Valley. This northeastward migration started before 6.5 Ma at Howe Point, after 5.4 Ma in the central portion of the basin, and sometime between the Pliocene and the early Pleistocene (our preferred guess is between 3 to 4 m.y.) near Lone Pine. Initial tilting in the central basin and near Lone Pine could be the same age because there is no TQol alluvium exposed in the central portion of southern Birch Creek Valley.

A northeastward migration of fault cessation, similar to the northeastward migration of initial tilt-

ing, is evident. This is clearly seen in the middle to late Pleistocene alluvium that is not offset by the Beaverhead fault south of Lone Pine but is offset by the fault north of Lone Pine. This pattern of fault cessation for the Beaverhead fault, as well as the Lost River and Lemhi faults, is discussed by Scott and others (1985) and Pierce and others (1988).

Basin evolution north and south of the Snake River Plain

North and south of the Snake River Plain, distinct differences in the style of faulting and remarkable similarities in the age progression of faulting are evident. South of the Snake River Plain, seismic reflection transects across several basins clearly show listric fault patterns. In Swan, Grand, and Star Valleys, tectonic tilts determined by paleomagnetic study of the tuff of Blacktail vary from 2° to 32° and appear to decrease exponentially as a function of distance away from the fault trace, as would be expected from a listric fault (Anders and others, 1989).

Basins north of the Snake River Plain have almost no published seismic profiles that can delineate fault geometry. However, aftershocks from the 1983 Ms = 7.3 earthquake showed that the Lost River fault is a planar fault surface down to 9 miles (15 km) (Richins and others, 1987). Our data supports interpretation of a planar fault geometry, in which the faults and fault blocks tilt domino-style to the east as suggested by Scott and others (1985) and Anders and others (1988). Paleomagnetic analyses of the tuff of Blacktail from the Beaverhead Mountains and the Lemhi and Lost River Ranges display an average northeast tilt of 10°, with a range of 9° to 15° (Anders and others, 1988). The variation in tilt amounts is less north of the Snake River Plain than south of it, and no east-west pattern of progressively smaller tilts is evident, suggesting that the Beaverhead Mountains and Lost River and Lemhi Ranges are uniformly tilted to the northeast.

As discussed above, in Birch Creek Valley there was a northward migrating pattern of incipient basin development followed by a northward-migrating pattern of fault cessation. Scott and others (1985) and Pierce and others (1988) have described this pattern of faulting throughout the northern circum-Snake River Plain. Similarly, south of the Snake River Plain in Swan, Grand, and Star Valleys, the age of faulting decreases away from the Snake River Plain. As discussed in Anders (this field trip, part 2), rapid extension and concomitant basin subsidence in Swan Valley started between 4.0 and 4.4 Ma and essentially stopped before 2 Ma. Farther to the south, Star Valley has been active during the latest Quaternary. The outward migration of fault activity in the circum-Snake River Plain is believed to be caused by migration of the Yellowstone hot spot, as discussed in detail in Anders and others (1989).

Road log and stop descriptions

From the Westbank Motel in Idaho Falls, drive west on Broadway Street to U.S. Interstate 15. Travel north on Interstate 15 for about 23 miles to exit 143, the interchange with State Highway 28 and 33. Leave the interstate and travel west (toward Salmon) on Highway 28 for about 30 miles to the intersection with State Highway 22. The road log is keyed to highway mileposts.

Milepost

30 Intersection of State Highways 28 and 22. This is the southern end of Birch Creek Valley, where it meets the Snake River Plain. To the west is the Lemhi Range, an east tilted fault block underlain by Proterozoic to Permian shelf strata. Howe Point, the southern tip of the Lemhi Range, is underlain by Neogene sedimentary and volcanic rocks (Kuntz and others, 1984; Morgan and others, 1984; Rodgers and Zentner, 1988) that record progressive east tilting from 10 to 4 Ma and uplift since that time. To the east is the southern Beaverhead Mountains, another east tilted fault block underlain by Proterozoic and Paleozoic shelf strata and Neogene rocks (Kuntz and others, 1984; Garmezy, 1981; Rodgers and Zentner, 1988). Continue north on Highway 28.

33 Just east of the highway is an outcrop of an undated ash-flow tuff. It is petrologically similar to both the tuff of Blue Creek and the tuff of Blacktail, but the results of our paleomagnetic analysis indicate that it is neither unit. In **Table 2,** this unit is listed as sample BHE and has an unusual shallow reversed inclination unlike any unit sampled in the circum-Snake River Plain.

34-35 The low hills to the east are underlain by basalt. The basalt flow located near the radio tower is sample 8T142 in **Table 1**. This unit's untilted position on valley-floor alluvium indicates it is probably a Quaternary basalt. Its age is further restricted to greater than 730 ka because the unit has reversed polarity. North of the radio tower, there are three buttes that are each capped by several flows. The largest butte is Scott Butte, whose basalt cap has been dated at 5.4 ± 0.8 Ma (Chase, 1972). Paleomagnetic analysis of one of the middle flows indicates a normal polarity (sample BHB, **Table 1**). The smaller butte to the south has been extensively trenched by prospectors. The trenching has exposed the tuff of Blacktail capped by reworked ashes, probably tuff of Blacktail ash. Paleomagnetic analysis of this tuff (sample BHM, **Table 2**) indicates it has tilted 9°. The dip on the capping basalt is 10,° indicating that tilting occurred after emplacement of the 5.4 Ma basalt.

43.0 For the next several miles, Birch Creek is located along the eastern edge of the valley, and is incised up to 82 feet (25 m) through middle Pleistocene alluvium. Scott (1982) suggested late Pleistocene to Holocene uplift of this region has occurred.

46.0 About one-half mile north of this mile marker, turn west on a gravel road numbered 181 by the Bureau of Land Management. Turn sharply north on another gravel road 1.8 miles west of the highway, cross a shallow irrigation ditch, continue up the small hill, and drive north. After driving 1.4 miles north along this road, follow the road as it turns west and drops to a lower elevation. The road forks here. Maintain a straight westerly course up the alluvial terrace. After driving west up the terrace 2.8 miles past the fork, stop and park at the crest before the road descends a hill. To the northwest is a basalt cliff that is Stop 6.

Stop 6. Birch Creek Valley overview

Located on the western edge of Birch Creek Valley, Stop 6 is a good locality for viewing the entire basin, lower Neogene units, and evidence for a normal fault. Walk northwest to the basalt cliff, and follow the base of the cliff northwest to the crest of the hill. Here, the basalt is underlain by Medicine Lodge Limestone, which to the west is in contact with a second basalt. The two basalt outcrops are believed to be the same unit, separated by a normal fault (refer to **Figure 1**).

The basalt units are tilted about 20°NE. After correcting for the tilt, the mean-site paleomagnetic remanence direction is correlative with a basalt flow near Highway 28 that caps the cliffs just south of Lone Pine (see **Figure 1**, sample site 8T134). This suggests that the flows around Lone Pine have dropped about 1,640 feet (500 m) relative to the flow at this locality. The distinct pattern of TRM directions exhibited by the Lone Pine Basalt flows makes them an excellent tool in reconstructing the Neogene tectonic history of Birch Creek Valley.

For an overview of Birch Creek Valley, walk a short distance east to the top of the eastern basalt cliff. To the west from here, the rolling hills are underlain by gently (15°) east dipping conglomerate of the Medicine Lodge Limestone. Along the range front are scattered outcrops of the Eocene (?) conglomerate, which underlie the Medicine Lodge Limestone and are distinguished by moderate (55°) east dips and high degree of cementing. To the east in the foreground, the drainage is underlain by limestone of the Medicine Lodge Limestone along its north side and Pliocene to early Pleistocene conglomerate (map unit TQol) along its south side. Farther east, basalt-capped hills are evident. In the distance across Highway 28, the rolling hills are Medicine Lodge Limestone gravels capped by basalt and offset along northwest striking normal faults (see **Figure 1**).

From the top of the eastern basalt, walk southeast to return to the parking spot. Patches of conglomerate (map unit TQol) are present, but at this locality the tuff of Blacktail is absent.

Return to Highway 28 following the same route as before and turn north on to the highway.

47.5 On the east side of the road, just north of an abandoned farm house, are four basalt flows tilting 15°NE. Paleomagnetic analyses of these flows showed that they record a magnetic reversal between the reversed lowermost three flows (LPB, 8T118 and 8T126) and the normal polarity of the topmost flow (8T134). Figure 3c shows progressively higher flows in the stack. This unusual pattern of site-means permits correlation of the limited number of basalt flows in Birch Creek Valley. Pressure ridges exposed on the bottom of the uppermost flow at this site constrain the direction of flow to northeast-southwest, which is transverse to the expected up-valley flow direction from the Snake River Plain.

51.0 A cliff of basalt east of the highway exposes two flows of the Lone Pine Basalt. Paleomagnetic analysis of these flows suggest that they are equivalent to the flows near the abandoned farm south of Lone Pine. The highest normal polarity flow has not been found at this location, but further work may locate it.

51.9 A few yards north of the county border, just beyond a gravel pit, turn west onto a gravel road, go through the gate and drive west. Drive 0.3 miles from the highway and take the left fork; at 1.1 miles beyond the highway take the left fork and drive south; at 1.4 miles stay right; at 1.7 miles the road turns west and downhill. At 2.2 miles take the left fork, and at about 3.3 miles the road ends at several prospect pits. Stop and park.

Stop 7. Tilted Neogene sediments with interbedded volcanic rocks

Walk a short distance to the prospect pits. At this stop, located about 4 miles north of Stop 6, the Neogene stratigraphy includes conglomerate of the Medicine Lodge Limestone, the Lone Pine Basalt, the tuff of Blacktail, and the upper conglomerate. The lower conglomerate forms an extensive, rather thin sheet that rests directly on Paleozoic basement. The tuff of Blacktail is exposed in the prospect pit, and the Lone Pine Basalt underlies the gently east dipping hill to the south. These rocks, like those at Stop 6, lie in the westernmost fault block in the valley.

Paleomagnetic analysis of the tuff of Blacktail at this location indicates the unit is tilted 12°±4° NE. This tilt is slightly steeper than the eutaxitic foliation, indicating that the tuff was deposited on a slightly west dipping counter slope. The basalt across the small ravine to the south is correlative with the highest flow south of Lone Pine and the basalt at Stop 6. The dip of the basalt is 11° NE, which agrees well with the 12°±4° tectonic tilt of the tuff of Blacktail.

Return to Highway 28 and travel north and then east to Nicholia, Several magnificent fault scarps along the range front of the Beaverhead Mountains are described in Haller (this field trip, part 4)

References cited

Anders, M.H., Geissman, J.W., Piety, L.A., and Sullivan, J.T., 1989, Parabolic distribution of circumeastern Snake River Plain seismicity and latest Quaternary faulting: migratory pattern and association with the Yellowstone hotspot: Journal of Geophysical Research, v. 94, no. B2, p. 1589-1621.

Anders, M.H., Hagstrum, J.T., and Rodgers, D.W., 1988, Late Cenozoic structural development of the southern Beaverhead and Lemhi Ranges, Idaho: Geological Society of America Abstracts with Programs, v. 20, n. 7, p. A63.

Armstrong, R.L., Harakal, J.E., and Neill, W.M., 1980, K-Ar dating of Snake River Plain (Idaho) volcanic rocks—new results: Isochron West, v. 27, p. 5-10.

Armstrong, R.L., Leeman, W.P., and Malde, H.E., 1975, K-Ar dating, Quaternary and Neogene volcanic rocks of the Snake River Plain, Idaho: American Journal of Science, v. 275, p. 225-251.

Chase, G.H., 1972, Potassium-argon ages from whole-rock analyses of igneous rocks in the area of the National Reactor Testing Station: U. S. Geological Survey Professional Paper 800-D, p. D123-D126.

Garmezy, L., 1981, Geology and tectonic evolution of the southern Beaverhead Range, east-central Idaho: M.S. thesis, Pennsylvania State University, 155 p.

Hackett, W.R. and Morgan, L.A., 1988, Explosive basaltic and rhyolitic volcanism of the eastern Snake River Plain, Idaho: Guidebook to the geology of central and southern Idaho: Idaho Geological Survey Bulletin 27, p. 283-301.

Harland, W.B., Cox, A., Llewellyn, P.G., Pickton, C.A.G., Smith, A.G., and Walters, R., 1982, A geologic time scale: Cambridge University Press, Cambridge, England, 131 p.

Kellogg, K.S., and Marvin, R.F., 1988, New potassium-argon ages, geochemistry, and tectonic setting of upper Cenozoic volcanic rocks near Blackfoot, Idaho: U.S. Geological Survey Bulletin 1806, p. 19.

Kellogg, K.S., Pierce, K.L., Mehnert, H.H., Hackett, W.R., Rodgers, D.W., and Hladky, F.R., 1989, New ages on biotite-bearing tuffs of the eastern Snake River Plain, Idaho: stratigraphic and mantle-plume implications: Geological Society of America Abstracts with Programs, v. 21, no. 5, p. 101.

Kuntz, M.A., Skipp, Betty, Scott, W.E., and Page, W.R., 1984, Preliminary geologic map of the Idaho National Engineering Laboratory and adjoining areas, Idaho: U.S. Geological Survey Open File Report 84-281, scale 1:100,000.

Leeder, M.R., and Gawthorpe, R.L., 1987, Sedimentary models for extensional tilt-block/half graben basins; *in* Coward, M.P., Dewey, J.F., and Hancock, P.L., editors, Continental extensional tectonics: Geological Society of London Special Publication 28, p. 139-152.

McBroome, L.A., 1981, Stratigraphy and origin of Neogene ash-flow tuffs on the north-central margin of the eastern Snake River Plain, Idaho: M.S. thesis, University of Colorado, Boulder, 74 p.

Morgan, L.A., Doherty, D.J., and Leeman, W.P.,1984, Ignimbrites of the eastern Snake River Plain: evidence for major caldera-forming eruptions: Journal of Geophysical Research, v. 89, p. 8665-8678.

Morgan, L.A., and Hackett, W.R., 1989, Explosive basaltic and rhyolitic volcanism of the eastern Snake River Plain: *in* Ruebelmann, K.L., editor, Field Trip Guidebook T305, Jackson, Wyoming to Boise, Idaho, July 21-29, 1989, 28th International Geological Congress,Washington, D.C., 1989, p. 39-46.

Pierce, K.L., Scott, W.E., and Morgan, L.A., 1988, Eastern Snake River Plain neotectonics—faulting in the last 15 Ma migrates along and outward from Yellowstone "hotspot" track: Geological Society of America Abstracts with Programs, v. 20, p. 463.

Richins, R.D., Pechmann, J.C., Smith, R.B., Langer, C.J., Goter, S.K., Zwollweg, J.E., and King, J.J., 1987, The 1983 Borah Peak, Idaho earthquake and its aftershocks: Bulletin of the Seismological Society of America, v. 77, no. 3, p. 694-723.

Rodgers, D.W., and Zentner, N.C., 1988, Fault geometries along the northern margin of the eastern Snake River Plain, Idaho: Geological Society of America Abstracts with Programs, v. 20, no. 6, p. 465.

Scott, W.E., 1982, Surficial geologic map of the eastern Snake River Plain and adjacent areas, 111° to 115°W, Idaho and Wyoming: U.S. Geological Survey Miscellaneous Investigations Map I-1372, scale 1:250,000.

Scott, W.E., Pierce, K.L., and Hait, M.H., Jr., 1985, Quaternary tectonic setting of the 1983 Borah Peak earthquake, central Idaho: Bulletin of the Seismological Society of America, v. 75, n. 4, p. 1053-1066.

Field trip no. 1, part 4

LATE QUATERNARY MOVEMENT ON BASIN-BOUNDING NORMAL FAULTS NORTH OF THE SNAKE RIVER PLAIN, EAST-CENTRAL IDAHO

Kathleen M. Haller
U.S. Geological Survey
Denver, Colorado 80225

Trip summary (see Figure 1, Introduction to field trip no. 1)

Stop 8. Cedar Gulch graben
Stop 9. Cliff Canyon graben

Regional overview

Three major basin-bounding normal faults of the northeastern Basin and Range province, the Lost River, Lemhi, and Beaverhead faults, are characterized by scarps on alluvium along much of their length and have impressive similarities in geometry and timing of late Quaternary faulting. The following discussion reviews the temporal and spatial distribution of late Quaternary surface faulting north of the Snake River Plain and provides a regional perspective for the last two stops of this field trip, which will be on the Nicholia segment of the Beaverhead fault.

The Lost River, Lemhi, and Beaverhead faults, which bound the southwest sides of the ranges bearing the same name (**Figure 1**), are between 88 and 93 miles (140 and 150 km) long; each fault has six segments that have distinct faulting histories. These faults have characteristics that are common to one another as well as other major faults in the Basin and Range province (Machette and others, 1987). The timing of the youngest events, determined on the basis of scarp morphology, is generally Holocene on the middle segments of the faults and older on the end segments. Late Quaternary recurrence intervals appear to be shorter on middle segments than the segments on the ends, which appear to be less active. The relative late Quaternary slip rates are probably high on the middle of the faults and low on the ends of the faults, as indicated by range-front morphology and the overall form of the range.

The Lost River, Lemhi, and Beaverhead faults strike generally NNW-SSE, a strike which is nearly perpendicular to the trend of the Snake River Plain to the south. Relative timing of faulting with respect to proximity to the Snake River Plain is similar to that on faults south of the Snake River Plain; faulting on parts of these faults nearest the Snake River Plain is older than that farther from the plain. The southern parts of the faults have been inactive for the past 30,000 years (Malde, 1985; 1987; Pierce, 1985; Haller, 1988), whereas the central parts have been active during the Holocene (Schwartz and Crone, 1988; Haller, 1988). The northernmost parts of these faults have not had any surface faulting in the past 30,000 years (Scott and others, 1985). However, distinct differences are apparent in the age distribution of late Quaternary faulting on either side of the Snake River Plain. Faulting on parts of the Lost River, Lemhi, and Beaverhead faults proximal to the Snake River Plain is probably younger and late Pleistocene faulting does not extend as far from the plain as similar-age faulting does south of the plain (Pierce and others, 1988).

Fault segmentation

The 1983 M_s = 7.3 Borah Peak earthquake clearly demonstrated that the Lost River is a segmented fault zone (Crone and others, 1985; 1987); that is, only a part of the fault zone ruptures during a large-magnitude earthquake (Swan and others, 1980; Schwartz and Coppersmith, 1984). Although there is abundant evidence of geologically young surface faulting in the region, historically this part of the northeastern Basin and Range province has been generally aseismic with the exception of the Borah Peak earthquake (**Figure 1**)

and its aftershocks (Dewey, 1985). Because of the detailed information from numerous geologic and geophysical studies conducted following this earthquake, we are able to better characterize the coseismic behavior of the Lost River fault as well as other faults in this area.

The ability to identify prehistorically active fault segments, and thereby the parts of a fault that will behave at least somewhat independently during a large-magnitude earthquake, is crucial to evaluating seismic hazards and estimating the maximum-magnitude earthquake expected on a given part of a fault. In an area such as central Idaho, where surface faulting is infrequent, many suitable parameters for estimating earthquake magnitude by existing statistical relations, such as surface-rupture length and surface-fault displacement (Bonilla and others, 1984), are obscured by time. Similarly, in areas where seismicity is sparse, little is known about the nature of the fault at depth; thus, the maximum expected rupture area (Wyss, 1979) is difficult to estimate. Segments can be defined on the basis of the timing of faulting, which can be estimated from the morphology of late Quaternary fault scarps

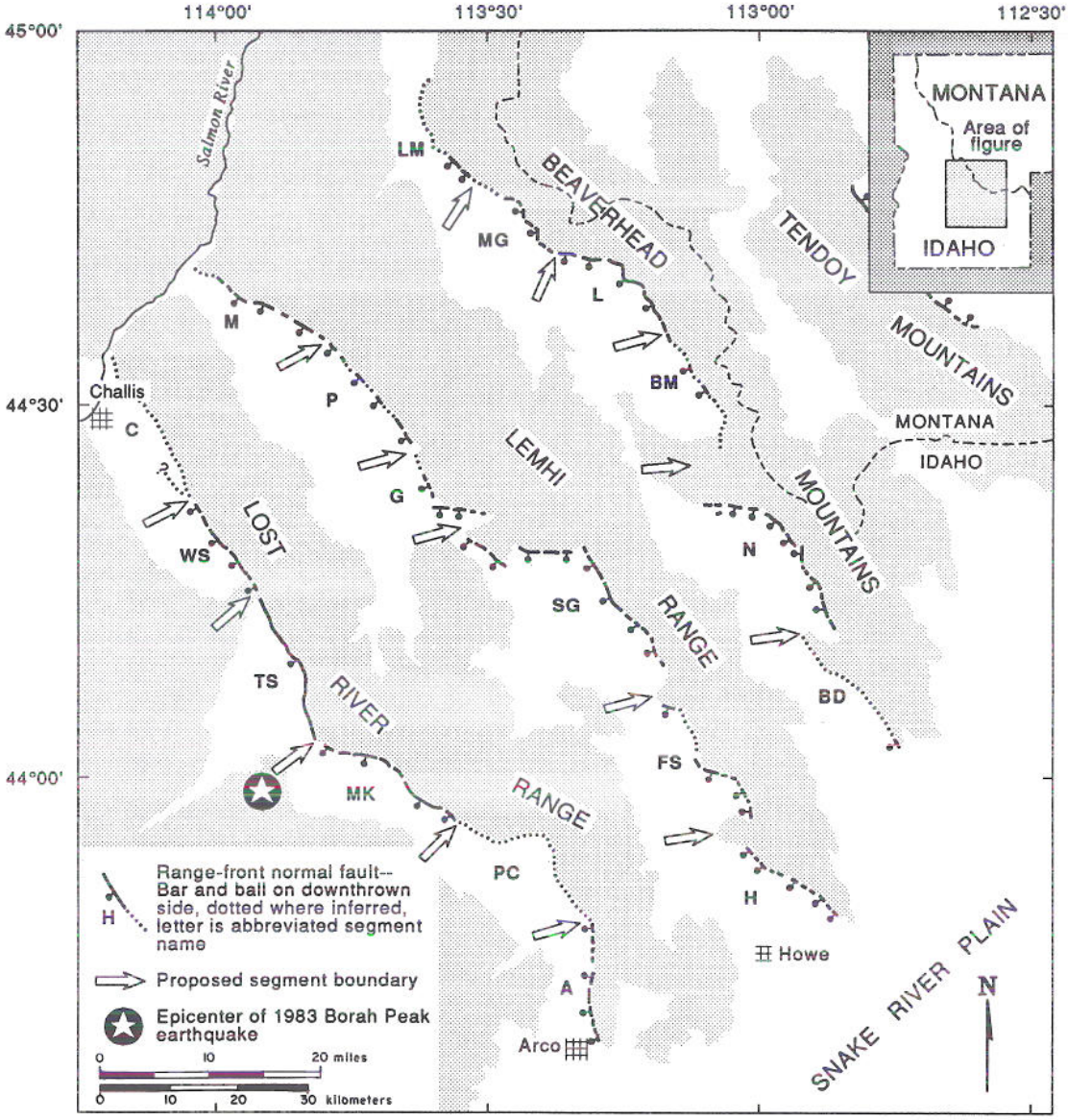

Figure 1. Map showing proposed segments of basin-bounding normal faults in northeastern Basin and Range province, north of the Snake River Plain. Segments on the Lost River fault are: C = Challis; WS = Warm Spring; TS = Thousand Springs; MK = Mackay; PC = Pass Creek; and A = Arco. Segments on the Lemhi fault are: M = May; P = Patterson; G = Goldburg; SG = Sawmill Gulch; FS = Fallert Springs; and H = Howe. Segments on the Beaverhead fault are: LM = Lemhi; MG = Mollie Gulch; L = Leadore; BM = Baldy Mountain; N = Nicholia; and BD = Blue Dome. Mountainous areas are stippled.

and range-front morphology. Thus, segment length can be used as a proxy for surface-rupture length (Crone and others, 1987); however, segment length may underestimate surface-rupture length because small scarps near the ends of the segment may be completely removed from the geologic record within a short time.

Segmentation of the Lost River fault and the Borah Peak earthquake

Fault-scarp morphology, range-front morphology, and structural relief all help to define the probable late Quaternary segmentation of the Lost River fault (Scott and others, 1985; Crone and others, 1987). This fault has six segments (**Figure 1**), which range from 11 to 18 miles (18 to 29 km) long, and each has distinct histories of faulting. The exact timing of faulting on the northernmost (Challis) segment and the two southern (Arco and Pass Creek) segments is poorly constrained, but deposits thought to be about 15,000 years old (Pierce and Scott, 1982) are not displaced. It is possible that faulting may not have occurred in the past 30,000 years on these segments (Pierce, 1985; Scott and others, 1985). In contrast, the three central segments of the Lost River fault are characterized by scarps on late Pleistocene alluvium, and recent trenching studies indicate that all three of these segments have ruptured at least once during the Holocene (Schwartz and Crone, 1985; 1988).

The coseismic behavior of the Lost River fault during the Borah Peak earthquake clearly demonstrates how a segmented fault ruptures and how the distribution of similar-age scarps can be used to define the segmentation of a fault. The Borah Peak earthquake was near the southern end of the Thousand Springs segment (**Figure 1**), and a 23-mile-long (36-km) surface rupture propagated unilaterally to the north along the Lost River fault (Crone and others, 1985; 1987). The most continuous and highest scarps, with a maximum displacement of 8.9 feet (2.7 m), formed on the Thousand Springs segment; smaller, less continuous scarps formed on the Warm Spring segment to the north (**Figure 1**). Therefore, surface faulting was not strictly confined to a single segment. Geological and geophysical data from the Borah Peak earthquake suggest that the primary rupture was confined to the Thousand Springs segment and faulting on the Warm Spring segment was secondary. Thus, the barrier between these segments was not completely effective in stopping the northward-propagating surface rupture during the Borah Peak earthquake. Additional geologic evidence does suggest that a rupture barrier at the Willow Creek hills, the intervening transverse bedrock ridge between the Warm Spring and Thousand Springs segments, has halted propagating ruptures in the past, and thereby serves as a segment boundary. In contrast, the barrier on the south end of the Thousand Springs segment (near the epicenter) was competent and prevented surface faulting to the south on the Mackay segment.

One earlier Holocene surface-faulting event has occurred on the Thousand Springs segment (Hanks and Schwartz, 1987), and several similarities exist between this prehistoric event and the 1983 event. For example, the 1983 earthquake caused complex faulting of the Doublespring Pass road site near the middle of the Thousand Springs segment. Trenching here revealed that these two earthquakes produced similar total amounts of displacement, and near-surface ruptures not only occurred along the same faults, but the sense and amount of displacements were also the same (Schwartz and Crone, 1985). This leads one to assume that the 1983 event was probably similar in magnitude to the previous event, and the Borah Peak earthquake was characteristic (Schwartz and Coppersmith, 1984) for this segment. In contrast, the small displacements and discontinuity of scarps on the Warm Spring segment suggest that the 1983 event was not a typical displacement event for this segment. Schwartz and Crone's (1988) trenching studies indicate that faulting on the Warm Spring segment has occurred independently of faulting on the Thousand Springs segment in the past. Thus, separating this part of the fault into two segments that have their own distinct seismic histories is reasonable even though part of the Warm Spring segment may have had sympathetic movement during the Borah Peak earthquake.

Segmentation of the Lemhi fault

The 93-mile-long (150-km) Lemhi fault is characterized by discontinuous scarps along its entire length. Six segments are defined on the basis of differences in scarp morphology along the length of the fault, range-front morphology, and the relation of scarp height to deposits of different age (**Figure 1**). Segments are between 8 and 27 miles (12 and 43 km) long, each of which has ruptured at least once in the past 30,000 years. As with the Lost River fault, the oldest segments of the Lemhi fault are the two nearest the Snake River Plain (Howe and Fallert Springs segments) and the northernmost (May) segment. The central part of the Lemhi fault displays evidence of surface faulting that is younger than the ends. The Sawmill Gulch and Patterson segments have ruptured during the Holocene and the Goldburg segment ruptured in late Pleistocene (about 15 ka).

Segmentation of the Beaverhead fault

Scarps on alluvium occur only on parts of the 93-mile-long (150-km) Beaverhead fault; thus, the parts of the fault along the mountain front that lack scarps may define old, less active segments. The Beaverhead fault has six segments that range from 12 to 26 miles (20 to 42 km) long (**Figure 1**). The timing of faulting is difficult to determine along segments that have few or no scarps. However, much of the range front is covered with alluvium that was probably deposited between 11 and 25 ka (Pierce and Scott, 1982), and thus the most recent faulting must predate the age of the alluvium. Three such segments on the Beaverhead fault are characterized by the absence of scarps; they are the northernmost (Lemhi) segment, the southernmost (Blue Dome) segment, and a central (Baldy Mountain) segment. Faulting probably has not occurred in the past 15,000 years on these segments. However, range-front morphology suggests a higher slip rate during the Quaternary along the Baldy Mountain segment than along segments on the ends of the fault. Of the other three segments, only the Leadore segment has Holocene displacement; the most recent movement on the Nicholia and Mollie Gulch segments probably occurred between 10 and 15 ka.

The temporal and spatial variation in surface faulting inferred from differences in scarp morphology that define the segmentation of the Lost River, Lemhi, and Beaverhead faults suggests impressively similar faulting histories for these faults. The faults are approximately the same length, they have the same number of segments, and surface rupture has occurred on segments comprising nearly half or more of the entire length of the fault in the past 30,000 years (**Table 1**). Four of the six segments on the Lost River fault have had at least one surface-faulting event in the

Table 1. Comparison of segment length, maximum topographic relief, and timing and number of events on the Beaverhead, Lemhi, and Lost River faults. Fault segments are listed from south to north. (Lost River fault data compiled from Crone and others, 1985, 1987; Pierce, 1985; Scott and others, 1985; Hanks and Schwartz, 1987; Schwartz and Crone, 1988.)

	Length km (miles)	Maximum topographic relief [m (ft.)]	Timing and number of faulting events			
			0-10 ka	10-15 ka	15-30 ka	>30 ka[1]
BEAVERHEAD FAULT						
Blue Dome segment	25 (16)	1,300 (4,265)				P?
Nicholia segment	42 (26)	1,485 (4,870)		1	1	
Baldy Mountain segment	21 (13)	1,250 (4,100)				IP?
Leadore segment	23 (14)	1,170 (3,840)	1		1	
Mollie Gulch segment	20 (12)	980 (3,215)		1?		
Lemhi segment	20 (12)	1,190 (3,905)				P?
LEMHI FAULT						
Howe segment	20 (12)	1,800 (5,905)			1	
Fallert Springs segment	29 (18)	1,820 (5,970)			1	
Sawmill Gulch segment	43 (27)	1,710 (5,610)	1	1		
Goldburg segment	12 (8)	1,413 (4,635)		1		
Patterson segment	23 (14)	1,700 (5,580)	1			
May segment	23 (14)	1,850 (6,070)			1	
LOST RIVER FAULT						
Arco segment	25 (16)				1	
Pass Creek segment	29 (18)					IP?
Mackay segment	22 (14)		1	1		
Thousand Springs segment	22 (14)		2			
Warm Spring segment	18 (11)		1			
Challis segment	25 (16)					P?

[1]IP = late Pleistocene; P = Pleistocene where more exact ages are unknown due to absence of scarps; queried where age is poorly constrained.

past 30,000 years; whereas all six segments on the Lemhi fault and three of the six segments on the Beaverhead fault have had similar-age movements. A minimum of 18 surface-faulting events have occurred on these three faults in the past 30,000 years, with the majority of events occurring on the central segments of each fault. Topographic relief is similar along strike of each fault, although topographic relief tends to decrease from southwest to northeast across the ranges.

Segment-boundary characteristics

Segment boundaries are commonly characterized by the absence of scarps at least for a few miles (kilometers) along strike of the fault. This is primarily due to a decrease in surface offsets near the segment boundaries; small scarps degrade more rapidly than large scarps formed during the same event and eventually disappear from the geomorphic record, leaving no evidence of surface rupture. In addition, many of the segment boundaries are associated with more prominent geometric changes in the range front or surface trace of the fault. These prominent changes include major en echelon offsets of the fault scarps or major salients in the range front. En echelon scarps are common surficial features of normal faults, but those that characterize segment boundaries have offsets of several miles (kilometers). Major salients are defined as local changes in the trend of the range front of tens of degrees; the abrupt 55° change in trend of the range front at the segment boundary between the Thousand Springs and Mackay segments (Crone and others, 1987) is one of the best examples in this area. It is near this salient that the Borah Peak earthquake nucleated. Other range-front salients are expressed as the major transverse bedrock ridges, which define one segment boundary on each of these three faults. The boundary between the Thousand Springs and Warm Spring segments on the Lost River fault is an example of this type of segment boundary.

Gravity data (Bankey and others, 1985) indicate that many of the salients coincide with relatively shallow bedrock beneath the valley fill (**Figure 2**) suggesting that the slip rate along these parts of the fault is low with respect to that along adjacent parts. During a typical surface rupture event, displacement is small near the segment boundary (or the end of the rupture) and increases to some maximum near the middle part of the segment; however, displacements are never a smooth curve as this brief discussion might suggest (see Figure 4 *in* Crone and others, 1987; Fig. 28 *in* Wallace, 1984, for examples). If segment boundaries persist through time, one would expect local gravity maxima to be expressed in the hanging wall at or near the segment boundary and closed gravity lows near the middle of the segment. Some of the segments defined on the basis of fault-scarp morphology do show these associations (**Figure 2**). The most notable are the segments on the Lemhi fault, but some segments on the Lost River and Beaverhead faults show similar associations. The segments of the Lost River fault associated with closed gravity lows are the Pass Creek, Thousand Springs, and Warm Spring segments and, to a lesser extent, the Mackay segment, although the gravity maxima separating these segments are not as conspicuous as those separating some of the segments of the Lemhi fault. Adjacent to the Beaverhead fault, closed gravity lows coincide with the Mollie Gulch and Leadore segments and, to a lesser extent, the Baldy Mountain segment, but only the local gravity maxima near the Mollie Gulch-Leadore segment boundary is well expressed.

Alignment of segment boundaries and other features

The transverse bedrock ridges, which form a drainage divide in each valley, appear to be aligned on a northeast trend that is subparallel to the trend of the Snake River Plain. Ruppel (1967) argued that these ridges are the surficial expression of a through-going structure, which locally elevated the landscape and divided drainage systems in the late Cenozoic. The divides align in a N70°E trend that intersects the Red Rock fault, in Montana, near the southern end of the Sheep Creeks segment (line A, **Figure 3**). A limb of the Snowcrest-Greenhorn thrust-fault system lies farther northeast along this projection, and Perry and others (1983) suggested it is a major through-going regional structure.

Other segment boundaries also align and appear to define through-going, subparallel, east to northeast trending zones of similar-age faulting that cross the four ranges north of the Snake River Plain at a high oblique angle (**Figure 3**). South of the drainage divides, segment boundaries align on N60°E trends. The alignment of the boundaries between the Mackay and Pass Creek, Sawmill Gulch and Fallert Springs, and Nicholia and Blue Dome segments (line B, **Figure 3**) projects to the southern limit of the topographic expression of the Tendoy Mountains in Montana. The zone between lines A and B contains faulting younger than 15,000 years old, and Holocene faulting characterizes the westernmost part of the zone.

Line B (**Figure 3**) is the southern limit of faulting occurring less than 15 ka; faulting is older south of this line. Its position also coincides with the interior parab-

ola of Anders and others (1989) that separates the active region to the northwest from the collapse shadow to the southeast, the latter of which is regarded as tectonically inactive. The zone between lines B and C contains the Pass Creek, Fallert Springs, and Blue Dome segments, all of which have not ruptured in the past 15,000 years, but at least one segment has ruptured in the past 30,000 years. The zone bounded by lines C and D contains the Arco and Howe segments, both of which had movements occurring approximately 30 ka.

North of the drainage divides, the alignments trend more easterly than those south of the divides (**Figure 3**), between N65°E and N75°E. The zone between lines E and A does not contain a predominant age of faulting. Instead, it contains two segments with Holocene displacement, one with displacement younger than 15,000 years, and one (Baldy Mountain segment) with late Pleistocene(?) displacement. The Baldy Mountain segment is the only segment in the area within a fault-zone interior that has not had surface rupture within the past 30,000 years; this suggests it is a likely candidate for movement. Neither line E or F project to a segment boundary on the Lost River fault, but the zone between lines E and F contains faulting that occurred less than 15 ka, with predominantly younger faulting in the westernmost part of the zone. The northernmost alignment (line G, **Figure 3**) intersects the ends of the Lost River and Lemhi faults, and the

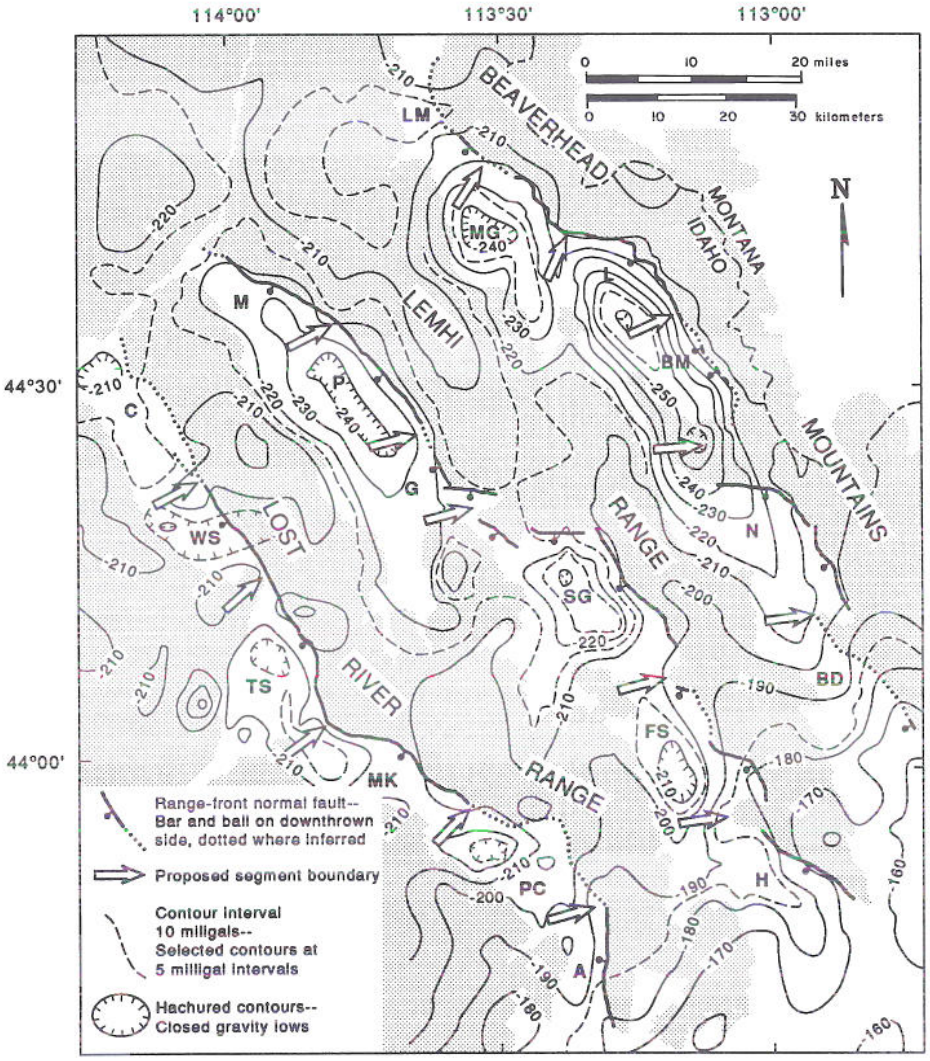

Figure 2. Generalized bouguer anomaly gravity map (modified from Bankey and others, 1985) of the northeastern Basin and Range province, showing the relation of segments to gravity lows in the valleys (unstippled areas). Bold letters designating segment names on Lost River, Lemhi, and Beaverhead faults are listed in Figure 1.

boundary between the Lemhi and Mollie Gulch segments. Interestingly, the westward projection of this line is at the abrupt northern termination of the Tendoy Mountains. The zone between lines F and G contains segments with faulting occurring before 15 ka. Anders and others' (1989) exterior parabola, which separates the active region to the south from the peripheral region to the northwest, is about 25 miles (40 km) north of the ends of these faults.

If the aligned segment boundaries that define these zones are related to deep-seated through-going structures, they are relict features. The orientation of these features in the present stress regime allow the structures to accommodate the differential motion (act as a decoupling zone) required to allow displacement on one segment when neighboring segments do not move or move minimally. These structures act not only as segment boundaries but also seem to bound zones of similar-age faulting, implying that regional extension is accommodated in broadly contemporaneous fashion within a zone. The pronounced north-northeast alignment of the segment boundaries in this area may be coincidental, or the boundary locations may be due only

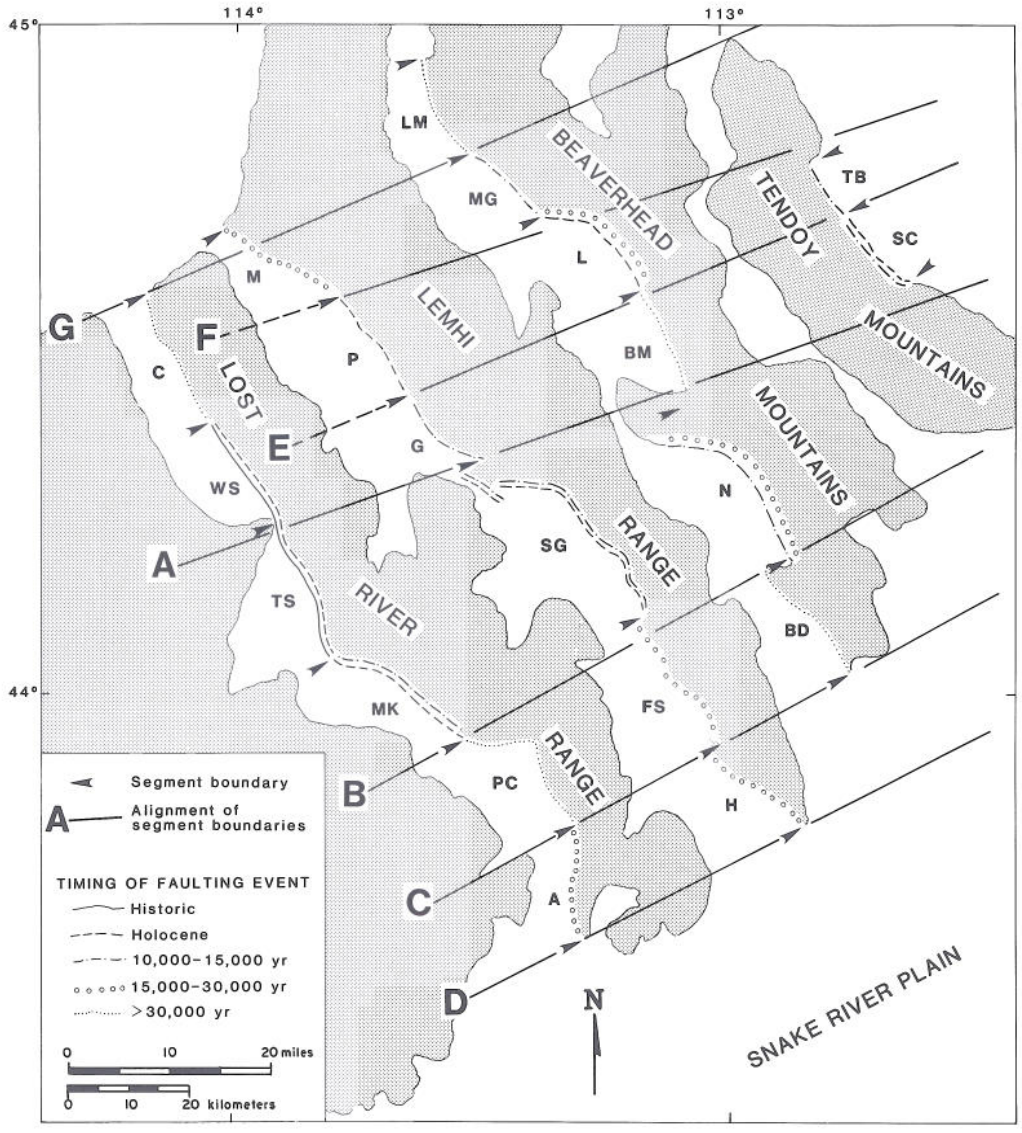

Figure 3. Map showing alignment of segment boundaries in the northeastern Basin and Range province and extending to the Red Rock fault, Montana. Double lines show timing of multiple events. Bold letters designating segment names on the Lost River, Lemhi, and Beaverhead faults are listed in Figure 1. Segments on the Red Rock fault are TB = Timber Butte and SC = Sheep Creek (Stickney and Bartholomew, 1987; Haller, 1988).

to segmentation of the faults into lengths determined by the size of the characteristic earthquake for that segment. However, the evidence that at least some of the boundaries have persisted throughout the late Quaternary or longer and have affected either the nucleation or termination of coseismic rupture, or both, suggests that the boundaries may involve some undetected deep-seated crustal structures. The existence of such structures is presently not well supported by available geologic or geophysical data. Further studies may resolve these questions, which, when answered, may improve our understanding of the temporal and spatial behavior of the seismogenic normal faults in this area.

Nicholia segment of the Beaverhead fault

The final two stops of this field trip are on the Nicholia segment of the Beaverhead fault. The characteristics of faulting at these stops, as well as other sites along this segment, demonstrate both the difficulties and benefits of using scarp morphology to define fault segmentation, determine the number of faulting events, and estimate time of faulting.

The 26-mile-long (42-km) Nicholia segment of the Beaverhead fault spans a major embayment in the range front and extends from Timber Canyon on the south to Gilmore Summit on the north (**Figure 4**). This is the longest segment of the Beaverhead fault and the second longest segment of these three faults. Nicholia segment is characterized by nearly continuous, prominent scarps along its southern 21 miles (34 km). Holocene alluvium is unfaulted, but all older alluvial terraces that cross the fault have scarps. In contrast, the segments to the north and south (Baldy Mountain and Blue Dome, respectively) have few scarps and those that are preserved are on bedrock and, therefore, are unsuitable for estimating the timing of faulting on these segments.

The two boundaries of the Nicholia segment coincide with bedrock ridges that extend into the valley. The Blue Dome-Nicholia (southern) boundary is at the northern end of the Blue Dome block (Skipp and Hait, 1977) and is coincident with a 3.3-mile-wide (5.5-km) en echelon step to the east in the Beaverhead fault. The Nicholia-Baldy Mountain (northern) boundary coincides with the major transverse bedrock ridge (Middle Range on **Figure 4**) that forms the drainage divide between the northwest-flowing Lemhi River and the southeast-flowing Birch Creek. This segment boundary is marked by a 4-mile-long (6-km) gap in scarps, a 6-mile (10-km) sinuous mountain-piedmont junction (Bull, 1987), and an absence of other indications of recent faulting. Scholten and Ramspott (1968) described Middle Range as the product of deep-seated wrench faulting, but the causative structures remain unmapped.

Timing of faulting of the Nicholia segment

The relation of scarp height to maximum slope angle for scarps of the Nicholia segment (**Figure 5**) does not present a clear indication of the timing of the event that produced them. The slope of the line of best fit is anomalously low with respect to the other lines given in **Figure 5** to provide a temporal perspective for data from the Nicholia segment. The majority of the scarp data lie below the 15-ka regression line and thus suggest the timing of the most recent faulting event occurred more than 15 to more than 30 ka. However, the timing of the most recent event on this segment probably occurred closer to 15 than 30 ka because: (1) the scarps are well preserved and generally continuous, (2) many small scarps are preserved, (3) single-event scarps are on late Pleistocene deposits inferred to be no more than 15,000 years old, and (4) multiple-event scarps are found on deposits thought to be more than 24,000 years old.

Unlike the discontinuous 30,000-year-old scarps of the Arco segment of the Lost River fault, scarps on this segment are generally continuous except where the fault is buried by Holocene alluvium. Without exception, all pre-Holocene deposits are faulted at least once and older deposits are faulted twice.

The ages of the alluvial deposits along the range front are poorly constrained; however, by using surface morphology, position on the landscape, and degree of soil development, one can approximate their ages, and thereby loosely constrain the upper limit of time of faulting. Nearly all of the surficial deposits seen along this segment are thought to have been deposited during major periods of glaciation (Pierce and Scott, 1982). The weakly developed soils found in this area indicate that the most extensive deposits at the range front were probably deposited since the last full glacial, which is regarded as the beginning of the most recent

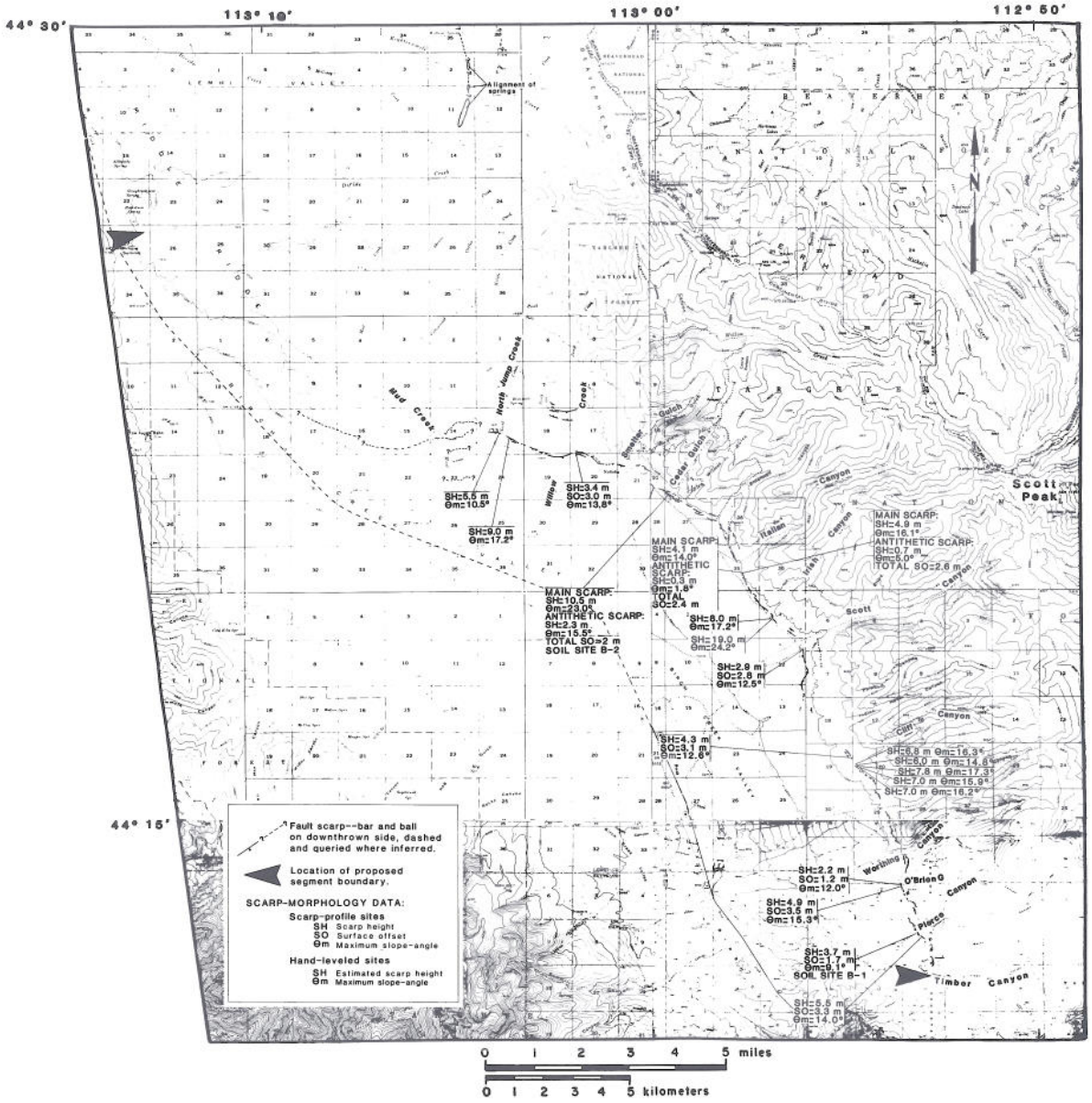

Figure 4. Map of scarps on the Nicholia segment of the Beaverhead fault, Idaho.

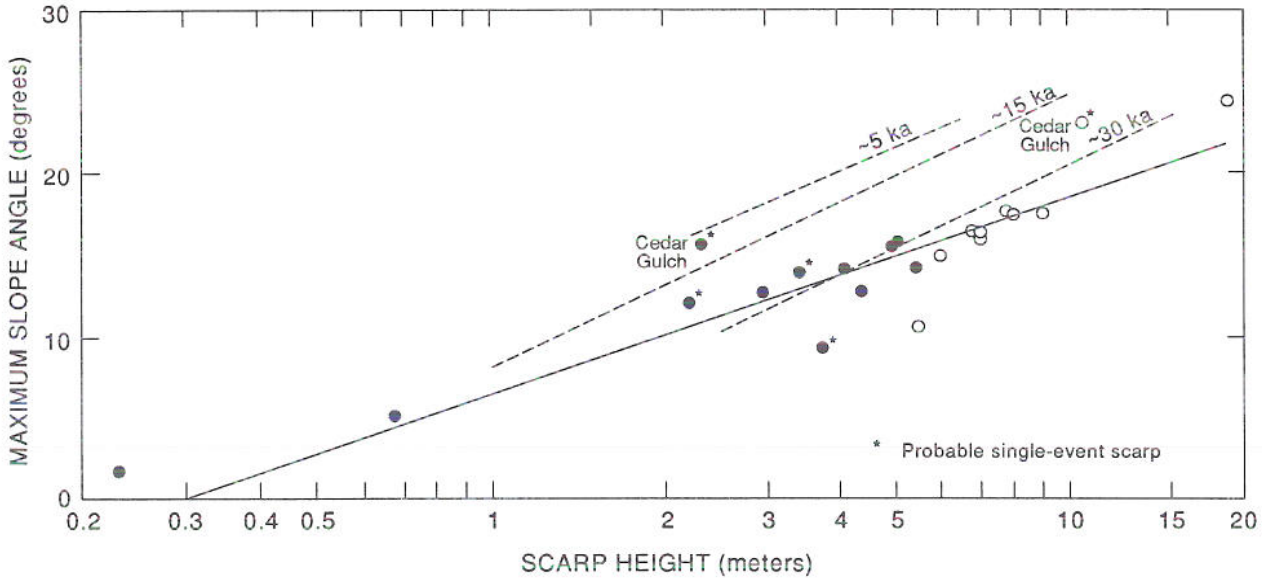

Figure 5. Plot of scarp height versus maximum slope angle (parameters defined by Bucknam and Anderson, 1979) for scarps on the Nicholia segment of the Beaverhead fault. Solid circles are data from profiled scarps, open circles are hand-leveled data. Dashed lines are lines of best fit, described by regression equations based on data from scarps on Mackay segment (5 ka) of the Lost River fault (A.J. Crone and others, unpublished data), west-facing fluvial scarps (15 ka) near Arco, Idaho (Pierce and Colman, 1986), and scarps on Arco segment (30 ka) of the Lost River fault (Pierce, 1985). Solid line is regression based on scarp data from Nicholia segment of the Beaverhead fault.

major fluvial activity and regrading of fan surfaces. At least two levels of latest Pleistocene fluvial terraces are common along this segment. The low terrace is composed of alluvium that was deposited during late-glacial time, assumed to be about 15 ka, and the alluvium of the high terrace was deposited during full-glacial time, about 18-20 ±4 ka (Pierce and Colman, 1986).

There are many probable reasons that the morphologic age of these scarps appears greater than the estimated age of the faulted deposits, but climate and the slope of the deposits are among the most obvious factors that influence the rates of degradation of scarps and apparent scarp age. There are probably no significant differences in microclimate due to aspect of the scarps between this segment and other segments in this area, however, the local climate may be an important factor. Many of the scarps on this segment are high above the valley floor where temperatures are slightly cooler; because of this factor alone, vegetation is less dense, which could cause an increase in erosion rates (Schumm, 1977). If the erosion rate is high, the scarp will degrade faster and its morphology will suggest an apparent age that is too old. Another factor that can affect the apparent morphologic age of a scarp is the slope of the faulted deposit (Hanks and Andrews, 1987). Along this segment, the surface of the faulted deposits has slopes at least 3° steeper than those at sites on other segments; this allows more sediment to be transported as a result of sheet wash and also results in increased degradation rates. Although a 3° increase in slope does not seem to be significant, a positive feedback may develop when coupled with sparse vegetation. In addition, the high scarps result from multiple-faulting events and this alone increases apparent age of the scarp (Machette and others, 1986).

Stop descriptions

Stop 8. Cedar Gulch graben

The largest probable single-event scarps on the Nicholia segment are at Cedar Gulch, where the steeply sloping (>5°) fan is extensively faulted. A large graben extends across the head of the fan north of the present drainage from Cedar Gulch, and numerous horst blocks are present within the graben. Several small down-to-

the-valley scarps are present northeast (rangeward) of the main scarp and southwest of the large antithetic scarp. At the apex of the high older fan, the main scarp is 34.4 feet (10.5 m) high with a maximum slope angle of 23.0°, and the antithetic scarp is 7.5 feet (2.3 m) high with a maximum slope angle of 15.5°. The relatively steep faces of these scarps, when compared to other scarps on this segment of similar size, may be due to the mantle of large boulders that armor the scarps. These boulders probably help preserve steep slopes longer than the slopes would be preserved in materials lacking such large clasts, but the steep slope also may reflect the single-event origin of these scarps. Note that the data from the Cedar Gulch scarps plot near and on both sides of the 15-ka regression line (**Figure 5**).

Although scarps are large at this site, the total surface offset, which is about 6.5 feet (2 m), could easily result from one faulting event. Stickney and Bartholomew (1987) implied that the Cedar Gulch scarps are possibly Holocene, but the morphology of the scarps indicates that they formed about 15 ka as the result of the most recent event rupturing this segment. The soil on this faulted deposit is weakly developed and indicates the deposit is latest Pleistocene in age (approximately 15,000 years). The 24-inch-thick (60-cm) solum contains a 6-inch-thick (15-cm) A horizon over a 11-inch-thick (27-cm) B horizon in which carbonate has stage I to weak stage II morphology (Gile and others, 1965). Carbonate morphology is better developed than might be expected for a deposit of this age due to accelerated accumulation of carbonate derived from limestone parent material (Rember and Bennett, 1979). This soil is characteristic of other "late Pinedale" soils in the area (Butler and others, 1983; Hait, 1985).

A small drainage at the north end of the fan provides good evidence for young faulting and demonstrates the effects of faulting on the flow of surface water. This stream drains only a small area and probably flows only a few times a year; because of this, the stream has not become graded to the new base level created by faulting. A prominent nick point can be seen on the upthrown block near the main scarp. The formation of the graben at this site dammed the course of the stream and diverted the flow to the northwest along the axis of the graben. The amount of sediment transported into the graben has been small, and therefore, the stream has not breached the antithetic scarp. Because of the ephemeral nature and small drainage area of the stream, these features have been preserved.

Stop 9. Cliff Canyon graben

There is a well-developed graben on either side of the mouth of Cliff Canyon (**Figure 4**), which is about 7 miles (11 km) south-southeast of Cedar Gulch (Stop 8). The Cliff Canyon graben is 0.1 mile (0.2 km) long, as much as 160 feet (50 m) wide, and contains as many as four scarps. Scarps are not present on the Holocene alluvium that covers approximately 0.8 mile (1.3 km) of the fault's length. South of the channel, a 26-foot-high (8-m) fluvial terrace has a 23-foot-high (7-m) fault scarp with maximum slope angles between 14.8° and 17.3°. Approximately 300 feet (100 m) north of the Cliff Canyon channel, there is a small remnant of a low-lying (5.6 ft-/1.7-m-high), complexly faulted terrace. The prominent graben on the high terrace is also obvious here, but these scarps are small by comparison. Displacement on the antithetic scarp is less than 1.6 feet (0.5 m). From the floor of the graben, the surface offset of the main scarp is 10.1 feet (3.1 m) and the scarp height is 14.1 feet (4.3 m). Relationships such as this increased height of fault scarps on progressively older terraces provide the best evidence of multiple-event faulting and the approximate timing of those events.

The heights of these subjacent scarps differ by a factor of approximately two, which suggests that at least the scarp on the high terrace is a multiple-event scarp. If the scarp on the low terrace is the result of one faulting event then the scarp on the high terrace is probably the result of two similar-sized faulting events. However, the morphology of the scarp on the low terrace suggests that it too may be the product of multiple displacements; it has a morphology similar to the multiple-event scarps near O'Brien Gulch and Pierce Canyon to the south (**Figure 4**). If this is the case, then the scarp on the high terrace at Cliff Canyon may be the result of as many as four events.

With the exception of the unfaulted Holocene deposits along the stream of Cliff Canyon, all of the alluvium here is of late Pleistocene age, probably time equivalent to late Pinedale (11-24 ka, Pierce and Scott, 1982). Thus, two to four faulting events are indicated in the past 24,000 years. Based on other sites along this segment of the Beaverhead fault, certainly the most conservative and likely the most plausible scenario for the faulting history of this part of the fault is that two events have occurred since 24 ka, and the last event occurred around 15 ka or toward the end of the period of alluviation during the most recent Pleistocene glaciation.

References cited

Anders, M.H., Geissman, J.W., Piety, L.A., and Sullivan, J.T., 1989, Parabolic distribution of circum-eastern Snake River Plain seismicity and latest Quaternary faulting—migratory pattern and association with the Yellowstone hotspot: Journal of Geophysical Research, v. 94, p. 1589-1621.

Bankey, V., Webring, M., Mabey, D.R., Kleinkopf, M.D., and Bennett, E.H., compilers, 1985, Complete bouguer gravity anomaly map of Idaho: U.S. Geological Survey Miscellaneous Field Studies Map MF-1773, 1 sheet, scale 1:500,000.

Bonilla, M.G., Mark, R.K., and Lienkaemper, J.J., 1984, Statistical relations among earthquake magnitude, surface rupture length, and surface fault displacement: Bulletin of the Seismological Society of America, v. 74, p. 2379-2411.

Bucknam, R.C., and Anderson, R.E., 1979, Estimation of fault-scarp ages from a scarp-height—slope-angle relationship: Geology, v. 7, p. 11-14.

Bull, W.B., 1987, Relative rates of long-term uplift of mountain fronts, *in* Crone, A.J., and Omdahl, E.M., editors, Proceedings of Conference XXXIX—Directions in Paleoseismology: U.S. Geological Survey Open File Report 87-673, p. 192-202.

Butler, D.R., Sorenson, C.J., and Dort, W., Jr., 1983, Differentiation of morainic deposits based on geomorphic, stratigraphic, palynologic, and pedogenic evidence, Lemhi Mountains, Idaho, U.S.A., *in* Evenson, E.B., editor, Tills and related deposits—genesis, petrology, application, stratigraphy—1981 INQUA symposium on the genesis and lithology of Quaternary deposits: Geo Books, Norwich, England, p. 373-380.

Crone, A.J., Machette, M.N., Bonilla, M.G., Lienkaemper, J.J., Pierce, K.L., Scott, W.E., and Bucknam, R.C., 1985, Characteristics of surface faulting accompanying the Borah Peak earthquake, central Idaho, *in* Stein, R.S., and Bucknam, R.C., editors, Proceedings of Workshop XXVIII on the Borah Peak, Idaho, Earthquake: U.S. Geological Survey Open File Report 85-290, v. A, p. 43-58.

Crone, A.J., Machette, M.N., Bonilla, M.G., Lienkaemper, J.J., Pierce, K.L., Scott, W.E., and Buchnam, R.C., 1987, Surface faulting accompanying the Borah Peak earthquake and segmentation of the Lost River fault, central Idaho: Bulletin of the Seismological Society of America, v. 77, p. 739-770.

Dewey, J.W., 1985, Instrumental seismicity of central Idaho, *in* Stein, R.S., and Bucknam, R.C., editors, Proceedings of Workshop XXVIII on the Borah Peak, Idaho, Earthquake: U.S. Geological Survey Open File Report 85-290, v. A, p. 264-284.

Gile, L.H., Peterson, F.F., and Grossman, R.B., 1966, Morphological and genetic sequences of carbonate accumulation in desert soils: Soil Science, v. 101, p. 347-360.

Hait, M.H., Jr., 1985, Doublespring Pass road trench, *in* Crone, A.J., Fault scarps, landslides and other features associated with the Borah Peak earthquake of October 28, 1983, central Idaho—A field trip guide, *in* Stein, R.S., and Bucknam, R.C., editors, Proceedings of Workshop XXVIII on the Borah Peak, Idaho, Earthquake: U.S. Geological Survey Open File Report 85-290, v. B, p 11-18.

Haller, K.M., 1988, Segmentation of the Lemhi and Beaverhead faults, east-central Idaho, and Red Rock fault, southwest Montana, during the late Quaternary: M.S. thesis, University of Colorado, Boulder, 141 p.

Hanks, T.C., and Andrews, D.J., 1987, Far-field slopes and the nature of general diffusion models of scarplike landforms in weakly consolidated terrains, *in* Crone, A.J., and Omdahl, E.M., editors, Proceedings of Conference XXXIX—Directions in Paleoseismology: U.S. Geological Survey Open File Report 87-673, p. 339-357.

Hanks, T.C., and Schwartz, D.P., 1987, Morphologic dating of the pre-1983 fault scarp on the Lost River fault at Doublespring Pass road, Custer County, Idaho: Bulletin of the Seismological Society of America, v. 75, p. 835-846.

Machette, M.N., Personius, S.F., and Nelson, A.R., 1987, Quaternary geology along the Wasatch fault zone—Segmentation, recent investigations, and preliminary conclusions, *in* Gori, P.L., and Hays, W.W., Assessment of regional earthquake hazards and risk along the Wasatch front, Utah: U.S. Geological Survey Open File Report 87-585, v. I, p. A-1—A-72.

Machette, M.N., Personius, S.F., Menges, C.M., and Pearthree, P.A., 1986, Map showing Quaternary and Pliocene faults in the Silver City 1°x 2° Quadrangle and the Douglas 1°x 2° Quadrangle, southeastern Arizona and southwestern New Mexico: U.S. Geological Survey Miscellaneous Field Studies Map MF-1465-C, 20 p., scale 1:250,000.

Malde, H.E., 1985, Quaternary faulting near Arco and Howe, Idaho, *in* Stein, R.S., and Bucknam, R.C., editors, Proceedings of Workshop XXVIII on the Borah Peak, Idaho, Earthquake: U.S. Geological Survey Open File Report 85-290, v. A, p. 207-235.

Malde, H.E.,1987, Quaternary faulting near Arco and Howe, Idaho: Bulletin of the Seismological Society of America, v. 77, p. 847-867.

Perry, W.J., Jr., Wardlaw, B.R., Bostick, N.H., and Maughan, E.K., 1983, Structure, burial history, and petroleum potential of frontal thrust belt and adjacent foreland, southwest Montana: American Association of Petroleum Geologists Bulletin, v. 67, p. 725-743.

Pierce, K.L., 1985, Quaternary history of faulting on the Arco segment of the Lost River fault, central Idaho, *in* Stein, R.S., and Bucknam, R.C., editors, Proceedings of Workshop XXVIII on the Borah Peak, Idaho, Earthquake: U.S. Geological Survey Open-File Report 85-290, v. A, p. 195-206.

Pierce, K.L., and Colman, S.M., 1986, Effect of height and orientation (microclimate) on geomorphic degradation rates and processes, late-glacial terrace scarps in central Idaho: Geological Society of America Bulletin, v. 97, p. 869-885.

Pierce, K.L., and Scott, W.E., 1982, Pleistocene episodes of alluvial-gravel deposition, southeastern Idaho, *in* Bonnichsen, B., and Breckenridge, R.M., editors, Cenozoic geology of Idaho: Idaho Bureau of Mines and Geology Bulletin 26, p. 685-702.

Pierce, K.L., Scott, W.E., and Morgan, L.A., 1988, Eastern Snake River Plain neotectonics—faulting in the last 15 Ma migrates along and outward from Yellowstone "hotspot" track: Geological Society of America Abstracts with Programs, v. 20, no. 6, p. 463.

Rember, W.C., and Bennett, E.H., compilers, 1979, Geologic map of the Dubois Quadrangle, Idaho: Idaho Department of Lands, Bureau of Mines and Geology, Geologic Map Series, scale 1:250,000.

Ruppel, E.T., 1967, Late Cenozoic drainage reversal, east-central Idaho, and its relation to possible undiscovered placer deposits: Economic Geology, v. 62, p. 648-663.

Scholten, R., and Ramspott, L.D., 1968, Tectonic mechanisms indicated by structural framework of central Beaverhead Range, Idaho-Montana: Geological Society of America Special Paper 104, 71 p.

Schumm, S.A., 1977, The fluvial system: John Wiley and Sons, New York, New York, p. 42-56.

Schwartz, D.P., and Coppersmith, K.J., 1984, Fault behavior and characteristic earthquakes—examples from the Wasatch and San Andreas fault zones: Journal of Geophysical Research, v. 89, p. 5681-5698.

Schwartz, D.P., and Crone, A.J., 1985, The 1983 Borah Peak earthquake—A calibration event for quantifying earthquake recurrence and fault behavior on Great Basin normal faults, *in* Stein, R.S., and Bucknam, R.C., editors, Proceedings of Workshop XXVIII on the Borah Peak, Idaho, Earthquake: U.S. Geological Survey Open File Report 85-290, v. A, p. 153-160.

Schwartz, D.P., and Crone, A.J., 1988, Paleoseismicity of the Lost River fault zone, Idaho—earthquake recurrence and segmentation: Geological Society of America, Cordilleran Section Abstracts with Programs, v. 20, no. 3, p. 228.

Scott, W.E., Pierce, K.L., and Hait, M.H., Jr., 1985, Quaternary tectonic setting of the 1983 Borah Peak earthquake, central Idaho: Bulletin of the Seismological Society of America, v. 75, p. 1053-1066.

Skipp, Betty, and Hait, M.H., Jr., 1977, Allochthons along the northeast margin of the Snake River Plain, Idaho, *in* Heisey, E.L., Lawson, D.E., Norwood, E.R., Wach, P.H., and Hale, L.A., editors, Rocky Mountain thrust belt geology and resources: Wyoming Geological Association 29th Annual Field Conference Guidebook, p. 499-515.

Stickney, M.C., and Bartholomew, M.J., 1987, Seismicity and late Quaternary faulting of the northern Basin and Range province, Montana and Idaho: Bulletin of the Seismological Society of America, v. 77, p. 1602-1625.

Swan, F.H., III, Schwartz, D.P., and Cluff, L.S., 1980, Recurrence of moderate to large magnitude earthquakes produced by surface faulting on the Wasatch fault zone, Utah: Bulletin of the Seismological Society of America, v. 70, p. 1431-1462.

Wallace, R.E., 1984, Faulting related to the 1915 earthquakes in Pleasant Valley, Nevada: U.S. Geological Survey Professional Paper 1274-A, p. A1-A33.

Wyss, Max, 1979, Estimating maximum expected magnitude of earthquakes from fault dimensions: Geology, v. 7. p. 336-340.

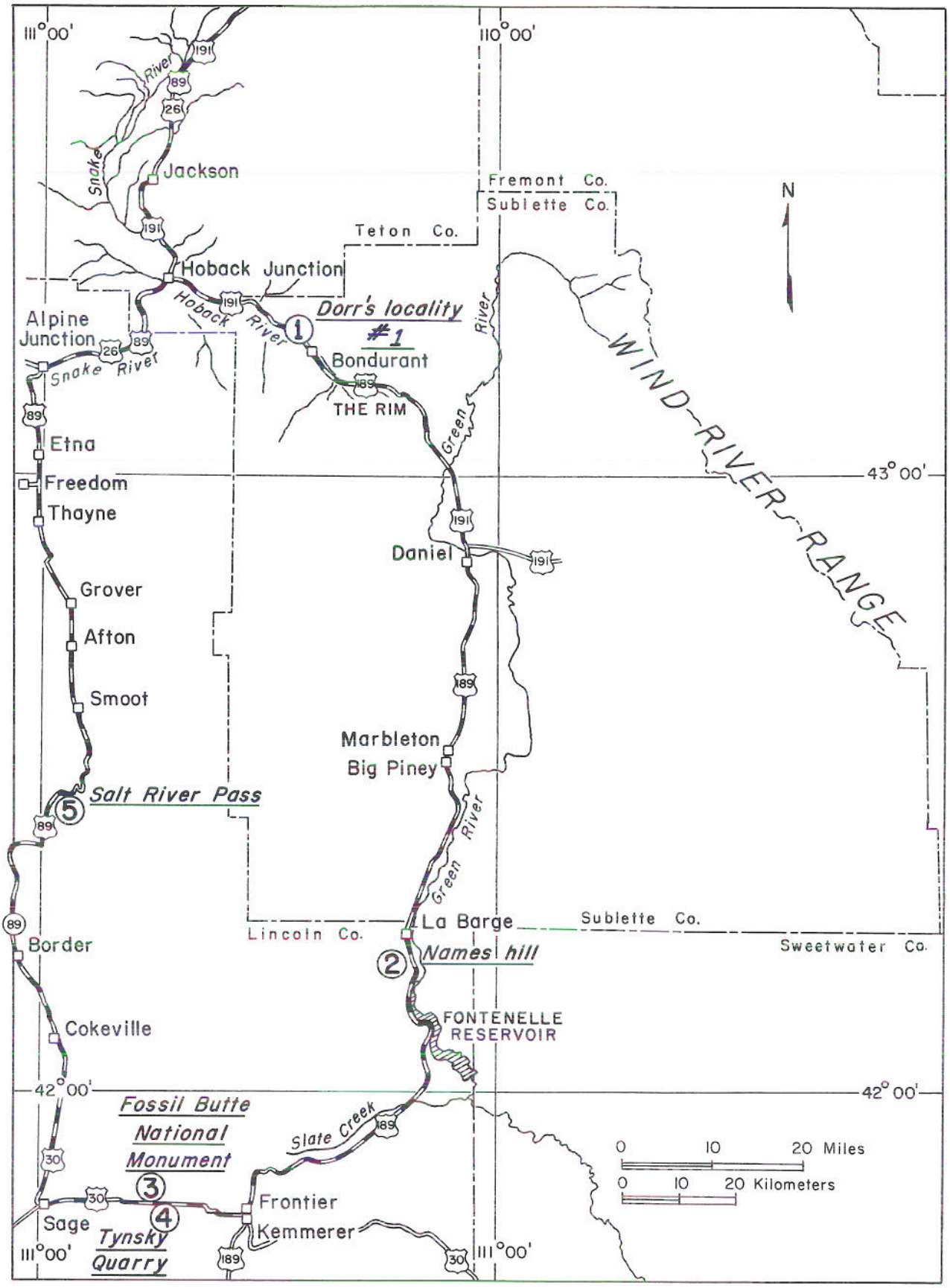

Figure 1. Trip route and stop locations, field trip no. 2

Field trip no. 2

EARLY TERTIARY FOSSILS AND ENVIRONMENTS OF WYOMING - JACKSON TO FOSSIL BUTTE NATIONAL MONUMENT

Brent H. Breithaupt
Geological Museum
Department of Geology and Geophysics
University of Wyoming
Laramie, Wyoming 82071

Trip Summary (See Figure 1)

Stop 1. Jack Dorr's locality no.1 (Hoback Formation), Hoback Basin
Stop 2. Names Hill (New Fork Tongue of the Wasatch Formation)
Stop 3. Fossil Butte National Monument (Fossil Butte Member of the Green River Formation), Fossil Basin
Stop 4. James E. Tynsky Quarry (Fossil Butte Member of the Green River Formation), Fossil Basin
Stop 5. Salt River Pass

Introduction

This field trip deals with the unique geology and history of western Wyoming. In the 1800s, trappers, people following the emigrant trails, railroad workers, and surveyors for the geological and geographical surveys made some of the first fossil discoveries in Wyoming in this part of the state. Early in the 1800s, the distinctive rocks and fossils of western Wyoming were recognized as suggesting an ancient environment very different than is seen in this part of the country today. In particular, early Tertiary specimens indicated that this part of Wyoming contained large river and lake systems in a warm-temperate to subtropical environment. A rich variety of plants and animals inhabited western Wyoming approximately 40 to 60 million years ago. The rivers and lakes teemed with water plants, mollusks, and fish. The banks and shores contained abundant insects, birds, reptiles, and mammals, as well as a lush flora. Excellent exposures of the Eocene Green River and Wasatch formations are present in the Green River and Fossil basins (especially at Fossil Butte National Monument). Interpretive displays on the environments and biota of these rock units are presented at the Fossil Butte National Monument Visitor's Center. Although fossils have been collected from western Wyoming for over 150 years, important scientific discoveries continue to be made in the early Tertiary rocks there.

Acknowledgments

Appreciation is extended to the Wyoming Council for the Humanities for help in funding parts of this project. Thanks to the University of Wyoming Department of Geology and Geophysics for logistical support.

Jackson to Dorr's locality number 1 (Hoback Formation)

Jackson to Hoback Junction via Highway 191

This roughly 13-mile route parallels the late Miocene Hoback normal fault. Along the route, Devonian (Darby Formation), Mississippian (Madison Limestone), and Pennsylvanian (Tensleep and Amsden formations) rocks are exposed. The Lower Cretaceous Aspen Shale can be seen in roadcuts along this route;

slumping in this area is often associated with this rock unit. The Miocene-Pliocene Camp Davis Formation may be seen cropping out occasionally above the Aspen Shale.

Hoback Junction to Hoback Basin via Highway 189-191

The route travels through the Hoback Range and into the Hoback Basin. Near Hoback Junction, along the Hoback River, is an historical marker commemorating John Hoback. Hoback helped guide the American Fur Company's Astorian Land Expedition (consisting of 61 men and 118 horses), under the leadership of Wilson Price Hunt, through this canyon on their way to the Pacific Ocean in the autumn of 1811. They were the first white men in this area of Wyoming. The group continued past the junction of the Snake and Hoback rivers into Jackson Hole over Teton Pass and on into Idaho. During the winter of 1813, Hoback was killed by Indians while trapping beavers in this area. This river was named by Wilson Price Hunt in memory of his guide.

Along the river, in Hoback Canyon, are drab Lower Cretaceous shales and sandstones of the Bear River and Aspen formations, as well as the Gannett Group. The Upper Cretaceous Frontier Formation forms ledges in this area.

Roughly 2.5 miles from Hoback Junction is the type area of the Camp Davis Formation. Here, a basal conglomerate (locally derived from Paleozoic carbonate rocks and reworked Precambrian quartzite clasts) overlies the Aspen Shale. The white ledges above the conglomerate are fresh water limestone beds overlain by pumicite, diatomite, and tuffaceous sandstones and shales. This formation is 5,365 feet (1,635 m) thick. Within the Camp Davis Formation are fossils of pelecypods, gastropods, ostracodes, and root casts. A tooth of *Pliohippus* was found in the upper member, suggesting a late Miocene to early Pliocene age for this formation (For a further discussion of this rock unit, see Dorr and others, 1977.)

Roughly 5 miles down the canyon is the "Hoback Gateway". The cliffs north of the highway are Madison Limestone. Farther down the canyon the Tensleep Formation also is a cliff former. Along this route, Devonian (Darby Formation), Mississippian (Madison Limestone), Pennsylvanian (Tensleep and Amsden formations), Permian (Phosphoria Formation), and Triassic (Dinwoody and Woodside formations) rocks are exposed. Continue down the highway across the Teton-Sublette County Line. Highly contorted and steeply dipping Ankareh Formation (Triassic), Nugget Sandstone (Triassic), Twin Creek Limestone (Jurassic), Stump Formation (Jurassic), Preuss Sandstone (Jurassic), and Gannett Group (Jurassic) can be seen in this area of the route.

Continue on Highway 189-191 out of the Hoback Range into the Hoback Basin. Formation of the Hoback Basin in the latest Cretaceous or early Paleocene was associated with the ancestral uplift of the Gros Ventre-Teton Range. During the early Tertiary, this basin was a central floodplain with associated marginal alluvial fans (Dorr and others, 1977). Most of the deposition in this basin occurred in the Paleocene and Eocene, when the Hoback, Wasatch, and Pass Peak formations were deposited.

The Paleocene Hoback Formation is seen in exposures roughly 13 miles from Hoback Junction. In a road cut north of the highway (approximately 17 miles from Hoback Junction) a basal conglomerate known as the "Hoback Conglomerate" is exposed. This unit overlies (with an erosional unconformity) the underlying Harebell Formation in the northern part of the basin. Pebbles and cobbles are rounded and composed of sandstone, limestone, and chert apparently derived locally from rocks of Paleozoic age to the west (Dorr and others, 1977). No granite or Precambrian quartzite (such as is characteristic of the Paleocene Pinyon Conglomerate) is found. The Hoback Formation is approximately 6,560 feet (2 km) thick (typically) and is exposed in the northern and western borders of the Hoback Basin. Shales make up 90 percent of this unit. Sandstones, limestones, coal seams, and conglomeratic layers are also present within the Hoback Formation. The formation lacks Precambrian-derived garnets, feldspars, and epidotes common in other Tertiary formations in this part of Wyoming (Dorr and others, 1977). Also absent are pressure-marked metaquartzite cobbles of the Pinyon Conglomerate type. In the southern and central parts of the basin, the upper part of the Hoback Formation intertongues with and is conformably overlain by the Chappo Member of the Wasatch Formation. This member is dated as earliest Eocene (Clarkforkian). In the eastern part of the Basin, this unit is overlain by the Eocene Pass Peak Formation.

The depositional environment of the Hoback Formation is interpreted as being a vegetated, fluviatile floodplain with meandering streams and numerous small interfluvial ponds and some swampy areas (Dorr and others, 1977). Cross-bedding analysis suggests a northern source (ancestral Teton-Gros Ventre uplift) for sediments of the Hoback Conglomerate. After the

deposition of this unit, the majority of the material appears to have come from the thrust belt to the west. The final phase of Hoback Formation deposition again derived material from a northern source.

Approximately 19 miles from Hoback Junction, near the Elk Horn Trading Post, the Dell Creek Road joins Highway 189/191 from the northeast. Locality no. 1 of Dorr (1952) is located a short distance up this road.

Stop 1. Jack Dorr's locality no. 1 (Hoback Formation), Hoback Basin

North of the highway, drab east dipping units of the Hoback Formation are exposed along the Dell Creek Road. Jack Dorr's (1952) vertebrate fossil locality no. 1 (see faunal list below) is located where the dark carbonaceous shales cross the road. The main productive fossil zone is an argillaceous limestone located below these shales and underlain by a sandstone layer (see **Figure 2**). In addition to fossil mammals of Tiffanian (late Paleocene) age, invertebrates (Dorr, 1977) and pollen (Guennel and others, 1973) are preserved. Dorr (1977) interpreted the Hoback Formation at this site as having been deposited under reducing conditions in a moist, poorly drained region, perhaps an oxbow lake or slough.

Dorr (1958, 1977, 1978) described the following animals from the Hoback Formation. Those taxa found at locality no. 1 are followed by an *.

INVERTEBRATES

CLASS GASTROPODA
- Order Archaeogastropoda
  - Family Grangerellidae
    - *Grangerella* sp. *
- Order Mesogastropoda
  - Family Viviparidae
    - *Campeloma* sp. *
- Order Basommatophora
  - Family Physidae
    - *Physa* sp. *
- Order Stylommatophora
  - Family Endodontidae
    - *Discus* sp. *
  - Family Oreohelicidae
    - *Oreohelix* sp. *

Figure 2. Locality no. 1 of Dorr (1952) within the Paleocene Hoback Formation.

VERTEBRATES

CLASS OSTEICHTHYES
- Order Lepisosteiformes
  - Family Lepisosteidae
    - *Lepisosteus* sp.

CLASS REPTILIA
- Order Chelonia
  - Family, genus, and species indet.
- Order Squamata
  - Suborder Lacertilia, Family indet.
    - *Haplodontosaurus excedens* *
- Order Crocodilia
  - Family Crocodylidae
    - *Allognathosuchus* sp. *

CLASS MAMMALIA
- Order Multituberculata
  - Family Ectypodontidae
    - *Neoplagiaulax fractus* *
    - *Ectypodus powelli* *
  - Family Ptilodontidae
    - *Ptilodus* cf. *P. montanus*
- Order Insectivora
  - Family Deltatheridiidae
    - cf. *Gelastops parcus* *
  - Family Adapisoricidae
    - *Leptacodon packi* *
    - *Leptacodon* cf. *L. ladae* *
  - Family Pantolestidae
    - *Palaeosinopa simpsoni* *
- Order Primates
  - Family Plesiadapidae
    - *Plesiadapis rex*
    - *P. fodinatus* *
    - *Chiromyoides potior* *
  - Family Carpolestidae
    - *Carpodaptes hobackensis* *
  - Family Paromomyidae
    - *Ignacius frugivorus* *
  - Family Palaeoryctidae
    - cf. *Gelastops* sp. *
- Order Carnivora
  - Family Miacidae
    - *Didymictis dellensis* *
- Order Condylarthra
  - Family Arctocyonidae
    - *Thryptacodon australis* *
    - *Chriacus* sp.
  - Family Hyopsodontidae
    - *Litaletes* sp.
    - *Haplaletes* cf. *H. disceptatrix*
    - *Haplatetes diminutivus* *
  - Family Phenacodontidae
    - *Ectocion* cf. *E. wyomingensis*
    - *Phenacodus grangeri*

Variegated rocks east of locality no. 1 are part of the Chappo Member of the Wasatch Formation and contain fossil mammals (Dorr's 1958 localities 7, 10 and 20) of Wasatchian (early Eocene) age. The Chappo Member of the Wasatch Formation is 1,970 feet (600 m) thick. It is variegated in color and consists of sandstones and shales. Minor limestone beds are present in the center of the basin. This member is conformable with the Hoback Formation and intertongues with this unit to the north and east (Dorr and others, 1977). The Chappo Member is overlain by the Pass Peak Formation in the Hoback Basin. The gray sandstone facies in the lower part of this unit is compositionally similar to and intertongues with the Lookout Mountain Conglomerate Member of the Wasatch Formation found in the southwestern corner of the Hoback Basin of the Wasatch Formation. Sediment for this facies was transported from the southwest to the northeast (Dorr and others, 1977). A yellow-tan sandstone facies located in the upper part of the section is compositionally identical with that of the Pass Peak Formation. The sediment for this facies was transported from northeast to southwest (Dorr and others, 1977).

Dorr (1958, 1978) described the following vertebrates from the Chappo Member of the Wasatch Formation in the Hoback Basin. Hackberry seeds of the genus *Celtis* are also known to be locally abundant (Dorr, 1978).

VERTEBRATES

CLASS OSTEICHTHYES
- Order Lepisosteiformes
  - Family Lepisosteidae
    - *Lepisosteus* sp.

CLASS REPTILIA
- Order Chelonia
  - Family, genus, and species indet.
- Order Squamata
  - Suborder Lacertilia
    - Family, genus, and species indet.
- Order Crocodilia
  - Family Crocodylidae
    - Subfamily Alligatorinae
      - Genus and species indet.

CLASS MAMMALIA
- Order Multituberculata
  - Family cf. Ectypodontidae
    - Genus and species indet.
- Order Tillodontia
  - Family Tillotheriidae
    - *Esthonyx* sp.
- Order Pantodonta
  - Family Coryphodontidae
    - *Coryphodon* sp.

Order Dinocerata
Family Uintatheriidae
Prouintatherium hobackensis
Order Primates
Family Apapidae
Pelycodus ralstoni
Order Condylarthra
Family Hyopsodontidae
cf. *Haplomylus speirianus*
Hyopsodus cf. *H. loomisi*
Family Phenacodontidae
Phenacodus vortmani
Phenacodus primaevus
Order Artiodactyla
Family Dichobunidae
Diacodexis sp.
Order Perissodactyla
Family Equidae
Hyracotherium sp.

On the skyline north of Dorr's locality no. 1 are the Gros Ventre mountains. Here the Madison Limestone is thrust to the southwest onto Triassic redbeds (visible in the wooded ravines). Farther to the southeast, Mesozoic rocks are thrust over the Hoback Formation.

Dorr's locality no. 1 to Names Hill

Dorr's locality no. 1 to Hoback Rim via Highway 189-191

Return to Highway 189-191 and continue southeast. Roughly 2 miles from Bondurant, on the skyline north of the road, is a rounded, timbered peak with a large landslide scar on the west face. This is the type area of the Eocene Pass Peak Formation. Here over 2,000 feet (610 m) of conglomerates and sandstones are present. The conglomerates are composed of highly rounded quartzite cobbles identical to and apparently derived from the Pinyon Conglomerate to the north in Jackson Hole (Dorr, 1969). The Pass Peak Formation encompasses more than half of the Hoback Basin; more than any other rock unit (Dorr, 1969). In the northern part of the basin, it is 3,280 feet (1 km) thick. It thins to the south to only 1,640 feet (.5 km) thick in the center of the basin. The Pass Peak Formation is in fault contact with Paleozoic rocks and angular unconformity with the Hoback Formation in the northern part of the basin. A quartzite-conglomerate facies is found mainly in the northern part of the basin. It consists of reworked Pinyon and Harebell (originally Precambrian) material. There is also some reworked Paleozoic and Mesozoic material. The sandstone-siltstone-floodplain environment facies of the Pass Peak Formation is found farther to the south in the basin. It contains some limestones indicating ponding. The main direction of transport for the sediments of the Pass Peak Formation is from northeast to southwest (Dorr and others, 1977). A secondary source from the east (Wind River Range) is also indicated.

Continue southeast on Highway 189-191; cross the Hoback River and Fisherman Creek. The outcrops of sandstone south and north of the road represent the base of the Pass Peak Formation. Continuous outcrops of the Pass Peak Formation can be seen in road cuts for many miles from here to the top of Hoback Rim. Quartzite cobble conglomerates within this unit are common. Most of the quartzite cobbles have a slight sheen and abundant percussion marks. The thick conglomeratic beds in the vicinity of Pass Peak pinch-out southward in a short distance, as only thin lenses are present along the highway. Near the top of Hoback Rim, carbonaceous shales (above the sandstones) in the Pass Peak Formation in north and south road cuts, contain fragments of fossil leaves (Dorr, 1969).

The following is the described fauna from the Pass Peak Formation (after Dorr, 1969, 1978). Associated with these taxa are abundant hackberry (*Celtis*) seeds, leaf fragments, coalified wood, and wood impressions. The transition zone between the Chappo Member of the Wasatch Formation and the overlying Pass Peak Formation is also represented.

INVERTEBRATES

CLASS GASTROPODA
Order Mesogastropoda
Family Viviparidae
Viviparus sp.
Order Stylommatophora
Family Bulimulidae
Oreoconus sp. (also in the transition zone)
Family Urocoptidae
Holospira sp.

VERTEBRATES

CLASS OSTEICHTHYES
Order Lepisosteiformes
Family Lepisosteidae
Lepisosteus sp.

CLASS REPTILIA
- Order Squamata
  - Family Anguidae
    - Genus and species undescribed
- Order Crocodilia
  - Family, genus and species indet.

CLASS AVES
- Order, family, genus, and species undescribed

CLASS MAMMALIA
- Order Insectivora
  - Family Adapisoricidae
    - *"Nyctitherium" celatum*
- Order Rodentia
  - Family Paramyidae
    - *Paramys copei*
- Order Condylarthra
  - Family Hyopsodontidae
    - *Hyopsodus* cf. *H. wortmani*
- Order Artiodactyla
  - Family Dichobunidae
    - *Diacodexis metsiacus*
- Order Perissodactyla
  - Family Equidae
    - *Hyracotherium angustidens* (found in the transition zone)
    - *Hyracotherium* cf. *H. vasacciense*

Hoback Rim to Daniel Junction via Highway 189-191

Continue on Highway 189-191 southeast from Hoback Rim [elevation 7,921 ft (2,414 m) above sea level] into the Green River Basin. Cross the Green River approximately 45 miles from Hoback Junction. On the skyline to the northeast is the Wind River Range. Hills around the highway are lateral moraine deposits. The Eocene Wasatch Formation can be seen in road cuts in this area. Continue on Highway 189-191 to Daniel Junction.

Daniel Junction to Names Hill via Highway 189

At Daniel Junction turn south on Highway 189. The highway crosses the Green River. Just outside of the town of Daniel is an historical marker east of the highway commemorating the Green River Rendezvous. From 1824 to 1840, this location was a market place for the fur trade, where trappers, traders, and Indians came to barter. Not only were furs exchanged, but also information of geographical importance that helped in the exploration of the west. A stone marker nearby commemorates the missionaries Naricissa Prentiss Whitman and Eliza Hart Spalding, the first white women in Wyoming and first women over the Oregon Trail (1836).

Continue on the highway through Daniel. To the west and north are Paleozoic and Mesozoic rocks of the Overthrust Belt. Sandstones and variegated shales of the Eocene Wasatch Formation crop out along the highway for the next 50 miles. Continue on the highway through Marbleton to Big Piney. On the skyline to the southeast across the Green River are outcrops of the Wasatch and Green River Formations. These can be seen better south of Big Piney. The most prolific collecting grounds in beds of the La Barge Member of the Wasatch Formation are found in the units that crop out between Big Piney and La Barge in the vicinity of the Green River (Gazin, 1952). Roughly 5 miles south of Big Piney, in the white-capped hill on the skyline to southeast, are the red banded shales of the La Barge Member of the Wasatch Formation. The grass-covered slope above contains the buff-colored marlstones, shales, and sandstones of the Fontenelle Tongue of the Green River Formation. The well-exposed green (with some red) shales and brown sandstones above the grass cover are the New Fork Tongue of the Wasatch Formation. The light colored marlstone, shale, and sandstone sequence at the top is the Laney Member of the Green River Formation. The complete sequence of the Wasatch and Green River formations described here can be seen on the slopes of the prominent white-capped hills to the northwest, west, and east as you continue south on Highway 189.

Green River Basin and Lake Gosiute

Roughly 46 to 54 million years ago (early to middle Eocene Epoch), basin downwarping resulted in the development of a large hydrogeographic basin approximately 1,000 feet (305 m) above sea level in southwestern Wyoming, as well as small parts of the adjacent states of Colorado and Utah. Within this basin, a lake formed, covering a maximum of 15,500 square miles (40,155 square km), and known as Lake Gosiute (Surdam and Wolfbauer, 1975). It was fed by numerous meandering drainages that originated in the nearby tectonic highlands. Within this lake and the two nearby Eocene lakes were deposited some of the largest accumulations of lacustrine sedimentary rocks in the world, the Green River Formation. This formation, with an average thickness of 2,000 feet (610 meters), is characterized by light gray-brown-buff dolomitic marlstones and shales often containing organic material; the latter exemplified by kerogen-rich oil shales. Climate during early to middle Eocene time ranged from warm-temperate to subtropical with an average overall temperature of 59 to 70 °F (15 to 21 °C). Climatic and sedimentologic fluctuations resulted in variations in the size and chemistry of Lake Gosiute, which is thought to represent an extensive playa lake (Surdam and Wolf-

bauer, 1975). Variations in the nature of this lake are reflected by the deposits of the members of the Green River Formation (Bradley, 1964). The Fontenelle Tongue and the Laney Member represent high stands of fresh water in the lake in the northwestern Green River Basin. Lake Gosiute teemed with life at these times. During deposition of the New Fork Tongue of the Wasatch Formation, deposition within the lake (as represented by deposits of the Wilkins Peak Member) was restricted to one-third of its maximum size. The hypersaline lake contained a paucity of life at that time and evaporites were precipitated. After the last high stand of the lake in middle Eocene time, sediments derived from local highlands filled the lake until it disappeared. Middle Eocene fluvial sediments from the Bridger Formation overlie the upper lacustrine deposits of the Green River Formation.

Deposition of the Green River Formation was contemporaneous with that of the Eocene Wasatch Formation, the various members of which underlie and interfinger with the lake deposits of the Green River Formation (see Bradley, 1964; Oriel, 1961). The lithologically heterogeneous, variegated beds of the Wasatch Formation represent fluviatile deposition into the Green River drainage basin marginal to the Green River lakes during early Eocene time. In the northwestern Green River Basin, the Wasatch Formation consists of three members. The lowest is the Chappo Member similar to that described above in the Hoback Basin. Above the Chappo Member is the La Barge Member, consisting of variegated mudstones, sandstones, and siltstones. Conglomeratic and calcareous units are also present. The Chappo and La Barge members are contemporaneous with the Main Body of the Wasatch Formation. Above the La Barge Member is the New Fork Tongue of the Wasatch Formation. The La Barge Member is separated from the New Fork Tongue by the Fontenelle Tongue of the Green River Formation. The New Fork Tongue consists of variegated mudstones with numerous layers of light colored, very fine- to medium-grained sandstones. Conglomeratic lenses are also present.

The following genera of mammals have been found in the La Barge Member of the Wasatch Formation between La Barge and Big Piney. Those genera followed by an * indicate genera also found in the New Fork Tongue of the Wasatch Formation slightly east of this area (after Gazin, 1952, 1962).

CLASS MAMMALIA
- Order Marsupialia
  - Family Didelphidae
    - *Peratherium*
- Order Leptictida
  - Family Leptictidae
    - *Diacodon* *
- Order Tillodontia
  - Family Esthonychidae
    - *Esthonyx* *
- Order Pantodonta
  - Family Coryphodontidae
    - *Coryphodon*
- Order Dinocerta
  - Family Uintatheriidae
    - *Bathyopsis* * (not found in the La Barge Member)
- Order Taeniodontia
  - Family Stylinodontidae
    - Genus and species indet.
- Order Primates
  - Family ?Microsyopsidae
    - *Microsyops*
  - Family Adapidae
    - *Pelycodus*
    - *Notharctus*
  - Family Omomyidae
    - *Absarokius*
    - *Tetonius*
- Order Creodonta
  - Family Hyaenodontidae
    - *Sinopa* *
    - *Proviverra*
    - *Prolimnocyon*
  - Family Oxyaenidae
    - *Ambloctonus* *
    - *Oxyaena*
- Order Carnivora
  - Family Miacidae
    - *Miacis*
    - *Didymictis*
    - *Vulpavus*
    - *Uintacyon*
  - Family Viverravidae
    - *Viverravus*
- Order Rodentia
  - Family Paramyidae
    - *Paramys*
  - Family Sciuravidae
    - *Sciuravus*
    - *Tillomys*
- Order Condylarthra
  - Family Arctocyonidae
    - *Thryptacodon*
  - Family Hyopsodontidae
    - *Hyopsodus* *
  - Family Phenacodontidae
    - *Phenacodus*
  - Family Meniscotheriidae
    - *Meniscotherium* *
- Order Artiodactyla
  - Family Dichobunidae
    - *Diacodexis*
    - *Hexacodus*
    - *Bunophorus*

Order Mesonychia
Family Mesonychidae
Pachyaena * (not found in the La Barge Member)
Order Perissodactyla
Family Equidae
Hyracotherium *
Family Helaletidae
Heptodon *
Hyrachyus *
Family Brontotheriidae
Lambdotherium *
Order Incertae Sedis, Suborder Palaeanodonta
Family Epoicotheriidae
Pentapassalus

Near La Barge, on the slopes to the west, are grass-covered Fontenelle shales overlain by green shales and brown sandstones of the New Fork Tongue, capped by white marlstone and shales of the Laney Member. Across the Green River to the southeast, the La Barge-Fontenelle contact dips south into the river. On the hill slopes above the river are the Fontenelle and New Fork members capped by Laney Shale. The Fontenelle and New Fork contact crosses the road several miles south of La Barge. Massive sandstones and green and red shales on the hill slope to the west are in the New Fork Tongue. Outcrops on the cliff east of the river are New Fork and Laney members.

Stop 2. Names Hill

Names of early Oregon Trail pioneers dating back to the 1850s are inscribed on the sandstone cliff of the New Fork Tongue of the Wasatch Formation. This area was a favorite camping place of pioneers at one of several crossings of the Green River along the Oregon Trail. Names Hill, or "Calender of the West", is a landmark on the Sublette Cutoff of the Oregon Trail (which shortened the route traveled by 65 miles). The sandstone outcrop of the New Fork Member of the Wasatch Formation contains the names and initials of hundreds of emigrants who passed this way. The earliest signature is 1825. Indians were also known to leave pictographs on Names Hill (Wyoming Recreation Commission, 1988). The most notable inscription is "Jim Bridger, Trapper, 1844." Bridger was a famous mountain man, explorer and scout. However, Jim Bridger was illiterate and signed his name with an "X", so someone probably carved this for him.

Names Hill to Fossil Butte National Monument

Names Hill to Kemmerer via Highway 189

Exposures of the New Fork and Laney members of the Wasatch and Green River formations respectively can be seen for several miles south of Names Hill. Excellent outcrops of the Laney Shale can be see on cliffs south of the highway and northeast of the river. The lake in the valley is the Fontenelle Reservoir formed by the Fontenelle Dam across the Green River. The Green River was called the Seeds-ke-dee-Agie (Prairie Chicken River) by the Shoshone Indians. The Astorians termed it the Spanish River near its headwaters and the Spaniards referred to it as the the Rio Verde (Green River) to the south. The forks of the Green River (La Barge, Hams, Blacks, Smith, Henry, etc.) commemorate the names of the early explorers in this area. The argillaceous siltstones of the Eocene Bridger Formation overlie the Green River Formation to the south.

Continue on Highway 189 southbound toward Kemmerer. Along the last 20 miles into Kemmerer, exposures of the Jurassic Nugget Sandstone and Twin Creek Formation; Jurassic-Cretaceous Beckwith Formation; Cretaceous Bear River, Frontier, and Adaville formations and Aspen and Hilliard shales; and Eocene Green River and Wasatch formations crop out along Slate Creek. Outside the town of Frontier is the type locality for the Frontier Formation. Continue on Highway 189 to the city limits of Kemmerer.

The founder of Kemmerer, Patrick J. Quealy, interested Mahlon S. Kemmerer of Pennsylvania in organizing the Kemmerer Coal Company in the late 1890s. Coal had been discovered in the Cretaceous units of this area in the late 1860s. The first mining operations began in 1897. The town became the headquarters for the Oregon Short Line (U.P.R.R.). With the creation of Lincoln County in 1911, it became the county seat. Kemmerer was built where the railroad crossed the Ham's Fork of the Green River. James Cash Penney opened his first store (then known as the Golden Rule Store) here April 14, 1902.

Kemmerer to Fossil Butte National Monument via Highway 30

At the intersection of Highway 189 and Highway 30 follow Highway 30 to the west. Cretaceous Hilliard Shale and Adaville Formation are exposed in this area. Pass the Pittsburg-Midway Coal Company mine to the south; it is the largest open pit coal mine in the United States. It is approximately 700 feet (215 m) deep, and

is projected to go as deep as 1,000 feet (305 m). Close to 4,000,000 tons of coal are produced annually from this mine. The coal is mined from multiple seams within the Adaville Formation. Within this mine, dinosaur tracks have also been discovered.

Continue on Highway 30 to the west. Pass by exposures of the Upper Cretaceous and early Tertiary Evanston Formation. This unit consists of drab mudstones, siltstones, sandstones, and conglomerates. The lower part of this formation contains dinosaur remains, leaves, and pollen indicating a Late Cretaceous age. The upper part of this unit contains Torrejonian and Tiffanian age mammal remains.

The following mammal genera are known from the Evanston Formation in the Fossil Basin (after McGrew and Casilliano, 1975).

CLASS MAMMALIA
- Order Multituberculata
  - Family Ectypodontidae
    - *Neoplagiaulax*
    - *Ectypodus*
  - Family Ptilodontidae
    - *Ptilodus*
- Order Insectivora
  - Family Adapisoricidae
    - *Leptacodon*
  - Family Pentacodontidae
    - *Aphronorus*
- Order Pantodonta
  - Family, genus, and species indet.
- Order Primates
  - Family Plesiadapidae
    - *Plesiadapis*
    - *Pronothodectes*
  - Family Paromomyidae
    - *Torrejonia*
- Order Carnivora
  - Family Miacidae
    - *Didymictis*
- Order Condylarthra
  - Family Arctocyonidae
    - *Thryptacodon*
    - *Chriacus*
    - *Tricentes*
    - *Claenodon*
  - Family Hyopsodontidae
    - *Litomylus*
    - *Haplaletes*
  - Family Phenacodontidae
    - *Phenacodus*
  - Family Meniscotheriidae
    - *Ectocion*
  - Family Mioclaenidae
    - *Litaletes*
    - *Promioclaenus*

Continue west on Highway 30. Ahead are the variegated red, purple, and gray beds of the Wasatch Formation overlain by the buff-white beds of the Green River Formation. Continue west to the junction of Highway 30 and the road to Fossil Butte National Monument. Take road to the north to the Visitor's Center at Fossil Butte National Monument.

Fossil Basin and Fossil Lake

Fossil Basin or Fossil syncline is a relatively small north-south oriented structural basin. Oyster Ridge separates Fossil Basin from the main part of the Green River Basin; both were separate basins of deposition in the Eocene.

Fossil Lake is one of the three extinct lakes preserved within deposits of the Green River Formation. The Green River Formation represents one of the earliest fresh water lake systems of North America that supported a modern (teleost) fish fauna (Grande, 1984). It was the shortest lived of the three lakes, being confined to the early Eocene (late Wasatchian and possibly Lost Cabinian; roughly 2 million years). Fossil Lake had the smallest surface area but the greatest depth of the three lakes. Fossil Lake appears to have expanded and contracted several times. Its deposits have produced the most taxonomically diverse assemblage of complete vertebrate fossils known from the Green River Formation (Grande, 1989). Vertebrate fossils from this lake are very well preserved. The Green River Formation in this area consists of 220 layers, sixty of which contain fossils. Roughly 28 species of fish are known from the Green River Formation.

Two members are recognized in the Green River Formation in Fossil Basin. The upper is the Angelo Member, which caps Fossil Butte. It has a maximum thickness of 200 feet (60 m). The lower member is the Fossil Butte Member, which is 200 to 250 feet (60-80 m) thick at the center of the lake. The main fossil-bearing units are in the Fossil Butte Member. The two main fish-bearing units in this member are locally named the "18-inch" layer (F-1 of Grande, 1984) and the "split-fish" layer (F-2 of Grande, 1984). The F-1 horizon is a laminated, whitish to buff-colored calcite limestone with well-differentiated light to dark brown laminae of fine organic material. It lies near the top of the Fossil Butte Member and averages between 15 and 20 inches (40 and 50 cm). These laminae may represent annual cycles of deposition. If these represent varves, then the F-1 horizon may represent as much as 4,000 years of deposition (Grande, 1984). However, the exact nature of these laminae remains in question (Buchheim and

Eugster, 1989). The unit is conformably bounded above and below by several inches of dark oil shale and organic-rich black limestones. These bounding units contain abundant plant, insect, and molluscan fossils. The F-1 layer represents the deep area of the lake far from shore. The lake may have been chemically or thermally stratified during deposition of this layer. The fossil-bearing units within Fossil Butte National Monument are all within the F-1 horizon.

The F-2 layer is a light colored limestone and marl only faintly laminated or massive and unlaminated. The matrix is almost pure calcite, with less preserved microorganic material. It is approximately 7 feet (2 m) thick. It is overlain by a massive mollusk-rich marlstone. F-2 has a diverse benthic fauna compared to the F-1 layer (i.e., stingrays, crayfish, shrimp, snails). This suggests better circulation of bottom waters than the environment represented by the F-1 deposits. The F-2 beds are interpreted as being deposited in a nearshore lacustrine environment, contemporaneous with the deeper water deposits of the F-1 layer (Grande, 1989).

Fossil Butte Member flora and fauna

PLANTS
(after Grande, 1984)

CLASS GYMNOSPERMAE
- Order Coniferales
  - Family Pinaceae
    - *Pinus* sp.

CLASS ANGIOSPERMAE
- Order Monocotyledonae
  - Family Typhaceae
    - *Typha* sp.
  - Family Palmae
    - *Sabalites* sp.
- Order Dicotyledonae
  - Family Salicaceae
    - *Populus cinnamomoides*
    - *P. wilmattae*
  - Family Fagaceae
    - *Quercus castaneopsis*
  - Family Ulmaceae
    - *Zelkova nervosa*
  - Family Rosaceae
    - *Prunus* sp.
  - Family Leguminosae
    - *Swartzia wardelli*
    - *Mimosites* sp.
  - Family Simaroubaceae
    - *Ailanthus* sp.
  - Family Burseraceae
    - *Bursera* sp.
  - Family Euphorbiaceae
    - Aleurites glandulosa
  - Family Anacardiaceae
    - *Astronium truncatum*
    - *Rhus nigricans*
    - *Sapindus* sp.
  - Family Aceraceae
    - *Acer lesquereuxi*
  - Family Sterculiaceae?
    - *Sterculia coloradensis*
  - Family Verbenaceae
    - *Holmskioldia speirii*

INVERTEBRATES
(after Grande, 1984; Oriel and Tracey, 1970)

CLASS BIVALVIA
- Order Unionacea
  - Family Unionidae
    - *Plesielliptia* sp.

CLASS GASTROPODA
- Order Mesogastropoda
  - Family Viviparidae
    - *Viviparus pauludinaeformis*
    - *Viviparus* cf. *V. trochiformis*
  - Family Pleuroceridae
    - *Goniobasis* sp.
- Order Basommatophora
  - Family Physidae
    - *Physa pleromatis*
- Order Stylommatophora
  - Family Bulimulidae
    - *Oreoconus* sp.

PHYLUM ANNELIDA
- Order, family, genus, species undescribed

PHYLUM ARTHROPODA

SUPERCLASS CRUSTACEA

CLASS OSTRACODA
- Order Podocopida
  - Family Cypridacae
    - *Hemicyprinotus watsonensis*
    - *Procyprois ravenridgensis*
    - *Pseudocypris* sp.

CLASS MALACOSTRACA
- Order Decapoda
  - Family Astacidae
    - *Procambarus primaevus*
  - Family Palaemonidae
    - *Bechleja rostrata*

SUPERCLASS HEXAPODA

CLASS INSECTA
- Order Homoptera
  - Family Fulgoridae
    - Genus and species undescribed
- Order Diptera?
  - Family Bibionidae
    - *Plecia pealei*

Order Coleoptera
Family Curculionidae
Eugnamptus sp.

VERTEBRATES
(after Grande, 1984)

CLASS CHONDRICHTHYES
Order Rajiformes
Family Dasyatidae
Heliobatis radians

CLASS OSTEICHTHYES
Infraclass Paleopterygii
Order Acipenseriformes
Family Polyodontidae
Crossopholis magnicaudatus
Infraclass Neopterygii
Order Amiiformes
Family Amiidae
Amia uintaensis
A. fragosa
Order Lepisosteiformes
Family Lepisosteidae
Lepisosteus simplex
L. atrox
L. cuneatus
Order Osteoglossiformes
Family Hiodontidae
Eohiodon falcatus
Family Osteoglossidae
Phareodus encaustus
P. testis
Order Clupeiformes
Family Clupeidae
Knightia eocaena
K. alta
Order Ellimmichthyiformes
Family Ellimmichthyidae
Diplomystis dentatus
Order Gonorynchiformes
Family Gonorynchidae
Notogoneus osculus
Order Siluriformes
Family Ictaluridae
Astephus antiquus
Order Percopsiformes
Family Percopsidae
Amphiplaga brachyptera
Order Incertae Sedis
Family Asineopidae
Asineops squamifrons
Order Perciformes
Family Percidae
Mioplosus labracoides
?M. suavagenus
Family Priscacaridae
Priscacara serrata
P. liops

CLASS AMPHIBIA
Order Urodela
Family, genus, and species undescribed

CLASS REPTILIA
Order Chelonia
Family Trionychidae
Trionyx sp.
Family Emydidae
Echmatemys sp.
Family Chelydridae
Genus and species undescribed
Family Baenidae
Genus and species undescribed
Order Squamata
Suborder Lacertilia, Family Varanidae
Genus and species undescribed
Suborder Serpentes, Family Boidae
Boavus idelmani
Order Crocodilia
Family Crocodylidae
Leidyosuchus sp.

CLASS AVES
Order Pelicaniformes
Family Fregatidae
Limnofregata azygosternon
Order Galliformes
Family Gallinuloididae
Gallinuloides wyomingensis
Order Coraciiformes
Family Primobucconidae
Primobucco mcgrewi
P. olsoni
Neanis schucherti
N. kistneri
Order Gruiformes
Family, genus, and species undescribed

CLASS MAMMALIA
Order Chiroptera
Family Icaronycteridae
Icaronycteris index
Order Perissodactyla
Family Equidae
Genus and species undescribed

The relative abundances of fish genera from the F-1 Fossil Lake deposits follows (after Grande, 1984, 1989). *Heliobatis* is rare (less than 1% of the total fish population); *Lepisosteus, Amia, Crossopholis, Astephus, Amphiplaga, Asineops,* and *Eohiodon* are extremely rare (known only from a few specimens); *Knightia* and *Diplomystus* are very common (between 25% and 50% of total fish population); and *Phareodus, Notogoneus,* and *Mioplosus* are uncommon (between 1% and 5% of total fish population). *Priscacara* is common to very common. Relative to this, *Heliobatis, Crossopholis,*

Eohiodon, Phareodus, Amphiplaga, and *Knightia* are more common in the F-2 Fossil Lake deposits. *Notogoneus* and *Priscacara* are less common in these units. F-1 deposits tend to produce more large (>15 in/ >38 cm) specimens of *Diplomystus* and large (>12 in/ >30 cm) *Mioplosus* than the nearshore F-2 deposits. Fossil plants and insects are much more common in F-1 than in F-2 (probably the result of differential preservation). F-1 has no decopod crustaceans (in contrast to F-2). *Goniobasis* is the common snail in the F-1 zone, but *Viviparus* is the common variety in F-2 deposits.

Below the Green River Formation in this area, is the brightly colored Wasatch Formation. The highly variegated unit consists of the following seven members in the Fossil Basin (McGrew and Casilliano, 1975): (1) Basal Conglomerate Member (channel deposit), (2) Lower Member (floodplain and stream deposited mudstones and siltstones), (3) Main Body (variegated, lithologically variable unit that makes up the spectacular badlands topography in Fossil Butte National Monument), (4) Sandstone Tongue, (5) Mudstone Tongue, (6) Bullpen Member (uppermost member), and (7) Tunp Member (a marginal basin unit). These deposits represent the ancient floodplains surrounding Fossil Lake.

The following genera of mammals have been found in the Wasatch Formation of the Fossil Basin. Those genera that have been found at Fossil Butte are followed by an * (after McGrew and Casilliano, 1975; Gazin, 1962).

CLASS MAMMALIA
- Order Leptictida
  - Family Leptictidae
    - *Diacodon* *
- Order Tillodontia
  - Family Esthonychidae
    - *Esthonyx*
- Order Pantodonta
  - Family Coryphodontidae
    - *Coryphodon* *
- Order Primates
  - Family Adapidae
    - *Pelycodus* *
  - Family ?Microsyopidae
    - *Microsyops*
- Order Creodonta
  - Family Hyaenodontidae
    - *Sinopa* *
    - *Proviverra*
- Order Carnivora
  - Family Miacidae
    - *Didymictis* *
    - *Vulpavus*
    - *Vassacyon* *
- Order Rodentia
  - Family Paramyidae
    - *Paramys*
    - *Reithroparamys* *
- Order Condylarthra
  - Family Hyopsodontidae
    - *Hyopsodus* *
    - *Haplomylus*
  - Family Phenacodontidae
    - *Phenacodus*
  - Family Meniscotheriidae
    - *Meniscotherium?* *
- Order Artiodactyla
  - Family Dichobunidae
    - *Diacodexis*
    - *Hexacodus* *
    - *Protodichobune*
- Order Mesonychia
  - Family Mesonychidae
    - *Pachyaena*
- Order Perissodactyla
  - Family Equidae
    - *Hyracotherium* *
  - Family Helaletidae
    - *Heptodon* *

Stop 3. Fossil Butte National Monument

Fossil Butte National Monument was established in 1972 by the U. S. Department of the Interior, National Park Service to commemorate one of the most extensive concentrations of fossilized fish in the United States, and one of only a few such areas anywhere in the world. It was the third national monument to be established in Wyoming. The first being Devils Tower National Monument established in 1906 and the second being Shoshoni Caverns National Monument established in 1909. The latter is no longer a national monument. Fossil Butte National Monument encompasses 8,180 acres of land. The top of the butte is over 1,000 feet (305 m) above the Twin Creek Valley (see **Figure 3**).

Fossil Butte was first described in Hayden's Survey Report of 1879 by A. C. Peale. Specimens collected by Peale were later described by Cope, Lesquereux, and Scudder. By 1897, fossil hunters such as Lee Craig, Samuel C. Small, and David C. Haddenham were collecting in the Fossil Butte Member of the Green River Formation. These fossils were sold to collectors, locals, tourists, and museums around the world. "After 100 years of concerted collecting, there is still an untapped resource to be collected and studied" (Grande, 1984).

Figure 3. Fossil Butte National Monument. Light colored beds are the Eocene Green River Formation; darker beds below are the Eocene Wasatch Formation.

Knightia: The Wyoming State Fossil

Wyoming's state fossil, *Knightia* is found commonly in the distinctive shales of the Fossil Butte Member of the Green River Formation. *Knightia* was a small (1-10 in/2.5-25 cm long), herring-like fish that probably ate algae, diatoms, ostracodes, insects, and occasionally smaller fish, and was eaten in turn by many of the larger fish that lived in the Eocene Epoch lakes (Grande, 1982). Apparently a schooling fish, it often is found in mass mortality layers, composed of hundreds of individuals overlapping and randomly arranged in a horizontal plane. These accumulations, that probably represent mass die-offs, may have resulted from the fish's inability to acclimate to fluctuating water temperatures.

Knightia, was the first described vertebrate fossil from Wyoming. In 1856 Dr. John Evans uncovered the remains of a small, herring-like fish in the buff-white, fine-grained, horizontally-bedded rocks that crop out along the Green River near the present town of Green River, Wyoming. Dr. Evans was a geologist on Dr. Ferdinand Vandiveer Hayden's Survey of the Territories working in what is now southwestern Wyoming. Hayden took the specimen to the Pennsylvanian anatomist Dr. Joseph Leidy at the Philadelphia Academy of Sciences for identification. Leidy named it *Clupea humilis* and described it in 1856 (Leidy, 1856; see **Figure 4**). Professor Hayden named the calcareous rocks that yielded the fossil the Green River Shales (Formation) in 1869 (Hayden, 1869).

Additional fossil fish from the Green River Shales in western Wyoming (including the Twin Creek site, now Fossil Butte National Monument), northeastern Utah, and northwestern Colorado were studied by Edward Drinker Cope (a paleontologist working in Philadelphia) in the early 1870s. In 1877, Cope (1877a,b,c) changed Leidy's name *Clupea humilis* to *Diplomystus humilis*, as the name, *C. humilis*, had been used 29 years earlier to describe another fish (Meyer, 1848). However, later he realized that the genus *Diplomystus* was composed of two distinct forms (Cope, 1883). Cope separated out one form based on Leidy's *Clupea humilis* and synonomized it with his *Clupea pusillae*, named in 1870 (Cope, 1870). Unfortunately, this name had also been used previously (Mitchill, 1815). Finally in 1907, Professor D. S. Jordan redescribed the form described by Leidy and Cope and named it *Knightia eocaena*; "in honor of the late Wilbur Clinton Knight, of the University of Wyoming, an indefatigable student of the palaeontology of the Rocky Mountains" (Jordan, 1907).

Knightia has been found in Colorado, Utah, Montana, and possibly China, Brazil, and the Isle of Wight.

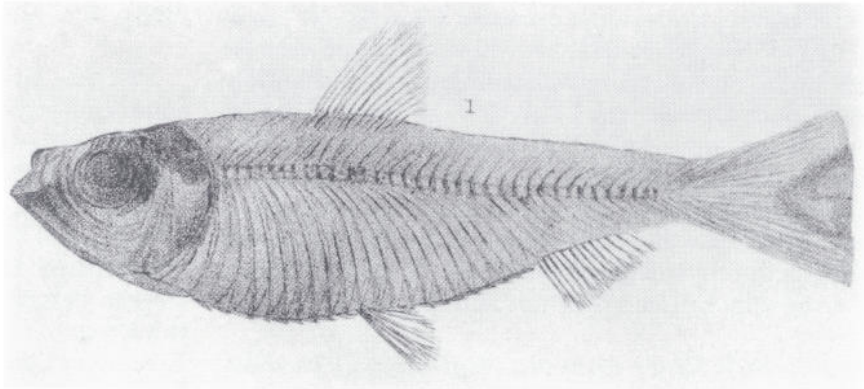

Figure 4. *Knightia eocaena*, originally described by Leidy in 1856 as *Clupea humilis*. (from Plate 18, Leidy, 1873).

It is one of the most common fossils to be found in the ancient lake deposits of the Green River Formation and "is one of the most common complete vertebrate fossils in the world" (Grande, 1984). On May 22, 1987, *Knightia* was adopted as Wyoming's State Fossil.

Fossil Butte National Monument to James E. Tynsky Quarry

Leave Fossil Butte National Monument, travel by Fossil, Wyoming. Founded in 1881, Fossil was a station servicing the Oregon Shortline Railroad. This railroad annexed the Union Pacific Railroad at Granger, Wyoming and ran to Huntington, Oregon (see Linville, 1989). It was named for the extensive fossil deposits found in this area. As the Fossil Basin was an excellent area for grazing, Fossil became an important cattle shipping station. Coal was discovered a short distance to the east of here; oil was discovered in this area in 1885. Travel on Highway 30 east towards Kemmerer and take a private road north onto the Lewis Ranch. Permission by the landowner is required to drive on this road and to enter the quarry.

Stop 4. James E. Tynsky Quarry

Located in the Fossil Butte Member of the Green River Formation of the Fossil Basin, is the Lewis Ranch Quarry #1. It represents a deep-water, far-from-shore paleoenvironment. This quarry is currently leased to commercial fossil quarriers, James E. and Karen Tynsky. It is located a few miles south-southeast of Fossil Butte National Monument. The horizon mined for fossils at this site is the "18-inch" layer (F-1 layer of Grande, 1984). F-1 deposits are quite extensive in the Fossil Basin area. This is just one of many fossiliferous localities in the "18-inch" layer. The tailings and disturbance of other commercial collectors are visible on the hillsides of this area.

According to Grande (1989), in general the faunal differences between the two contemporaneous Fossil Lake horizons (F-1 and F-2) reflect the contrasting paleohabitats of the off-shore and near-shore areas of the lake during the early Eocene. Reasons for the major faunal differences between these deposits and the somewhat younger (possibly 2-3 million years) main fossiliferous deposits of lakes Gosiute and Uinta are unclear and may be due to environmental differences causing ecological barriers to specific taxa or geographic barriers between taxa, and/or differences in evolution of the community through extinction and immigration (Grande, 1989).

Tynsky Quarry to Salt River Pass

Tynsky Quarry to Sage via Highway 30

Rejoin Highway 30 and travel west to Sage. Exposures of Permian Phosphoria Formation; Triassic Dinwoody Formation, Woodside Shale, Ankareh Shale and Thaynes Limestone; Jurassic Twin Creek Limestone and Nugget Sandstone (this is the type area for this unit), Jurassic-Cretaceous Beckwith Formation; and Lower Cretaceous Cokeville and Sage Junction formations can be seen along this route. Wasatch Formation (Tunp and Bullpen members) caps some of the hills in this area. Just before Sage Junction (Intersection of Highway 30 and Highway 89), see an 1875 coal mine in the Bear River Formation. Wasatch Formation caps the hill and overlaps this formation.

Sage to Salt River Pass via Highways 30 and 89

Travel north on Highway 30 out of Sage to Cokeville and Border. At Border, continue north on Highway 89 to Salt River Pass. Folded and faulted Paleozoic and Mesozoic rocks can be seen east of the highway between Sage and Salt River Pass. The Wasatch Formation unconformably caps some of these.

Stop 5. Salt River Pass

At Salt River Pass (elevation 7,610 ft/2,319 m), a commemorative plaque discusses the Lander Cutoff. It was an emigration route and the first military road constructed west of the Mississippi River. Roughly 10,000 people used this trail. Constructed in 1858 by a detachment of men under the command of Colonel Frederick W. Lander, it provided a shorter route to the Oregon Territory and the California gold fields. It left the Oregon Trail at Burnt Ranch on the Sweetwater River near South Pass City and rejoined it northeast of Pocatello at Ross Fork Creek. The Lander Cutoff trail crosses the highway near Smoot. Another plaque at Salt River Pass discusses Periodic Spring, a large

seasonally fluctuating periodic spring. The unusual flow is caused by the associated cavern geometry. It is located 4 miles east of Afton. The Salt River Range can be seen to the east.

Salt River Pass to Jackson

Continue on Highway 89 through Smoot, Afton, and Grover. The Star Valley Narrows border the highway outside of Grover with exposures of Twin Creek Limestone. Continue north on the highway past the Star Valley rest stop. Star Valley was first inhabited by Shoshone and Blackfoot or Crow Indians. The first white men to descend into this valley were the Astorians, led by Wilson Price Hunt in 1812. This was a rich fur trapping area and was exploited by the Hudson Bay Company until the decline of the fur trade in 1840. Because of the topographic features and high precipitation, this is one of the most productive and diverse wildlife areas in Wyoming. Continue on Highway 89 through Thayne, Freedom (named because the early settlers came to the valley to escape persecution for polygamy), and Etna onto Alpine Junction. Along the banks of Salt River, just before Alpine Junction, are exposures of the white, middle Pliocene Teewinot Formation. From Alpine Junction, travel up the Snake River Canyon to Hoback Junction on Highway 26-89. At Hoback Junction, travel north on Highway 191 to Jackson.

References

Bradley, W. H., 1964, Geology of the Green River Formation and associated Eocene rocks in southwestern Wyoming and adjacent parts of Colorado and Utah: U. S. Geological Survey Professional Paper 496-A, p. A1-A86.

Buchheim, H. P. and Eugster, H. P., 1989, Depositional environments of oil shales and associated lithofacies within the Eocene Green River Formation of Fossil Basin, Wyoming: unpublished manuscript, 66 p.

Cope, E. D., 1870, Observations on the fishes of the Tertiary Shales of Green River, Wyoming Territory: American Philosophical Society, Proceedings, v. 11, p. 380-384.

Cope, E.D., 1877a, A contribution to the knowledge of the ichthyological fauna of the Green River Shales, *in* Hayden, F. V. (geologist-in-charge), United States Geological and Geographical Survey of the Territories Bulletin, v. 3, art. 34: Department of the Interior, Government Printing Office, Washington, D.C., p. 807-819.

Cope, E.D., 1877b, New fossil fishes from Wyoming: American Naturalist, v. 11, p. 570.

Cope, E.D., 1877c, Verbal communication on a new locality of the Green River Shales containing fishes, insects and plants in a good state of preservation: Palaeontological Bulletin, no. 25, p. 1.

Cope, E.D., 1883, The Vertebrata of the Tertiary formations of the West, *in* Hayden, F. V. (geologist-in-charge), 1884, Report of the United States Geological Survey of the Territories, v. 3: Department of the Interior, Government Printing Office, Washington, D.C., 1002 p.

Dorr, J. A., Jr., 1952, Early Cenozoic stratigraphy and vertebrate paleontology of the Hoback Basin, Wyoming: Geological Society of America Bulletin, v. 63, p. 59-94.

Dorr, J.A., Jr., 1958, Early Cenozoic vertebrate paleontology, sedimentation, and orogeny in central western Wyoming: Geological Society of America Bulletin, v. 69, p. 1217-1244.

Dorr, J.A., Jr., 1969, Mammalian and other fossils, early Eocene Pass Peak Formation, central western Wyoming: University of Michigan, Museum of Paleontology Contributions, v. 22, no. 16, p. 207-219.

Dorr, J.A., Jr., 1977, Partial skull of *Paleosinopa simpsoni* (Mammalia. Insectivora), latest Paleocene Hoback Formation, central western Wyoming, with some general remarks on the Family Pantolestidae: University of Michigan, Museum of Paleontology Contributions, v. 24, no. 23, p. 281-307.

Dorr, J.A., Jr., 1978, Revised and amended fossil vertebrate faunal lists, early Tertiary, Hoback Basin,

Wyoming: University of Wyoming Contributions to Geology, v. 16, no. 2, p. 79-84.

Dorr, J. A., Jr., Spearing, D. R., and Steidtmann, J. R., 1977, Deformation and deposition between a foreland uplift and an impinging thrust belt: Hoback Basin, Wyoming: Geological Society of America Special Paper 177, p. 1-82.

Gazin, C. L., 1952, The lower Eocene Knight Formation of western Wyoming and its mammalian faunas: Smithsonian Miscellaneous Collections, v. 117, no. 18, 82 p.

Gazin, C.L., 1962, A further study of the lower Eocene mammalian faunas of southwestern Wyoming: Smithsonian Miscellaneous Collections, v. 144, no. 1, 98 p.

Grande, L., 1982, A revision of the fossil genus *Knightia*, with a description of a new genus from the Green River Formation (Teleostei, Clupeidae): American Museum of Natural History Novitates, no. 2731, p. 1-22.

Grande, L., 1984, Paleontology of the Green River Formation, with a review of the fish fauna: Geological Survey of Wyoming Bulletin 63, 333 p.

Grande, L.,1989, The Eocene Green River Lake System, Fossil Lake, and the history of the North American fish fauna, *in* Flynn, J. J., editor, Mesozoic/Cenozoic vertebrate paleontology: clastic localities contemporary approaches: 28th International Geological Congress Field Trip Guidebook T322, p. 18-28.

Guennel, G. K., Spearing, D. R., and Dorr, J. A., Jr., 1973, Palynology of the Hoback Basin: Wyoming Geological Association 25th Annual Field Conference Guidebook, p. 173-185.

Hayden, F. V., 1869, Third annual report of the United States Geological Survey of the Territories embracing Colorado and New Mexico, *in* Hayden, F. V. (geologist-in-charge), 1873, 1st, 2nd, and 3rd annual reports of the United States Geological Survey of the Territories for the years 1867,1868, 1869: Department of the Interior, Government Printing Office, Washington, D.C., p. 103-251.

Jordan, D. S., 1907, The fossil fishes of California; with supplementary notes on other species of extinct fishes: Department of Geology, University of California Bulletin, v. 5, p. 95-145.

Leidy, J.,1856, Notice of some remains of fishes discovered by Dr. John E. Evans: Academy of Natural Sciences of Philadelphia Proceedings, p. 256.

Leidy, J., 1873, Contributions to the extinct vertebrate fauna of the western territories, *in* Hayden, F. V. (geologist-in-charge), Report of the United States Geological Survey of the Territories: v. 1, Fossil vertebrates: Department of the Interior, Government Printing Office, Washington, D.C., 358 p.

Linville, M. D., 1989, Fossil, Wyoming: A trip through time and memories: Dinosaur Nature Association, Jensen, Utah, 14 p.

McGrew, P. O. and Casilliano, M., 1975, The geological history of Fossil Butte National Monument and Fossil Basin: National Park Service Occasional Paper No. 3, 37 p.

Meyer, H., von, 1848, Fossile Fische aus dem Tertiarthon von Unter-Kirchberg an der Iller: Palaeontographica, v. 2, p. 85-113.

Mitchill, S. L., 1815, The fishes of New York, described and arranged: Literary and Philosophical Society of New York Transactions, v. 1, p. 355-501.

Oriel, S. S., 1961, Tongues of the Wasatch and Green River formations, Fort Hill area, Wyoming: U.S. Geological Survey Professional Paper 424B, p. B151-B152.

Oriel, S. S. and Tracey, J. I., Jr., 1970, Uppermost Cretaceous and Tertiary stratigraphy of Fossil Basin, southwestern Wyoming: U.S. Geological Survey Professional Paper 635, p. 1-53.

Peale, A. C., 1879, Report on the geology of the Green River district, *in* Hayden, F. V. (geologist-in-charge), 11th annual report of the United States Geological Survey of the Territories: Department of the Interior, Government Printing Office, Washington, D.C., p. 509-646.

Surdam, R. C. and Wolfbauer, C. A., 1975, Green River Formation, Wyoming: a playa-lake complex: Geological Society of America Bulletin, v. 86, p. 335-345.

Wyoming Recreation Commission, 1988, Wyoming: A guide to historic sites: House of Printing, Casper, 327 p.

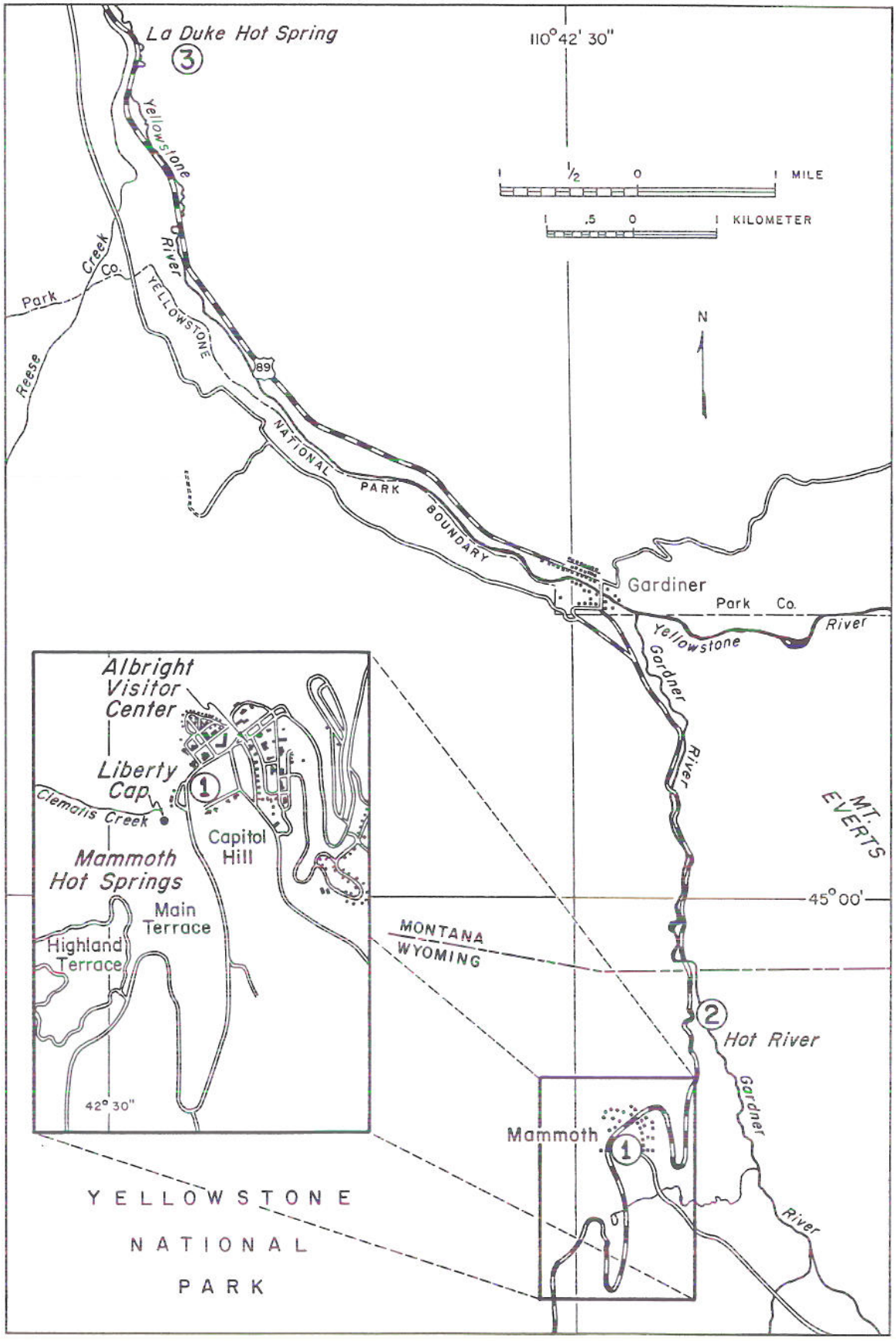

Figure 1. Trip route and stop locations, field trip no. 3.

Field trip no. 3

INVESTIGATIONS OF GEOTHERMAL CONNECTIONS, MERCURY ANOMALY MAPPING, NORTHERN BOUNDARY OF YELLOWSTONE NATIONAL PARK

Wayne L. Hamilton
Research Geologist
National Park Service
Yellowstone National Park

Trip summary (see Figure 1)

Stop 1. Mammoth Hot Springs area
Stop 2. Hot River
Stop 3. La Duke Spring

Introduction

This field trip covers the Mammoth Hot Springs area, the nearby Hot River in Yellowstone National Park, and the La Duke Spring, located 1.6 miles north of the park, where geothermal development is being considered on private land nearby. The results of an ongoing soil mercury investigation at these hot spring areas and along faults that connect them suggest that depletion of mercury anomalies along faults in the Norris-Mammoth-La Duke corridor can be used to infer reasonable directions of hydrothermal flow (Hamilton, et al., 1990) that are in agreement with flows inferred by other means (Clark and Turekian, 1990).

The investigation is part of a larger study in collaboration with the U.S. Geological Survey, in which we are attempting to determine the extent that geothermal development north of the park might affect significant thermal features in Yellowstone. Publication of results is planned shortly after the conclusions are reported to Congress by the U.S. Geological Survey at the end of 1990.

Stop descriptions

Stop 1. Mammoth Hot Springs area

The Mammoth Hot Springs area was described by Bargar (1978). Travertine fills gullies developed on early post-glacial topography, forming lobes that descend eastward toward the Gardner River. At McCartney Cave, a sinkhole near Albright Visitor Center, travertine thickness exceeds 110 feet. Intermittent surface-water discharge from Clematis Creek has infiltrated the travertine at Liberty Cap and, over time, has produced a system of solution channels and karst features that align with buried topography. Radon anomaly mapping (Colvard and Hamilton, 1988), alignment of warm vapor vents, and mercury anomalies suggest an association of hydrothermal flows with the principal solution channel between Liberty Cap and Hot River, 1 mile to the northeast. This alignment coincides with a concealed fault shown by U.S. Geological Survey (1972) mapping.

At Liberty Cap (at Mammoth Hot Springs), ascend halfway up the active travertine terraces on a boardwalk trail. The ephemeral character of these springs is probably a result of "piping" and rapid destruction of

pipes by reentry of cooled discharge into sinks. The traces of two concealed faults that supply these springs have associated mercury and radon anomalies. Capitol Hill, and other nearby mounds, are thermal kames. Several large sinkholes are evident in the level travertine sheet between this point and Albright Visitor Center. Radon venting is of such magnitude at Mammoth that the Park Service has been actively involved in remediation efforts to reduce concentrations of radon in park housing. Some structures had levels exceeding 100 pCi/l a few years ago.

Mammoth spring discharge temperature seldom exceeds 165° F. The calcareous, bicarbonate waters rapidly deposit travertine and some sodium bicarbonate. Chemically, Mammoth water appears to represent Norris-type water that has moved northward along extensional faults, encountering Madison Limestone at depth (Truesdell and Fournier, 1976). The chemistries of Mammoth and La Duke waters are so different that if faults in Yellowstone contribute hot water to the aquifer at La Duke, significant mixing of different waters must occur.

This is also a good vantage point for viewing the Upper Cretaceous section exposed on Mt. Everts to the east. It is capped by the Quaternary Huckleberry Ridge Tuff, representing Yellowstone's earliest silicic caldera eruption.

Stop 2. Hot River

The second stop, at Hot River, involves a 1.2-mile round-trip walk up the Gardner River, starting at the U.S. Geological Survey 45th-parallel gaging station. A popular bathing area, Hot River flows from a cave developed in the distal end of the main travertine lobe that descends from the Mammoth Terraces. It has long been recognized that some surface recharge at Mammoth enters solution channels in the travertine and rapidly finds its way into Hot River (Dole, 1914). Recent tracer studies have added important new information on this connection (Kharaka and others, 1989) and on a newly discovered sink, where Gardner River water mixes underground with thermal water and reemerges at Hot River. Debris flows to the east have aggraded the river channel, raising river level to a point where it has produced a solution channel in the travertine. The U.S. Geological Survey operates automated monitoring equipment at the point where Hot River emerges. Water temperature varies between 104° and 126° F, depending on the amount of dilution by river water and underflow from the Mammoth area.

Stop 3. La Duke Spring

This is a roadside stop. La Duke Spring is situated at the intersection of the Reese Creek and Gardiner faults (mapping of these faults is in progress). Reese Creek fault is a north-south normal fault in the Reese Creek canyon in Yellowstone, and Gardiner fault is a Laramide thrust that parallels U.S. Highway 89 northeast of Yellowstone River between Gardiner and La Duke. Hydrothermal sulfate and carbonate mineralization is evident in upturned Paleozoic strata above the spring. A geothermal well has been drilled on private land several hundred meters west of this location, across the Yellowstone River. During pumping tests on the well, discharge at La Duke practically ceased.

Discharge temperature is usually close to 136° F. The water is high in sulfate (1,200 ppm) and low in chloride (47 ppm). Sediment in the concrete spring box contains more than 1.8 ppm mercury. Soil mercury determinations on traverses crossing these and other faults trending northward across the park boundary suggest ways in which mercury-bearing waters may be mixed on their way to the La Duke area. La Duke and other hot springs in the north boundary area are now jointly monitored by the U.S. Geological Survey and the National Park Service.

References cited

Bargar, K.E., 1978, Geology and thermal history of Mammoth Hot Springs, Yellowstone National Park, Wyoming: U.S. Geological Survey Bulletin 1444, 55 p.

Clark, J.F., and Turekian, K.K., 1990, Reaction time scale of hot spring waters from the Norris-Mammoth corridor, Yellowstone National Park, based on radium isotopes and radon: Journal of Volcanology and Geothermal Research, in press.

Colvard, E.M., and Hamilton, W.L., 1988, Radon surveys, mercury surveys, and monitoring history in the north boundary geothermal study area [abstract], *in* Proceedings of the North Boundary Geothermal Area Symposium: U.S. Geological Survey-National Park Service, Mammoth Hot Springs, March, 1988, p. 2.

Dole, R.B., 1914, Report on sanitary conditions in the Yellowstone National Park: Report to the Secre-

tary of the Interior, Yellowstone National Park archives, 10 p.

Hamilton, W.L., Chambers, R.L., Colvard, E.M., and Hudgings, J.A., 1990, Mercury anomalies associated with hydrothermal systems in the Norris-Mammoth-La Duke corridor and Mud Volcano in and near Yellowstone National Park, Wyoming and Montana: [National Park Service Files], unpublished, 64 p.

Kharaka, Y.K., Ambat, G., Evans, W., and White, L.,1989, Tracer tests in the Mammoth-Hot River corridor, Yellowstone National Park, [abstract]: Proceedings of the Seventh Annual Yellowstone Physical Science Symposium, Mammoth Hot Springs, September, 1989, p. 3.

Truesdell, A.H., and Fournier, R.O., 1976, Conditions in the deeper parts of the hot spring systems of Yellowstone National Park, Wyoming: U.S. Geological Survey Open File Report 76-428, 29 p.

U.S. Geological Survey, 1972, Geologic map of Yellowstone National Park: U.S. Geological Survey Miscellaneous Investigations Map I-711, scale 1:125,000.

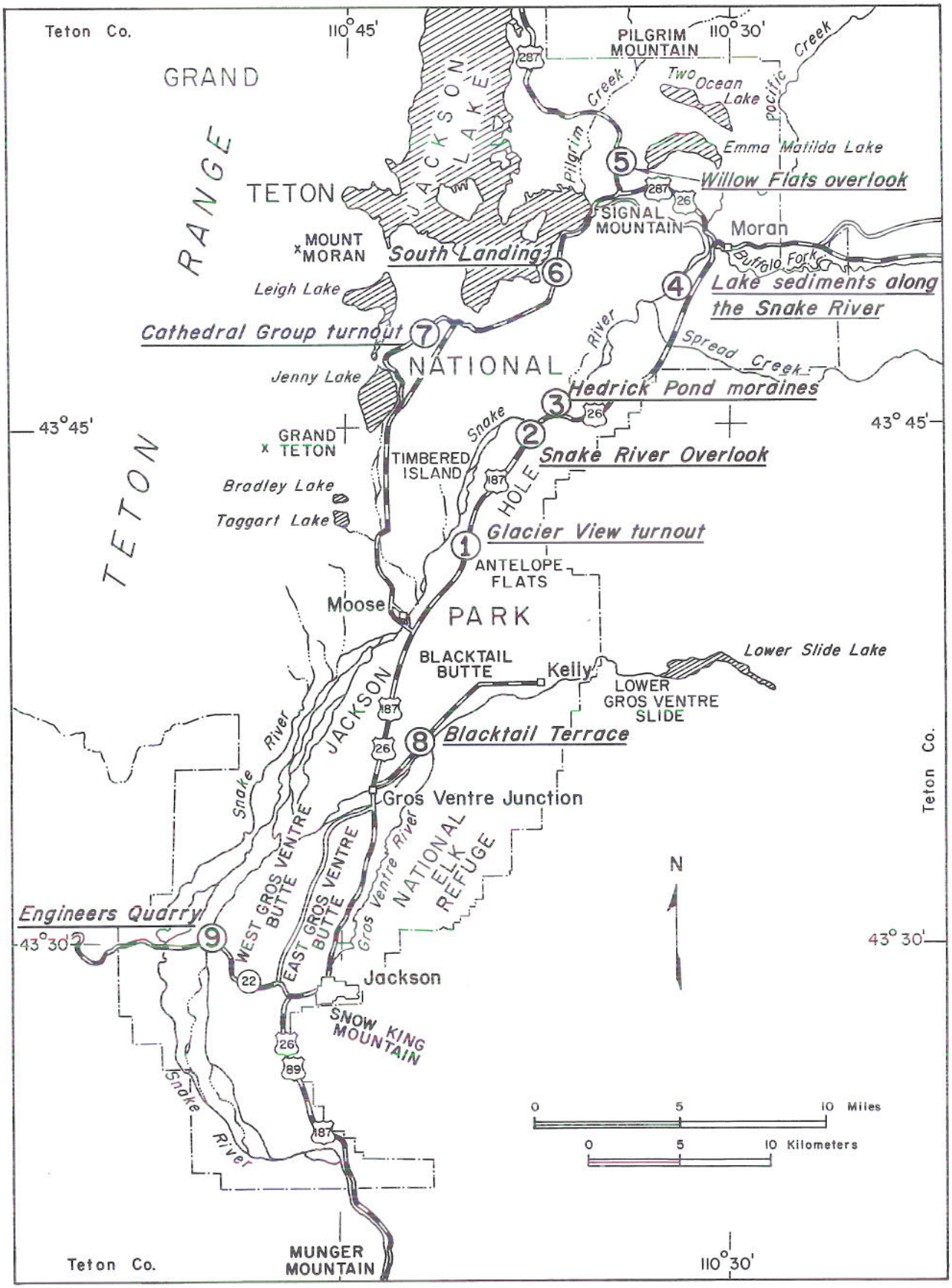

Figure 1. Trip route and stop locations, field trip no. 4.

Field trip no. 4

QUATERNARY GEOLOGY OF JACKSON HOLE, WYOMING

Kenneth L. Pierce
U.S. Geological Survey
Denver, Colorado 80225

and

John M. Good
National Park Service, Retired
Jackson, Wyoming 83001

Trip summary (see Figure 1)

Stop 1. Glacier View turnout
Stop 2. Snake River Overlook
Stop 3. Hedrick Pond moraines
Stop 4. Lake sediments along the Snake River
Stop 5. Willow Flats overlook
Stop 6. South Landing, Jackson Lake
Stop 7. Cathedral Group turnout
Stop 8. Blacktail Terrace
Stop 9. Engineers Quarry

Introduction

The stratigraphic names and the sequence of events for the later Quaternary geology of Jackson Hole are shown diagramatically on **Table 1**. In addition, a proposed correlation of the Jackson Hole sequence, with deposits and dated chronologies outside of Jackson Hole, is given on the left side of **Table 1**.

The main part of the field trip is to northern Jackson Hole, where we will examine three moraine/outwash systems, representing three phases of the last glaciation (Pinedale) that we relate to changes in the Yellowstone/Absaroka glacial source area (**Table 2**). The southern part of the Yellowstone/Absaroka ice mass formed three glacial lobes that flowed into Jackson Hole. These lobes are named for the drainages they occupied (from east to west): Buffalo Fork, Pacific Creek, and Snake River. Differing combinations of these three glacial lobes built these moraines as follows: (1) Burned Ridge phase by Buffalo Fork/Pacific Creek lobes, (2) Hedrick Pond/Dogleg phase by Pacific Creek/Snake River lobes, and (3) Jackson Lake phase by Snake River/Pacific Creek lobes (**Tables 1** and **2**). This succession reflects westward migration of the center of gravity of the Yellowstone/Absaroka glacial source area, probably in response to orographic buildup on the western, downwind side of the icecap. Great volumes of quartzite-rich outwash accumulated and buried much of these moraines.

We will also examine: (1) an outwash terrace deposited early in the last glacial cycle and now mantled by as much as 10 feet (3 m) of loess, (2) scour basins now filled by lake sediments and other deposits in the Deadmans Bar/Moran area and beneath the Jackson Lake Dam, (3) evidence for the Hedrick Pond low-gradient advance across a lake in the Deadmans Bar/Moran area, (4) landforms of floods about 30 feet (10 m) deep that rushed down a flume about 1 mile (1.5 km) wide downstream from Deadmans Bar, (6) a set of moraines from a Teton glacier that encompasses Jenny Lake, and the relations between this glacier and the outwash from the Yellowstone icecap source.

Table 1. Quaternary stratigraphic terms and correlations, Jackson Hole, Wyoming.

Beyond Jackson Hole			Jackson Hole Terms and Events			
Time divisions[1]	Marine isotope stages[2]	Regional terms[3]	Names for glacial deposits	Correlative outwash locations	Lakes	Loess or soil formation
-0 ka	-0 ka	Neoglaciation -4 ka Altithermal -9 ka	Cirque moraines		Present Jackson Lake	soil
Holocene	1					
-10 ka						
	-11 ka		->11 ka			
late Pleistocene	2	Pinedale glaciation	Jackson Lake 4**2**	4 Channelways	? Triangle X	loess
	-35 ka		Hedrick Pond/Dogleg 4**2**? or **3**?	Snake River & Dogleg moraine	Pre-Hedrick Pond	
	3		Burned Ridge 4**2**? or **3**? or **4**? #3 #2 #1	Antelope Flats		soil
	-65 ka 4			Blacktail terrace		loess
	-79 ka 5					loess soil loess
-132 ka	-132 ka	-132 ka	-132 ka			
middle Pleistocene	6	Bull Lake(?) glaciation	Munger glacial deposits 4**6**? recessional maximum	Timbered Island Windy Point SE Jackson Hole		loess

[1] From Richmond and Fullerton (1986).
[2] After Shackleton and Opdyke (1973); recalibrated by Richmond and Fullerton (1986) based on astronomical age of Matuyama/Brunhes boundary of Johnson (1982).
[3] Partly from Pierce (1979).
[4] Underlined bold numbers indicate possible marine-isotope stage correlations.

Table 2. Relative size at terminus among three glacial lobes in the northern Jackson Hole during three phases of the last glaciation. Phases are listed from youngest to oldest.

Phase (informal)	Lobe		
	Buffalo Fork	Pacific Creek	Snake River
Jackson Lake	0	X	XXX
Hedrick Pond/Dogleg	0?	XX	XX
Burned Ridge	XXX	X	0

Explanation of symbols:
XXX, lobe confluent and dominant at glacial terminus
XX, lobe confluent and of similar size at terminus
X, lobe confluent but subordinate at terminus
0, lobe not confluent with others at terminus

Near the end of the field trip, in southern Jackson Hole, we will examine deposits we informally assign to the Munger glaciation (Bull Lake ?) that are mantled by loess resting on a well-developed buried soil.

An important dimension of the Quaternary geology of Jackson Hole is tectonism, particularly downdropping on the Teton fault. Normal faulting and associated tilting of Jackson Hole into the Teton fault has produced the following: (1) tilting at Signal Mountain of 2, 6(?), and 9 Ma strata at dips of 11°, 22°, and 22° into the fault (Love and others, in press; Gilbert and others, 1983); (2) tectonic submergence in the last 15 ka of about 10 paleoshorelines below the pre-dam level of Jackson Lake; (3) a tectonic basin into which outwash deposits have accumulated; and (4) as much as 65 feet (20 m) offset of moraines estimated to be 15 ka.

Acknowledgments

We wish to thank Dave Love for sharing with us his vast knowledge of the bedrock and surficial geology of Jackson Hole. Some of this information is summarized in Love and Reed (1971). Both the bedrock and surficial geology is shown at a scale of 1:62,500 on Love and others (in press). We have also drawn on the classic work of Fryxell (1930), who described most of the prominent glacial features of Jackson Hole; we differ from Fryxell in attributing a lesser role to glaciers from the Teton Range and a larger role to the southern part of the Yellowstone ice mass.

Road log and stop descriptions

This guide is intended for use with the 1:62,500-scale topographic map of Grand Teton National Park. The first number is the distance in miles from the start of each segment; the number in parentheses is the distance from the last logged feature.

Jackson to Moose Junction

0.0 (0.0) Jackson Town Square; proceed north on U.S. Highway 89. Jackson is built on an alluvial fan deposited by Cache Creek, mostly of Pinedale age.

0.4 (0.4) Note marshy land on the National Elk Refuge where Cache Creek alluvial fan dams Flat Creek.

4.0 (3.6) Road climbs onto gravel of Munger age mantled by several feet (meters) of Pinedale loess. A soil displaying better development than the surface soil occurs near the base of the loess. West sloping gravel is probably outwash of the Gros Ventre River, which enters Jackson Hole from the east.

4.9 (0.9) Enter Grand Teton National Park (GTNP).

6.4 (1.5) Cross the Gros Ventre River. The river channel is currently aggrading and has been used as a source of gravel. Low terraces of Pinedale age occur on both sides of the river. The Gros Ventre River flooded catastrophically in 1927, when the 1925 Gros Ventre landslide-dam failed.

6.9 (0.5) Gros Ventre Junction. Stop later on trip will be along road to east (right). North of Gros Ventre Junction, the highway descends the slope of an alluvial fan built northward by the Gros Ventre River onto the south sloping Pinedale outwash terrace, on which the airport is built.

8.9 (2.0) Airport turnoff. The bench to the east is same one as at Stop 9, and can be seen to be mantled by up to 10 feet (3 m) of loess .

10.7 (1.8) South end of Blacktail Butte. The nearly horizontal line on alluvially faceted slopes is the top of a gravel terrace that is overlain by loess and colluvium.

11.7 (1.0) Descend a terrace scarp of Pinedale age.

12.7 (1.0) Moose Junction.

Moose Junction to Moran Junction

0.0 (0.0) Moose Junction; continue north on U.S. 89.

1.1 (1.1) Cross Ditch Creek at the north end of Blacktail Butte. Ditch Creek has deposited large alluvial fans of Munger and Pinedale ages to the east of here.

2.9 (1.8) Climb across an intermediate terrace up onto Antelope Flats. Antelope Flats is a composite, nearly concordant terrace surface ranging in age from Burned Ridge #1, #2, and #3 to Hedrick Pond.

Stop 1. Glacier View turnout

3.4 (0.5) At 9:00 (west) across the valley at the base of the Teton Range are Pinedale moraines enclosing Bradley Lake and Taggart Lake. At 10:00 is Timbered Island, one of the farthest up-valley remnants of loess-mantled till and outwash of Munger age. At 3:00, covered by cottonwoods, is Ditch Creek alluvial fan of Munger age, mantled by loess. At 4:00 is Sheep Mountain, glaciated by Munger ice to above timberline (about 9,800 ft/2,990 m). Up Gros Ventre valley is the Gros Ventre Slide that released along a dip slope in 1925. When the thick glacier filling the Gros Ventre drainage melted out in late Munger time, ice from the Snake River drainage blocked the Gros Ventre valley and resulted in deposition of kame and lake sediments up the Gros Ventre valley. West from this viewpoint, the surface of the prominent inset terrace of the Snake River is marked by large-scale flood bars and channels. These flood features were formed by the last of proba-

bly many floods that rushed from the Deadmans Bar area down this flood flume. The highest and oldest of this flood sequence left longitudinal flood bars near the edge of the highest terrace. The walls of the flood flume have an unusual deposit of pebble gravel that blankets the lower terrace scarp and extends up to a height of 30 feet (10 m). The last flood is estimated to have been 30 to 45 feet (10-15 m) deep and 1 mile (1.5 km) wide.

5.3 (1.9) Teton Point turnout. At 3:00, note the terrace scarp of Hedrick Pond age cut in Burned Ridge outwash. At 9:00, on the surface of the terrace inset below that of the road, are the best-displayed large-scale bedforms formed by flood waters 30 to 45 feet (10-15 m) deep and 1 mile (1.5 km) wide.

6.7 (1.4) Fluvial scarp at 3:00 (east), beyond which are Burned Ridge #2 moraines. At the foot of the valley wall, where a grassy ridge comes down to the outwash level, is a large kettle representing Burned Ridge #1 ice margin.

7.0 (0.3) About 650 feet (200 m) to the east is a low fault(?) scarp in Burned Ridge outwash.

Stop 2. Snake River Overlook

8.4 (1.4) Walk east and climb to the crest of Burned Ridge #3 moraine to examine Burned Ridge moraines and outwash. Stones in this moraine and those to the south are dominated by roundstones of Pinyon-type quartzite with lesser amounts of Paleozoic limestone, Pennsylvanian sandstone, Mesozoic sandstone, Eocene andesitic rocks, and Precambrian crystalline rocks. Note burial of Burned Ridge #1, #2, and #3 moraines by outwash and formation of kettles near the head of the outwash. The dropoff to the north is a depositional, ice-contact slope formed by the Burned Ridge #3 ice front. South of the Burned Ridge #3 moraine; the trend of the channels and slope of the outwash are from east to west. The Burned Ridge #2 ice margin is 1.6 miles (2.6 km) to south, and the Burned Ridge #1 ice margin is 2.2 miles (3.5 km) to south. The Burned Ridge moraines here were deposited by a glacial lobe that flowed down Buffalo Fork. The outwash was largely carried by Spread Creek, which flowed from the Togwotee Pass area along the south side of the glacier to the head of the outwash fan near the Lost Creek Ranch to the east.

Walk from the moraine across the highway to Snake River Overlook. Note Burned Ridge and associated outwash across the river. Inside (north) the Burned Ridge moraines is outwash of Jackson Lake age in The Potholes channelway. At Deadmans Bar, this outwash is graded to levels that range in altitude (alt.) from 6,800 to 6,730 feet (2,073-2,051 m). Looking down the Snake River, the prominent inset terrace level is the lowest level eroded by multiple floods of Jackson Lake age. Hedrick Pond outwash levels are about 6,800 to 6,820 feet (2,073-2,079 m). The exposure in the bluffs across the river is a gray gravel mantled by loess(?) and overlain by a yellow gravel overlain in turn by a gray gravel of Jackson Lake age.

8.9 (0.5) Deadmans Bar turnoff. Turn west (left).

Stop 3. Hedrick Pond moraines

9.0 (0.1) Stop at parking area. Hike about 0.4 miles across the low Hedrick Pond moraines and kettled outwash (alt. 6,800-6,830 ft/2,073-2,082 m) to an exposure in the Snake River bluffs. There Hedrick Pond outwash gravel and sand overlies and interfingers with till of Hedrick Pond age. The following section is exposed along the ridge line:

Thickness ft (m)	Description
16 (5)	Gravel with scattered lenses of flow till. Bedded but beds discontinuous. Surface kettled.
6 (1.8)	Diamicton, flow till
11 (4.3)	Gravel
11 (3.4)	Sand, cross bedded
2.5 (0.8)	Gravel
80 (24.1)	Diamicton, muddy sand matrix with scattered pebbles, locally wispy bedding.

Below the diamicton is a covered interval and gravel exposed near the river.

The till is rich in fines and poor in gravel and was probably eroded from lake sediments that accumulated in a pre-Hedrick Pond phase of a lake extending from Deadmans Bar to Moran Junction. Glacial flow across this muddy-bottomed lake is probably responsible for the local gradient of Hedrick Pond ice, which is about one-half that of Burned Ridge ice in the same area. The till overlies an older gravel near river level.

9.1 (0.1) Return to U.S. 89 and turn left (north).

10.1 (1.0) Hedrick Pond, a deep kettle for which the Hedrick Pond phase is named, is briefly visible on the right beyond the forested moraine.

10.6 (0.5) Lake sediments at 6,720 feet alt. (2,048 m). A delta front is to the left of the road.

10.8 (0.2) Light gray lake sediments in road cut.

11.2 (0.4) Lake sediments to the right (east) of Triangle X lake. The nearly white color reflects the presence of ash reworked from the ash-rich Teewinot Formation (Miocene).

11.5 (0.3) More lake sediments at the front of Triangle X fan-deltas. Fan-delta fronts descend in altitude from about 6,800 to 6,720 feet (2,073-2,048 m), indicating progressive lowering of the lake threshold at Deadmans Bar.

11.8 (0.3) Triangle X Ranch Road. (Optional stop 0.3 miles up the road. Park there and walk south to examine fine-grained, lacustrine sediment rich in reworked ash from the Teewinot Formation, which is locally inclined at 11° along the delta front.)

12.5 (0.7) Cunningham Cabin road on left.

13.0 (0.5) On the right, about 10 feet (3 m) above the flats, is a strandline platform formed by the highest level of Triangle X lake.

13.4 (0.4) Gravel road up late Holocene Spread Creek alluvial fan on the south side of Spread Creek hill, which is at 1:00.

14.1 (0.7) Spread Creek, aptly named due to continued alluviation of quartzite-rich gravel. The south side of Spread Creek hill is a high scarp, which has been considered to be either a fault scarp or a fluvially undercut scarp.

14.4 (0.3) Wolff Ranch road, turn right.

14.6 (0.2) Gravel pit on the left.

14.7 (0.1) Wolff Ranch driveway. Pull into the driveway , and then back 150 feet (50 m) to the northeast to observe delta fronts built into Triangle X lake at its highest level and at a level about 50 feet (15 m) lower.

15.0 (0.3) Return to U.S. 89 and turn right (north).

15.5 (0.5) Scarp is at the boundary between the surface of the lower fan-delta seen at Wolff Ranch and a Holocene alluvial fan deposited by Spread Creek when it spilled around the east end of Spread Creek hill. Gravels of this fan are mantled by mud derived from Mesozoic terrain to the east.

Stop 4. Triangle X lake sediments along the Snake River

16.3 (0.8). Park on the shoulder in the middle of a straight section of highway. To the east on the north side of Spread Creek hill, Hedrick Pond moraines actually slope up a valley separated only by a low divide from Buffalo Fork, indicating the Buffalo Fork lobe was not important in deposition of Hedrick Pond moraines.

Hike about 1/4 mile west to a meander bend of the Snake River to observe the following stratigraphic section exposed in river bluffs (from river level up):

Thickness ft (m)	Description
8 (2.5)	Gray, laminated lake sediments. These sediments were deposited near the center of the Triangle X lake. They also extend to the river bottom and may extend more than 300 feet (100 m) deeper and fill a basin scoured by the Buffalo Fork glacial lobe in Burned Ridge time.
11 (3.5)	Snake River gravel with basal erosional unconformity. Holocene or late glacial in age.
7 (2)	Clayey alluvium with a prominent humic buried soil at its base and a less prominent buried soil in the middle. Deposited by muddy discharges across the older part of the Spread Creek alluvial fan.

Return to vehicle and proceed north.

17.0 (0.7) Triangle X lake sediments exposed in the banks on the far side of the Snake River.

17.7 (0.7) Gravel road on right just after descending a scarp from the mud-mantled fan of Spread Creek onto bottomlands of Buffalo Fork.

18.2 (0.5) Buffalo Fork.

18.4 (0.2) Moran Junction. Continue straight ahead (east) up Buffalo Fork on U.S. 287.

19.8 (1.4) On the right, observe backfill by Pacific Creek glacial lobe up into the valley of Buffalo Fork during Jackson Lake time. Note the aligned ridges in kame moraines trending up into the valley of Buffalo Fork. Across Buffalo Fork and about 500 feet (152 m) higher, Hedrick Pond moraines slope up Buffalo fork, indicating Pacific Creek ice reached this level when Buffalo Fork ice had receded up the valley. During

Burned Ridge time, Buffalo Fork ice covered much of the terrain you see up Buffalo Fork, was more than 1,000 feet (300 m) deep here, and excavated a scour basin probably much deeper than the minimum depth of 100 feet (30 m) shown by wells.

20.3 (0.5) Lake sediments overlying kame gravels, probably deposited when Buffalo Fork was dammed by the Pacific Creek glacial lobe in Jackson Lake time. On the divide to the north, glacial scour features show the flow of Pacific Creek ice into deglaciated Buffalo Fork in Jackson Lake time.

20.6 (0.3) Turn around at Grand Teton National Park Entrance sign. Note the wide, flat-bottomed valley of Buffalo Fork scoured to an unknown depth during Burned Ridge time and filled with lake and other sediments.

22.8 (2.2) Moran Junction.

Moran Junction to Jackson Lake Lodge

0.0 (0.0) Moran Junction, turn north on U.S. 89 and pass Park Entrance Station.

0.3 (0.1) A side road climbs up onto a 6,820-feet-alt. (2,079-m) delta of Triangle X lake.

0.9 (0.6) Pacific Creek. A few miles north along Pacific Creek, drilling shows a glacial scour basin of Burned Ridge age at least 300 feet (90 m) deep filled by unconsolidated sediment.

1.6 (0.7) Climb onto the higher fan level of Pacific Creek.

1.9 (0.3) The Pond on the left is not a kettle, but a low place between an alluvial fan of Pacific Creek and the sandy shoreline deposits of the 6,800-foot (2,073-m) level of Triangle X lake.

2.4 (0.5) The parking area overlooks lush meadows on an abandoned lake floor and Oxbow ridge of sandy strandline deposits extending to an altitude of 6,800 feet (2,073 m).

2.8 (0.4) Oxbow Bend turnout. An old lake floor to the east (alt. 6,740 ft/2,054 m). Oxbow channels are up to 17 feet (5 m) deep (Arlene Pillmore, written communication, 1987).

4.1 (1.3) T-junction, continue straight ahead. The road swings right and climbs onto a gravel bench.

Stop 5. Willow Flats overlook

4.6 (0.5) Turn east (right) onto paved road and park on an outwash gravel surface built into the upper end of the Triangle X lake. Climb up onto a ridge of kame gravel north of the parking area and observe: (1) kame topography of recessional Jackson Lake age that extends from the ridge north to the Christian Pond area; (2) Willow Flats to the west on the post-glacial Pilgrim Creek alluvial fan, on which is built the Jackson Lake Dam; (3) Jackson Lake Lodge and Willow Flats overlook on the outwash/delta of a 6,840 to 6,820-foot-alt. lake (2,085-2,079 m); and (4) Lunch Tree Hill to the northwest, built on a recessional moraine of Jackson Lake age.

Traverse the kame ridge to the east and note: (1) development kame terrace (alt. 6,950 ft/2,118 m) between Christian Pond and Emma Matilda Lake required simultaneous presence of Pacific Creek ice on the east side and Snake River ice on the west side of the kame terrace during recessional Jackson Lake time; (2) 2 and 6 Ma tuffs on Signal Mountain dipping 11° and 22° into the Teton fault; (3) the location of a glacial scour basin north of Signal Mountain, which extends as much as 600 feet (180 m) below the Jackson Lake Dam; (4) Pilgrim Mountain to the north, with the upper limit of the Snake River lobe at an altitude of about 8,100 feet (2,470 m), just below the 8,274-foot (2,522-m) crest; (5) large kame benches and terraces (alt. 7,600-7,200 ft/2,320-2,200 m) built along the margin of the Snake River lobe from Pilgrim Peak to the eastern side of Pilgrim Creek; (6) the Pacific Creek glacial lobe, which reached an altitude of about 8,800 feet (2,680 m) between Whetstone and Gravel Mountains and flowed into Jackson Hole from high country in and near southern Yellowstone National Park. Follow the power line back down to the road, drive back to U.S. 89, and turn left (south).

5.1 (0.5) Descend gravel benches to T Junction.

Willow Flats to North Jenny Lake Junction

0.0 (0.0) Willow Flats junction, head south on "inner" GTNP road. The junction is underlain by gravels on lake sediments.

1.2 (1.2) The road climbs up onto Jackson Lake Dam, built above a 600-foot-deep (180-m) basin scoured by the Pacific Creek lobe in Burned Ridge time and filled with lake sediments and Pilgrim Creek alluvial fan deposits.

1.4 (0.2) The south abutment of the dam, built on 2.0 Ma Huckleberry Ridge Tuff that dips towards the Teton fault at about 11°.

3.1 (0.6) Signal Mountain Lodge turnout on west.

4.2 (1.1) Road to the summit of Signal Mountain on left. Optional side trip for spectacular views of Jackson Hole.

Stop 6. South Landing, Jackson Lake

4.4 (0.2) Turn north (right) into South Landing parking area. On the northeast side of the parking area, climb up onto a moraine deposited by the Snake River lobe in Jackson Lake time . The moraine has erratics of Pinyon-type quartzite, Huckleberry Ridge Tuff, and Precambrian crystalline rocks. The viewpoint overlooks the South Landing outwash channelway, with multiple terrace levels indicating progressive incision during Jackson Lake time. Across the sewage ponds at the margin of Jackson Lake, an esker ridge at lake level indicates a pressurized subglacial jet of water fed a fountain at the head of this channelway. The outwash fan continues a couple of miles to the southeast, where it built a prograding delta into the Triangle X lake. Deposits that accumulated on the west side of the Pacific Creek lobe during Hedrick Pond time form the knolls with trees to the south. Return to the paved road and continue southwest (right).

4.6 (0.2) Cross the lowest of South Landing channelways (alt. 6,860 ft/2090 m).

5.3 (0.5) Road climbs through moraines and different outwash levels.

5.8 (0.5) Paved road to parking area on left. In Hedrick Pond time, this high-altitude (6,900 ft/2,100 m), low-gradient outwash surface was constructed between glaciers of the Snake River lobe to the north and those of the Pacific Creek lobe to the south. Tree-covered knobs and kettles to the southeast define the western margin of Pacific Creek lobe during Hedrick Pond time. Moraines of the Snake River lobe of both Hedrick Pond and Jackson Lake age are to the northwest. Burned Ridge moraine forms the tree-covered ridge in the distance to south.

6.8 (1.0) Start the descent into The Potholes channelway of the Snake River lobe of Jackson Lake age. We viewed the lower end of this channelway from the Snake River overlook earlier in the day. The Potholes channel is marked by deep kettles, many of which are aligned, from its head all the way to the Snake River. Across The Potholes channelway, the Burned Ridge landform consists of Burned Ridge moraine at its southern end; we think the northern end has a moraine of Dogleg age draped around it.

7.2 (0.4) Lowest channel in The Potholes system (alt. 6,820 ft/2,079 m).

7.6 (0.4) The road traverses an ice-marginal channel (alt. 6,870-6,885 ft/2,994-2099 m) that was occupied by east-flowing meltwater during Jackson Lake time. This channel was active after meltwater ceased flowing down the north Jenny Lake Junction channelway (minimum alt. 6,930 ft/2,110 m).

8.6 (1.0) Note the deeply kettled glacial topography at the margin of Spaulding Bay sublobe of the Snake River lobe. Spaulding Bay of Jackson Lake is about half a mile to the north.

9.0 (0.4) North Jenny Lake Junction. The lowest channelway has a threshold of 6,930 feet (2,110 m) and is of Jackson lake age. Continue on the main road to turn around at viewpoint.

10.3 (1.3) Large turnout on the floor of North Jenny Lake Junction channels. East of North Jenny Lake Junction channelways, Dogleg moraines and outwash level form the higher terrain above the channelway. Nash (1987) studied the degradation rates of the terrace scarps in the channelway. Using the linear diffusion equation model, he found a clear dependence of rate on height, but not on orientation. Large boulders of crystalline rocks in channelway represent an ice margin, possibly of Dogleg age. Turn around and return 1.3 miles to North Jenny Lake Junction.

North Jenny Lake to Moose Junction

0.0 (0.0) North Jenny Lake Junction; proceed southwest on the one-way road.

0.1 (0.1) Gravel road to Spaulding Bay. Note multiple outwash terrace levels of Jackson Lake age of Spaulding Bay sublobe. The paved road climbs up onto an outwash terrace that slopes southwest to the next stop. Northeast of this terrace, moraines and/or an ice-contact terrace scarp represent the ice margin of the combined Snake River and Teton glacial lobes of Jackson Lake age.

Stop 7. Cathedral Group turnout

2.1 (2.0) View the Teton fault scarp on the Teton front, with 63 feet (19 m) vertical offset of slope depos-

its, and Pinedale moraines of a slab glacier on the Teton front. The turnout is on outwash of Jackson Lake age rich in quartzite from northeastern Jackson Hole. The slope *and* channel pattern of outwash trend obliquely toward the Teton front, indicating a source to the northeast and filling of a tectonic depression created by down dropping on the Teton fault. Walk 600 feet (200 m) north from the turnout to forested moraines of Jackson Lake age with large boulders of Precambrian crystalline rocks deposited by Leigh Canyon sublobe from the Teton Range, which was confluent with the Snake River glacial lobe. Quartzite roundstones are common in the outwash in front of the moraine, but quite uncommon in the moraine itself.

2.8 (0.7) T-junction, turn left. Quartzite-rich outwash, on which the road is built, buries the outer set of Cascade Canyon moraines of Pinedale age that loop around Jenny Lake. These buried moraines were encountered in a water well for Jenny Lake Lodge; the low permeability of the glacial till required drilling a new water well farther to the east, which penetrated about 280 feet (85 m) of gravel above a silty sediment.

5.4 (2.6) Jenny Lake Ranger Station. The Ranger Station and campground are built on the inner moraines of Cascade Canyon glacier, which are correlated by outwash relations with the Jackson Lake moraines. The channel to the east carried meltwater from the Leigh Lake-String Lake area. This meltwater would have spilled into Jenny Lake if there had not been a glacier in the Jenny Lake basin.

5.8 (0.4) South Jenny Lake Junction; turn right (south). The road is on outwash carried down the North Jenny Lake channelway during Jackson Lake time. To the east, Timbered Island is a recessional deposit of Munger age. The northern part of Timbered Island contains moraines with large erratics of Precambrian crystalline rocks from the Tetons; the southern part consists largely of outwash rich in Pinyon-type quartzite cobbles. This outwash is mantled by 8 to 15 feet (2 -4 m) of loess with a well-developed buried soil at the base of the loess and extending into the outwash.

9.4 (3.6) Cottonwood Creek bridge. To the west are the Bradley Lake and Taggart Lake moraines of Pinedale age.

11.0 (1.6) Windy Point turnout. The forested bench to the south is till and outwash of Munger age mantled by loess. An auger hole on this bench encountered a well-developed buried soil near the base of the loess. After this turnout, the road descends through outwash terraces to a broad left turn on the lowest outwash surface associated with flooding down the flood flume.

12.7 (1.7) Moose Visitor Center.

13.3 (0.6) Moose Junction, turn south (left).

Moose Junction to Gros Ventre Junction

0.0 (0.0) Drive south on U.S. 89. and retrace earlier route to the next intersection. The road climbs up onto the highest outwash terrace of the last glaciation.

5.8 (5.8) Gros Ventre Junction. Turn left (east) on a paved road up the Gros Ventre River.

Stop 8. Blacktail Terrace (older Pinedale age)

7.7 (1.9) Terrace gravel extends north from here to Blacktail Butte and is mantled by 3 to 6 feet (1-2 m) of loess. The absence of a buried soil at the base of the loess indicates the underlying gravel is old enough to have accumulated up to 10 feet (3 m) of loess, but not as old as the last interglacial. Toward the airport from here, a soil pit exposed 8 feet (2.5 m) of loess with a moderately developed Pinedale soil at the surface and a very weak soil in the lower part of the loess. Channels and terrace scarps on this bench indicate deposition by the southwest-flowing Gros Ventre River. The slope of this terrace has probably been increased by tilting into the Teton fault since early Pinedale (early Wisconsin?) time. A north-south fault between this stop and Blacktail Butte offsets this terrace.

Toward the east, the hills of the National Elk Refuge, underlain by Miocene Teewinot Formation, were extensively scoured during the Munger glaciation. On Sheep Mountain, Munger ice reached an altitude of about 9,800 feet (3,000 m). The Gros Ventre valley was filled with ice at this time. During Munger recession, much of the Gros Ventre valley deglaciated and a large glacier still remaining in Jackson Hole advanced several miles up the Gros Ventre, resulting in accumulation of ice-marginal fluvial and lacustrine deposits in the Gros Ventre valley.

9.6 (1.9) Return west to Gros Ventre Junction; cross U.S. 89 and continue straight ahead on Spring Creek Road.

Gros Ventre Junction to U.S. 22 Bridge across Snake River

0.0 (0.0) Proceed west on Spring Creek Road. Road to U.S. 22 traverses mostly Pinedale outwash, including an alluvial fill between East and West Gros Ventre Buttes.

8.7 (8.7) Highway 22, turn west (right).

Stop 9. Munger till and loess mantle at Engineers Quarry

12.0 (3.3) Turn off the road just east of U.S. 22 bridge across the Snake River. Park and walk into the quarry area to observe the following sequence:

1. Glacially polished bedrock with north-south striations. The glacier of Munger age filled all of Jackson Hole and extended to an altitude of 8,100 feet on Phillips Ridge (about 2,600 ft/790 m) above this stop).
2. Till of Munger age up to 6 feet (2 m) thick.
3. Loess mantle up to 25 feet (8 m) thick.

In the lower 3 to 5 feet (1-2 m) of loess, a buried soil complex is present with up to three buried soils, the lower of which extends into the till of Munger age. This buried soil complex merges into a single soil away from the outwash plains flooring Jackson Hole.

The main section of loess is relatively unaltered except for a weak buried soil in the middle part and the relatively well-developed surface soil with a B-horizon extending to 50 inches (130 cm), and leaching to 70 inches (170 cm). Return on the road east to Jackson.

U.S. 22 Bridge across Snake River to Jackson

0.0 (0.0) Engineers Quarry just east of U.S. 22 bridge across Snake River.

1.6 (1.6) Crest of hill; thick loess in road cuts is mostly of Pinedale age.

1.9 (0.3) North of the road, a deep glacial channel of Munger age cuts into the southern end of West Gros Ventre Butte.

2.3 (0.4) Snow King ski area straight ahead. The top of the ski area is about the upper limit of Munger glacial ice. To the south (right), Munger Mountain forms the largest mountain at the southern end of Jackson Hole. Munger moraines reach an altitude of 7,400 feet on the north side of Munger Mountain, 1,400 feet (430 m) above the Snake River.

3.1 (0.8) Flat-floored valley built up by outwash in Pinedale time.

3.8 (0.7) U.S. 22 and 89 "Y" intersection. Turn left and go upstream along Flat Creek.

5.3 (1.5) Jackson Town square.

References cited

Fryxell, F.M., 1930, Glacial features of Jackson Hole, Wyoming: Augustana Library Publications No. 13, 129 p.

Gilbert, J.D., Ostenaa, Dean, and Wood, Christopher, 1983, Seismotectonic study, Jackson Lake Dam and Reservoir, Minidoka Project, Idaho-Wyoming: U.S. Bureau of Reclamation Seismotectonic Report 83-8, 122 p. and 11 appendices.

Johnson, R.G., 1982, Brunhes Matayama magnetic reversal dated at 790,000 yr B.P. by marine astronomical correlations: Quaternary Research, v. 17, p. 135-147.

Love, J.D., and Reed,J.C., Jr., 1971, Creation of the Teton Landscape—a geologic story of Grand Teton National Park: Grand Teton Natural History Association, Moose, Wyoming, 130 p.

Love, J.D., Reed, J.C., Jr., and Christiansen, A.C, in press, Geologic Map of Grand Teton National Park, Teton County, Wyoming: U.S. Geological Survey Miscellaneous Investigations Map I-2031, scale 1:62,500.

Nash, David, 1987, Reevaluation of linear-diffusion model for morphologic dating of scarps, *in* Crone, A.J., and Omdahl,E.M., editors, Directions in paleoseismology: U.S. Geological Survey Open File Report 87-673, p. 325-338.

Pierce, K.L., 1979, History and dynamics of glaciation in the northern Yellowstone National Park area: U.S. Geological Survey Professional Paper 729F, 90 p.

Richmond, G.M., and Fullerton, D.S., 1986, Introduction to Quaternary glaciations in the United States of America, *in* Sibrava, V., Bowen, D.Q., and Richmond, G.M., editors, Quaternary glaciations in the Northern Hemisphere: Quaternary Science Reviews, v. 5, p. 3-10.

Shackleton, N.J., and Opdyke, N.D., 1973, Oxygen isotope and paleomagnetic stratigraphy of equational Pacific core V 28-238: Oxygen isotope temperatures and ice volumes on the 10^5 year and 10^6 year scale: Quaternary Research, v. 3, p. 39-55.

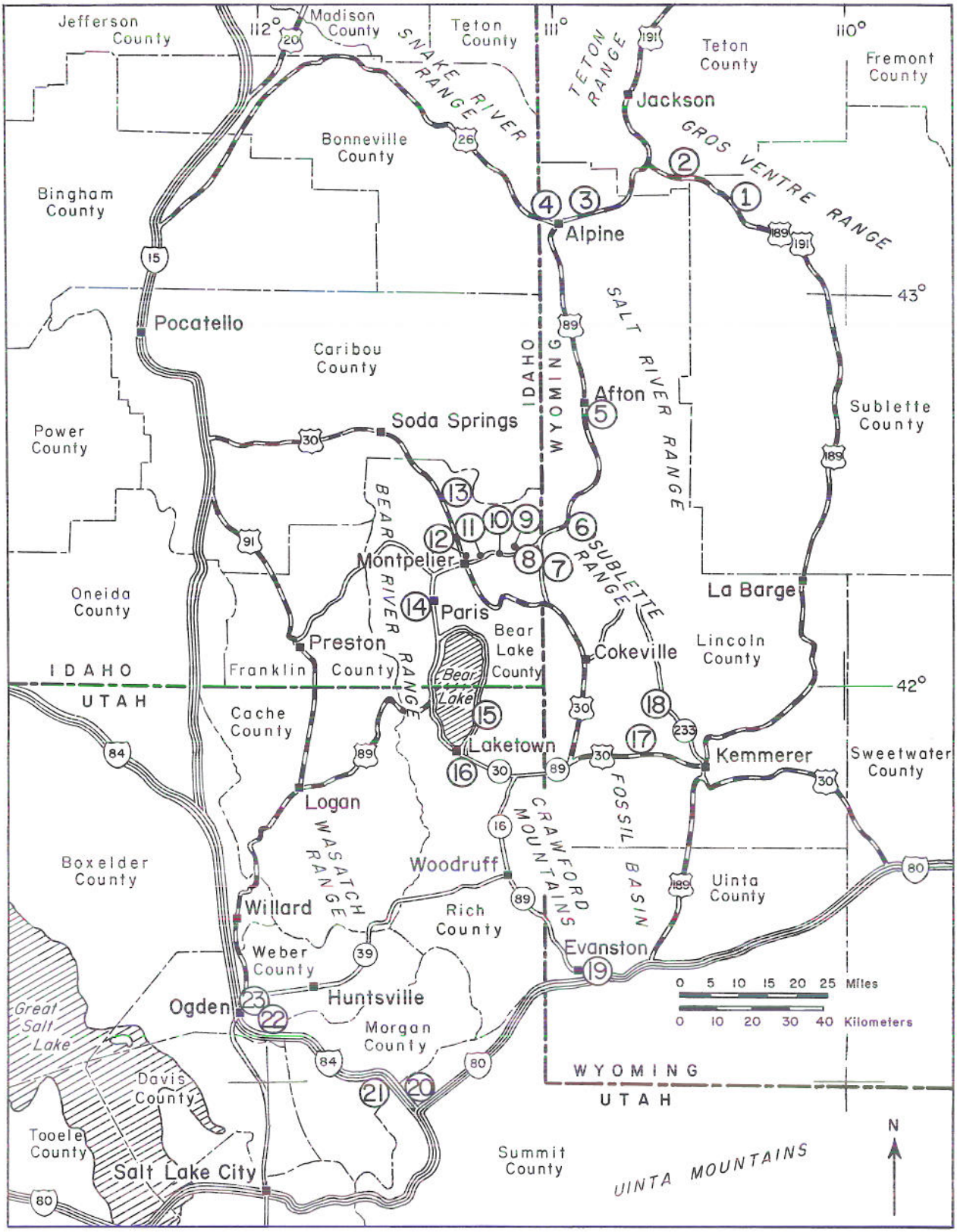

Trip route and stop locations, field trip no. 5.

Field trip no. 5

OVERVIEW OF RECENT DEVELOPMENTS IN THRUST BELT INTERPRETATION

James C. Coogan[1] and Frank Royse, Jr.[2]

[1]Department of Geology and Geophysics
University of Wyoming
Laramie, Wyoming 82071

[2]Chevron U.S.A., Retired
6984 Urban Street
Arvada, Colorado 80004

Trip summary (see Figure 1)

Stop 1. Granite Creek overview of Prospect thrust
Stop 2. Shepard thrust and Hoback fault at the mouth of Hoback Canyon
Stop 3. Absaroka thrust and Little Grays River anticline
Stop 4. Grand Valley fault at Alpine Junction
Stop 5. Swift Creek Canyon, Star Valley normal fault scarp
Stop 6. Salt spring in core of Afton anticline, Salt River Pass area
Stop 7. Sublette anticline
Stop 8. Preuss anticline near Geneva
Stop 9. Cleavage in Twin Creek Limestone at Geneva Summit
Stop 10. Home Canyon thrust fault near Montpelier Reservoir
Stop 11. Hellhole and Waterloo thrust faults at Home Canyon
Stop 12. Meade thrust fault, mouth of Montpelier Canyon
Stop 13. Bear Lake Valley fault and Meade thrust at Georgetown Canyon
Stop 14. Paris thrust in Paris Canyon
Stop 15. Laketown thrust footwall folds at South Eden Canyon
Stop 16. Laketown thrust hanging wall and Laketown Dolomite at Old Laketown Canyon
Stop 17. Fossil Butte National Monument
Stop 18. Hams Fork Conglomerate, Absaroka thrust front, and Lazeart syncline northwest of Kemmerer
Stop 19. View of Almy and Acocks normal faults, Evanston
Stop 20. Echo Canyon Conglomerate at Echo
Stop 21. Devils Slide, eastern edge of the Wasatch basement uplift
Stop 22. Devils Gate
Stop 23. Overview of Wasatch fault at the mouth of Ogden Canyon

Introduction

The Wyoming-Idaho-Utah thrust belt (**Figure 2**) is often cited as one of the most completely explored and best understood fold and thrust belts in the world. Certainly, this belt is remarkable in two respects: (1) it exposes a wide range of structural levels along strike that are well delineated by modern mapping and stratigraphy; and (2) it contains much recent subsurface control from over a decade of extensive oil and gas exploration. Still, many contemporary studies of the region do not incorporate these recent data, and rely

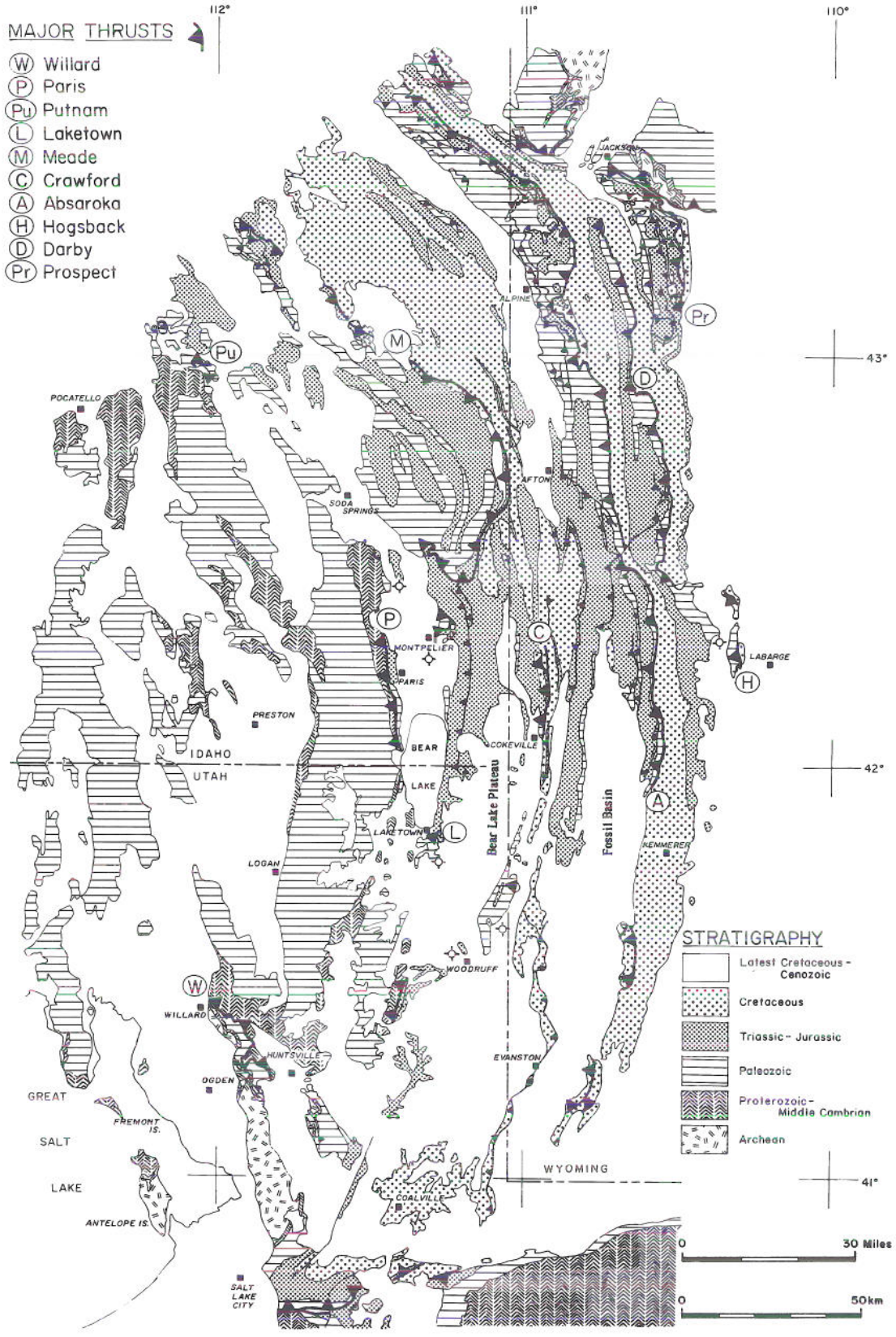

Figure 2. Generalized geologic map of the Wyoming-Idaho-Utah thrust belt (compiled by J.C. Coogan).

instead on earlier regional syntheses to constrain the structural history of the belt. This field trip is designed to provide an overview of specific areas where studies have led to a reevaluation or refinement of certain points of thrust belt interpretation. Not suprisingly, many of these points are presently matters of debate between the two field trip leaders. We hope that the germ of debate will infect other field trip participants as well.

Certain themes recur throughout the trip. First, we will stress the importance of thrust-sheet stratigraphy as we travel across the shortened Proterozoic through Jurassic miogeoclinal wedge. Second, the sequence of thrusting in each area will be discussed in light of Cretaceous through early Eocene tectogenic sediments as well as cross-cutting structural relationships. A third point of discussion will be the organization of individual thrust faults into thrust systems. We will view areas that preserve important linking geometries between thrust faults and we will outline arguments concerning the shared decollement levels between thrusts. Finally, we will drive through many Miocene-Holocene grabens that serve as points of discussion concerning the inheritance of earlier thrust structures by Basin and Range normal faults.

Stratigraphic framework

Basement rocks

The entire region of this field trip is underlain by metamorphic and igneous rocks of the Wyoming Archean province (Lush and others, 1988), which forms the basement below the thin-skinned thrust sheets we will traverse. These basement rocks are exposed east of the thrust belt in the Teton, Gros Ventre, and Wind River uplifts of the Wyoming foreland (**Figures 2** and **3**). In the subsurface, the Moxa arch foreland basement uplift underlies the frontal thrust sheets near La Barge, Wyoming. Basement rocks in front of and beneath the eastern thrust belt are not directly involved in thrust structures, although uplift of the Teton-Gros Ventre and Moxa arch areas provided a buttressing effect on the coeval frontal thrusts of the belt (Royse, 1985). A wealth of geophysical data demonstrates that the basement dips gently (< 4°) to the west beneath the eastern thrust sheets below a regional sole decollement in shales of the Cambrian Gros Ventre Formation. The only significant involvment of basement rocks in thrust-related shortening occurs in the Wasatch Range near Salt Lake City, Utah, where Archean rocks crop out at the surface. Farther to the west, Archean basement is exposed in the Albion-Raft River (Armstrong, 1982) and East Humboldt (Lush and others, 1988) metamorphic core complexes, where Cretaceous metamorphic ages imply an early metamorphic history coeval with the nonmetamorphic structures seen in this part of the Cordillera.

Early miogeocline

The sedimentary sequence that comprises the thrust sheets of the region can be subdivided based on three stages of sedimentation that have been previously summarized by Armstrong and Oriel (1965) and Oriel (1986). The earliest stage is preserved as a westward thickening Proterozoic through mid-Paleozoic miogeoclinal wedge deposited along the rifted and attenuated passive margin of the North American craton. A Proterozoic through Middle Cambrian shallow marine clastic sequence forms the base of the miogeoclinal wedge. In the foreland to the east, this sequence is represented only by the Middle Cambrian Flathead Sandstone, which is less than 330 feet (100 m) thick where it overlies Archean basement rocks in the Teton-Gros Ventre uplift. The Flathead Sandstone is not carried in any of the eastern thrust sheets, but it underlies the regional sole decollement beneath the thrusts until it crops out in northern Utah as the 1,200-foot-thick (365-m) Tintic Quartzite above the basement rocks of the Wasatch Range (**Figure 4**). In contrast, the argillites and quartzites of the Upper Proterozoic Pocatello Formation and Upper Proterozoic-Middle Cambrian Brigham Group of the western thrust belt reach a thickness of 15,000 feet (5 km) where they have been stripped from their basement above the Willard and Paris thrust faults (**Figure 4**).

Upper Cambrian through Devonian rocks of the miogeocline are largely carbonates with interbedded quartzites and shales. The eastern thrusts (Crawford, Absaroka, Darby-Hogsback, and Prospect) carry a relatively thin (1,800-2,300 ft/550-700 m) sequence representative of the Wyoming shelf. The Silurian System is conspicuously absent in these eastern thrust sheets above the sole decollement in the Cambrian Gros Ventre Formation. The western thrusts carry a much thicker (13,000 ft/4 km) Upper Cambrian through Devonian sequence that includes the Silurian Laketown Dolomite in the Willard, Paris, Meade, and Laketown thrust sheets (**Figure 4**).

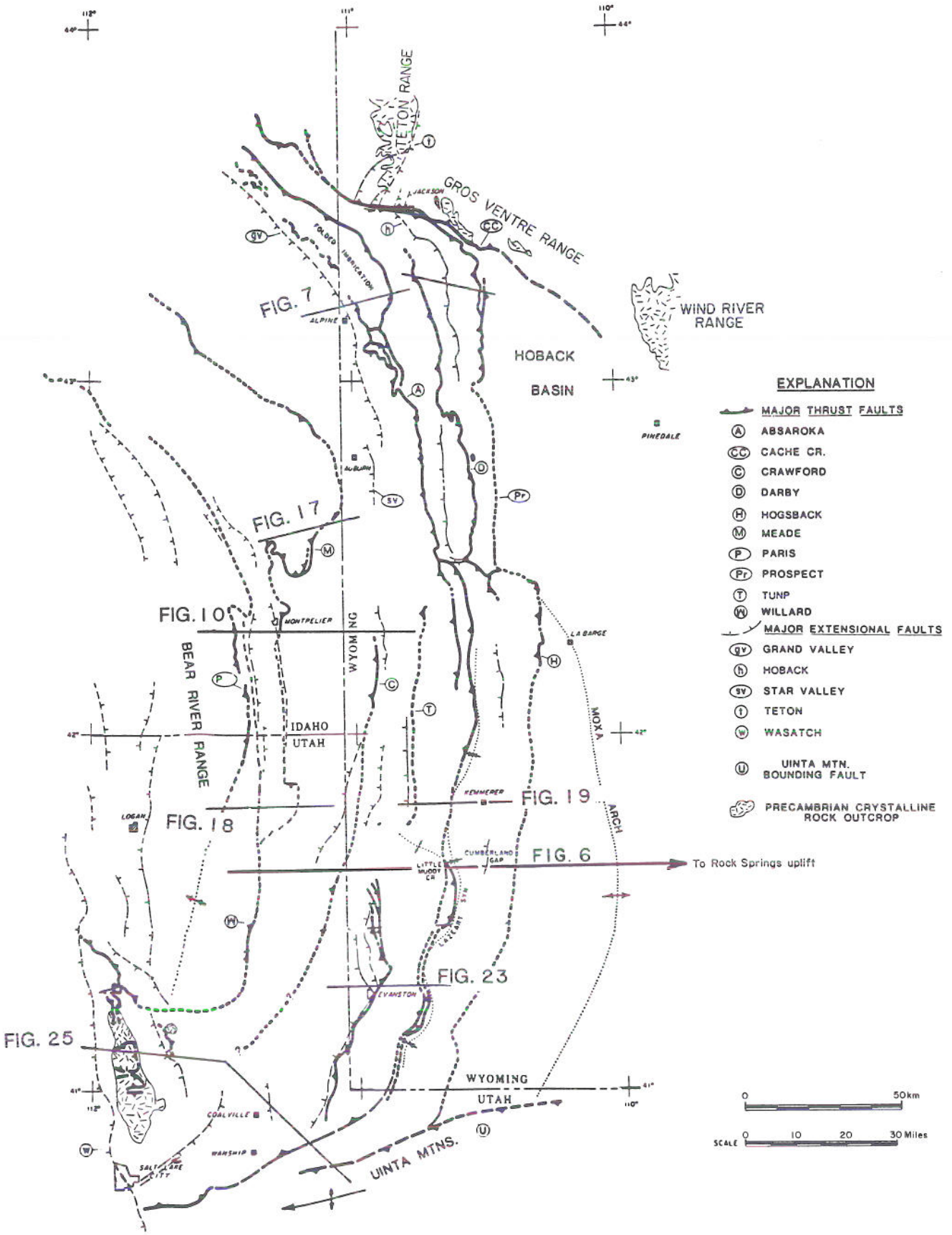

Figure 3. Tectonic map of principal thrust and extensional faults in the Wyoming-Idaho-Utah thrust belt, showing locations of Figures 6, 7, 10, 17, 19, 18, 23, and 25. (Modified from Royse and others, 1975.)

Tectonically influenced miogeocline

A second stage of sedimentation for the region was characterized by successive eastward shifts of depocenters from Mississippian through Jurassic time. The principal stratigraphic units of this period are summarized in **Figure 5.** The tectonic events responsible for interruptions in miogeoclinal deposition include the Mississippian Antler Orogeny (Speed and Sleep, 1982), the Pennsylvanian Ancestral Rocky Mountain uplift and the related Oquirrh basin subsidence (Jordan and Douglass, 1980), the early Triassic Sonoma event (Carr and Paull, 1983), and a poorly known Middle to Late Jurassic thrusting event associated with the Manning Canyon detachment in western Utah and eastern Nevada (Allmendinger and Jordan, 1981).

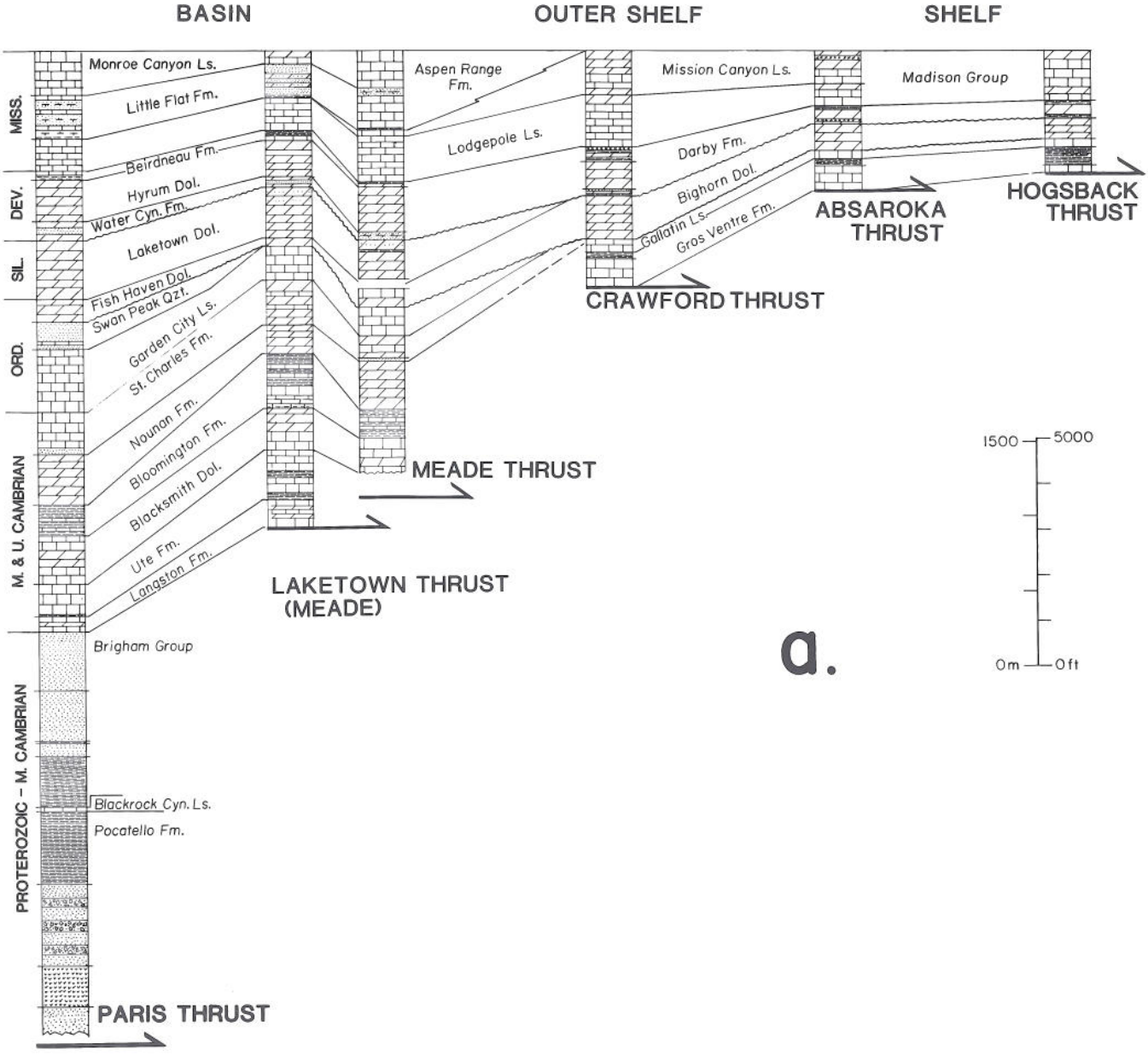

Figure 4. Composite Paleozoic thrust-sheet stratigraphy from surface and well data for the (a) central thrust belt and (b) southern thrust belt (next page) (compiled by J.C. Coogan). Specific subsurface stratigraphic information for the Meade thrust hanging wall is from the American Quasar #22-1 Jensen, sec. 22, T.13N, R.44E, Bear Lake County, Idaho and the Ladd # 3-24 Bennington, sec. 3, T.12N, R.44E, Bear Lake County, Idaho.

Cretaceous to early Eocene foreland basin

The third stage of sedimentation was the accumulation of tectogenic sediments in the foreland basin associated with the emplacement of the thrust sheets that we will visit during this excursion. Proximal clastic deposits derived from advancing thrust fronts are successively younger eastward. The preservation of the oldest proximal clastics, and thus preservation of a rather complete record of thrust timing, is largely due to the shallow erosional level of this thrust belt. Since the earliest thrust-derived conglomerates were incorporated into the hanging walls of later thrust sheets, we are looking not only at a shortened miogeoclinal wedge, but also at a shortened foreland basin. The relationship between individual thrust faults and the proximal clastic deposits used to date them is summarized in **Figure 6.**

Thrust structure and thrust systems

Exposures of nine major thrust traces represent the fundamental structural elements of the Wyoming-Idaho-Utah thrust belt. From southwest to northeast, these fault exposures are the Willard, Paris, Laketown, Meade, Crawford, Absaroka, Hogsback, Darby, and Prospect thrusts (**Figures 2** and **3**). The degree of connection between these individual exposures has long been a matter of debate that can be partially

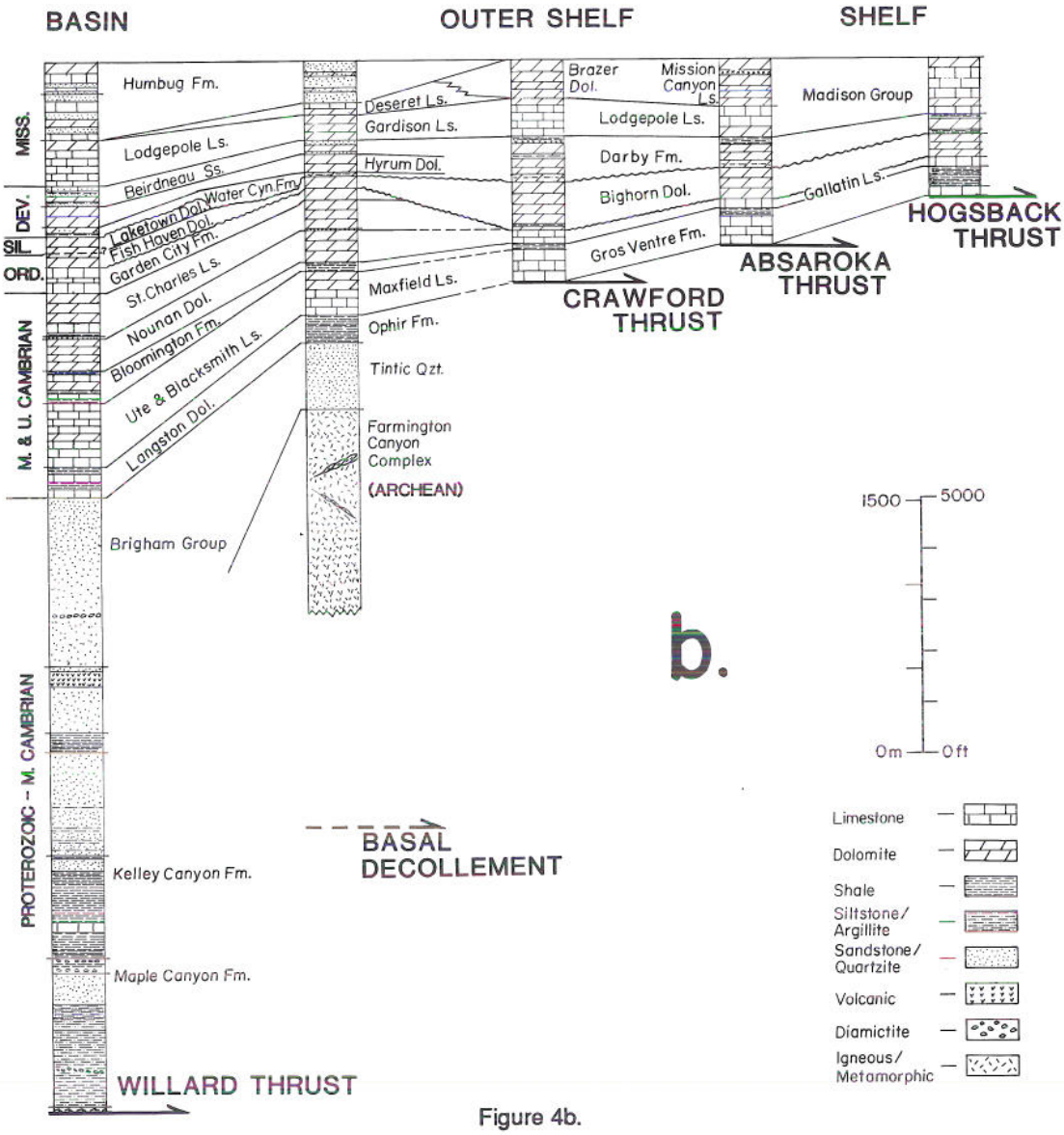

Figure 4b.

resolved through modern subsurface control. The dashed lines in **Figure 3** outline the present knowlege of the subsurface extent and the implied connections between thrust exposures based on subsurface data.

One goal of regional structural geology in thrust belts is to organize individual thrust traces into "systems" of thrusts that were geometrically, mechanically, and kinematically linked in their development. A thrust system is a branching array of individal thrusts that share a common sole decollement. In terms of sole decollements, the Wyoming-Idaho-Utah thrust belt can be divided into two separate thrust systems, west and east (Coogan, 1987). Whereas the Paris and Willard thrust traces expose a common hanging wall decollement level in Proterozoic argillites characteristic of the western thrust belt, the Crawford, Absaroka, and Darby-Hogsback-Prospect thrusts all share a sole decollement in the shales of the Cambrian Gros Ventre Formation that is characteristic of the eastern thrust belt. Between the two areas, surface exposures of the Laketown thrust and well control on the Meade thrust hanging wall beneath Bear Lake Valley indicate that these thrust sheets carry a Paleozoic section similar to that found above the Proterozoic of the Paris and Willard thrust sheets (**Figure 4**). The implication is that the Meade and Laketown thrusts eventually sole into the same Proterozoic decollement that underlies the Paris and Willard thrusts to the west.

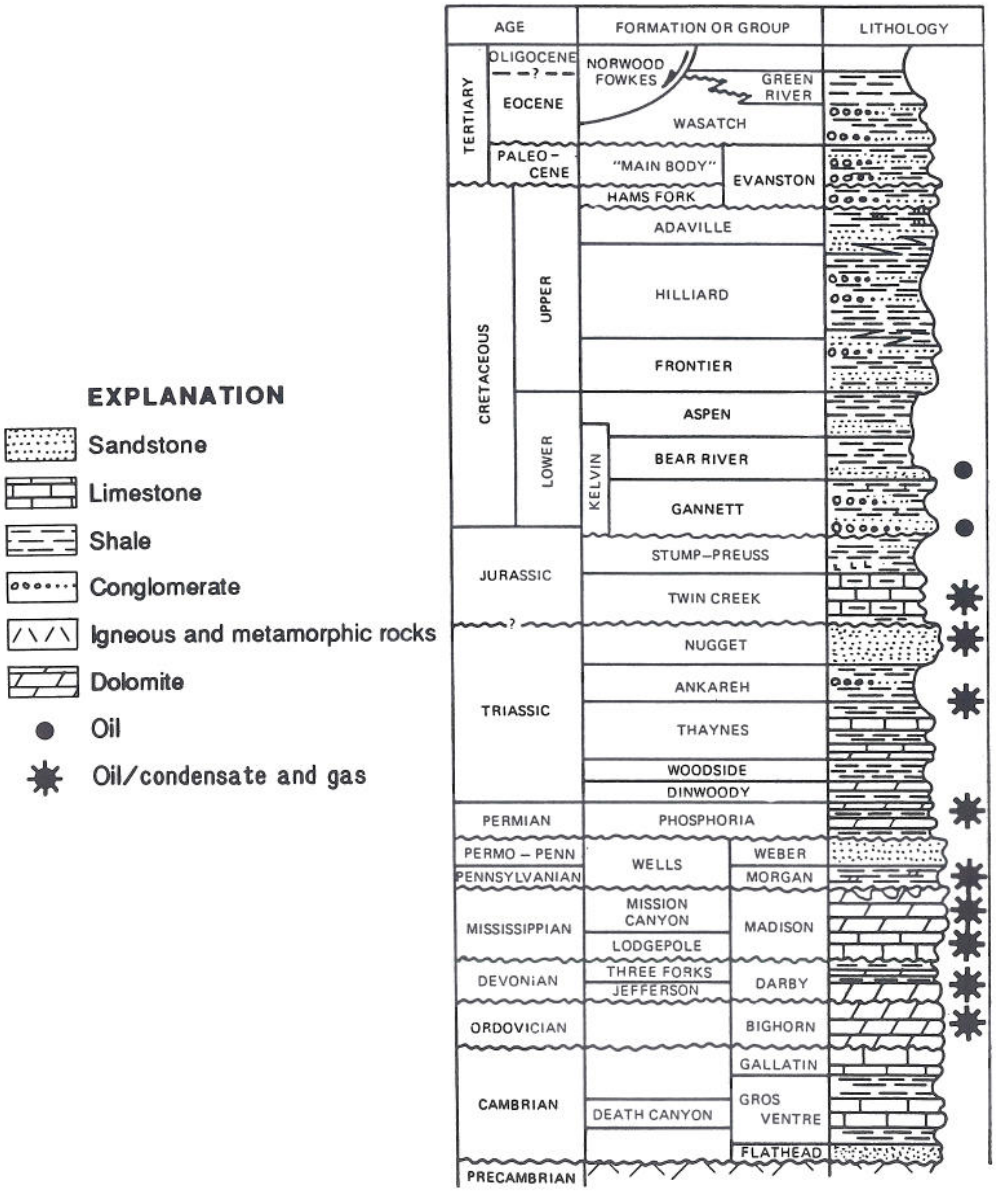

Figure 5. Stratigraphic column for the Wyoming-Idaho-Utah thrust belt (from Lamerson, 1982).

Detailed analysis of thrust decollements, connections, and terminations in this belt is now possible with the wealth of well data, seismic data, and surface mapping that has accumulated since 1975. Important revisions to the regional thrust relationships are summarized as follows:

(1) The Willard and Paris thrust traces are two separate thrust imbricates that share the western Proterozoic hanging wall decollement;

(2) The frontal thrust trace of the western thrust system is marked by the Willard thrust trace in the southern thrust belt and by the Laketown and Meade thrust traces to the north;

(3) The Meade and Crawford thrust faults do not represent equivalent shortening episodes in the northern and southern thrust belt as previously assumed; and

(4) The Crawford thrust shares the sole decollement in the Cambrian Gros Ventre Formation that is characteristic of the Absaroka and Darby-Hogsback-Prospect thrusts of the eastern thrust belt. This shortening of the sedimentary section is equivalent to the basement shortening seen in the Wasatch Mountains.

Cenozoic extension

Many of the north-south trending valleys that we will pass through on this field trip are extensional half grabens. In particular, we will drive through the valley of the Hoback River, Grand Valley, Star Valley, Bear Lake Valley, Bear River Valley, and Rock Creek Valley (**Figure 3**), all of which are in some way associated with the position of former thrust ramps. The graben fill ranges in age from Eocene to Holocene, and many fault scarps demonstrate that the bounding normal faults have been active in the very recent past. The normal faults represent an upper crustal extensional overprint on preexisting thrust structures along the

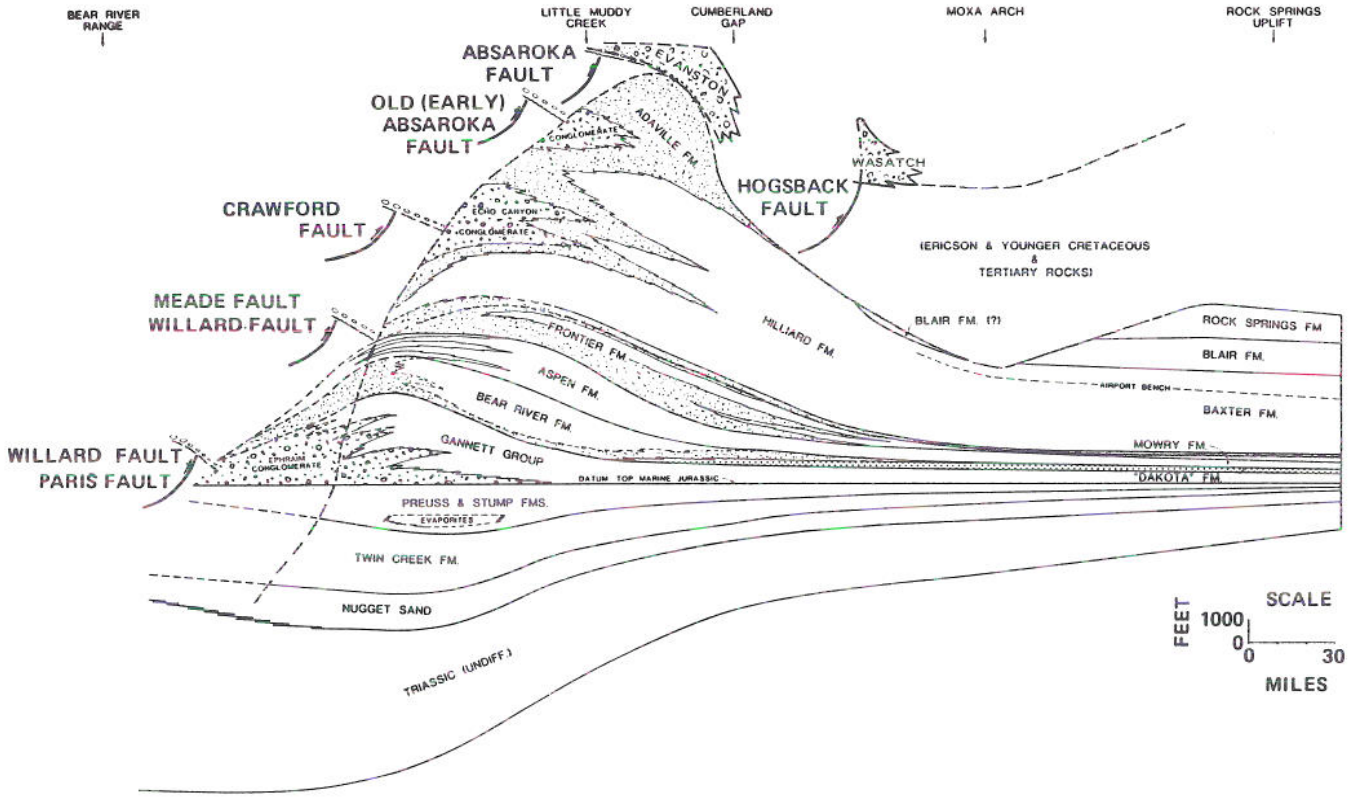

Figure 6. Stratigraphic diagram of restored Mesozoic and Tertiary rocks in western Wyoming and northern Utah, showing the relationship between thrust faulting and sedimentation (modified from Royse and others, 1975).

eastern edge of the Basin and Range. The uninterrupted dip of basement beneath the grabens indicates that the normal faults are confined to the formerly thrusted section above the regional sole decollement.

Field trip route and stop descriptions, day 1

Stop 1. Granite Creek overview of Prospect thrust fault

From this position at the confluence of the Hoback River and Granite Creek, we can view features of the Prospect thrust fault and discuss some surprises that resulted from drilling in this area, particularly with regard to the sequence of thrust imbrication here. To the south on Battle Mountain, the Jurassic Nugget Sandstone in the Prospect (Cliff Creek) thrust hanging wall has been thrust eastward over the Paleocene Hoback Formation of the footwall. To the west is a high ridge of Nugget that is also part of the Prospect thrust sheet. Across Granite Creek to the east is the reclaimed site of the Chevron # 1-34 Game Hill Unit well (**Figure 7**). The well penetrated the east dipping Game Hill thrust near the surface; drilled Hoback Formation to a depth of (3,562 ft/1,086 m), where Jurassic Nugget Sandstone was penetrated; and then drilled structurally complex Jurassic and Triassic rocks to a depth of (7,440 ft/2,268 m), where Upper Cretaceous rocks were found below a major blind (cryptic) thrust fault. This hidden thrust is informally named the Granite Creek thrust. The total depth of the well was (16,499 ft/5,029 m) and the rocks at the bottom were Upper Cretaceous Frontier Formation. Supernormal pressures were encountered while drilling in Cretaceous rocks, a feature which is related to hydrocarbon generation.

The blind thrust plate found by the Chevron #1-34 well does not crop out on the surface. Its presence in the subsurface below unconformable Hoback Formation (Paleocene) was a surprise, and knowledge of its existence markedly changes the interpretation of the structural history of this area. The first interpretive change concerns the magnitude and time of thrusting. The main thrust displacement is on the cryptic Granite Creek thrust fault, not the Prospect thrust fault. Also, the time of main displacement is pre-middle Paleocene, not post-Paleocene. A second change is in the kinematic interpretation of thrust sequence. Where the regional sequence of thrusting is well documented as younger toward the foreland (Armstrong and Oriel, 1965; Royse and others, 1975), the imbricates above the Granite Creek thrust are younger to the west. Recently, Hunter (1987) documented the cross-cutting relations that define the Prospect hanging-wall imbricates as succesively younger toward the west. Contemporaneous early uplift of the Gros Ventre Range may have established a foreland buttress that influenced the imbrication sequence. Along the highway to our next stop, the Prospect imbricates include, from east to west, Bull Creek, Game Creek, Bear, and Shepherd thrusts.

On the drive west to the head of Hoback Canyon, the highly contorted Jurassic and Cretaceous rocks seen on the north side of the road were deformed by slip on the Bull Creek and Game Creek thrusts. The two thrusts have small displacements and are difficult to see. Their importance lies in the fact that each thrust truncates structures associated with the thrust sheet beneath it, thus establishing the back-breaking sequence of thrusting (Hunter, 1987). Farther west in Hoback Canyon, a prominent gray ridge comes into view. The ridge consists of resistant sandstone of the Pennsylvanian Wells Formation in the hanging wall of the Bear thrust, which is juxtaposed against overturned and contorted Triassic redbeds in the footwall. Pass through an impressive series of cliffs of the Mississippian Madison Group carbonate rocks in the Bear thrust hanging wall. The low dip of these strata reflects a footwall decollement or "flat", probably in Triassic shales, along the underlying Bear thrust.

Stop 2. Shepard thrust and Hoback fault at the mouth of Hoback Canyon

At the mouth of Hoback Canyon near Stinking Springs, complexly folded and thrust-faulted Mississippian carbonate rocks are exposed in the canyon wall north of the river. These structures are in the hanging wall of the Shepard thrust, a minor backlimb imbricate of the Bear thrust that originates at a ramp where the Bear thrust plane cuts obliquely across footwall beds (**Figure 7**). Look closely and try to follow specific bed offsets and folds. This type of structural complexity is localized over ramps or steps in the thrust-fault plane, and occurs at various scales from mountain range size to small areas such as this one, depending on the magnitude of the ramp.

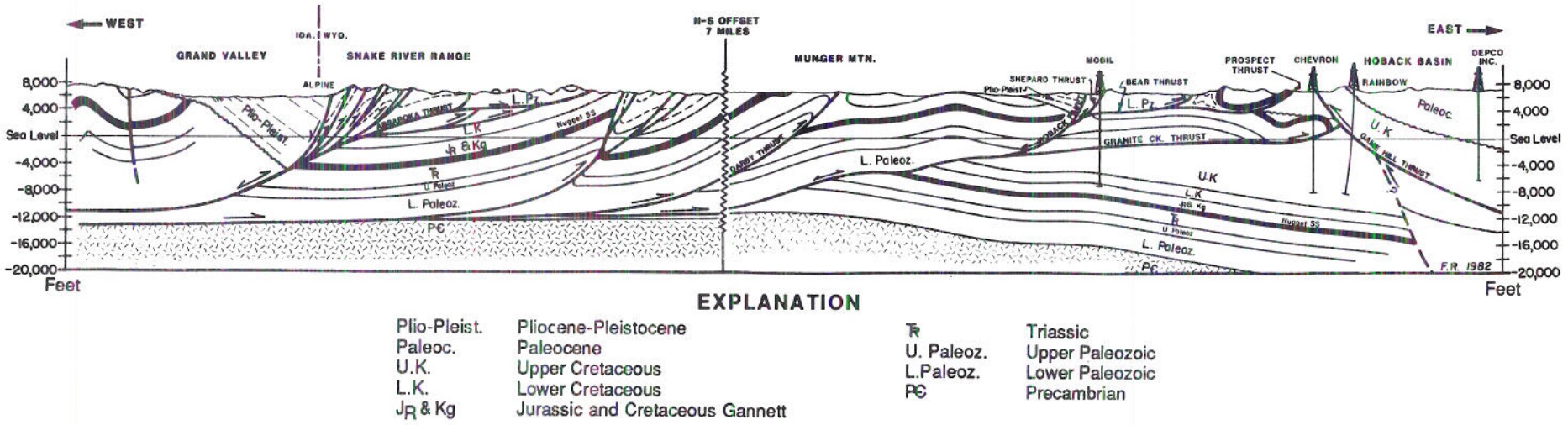

Figure 7. Geologic structure section from the Prospect thrust to Grand Valley along the route of Stops 1 to 4. (No vertical exaggeration.)

The trace of the Hoback normal fault can be viewed north of the river west of the parking area where a reddish sequence of Plio-Pleistocene tuffaceous sediments called the Camp Davis Formation has been down-dropped against Mississippian carbonate. The position of the Hoback normal fault is localized by a ramp in the Bear thrust, where the thrust plane cuts up section in the footwall to a Triassic decollement. Such inheritance of steeply inclined thrust structures by later extensional faults is a common feature seen repeatedly across the Wyoming-Idaho-Utah thrust belt. Seismic and well data indicate that the Hoback fault eventually merges with the older Prospect thrust fault plane at depth. Over 10,000 feet (3 km) of shallow-seated post-Miocene horizontal extension is indicated here.

Drive to Stop 3

On the drive north from Hoback Canyon, the side canyons to the west of the highway provide a view of Willow Creek anticline in Cretaceous rocks (**Figure 8**). The east limb of this anticline, along with the east dip of the Camp Davis Formation along the roadside, provides one of the best surface exposures of rotation into a listric normal fault to be found anywhere. On the east side of the highway are coarse conglomerates in the Camp Davis Formation. These lower conglomerates appear to have been deposited by a braided stream system before major displacement on the Hoback normal fault, but more poorly sorted conglomerates exposed in hillsides to the east were deposited in alluvial fans that were sourced from the uplifted footwall of the Hoback fault (Olson and Schmitt, 1987).

After turning west along the Snake River at Hoback Junction, the field trip route passes Astoria Hot Springs near the surface termination of the Darby thrust. The springs issue from the Mississippian Mission Canyon Limestone in the core of a north-plunging anticline, located in the hanging wall of the Darby thrust. For 45 miles (70 km) to the south, the hanging wall of the Darby thrust dips homoclinally westward and juxtaposes lower and upper Paleozoic rocks over Cretaceous strata. At this location however, the Darby thrust truncates the steep east limb of an anticline where it places Pennsylvanian through Triassic rocks over Jurassic strata in the footwall. Just 1 1/4 miles (2 km) to the north, the stratigraphic throw on the Darby is minimal where it juxtaposes Lower Cretaceous Aspen Shale in both the hanging wall and footwall. The Darby thrust termination illustrates the conversion from thrust to fold shortening near the tip points of thrust faults.

Stop 3. Absaroka thrust fault and Little Greys River anticline

Both the Absaroka thrust fault and a footwall fold, Little Greys River anticline, are easily viewed from this stop (1 km) west of Station Creek campground. Little

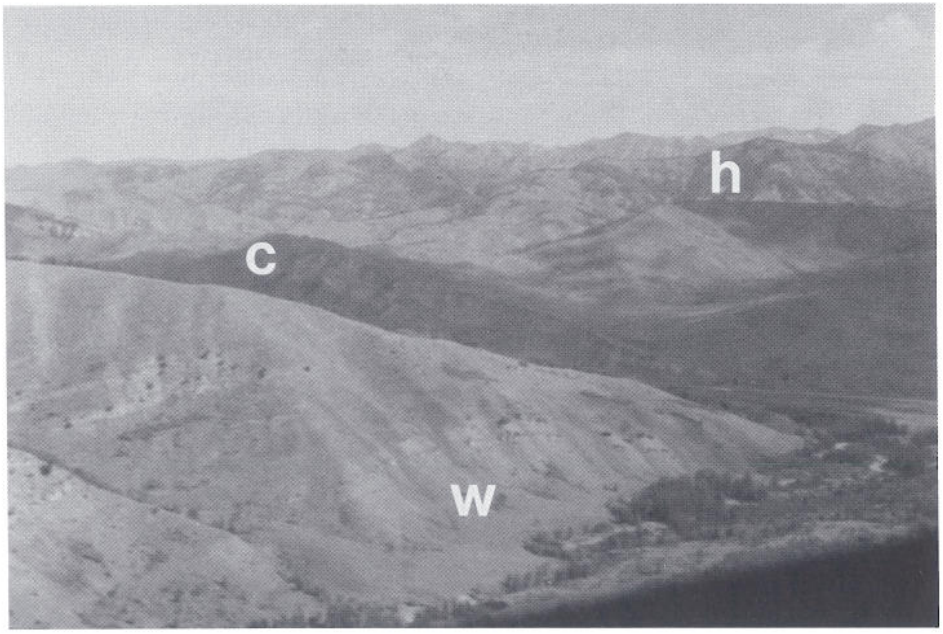

Figure 8. View to the east, showing the crest of Willow Creek anticline (w) in the Cretaceous Frontier Formation, as well as the rotated east dip of the Miocene-Pliocene Camp Davis Formation (c) into the Hoback normal fault, exposed in the strike valley below (h) in the photo.

Greys anticline is an east vergent, asymmetric anticline, a fault-cored intraplate fold in the hanging wall of the Darby thrust. In 1972, True Oil drilled a 14,775-foot (4,500-m) test on the crest of the anticline 4.3 miles (7 km) to the south. At the bottom of the hole, they encountered an imbricated upper Paleozoic section. At road level, the anticline is cored by the Jurassic Twin Creek Limestone. The steep to overturned east limb of the anticline is particularly apparent from the vertical carbonate ribs in the Jurassic Stump Sandstone. Note the extensional fractures in this outcrop. In contrast, we will drive through the gentle west limb of the fold, where excellent exposures of Lower Cretaceous Bear River rust-colored sandstone, black shale, and Aspen greenish sandstone, shale, and porcellanite dip beneath the Absaroka thrust fault.

The Absaroka thrust is exposed immediately to the west. Mississippian carbonate rocks (the high gray ridge) are thrust over the Lower Cretaceous Aspen Shale. It is instructive to note that the stratigraphic separation seen here is the same as that at the giant Whitney Canyon-Carter Creek gas field in the southern Absaroka thrust sheet, where the Mississippian Madison reservoir is juxtaposed against footwall Cretaceous black shale source rocks (Warner, 1982). Why are there no hydrocarbon reserves found in this northern part of the Absaroka thrust sheet? One obvious reason is that the potential reservoirs are breached here, whereas at Whitney Canyon the Mississippian reservoir is some 15,000 feet (4,600 m) beneath the surface. This observation is important since it points out that the structural elevation of the entire thrust belt is much higher here from the level of crystalline basement upward.

Drive to Stop 4

The high structural level of the northern Absaroka thrust sheet exposes a spectacular roadside cross section through the deepest structural and stratigraphic levels of the Absaroka thrust system along Snake River Canyon, where imbricates of the Absaroka thrust include the St. John and Ferry thrusts. The St. John thrust is well exposed on the north wall of Snake River Canyon, with Ordovician Bighorn Dolomite over a folded and imbricated Mississippian through Pennsylvanian section. The Ferry, St. John, and Absaroka thrusts all share a decollement in the Cambrian Gros Ventre Formation. This Cambrian sole decollement is also shared by the Prospect thrust system where it is exposed in fault slices at Teton Pass, and by the Crawford thrust where it has been penetrated by four wells. W.W. Rubey recognized this regional decollement during his mapping of the Bedford, Afton, Cokeville, and Sage and Kemmerer quadrangles immediately to the south (Rubey, 1958, 1973; Rubey and others 1975, 1980). Certainly, Rubey's field observations in this area were instrumental in the development of the Hubbert-Rubey fluid pressure model of thrust propagation (Hubbert and Rubey, 1959).

Stop 4. Grand Valley fault at Alpine Junction

The purpose of this stop at Alpine Junction, Wyoming is to view the features of the normal fault system on the east side of the valley. This is part of a post-Eocene extensional fault system within the thrust belt that extends southward out of the Snake River Plain into Utah, about 186 miles (300 km.). The geometry of the Grand Valley fault(s) at this locality is illustrated in **Figure 9**. The listric fault shape and eastwardly rotated down-dropped block are similar to features of other normal faults in the thrust belt, such as the Hoback fault at stop 2. The interpretation shown is supported by seismic data and exposures of Pliocene-Pleistocene beds that dip continuously into the fault. Of special interest at this stop is a view of a large block of Paleozoic beds that apparently slid westward off the highlands across the fault and out over Pliocene beds. The block was then rotated eastward into the fault plane by continued fault motion and was subsequently overlain by younger Pliocene-Pleistocene sediments that were also rotated. Many smaller blocks of Paleozoic rocks slid west off the upthrown side of the fault and were incorporated in the rotated Pliocene-Pleistocene section. With continued rotation into the Grand Valley fault, the exotic Paleozoic blocks have assumed the same rotated dip as the Pliocene-Pleistocene sediments in which they are now encased.

As discussed earlier for the Hoback normal fault, the position of major extensional faults may be localized by major ramps in older thrust fault systems. The Grand Valley normal fault may be controlled by the Paleozoic to Cretaceous footwall ramp of the Absaroka thrust system (**Figure 9**; Figure 6 of Royse and others, 1975). Further steepening of the Absaroka ramp by the underlying Firetrail thrust may have contributed to rotating the fault plane to a mechanically favorable orientation for later extension. Net slip on the fault here is approximately 18,000 feet (5.5 km).

Drive to Stop 5

The drive south from the Alpine area to the lunch stop near Afton passes through a linked system of half grabens that form Grand and Star valleys. The faceted mountain fronts of the Salt River Range to the east are

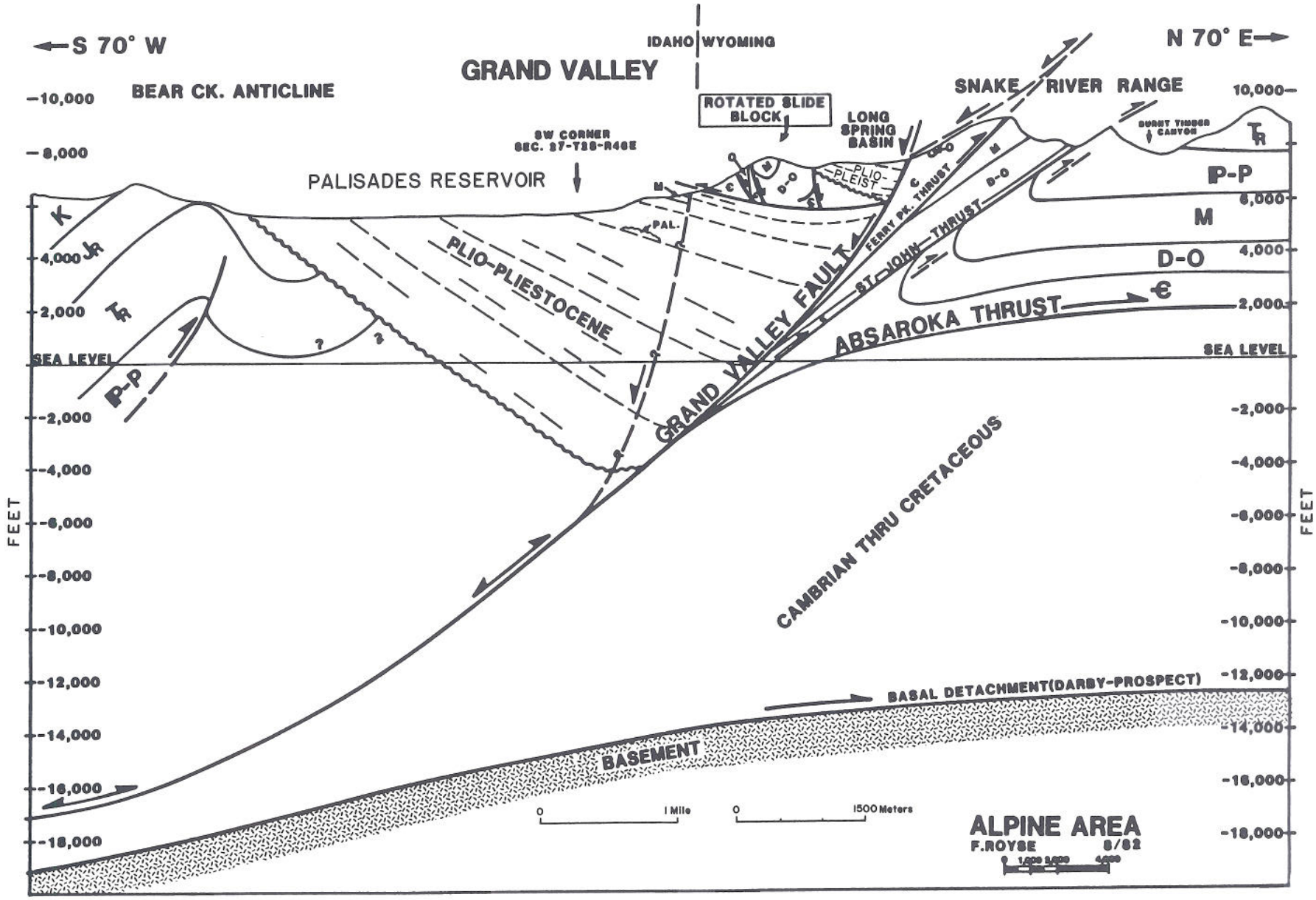

Figure 9. Schematic cross section of the Alpine area, showing the relationship between the footwall Cambrian through Cretaceous ramp of the Absaroka thrust plane and the position of the later Grand Valley extensional fault. Notice the slide block of Paleozoic strata that was encased in and rotated with the Pliocene-Pleistocene valley fill.

the geomorphic expression of a series of normal faults along which displacement terminates and transfers along strike in an en echelon map pattern. The clearest example of such transfer is in the Narrows area near Thayne, Wyoming. Here, displacement on the southern Grand Valley fault decreases markedly immediately southeast of Thayne as the lower Star Valley normal fault gains displacement southwest of Thayne. The normal fault system along Grand and Star valleys has been inactive along most of its length during the Holocene. However, the southern ends of the two fault segments exhibit well-developed scarps in Quaternary alluvium and colluvium (Piety and others, 1986).

Stop 5. Swift Creek Canyon, Star Valley normal fault scarp

Stop for lunch at Swift Creek Canyon, where you can view the scarp of the Star Valley normal fault at the mouth of the canyon.

Stop 6. Salt spring in the core of the Afton anticline, Salt River Pass area

Stop 6 is a view of a salt spring in the core of Afton anticline, located on the south side of the highway, 1.4 miles (2.5 km) south of Allred Campground.

The drive to Stop 6, through Salt River Pass from Afton transects short-wavelength (± 3 miles/5 km), high-amplitude (± 1,000 ft/3,000 m) symmetrical folds in Jurassic and Lower Cretaceous strata along the leading edge of the Crawford thrust system. The tightest folding is restricted to the Jurassic Preuss Redbeds and younger units. The Preuss is the oldest unit carried by thrusts that cut this fold train, namely the Porcupine Creek thrust and Muddy Ridge backthrust (**Figure 10**). A salt interval in the lowermost Preuss Redbeds is the primary decollement for Crawford thrust shortening in this area. The salt manifests itself surficially by numerous salt springs that are generally found in solution valleys that occupy the cores of anticlines such as Afton anticline, and that are found along the traces of major thrust faults, for example along the Meade thrust to the northwest (Coogan and Yonkee, 1985). In the subsurface, the salt interval is abnormally thickened where it has been penetrated in the Crawford thrust zone. Over 5,600 feet (1,700 m) of salt were encountered in the core of Afton anticline immediately east of the Crawford ramp anticline (Sublette anticline) (Coogan and Yonkee, 1985). A "normal" salt thickness in the area is 300 feet (100 m).

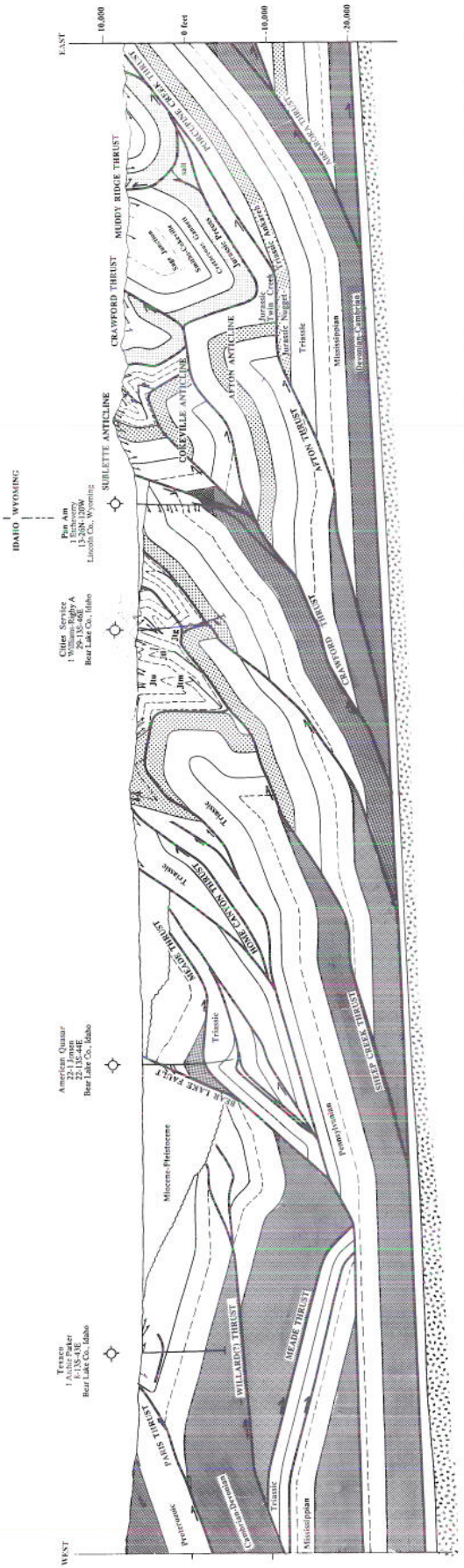

Figure 10. Geologic cross section from the frontal Crawford thrust salt decollement to the Paris thrust front (see Stops 6-15) (by J.C. Coogan). The highly folded strata of the Twin Creek Limestone are represented by: Jtu = upper Giraffe Creek and Leeds Creek members; Jtm = middle Watton Canyon and Boundary Ridge members; Jtl = lower Rich and Sliderock members; and Jtg = Gypsum Spring Member.

Stop 7. Sublette anticline

Sublette anticline is the main surface expression of the northern Crawford thrust. Well control on the forelimb and backlimb of Sublette anticline (**Figure 10**) demonstrates that the anticline is the result of a hanging wall ramp in the Crawford thrust plane from the Paleozoic level to the Jurassic Preuss salt decollement. The present structural elevation of Sublette anticline is the composite result of uplift above Cokeville and Afton anticlines, as well as uplift above the Crawford ramp itself. Afton anticline plunges south from our previous stop into the line of section in **Figure 10**. Both limbs of Afton anticline were drilled 6 miles (10 km) north of the line of section (Figure 7 of Coogan and Yonkee, 1985). Cokeville anticline is exposed 9 miles (15 km) south of this section where it plunges north into the line of section. The drive into Thomas Fork Valley transects the north plunging nose of Sublette anticline in Salt River Canyon (**Figure 11**). Here, the Jurassic Twin Creek Limestone is folded into a box fold. The steep limbs and flat crest of Sublette anticline can be seen on the north canyon wall.

Driving south through Thomas Fork Valley, Sublette anticline can be viewed at successively deeper stratigraphic levels to the east until Pennsylvanian strata are exposed in the core of the fold near Raymond Canyon. The faceted mountain front marks the approximate location of the Thomas Fork normal fault (**Figure 11**). The Thomas Fork fault is localized on the oversteepened Crawford thrust ramp. The approximate fault location and throw is constrained by well control immediately west of the mountain front (**Figure 10**). Vertical throw on the fault is approximately 3,600 feet (1,100 m) along the line of section.

Raymond Canyon presents a well-exposed cross section through the overturned limb of a tightened ramp anticline (**Figure 10**). The canyon cuts from the Pennsylvanian Wells Formation through the Jurassic Twin Creek Limestone and permits identification of the different structural styles encountered in the various lithologies. The entrance to the canyon is marked by vertical walls of the highly fractured Wells quartzites, but it is most notable for the "gateway" through a wall of the Rex Chert Member of the Permian Phosphoria Formation. Higher in the section, small-scale kinking and out-of-the-syncline folding and thrusting are observed in the shaley intervals of the Triassic. The Twin Creek Limestone displays well-developed refracted cleavage and small-scale thrusting at the east end of the canyon.

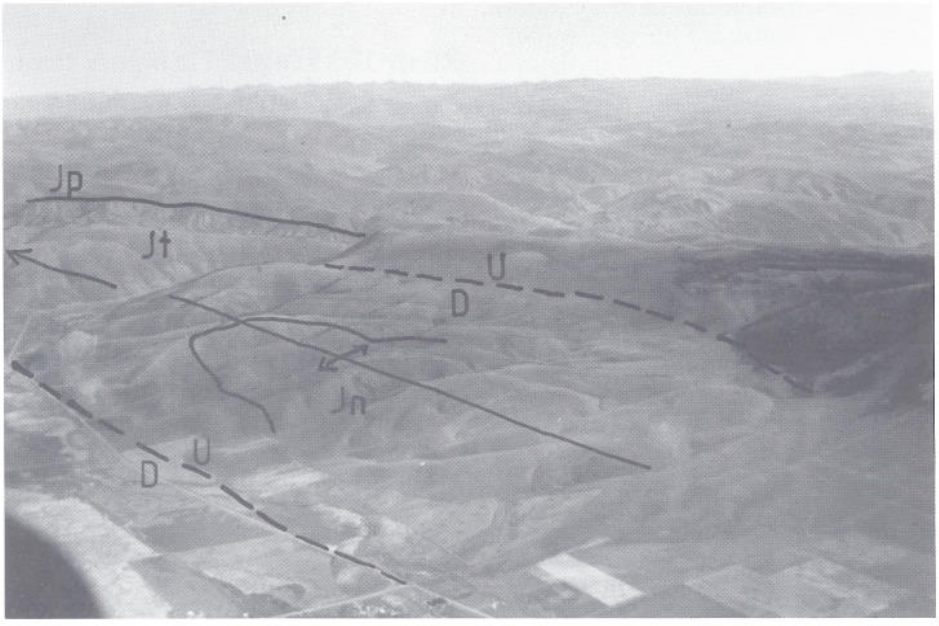

Figure 11. View of the north plunge of Sublette anticline in the Thomas Fork Canyon area. The Jurassic Nugget Sandstone (Jn) cores the fold with Jurassic Twin Creek Limestone (Jt) and Preuss Sandstone (Jp) on the fold limbs. Two small extensional faults are superimposed on this ramp anticline.

Stop 8. Preuss anticline near Geneva, Idaho

The drive west from Raymond Canyon provides a good perspective for viewing a spectacular decollement fold train on the west side of the valley (**Figure 12**). The folds are wholly within the Twin Creek Limestone, which is divided into seven members. The folds are expressed topographically by the ridge-forming Watton Canyon Member as well as by vegetation bands in the shales of the underlying Boundary Ridge Member. If time permits, stop to view the anhydrite-bearing Gypsum Spring Member of the Twin Creek in the core of Preuss anticline. A down-plunge projection of Preuss anticline (**Figure 12**) illustrates that the anhydrite-bearing Gypsum Spring Member fills the core of the anticline and the salt interval of the lower Preuss Redbeds fills in the tight troughs of adjacent synclines. Both anticlines and synclines have undergone hinge collapse. The down-plunge view illustrates that the upper sandstone interval of the Preuss Redbeds is only gently folded, hence an upper decollement to the folding must exist in the underlying salt interval. The salt interval is expressed on the surface as strike solution valleys. We will drive across the salt and sandstone interval as we proceed west past Geneva, Idaho.

Additional information on this fold chain is provided by Cities Service #1 Williams-Rigby well drilled on the crest of an anticline southwest of Preuss anticline (**Figures 10** and **12**), which further demonstrates that the Nugget Sandstone is not involved in the high-amplitude folding above the Gypsum Spring Member. In short, the Twin Creek Limestone forms a disharmonic fold train that provides an excellent example of angular parallel folding between upper and lower decollement horizons of mechanically weak material (Coogan and Boyer, 1985). The shortening in this fold belt is associated with the underlying Sheep Creek blind thrust that was drilled beneath Sheep Creek anticline in two wells to the southwest. Sheep Creek anticline is cored by an anhydrite interval in the Pennsylvanian Amsden Formation. The folding in the Twin Creek is simply fold shortening equivalent to the fold and thrust shortening of older units to the west (**Figure 10**).

Stop 9. Cleavage in Twin Creek Limestone at Geneva Summit

Proceeding west toward Montpelier, Idaho, stop about 300 feet (100 m) west of Geneva Summit to view the well-developed cleavage in the Twin Creek Limestone. Look closely and you will find that bedding is locally defined by thin, tan silt partings and is subvertical. The main cleavage is subhorizontal with a north-south strike. Throughout the region, this dominant Twin Creek cleavage is a fanned cleavage, indicating that it formed before the main fold event. This early layer-parallel shortening was estimated by Adolph Yonkee (Yonkee, 1983; Mitra and Yonkee, 1985) to be on the order of 15 to 20 percent by comparison of clay to carbonate volumes between the cleavage seams and the intervening micrite lithons. Protzmann (1985) measured 35 to 48 percent of early layer-parallel plastic strain from deformed Pentacrinus ossicles in an area immediately beneath the Meade thrust to the northwest. Yonkee (Yonkee, 1983; Mitra and Yonkee, 1985) also estimated temperatures from 130° to 200° C during cleavage development, using the crystallinity of illite in the cleavage seams as a thermal index. Estimated temperatures increase from east to west across the Crawford thrust plate and Meade footwall, a result that Mitra and Yonkee (1985) attributed to a westward increase in the depth of burial beneath the Meade thrust sheet.

A weak second cleavage is also well displayed at this location along north-south oriented outcrops. This cleavage is near vertical, but its strike is east-west. The second cleavage is subparallel to the axial planes of east-west trending cross folds that fold both bedding and the first cleavage. It is attributed to north-south shortening associated with a lateral ramp in the underlying Crawford thrust plane (Yonkee, 1983; Mitra and Yonkee, 1985).

Stop 10. Home Canyon thrust fault near Montpelier Reservoir

This stop, immediately west of the Montpelier Reservoir turnoff, provides an opportunity to view the Home Canyon thrust fault. The thrust has a persistent surface exposure for 27 miles (45 km) southward, along which it places Triassic Ankareh and Thaynes formations over the Triassic Ankareh, Jurassic Nugget Sandstone, and the Gypsum Spring Member of the Jurassic Twin Creek. The thrust lies in the footwall of both the Meade and Laketown thrusts. The surface trace of the fault has been mapped from 4.3 miles (7 km) north of this location to North Eden Canyon, Utah, where the thrust is folded by the underlying Sheep Creek anticline.

At our present location in Montpelier Canyon (**Figure 13**), the Home Canyon thrust places Triassic Thaynes over Triassic Ankareh. The footwall of the thrust is highly contorted; the Portneuf Limestone and Timothy Sandstone are folded into an antiformal syn-

cline and a synformal anticline from west to east. These footwall folds are in turn underlain by an eastern splay of the Home Canyon thrust named the Montpelier Reservoir thrust, which continues north and joins the Meade thrust trace south of Snowdrift Mountain. The Preuss salt horizon behaves as a footwall decollement for the Meade thrust and as an upper decollement (roof thrust) for the Montpelier Reservoir thrust.

Overnight at Montpelier, Idaho

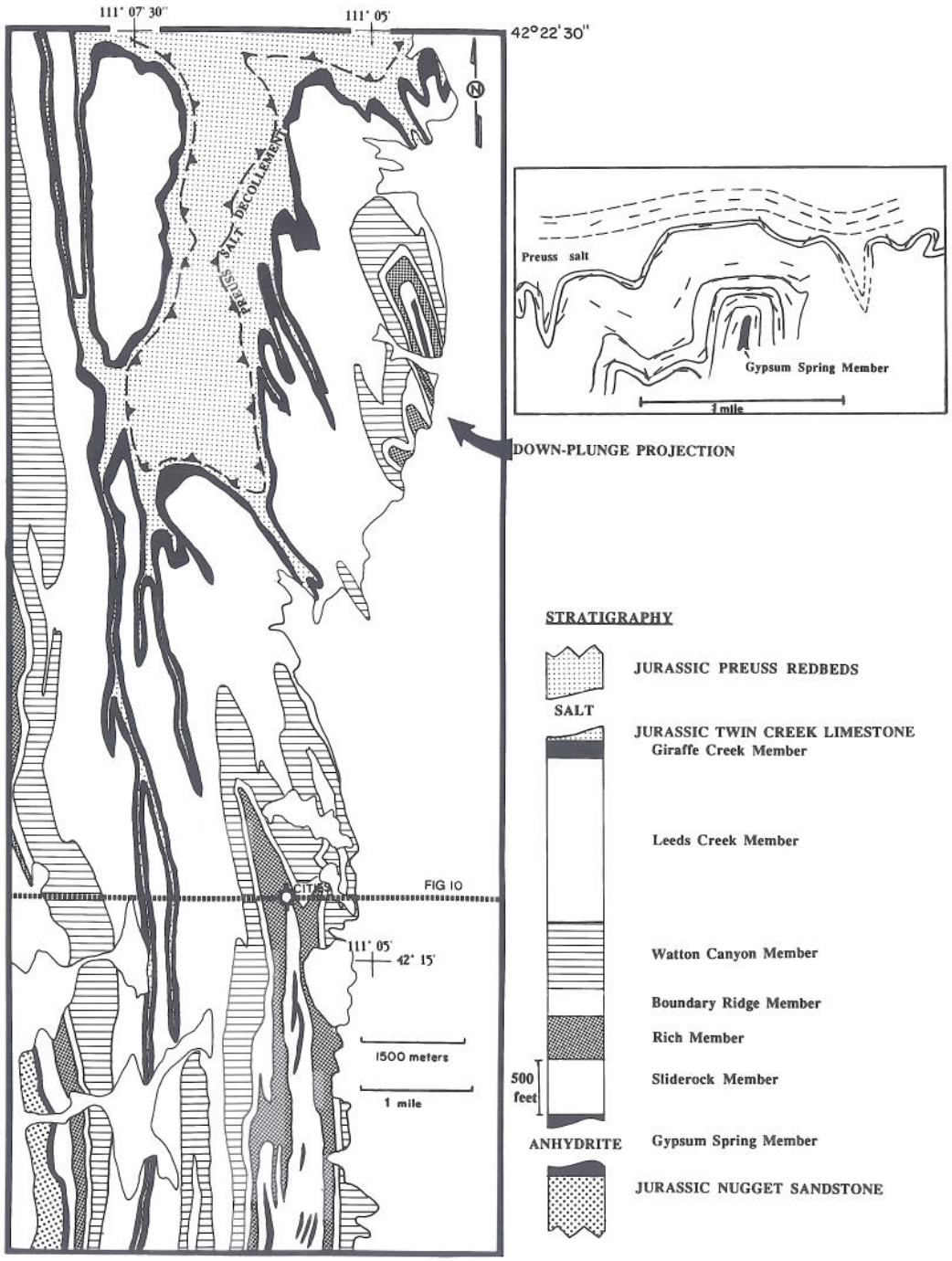

Figure 12. Geologic map, stratigraphic section, and down-plunge view of fold train in the Jurassic Twin Creek Limestone along the west side of Thomas Fork Valley (geology by J.C. Coogan).

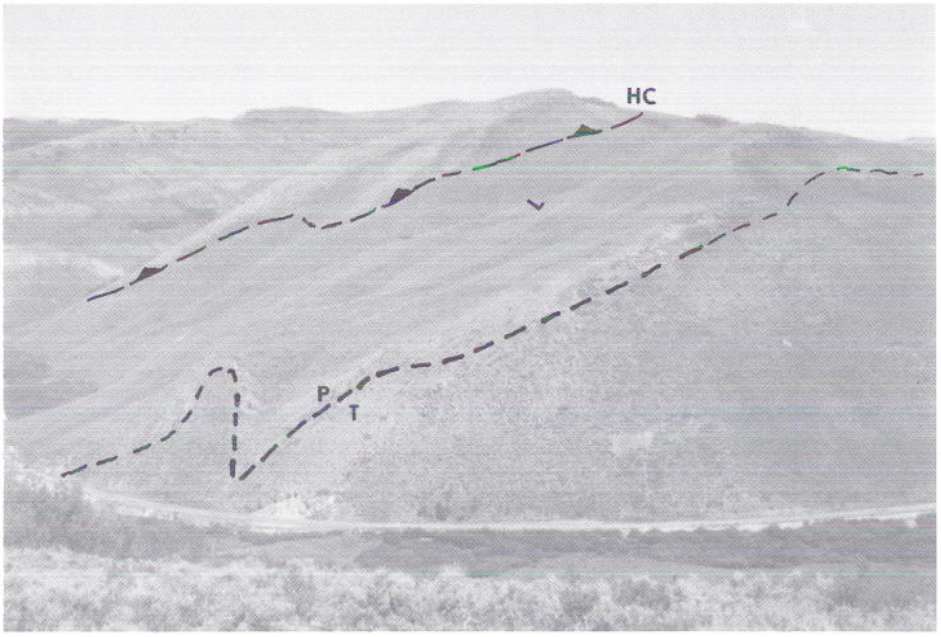

Figure 13. View to the northwest of the Home Canyon thrust (HC) in Montpelier Canyon, Idaho at Stop 10. The upper calcareous siltstone member of the Triassic Thaynes Limestone lies over an overturned section of the Lanes Tongue of the Triassic Ankareh Formation (L) in the footwall. The overturned footwall section is tightly folded, as seen by the contact between the Portneuf Limestone (P) and the Timothy Sandstone (T).

Field trip route and stop descriptions, day 2

Stop 11. Waterloo thrust faults at Home Canyon, Idaho

From Montpelier, we will return briefly to Montpelier Canyon to look at footwall imbricates of the Meade thrust as well as the southernmost surface exposure of the Meade thrust trace itself. Stop 12 is at the mouth of Home Canyon, where a view to the south encompasses the Hellhole and Waterloo thrusts (**Figure 14**). The decollement folds above the Hellhole thrust are particularly scenic. They are cored by the upper part of the Wells Formation and the resistant ridges on the limbs are the Rex Chert. At road level, the gray contorted rocks on the west side of the mouth of Home Canyon are the Wells, whereas the shallowly west dipping redbeds on the east side are the Lanes Tongue

Figure 14. View to the west above Montpelier Canyon showing the approximate position of the Waterloo thrust (WT) and the Hellhole thrust (HT) at Stop 11. Note the decollement fold train in the Pennsylvanian-Permian section above the Waterloo thrust.

of the Ankareh Formation. The canyon mouth sits astride the Hellhole thrust trace.

Stop 12. Meade thrust fault, mouth of Montpelier Canyon

The southernmost exposure of the Meade thrust is seen at the mouth of Montpelier Canyon where it juxtaposes the Mississippian carbonates in the hanging wall against the upper calcareous siltstone member of the Thaynes Limestone in the footwall. The upper calcareous siltstone is in the overturned west limb of an isoclinal footwall syncline, well exposed for 1.25 miles (2 km) east on the north slope of the canyon (**Figure 15**). The fault contact exhibits intense brecciation of the hanging wall carbonate rocks and a local crenulation cleavage in the footwall siltstones. South of this location 3.4 miles (5.5 km), the American Quasar # 22-1 Jensen drilled the Meade thrust beneath Bear Lake Valley (**Figure 10**). The well penetrated the Mississippian section, drilled through the Devonian, and eventually into the Silurian Laketown Dolomite, beneath which it penetrated the Meade thrust plane. A steeply east dipping footwall section consisting of the Triassic Woodside and Dinwoody, Permian Phosphoria, and Pennsylvanian Wells formations was encountered to the total depth of the well.

The well data reveal two highly significant facts. First, the presence of the Silurian section in the Meade hanging wall contrasts with the Crawford, Absaroka, and Prospect thrust sheets to the east, where the Silurian is missing along a regional unconformity. As we will see later in the day, the easternmost outcrop of the Silurian Laketown Dolomite is at the type locality on the Laketown thrust sheet. This and other stratigraphic observations are important in linking the Meade and Laketown thrust traces as part of the same fault system. The subsurface control is crucial, since the area between the exposed thrust traces has been dropped down beneath Bear Lake Valley. A second important observation is that the eastern Bear Lake Valley normal fault marks the approximate position of a hanging-wall ramp in the Meade thrust plane, where the Meade thrust cuts up section from at least the Silurian section in the borehole to where the thrust follows a Mississippian decollement that is better seen at the next stop.

Drive to Stop 13

On the drive north from Montpelier to Georgetown Canyon, drive down the axis of an asymmetric half graben filled with approximately 11,500 feet (3,500 m) of Miocene to Holocene sediments. The main bounding fault is adjacent to the east edge of the valley. The mountain front to the east is made up of the Jurassic Nugget Sandstone and the Twin Creek Limestone. The highest broad peak is Bald Mountain. The Watton Canyon Member of the Twin Creek Limestone forms the crest of the mountain and also lies in the core of Bald Mountain syncline, which trends about N30°W. Northeast of Bald Mountain, the Nugget Sandstone is exposed in the core of Home Canyon anticline, which plunges northwest into the Georgetown Canyon area (**Figure 16a**). You will stop in Georgetown Canyon, where Home Canyon anticline has folded the Meade thrust, exposing the thrust plane and allowing a view of both the hanging-wall and footwall deformation. On the drive west from Georgetown, Idaho, into Georgetown Canyon, the sagebrush-covered hills to the north and south are underlain by the Miocene to Pleistocene Salt Lake Formation, which dips from 50°E to 20°E into the Bear Lake Valley normal fault.

Stop 13. Bear Lake Valley fault and Meade thrust fault at Georgetown Canyon

The main normal fault is crossed approximately 2.5 miles (1.5 km) east of the mouth of Georgetown Canyon, where the prominent thin-bedded, dark gray Mississippian Lodgepole Limestone comes into view on the north side of the canyon in the fault footwall. The Lodgepole here is a down-dropped portion of the Meade hanging wall. A second normal fault juxtaposes the Lodgepole against the Twin Creek Limestone in the Meade footwall on the north side of the canyon.

Figure 16b is a down-plunge projection of the Meade hanging wall and footwall relationships (Adolph Yonkee, *in* Mitra and others, 1988). Walk across the area of this projection, which shows a recumbent syncline in the Twin Creek Limestone that is cored by the Preuss Redbeds. Along the north side of Georgetown Canyon, the Meade thrust juxtaposes a Mississippian hanging wall decollement against a footwall ramp through the Twin Creek and a footwall decollement in the lower, salt-bearing part of the Preuss (Coogan and Yonkee, 1985). The cleavage in the Twin Creek (S_1) is generally at a high angle to the steeply overturned, west dipping bedding (So). Near the thrust, cleavage-bedding angles decrease and the cleavage intensity increases, an observation that indicates that cleavage developed, at least in part, during slip and simple shear across the Meade thrust plane (Mitra and others, 1988). Locally, a second weak cleavage (S_2) developed parallel to the axial planes of small-scale

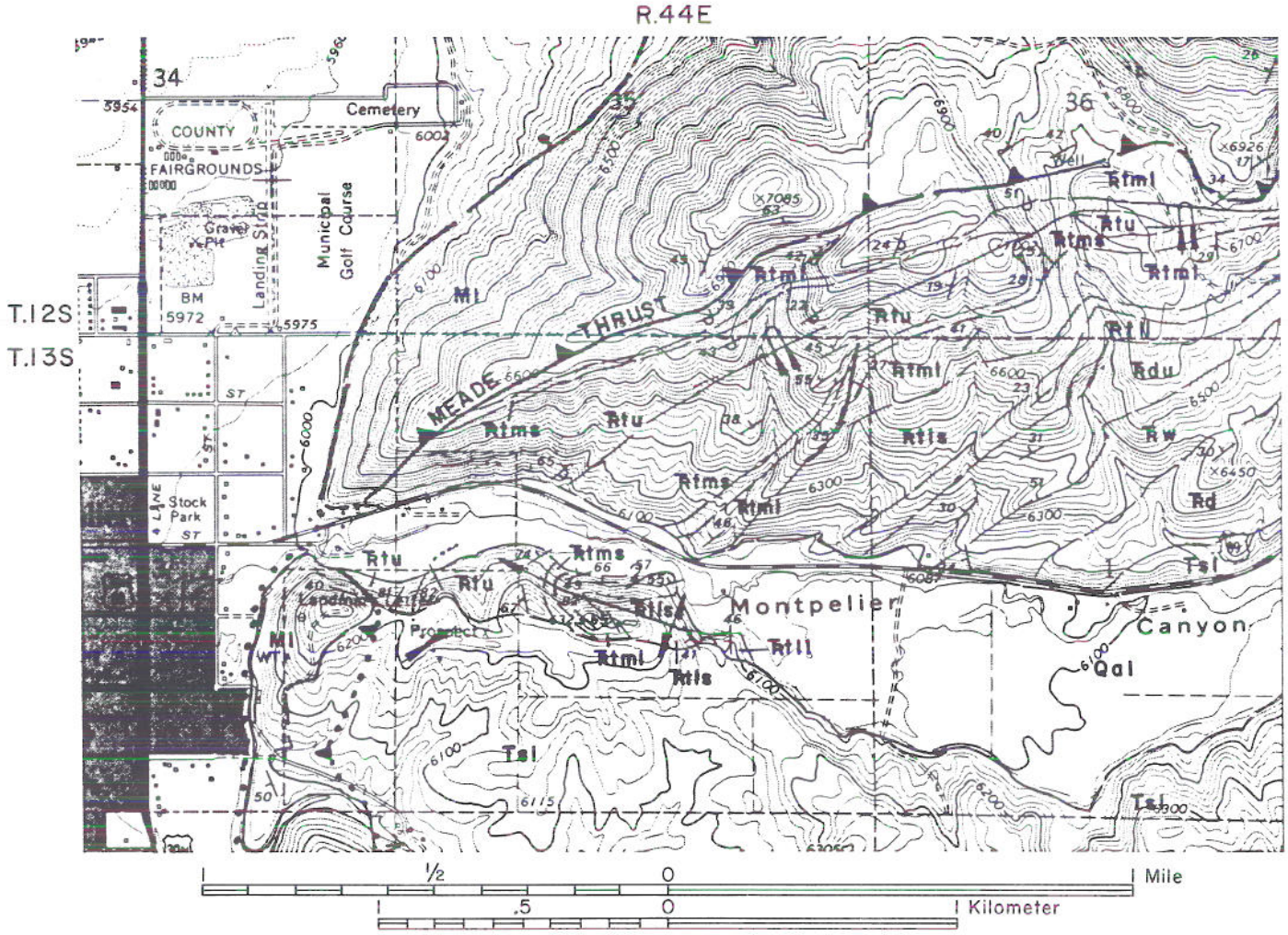

Explanation

Tsl = Miocene-Pleistocene Salt Lake Fm.
Thaynes Formation
- Rtu = upper calcareous siltstone
- Rtms = middle shale
- Rtml = middle limestone
- Rtls = lower shale
- Rtll = lower limestone

Rdu = upper tongue of Dinwoody Fm.
Rw = Woodside Formation
Rd = Dinwoody Formation
Mi = Mississippian rocks

- Geologic contact
- Normal fault, dotted where inferred
- Thrust fault, dotted where inferred
- 50 Strike and dip of bedding
- Syncline
- Overturned syncline
- Anticline, end arrow shows plunge

Figure 15. Geologic map of the Meade thrust at the mouth of Montpelier Canyon, Idaho, Stop 12 (geology by J.C. Coogan).

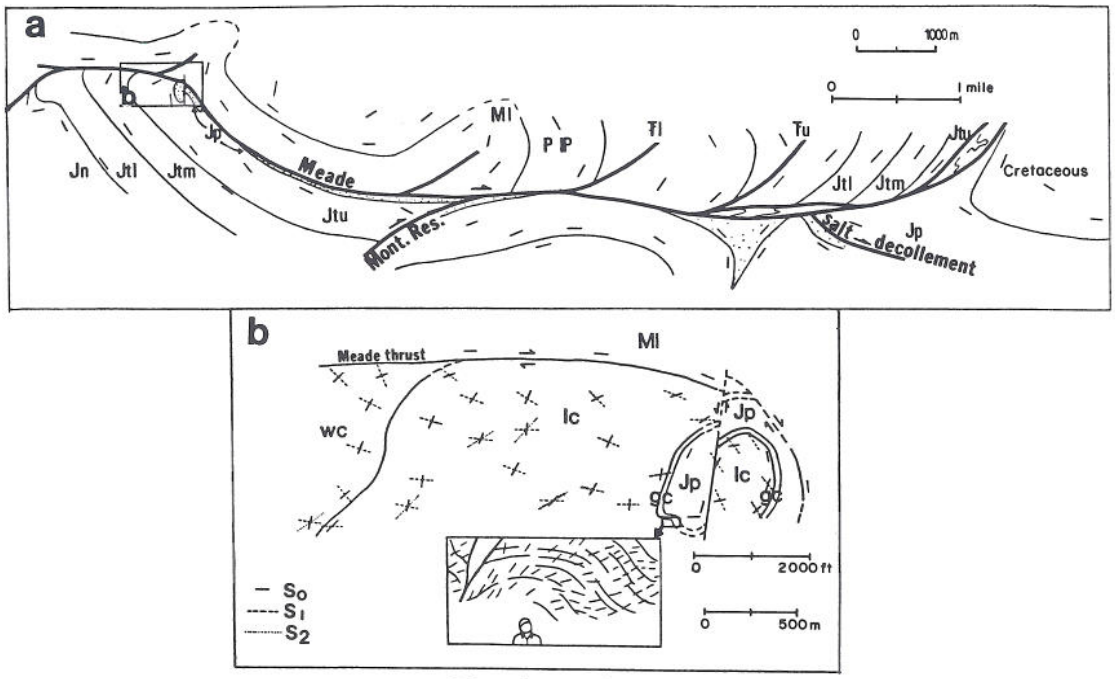

Explanation

a. M = Mississippian; P IP = Permian and Pennsylvanian; Tl = lower Triassic; Tu = upper Triassic; Jn = Nugget Sandstone; Jtl, Jtm, and Jtu = lower, middle, and upper Twin Creek Limestone; Jp = Preuss Redbeds

b. MI = Mississippian Lodgepole Limestone; wc, lc, and gc = Watton Canyon, Leeds Creek, and Giraffe Creek members of the Twin Creek Limestone; and Jp = Jurassic Preuss Redbeds. So = bedding, S1 = first cleavage, S2 = second cleavage

Figure 16. Down-plunge projections of the Meade thrust fault in the Georgetown Canyon area, Idaho, Stop 13. (a) Down-plunge projection of large-scale folding of Meade thrust plane (from Coogan and Yonkee, 1985). (b) Down-plunge projection of bedding-cleavage relationships in the Meade footwall (from Mitra and others, 1988).

buckle folds that shorten the first cleavage, possibly as a result of late contraction in front of the Meade ramp (Mitra and others, 1988). The entire package was subsequently rotated on the east limb of Home Canyon anticline.

Along the Meade thrust trace at Georgetown Canyon, a well-developed breccia zone is exposed that contains angular blocks of the Lodgepole Limestone in a calcite spar and cataclastic matrix. Small contraction faults and buckle folds are also seen above the thrust plane.

On a larger scale, well control into the Meade thrust footwall shows a more complex history than could be assumed by this location alone. The Union Texas #1-13 Big Canyon well penetrated the Meade thrust 5.5 miles (9 km) northwest of the field trip stop (**Figure 17**). The well drilled into a nearly complete Twin Creek section west of the northernmost exposure of Home Canyon anticline in the Left Hand Fork of Georgetown Canyon (Cressman, 1964). Along Left Hand Fork, the Meade thrust locally cuts down section eastward from the Jurassic Twin Creek into the Triassic Ankareh Formation. As represented in **Figure 17**, this cross-cutting geometry implies that the Meade thrust trace in this area is older than the Home Canyon fold. A similar relationship was discussed by Protzman (Mitra and others, 1988) for footwall folds in the frontal part of the Meade thrust as represented on **Figure 16a**. One scenario for such relationships would call for propagation of footwall imbricates in front of the Meade thrust during initial Meade slip. The minor imbricates in the Triassic above the Home Canyon thrust in the Union Texas well are candidates for such slip. Later slip along the Meade thrust might have truncated the

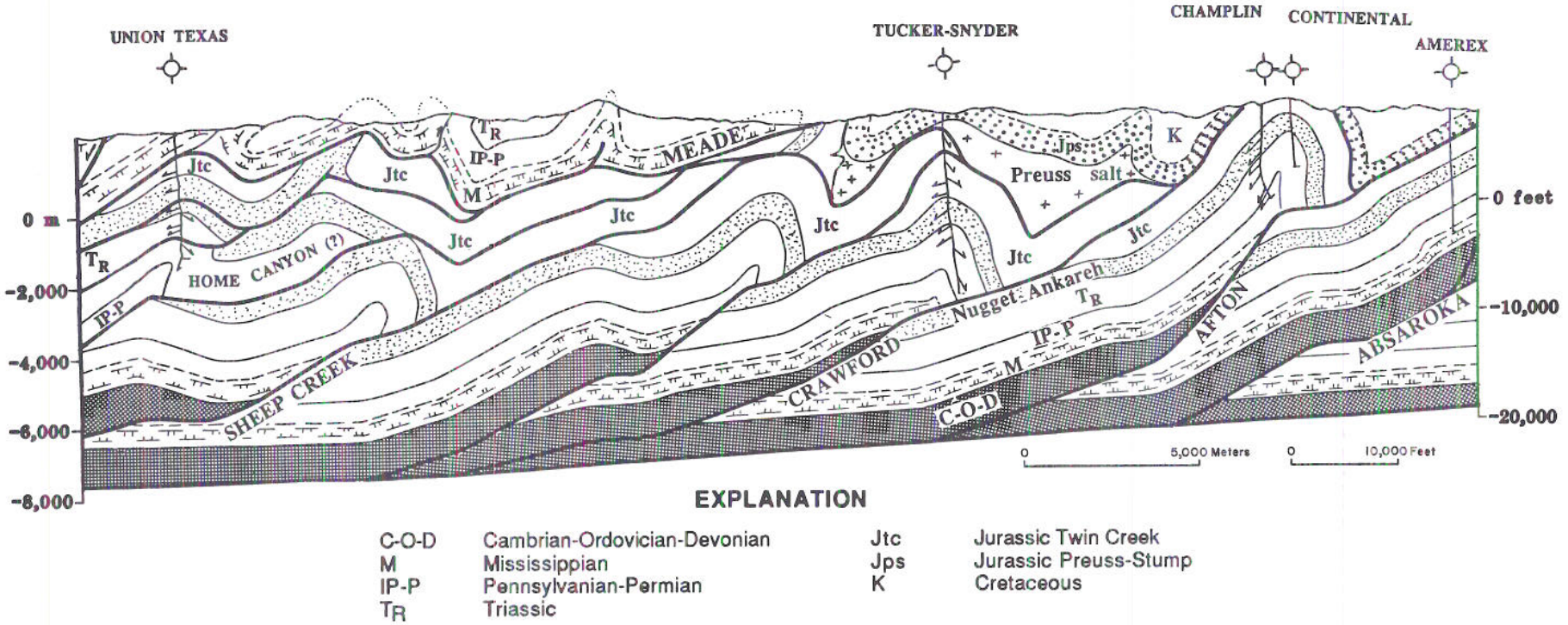

Figure 17. Generalized geologic cross section, showing well control of structures in the Meade thrust footwall between the Georgetown area (Stop 13) and Elk Valley, Idaho (by J.C. Coogan).

pre-existing imbricate-cored folds as fault plane asperities. Subsequent folding by the structurally lower fold above the Home Canyon thrust could account for the late rotation of the Meade thrust and its footwall seen at the Georgetown Canyon stop.

Well control beneath the Meade thrust also provides insight into the relationship between the Meade and Crawford thrusts (**Figure 17**). Until recently, Meade shortening in the northern thrust belt was thought to be equivalent to and coeval with Crawford shortening to the south, with the area between the two thrusts representing an area of simple displacement transfer between the two thrust traces (Royse and others, 1975; Wiltschko and Dorr, 1983; Evans and Craddock, 1985). **Figures 10** and **17** illustrate the subsurface constraints that lead to the conclusion that the Meade and Crawford thrusts are not geometrically linked in any simple manner. The Crawford thrust is structurally much lower than the Meade, and all evidence indicates that the Crawford thrust branches from a sole decollement in the Cambrian Gros Ventre Formation well to the east of any Meade thrust ramp. In addition, there are many intervening thrust faults, such as the Home Canyon and Sheep Creek thrusts, that underlie and fold the Meade hanging wall well to the west of the Crawford trailing ramp. The Crawford thrust is probably younger than the main displacement on the Meade thrust. Along the cross section in **Figure 17**, the Crawford ramp anticline (Sublette anticline) was drilled by the Tucker-Snyder #1-8 Elk Valley #2 just south of where it plunges beneath the Meade thrust. The jog in the Meade thrust trace immediately north of Elk Valley probably represents folding of the Meade thrust plane by the younger ramp anticline of the Crawford thrust.

Well control also sheds light on the hanging-wall structure and stratigraphy of the Meade thrust sheet in this area. The Ladd # 3-24 Bennington well drilled the Meade hanging wall 4.5 miles (7 km) southwest of Georgetown in Bear Lake Valley. At Georgetown Canyon, the Meade thrust carries only Mississippian and younger strata, but the Ladd well penetrated the Triassic through basal Mississippian section, encountered a normal fault, and continued drilling through the Ordovician Garden City and Cambrian St.Charles, Nounan, Bloomington, and Blacksmith formations, to a total depth of 13,530 feet (4,124 m). This hanging-wall section is remarkably similar to that encountered on the Paris thrust sheet and is nearly identical in thickness and lithology to the Laketown hanging wall that we will visit later in the day (**Figure 4**). The similar stratigraphy and structural position provide arguments for linking the Meade and Laketown thrusts beneath the length of Bear Lake Valley.

Stop 14. Paris thrust fault in Paris Canyon

The eastern section of Paris Canyon transects the Triassic Thaynes and Dinwoody Formations in Paris anticline on the footwall of the Paris thrust. This structure was drilled 5.5 miles (9 km) north of this location by the Texaco # 1 Archie Parker well. The well drilled a fairly low-dipping section to a total depth of 10,012 feet (3,052 m) in the Ordovician(?) (**Figure 10**). The trend drilled is underlain by a seismically defined imbricate in front of the Paris thrust that can be traced south to the southeast corner of Bear Lake. This imbricate may be the northern continuation of the Willard thrust, an interpretation that seems justified by the Proterozoic through Cambrian outcrop pattern to the south as mapped by Dover (1985). Southwest of Garden City, Utah, the Proterozoic through Cambrian outcrops of the Paris hanging wall diverge from a series of Proterozoic outcrops to the east. The eastern outcrop belt may be the leading edge of the Willard hanging wall.

In Paris Canyon, the Paris thrust places the Proterozoic to middle Cambrian Geertzen Canyon Quartzite over the Pennsylvanian Wells and Permian Phosphoria formations in the overturned west limb of Paris syncline. This syncline was drilled 4.3 miles (7 km) to the south by the Murphy Oil #1 Worm Creek well. The well drilled an overturned and imbricated Mississippian(?) and Pennsylvanian section, encountered the Permian Phosphoria and Triassic Dinwoody formations in the tight hinge of the syncline, and then drilled an upright Permian and Pennsylvanian section to a total depth of 7,493 feet (2,284 m). The overturned limb is clearly seen in Paris Canyon, where the phosphatic shales of the Phosphoria Formation are accentuated by old mine workings on the north side of the canyon. The Paris thrust itself is defined by a break in slope west of the prospect pits where the highly fractured pink and tan quartzites and conglomeratic quartzites of the Geertzen Canyon overlie the white, finer grained, fractured quartzites of the Wells. Paris Canyon is a good lunch stop.

Drive to Stop 15

The road from Paris Canyon to South Eden Canyon on the east shore of Bear Lake, passes a prominent hill 4.3 miles (7 km) south of Garden City, Utah, along the west side of the highway. Across this hill, the Geertzen Canyon Quartzite is folded into an east vergent overturned anticline. The highly sheared east limb of the anticline is underlain by a thrust fault, possibly the northern continuation of the Willard thrust, that jux-

taposes Geertzen Canyon Quartzite against Ordovician rocks to the south (Valenti, 1982). The Paris thrust trace lies 3 miles (5 km) west of this location where Dover (1985) mapped a thrust that places Geertzen Canyon Quartzite over Cambrian St. Charles Limestone along Richardson Fork Creek. The inferred relationship between the Paris, Willard, and Laketown thrusts is illustrated in **Figure 18**.

Bypass Laketown for now and turn north up the East Shore road toward South Eden Canyon. The only exposure of the Laketown thrust trace can be viewed 1 mile (1.5 km) north of Laketown on the round hillside to the east. Here the Laketown thrust places the Devonian Hyrum Formation over the Jurassic Nugget Sandstone, as mapped by Valenti (1982, Plate 2), although personal reconnaissance indicates that a thin layer of the Gypsum Spring Member of the Twin Creek Limestone might immediately underlie the thrust plane. The thrust plane itself is not exposed, but a crude three-point solution on the trace mapped by Valenti (1982) gives a dip direction of 50° toward 204°, approximately the same dip as the underlying Nugget Sandstone. The apparent concordance between the Laketown thrust and the footwall strata indicate that the thrust had initially overlain a flat footwall decollement, possibly at the base of the Gypsum Spring Member, which was subsequently folded in a south plunging anticline. The Triassic strata in the core of this anticline are seen in the red hillsides immediately to the northeast. Proceed north to South Eden Canyon where this footwall deformation is more readily seen.

Stop 15. Laketown thrust footwall folds at South Eden Canyon

At the turnoff to South Eden Canyon, the red and yellow mottled slope of the mountain front to the southeast is a dip slope of the Gypsum Spring Member of the Twin Creek. Local tight, disharmonic folding in dolomites within the Gypsum Spring indicate that this dip slope marks the position of an important decollement horizon. Across the canyon mouth to north, the steep lake front ridge is comprised of overturned Nugget that is thrust above a continuation of the Gypsum Spring dip slope. The thrust lies in the drainage (Little Creek) on the north side of the canyon immediately east of the ridge. One important observation here is that a Quaternary alluvial terrace at the mouth of Little Creek is offset with normal displacement along this fault trend. Once again, we see an example of the inheritance of early west dipping thrust fault planes by later extensional faults. Other Quaternary faults are evident in scarps across the alluvial terrace deposits of South Eden delta immediately to the west, as well as across alluvial fan and colluvial deposits at the foot of the faceted mountain front to the north and south.

About .6 mile (1 km) east of the canyon turnoff, an anticline-syncline pair in the Nugget Sandstone lies beneath the Gypsum Spring dip slope. The east limb of the syncline is tightly folded and it is bound by a thrust that places Nugget over the Gypsum Spring decolle-

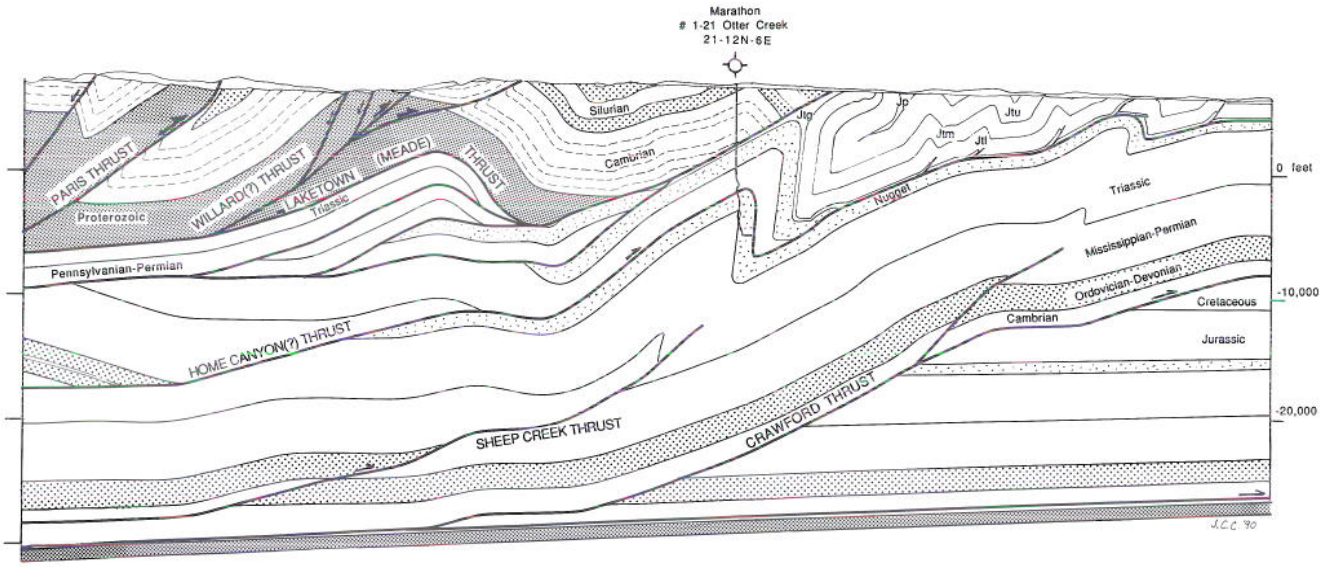

Figure 18. Structure section through the frontal part of the Laketown thrust sheet, showing the Marathon #1-21 Otter Creek well and the structural position of footwall folds at Stop 15 in South Eden Canyon along strike. Folded footwall strata of the Twin Creek Limestone are represented by: Jtu = upper Giraffe Creek and Leeds Creek members; Jtm = middle Watton Canyon and Boundary Ridge Members; Jtl = lower Rich and Sliderock members; Jtg = Gypsum Spring Member; and Jp = Preuss Redbeds. (No vertical exaggeration.)

ment. East of the thrust 1,300 feet (400 m), the crest of another anticline in the Nugget lies beneath the Gypsum Spring decollement.

To the east, the Gypsum Spring is spectacularly folded above the upper decollement to the Nugget folds. Below this decollement, the lower part of the Gypsum Spring is concordant with the Nugget. Above the decollement, dolomites in the Gypsum Spring are tightly folded. The decollement is a decoupling zone between Nugget structures and those of the overlying members of the Twin Creek. The Sliderock Member of the Twin Creek Limestone forms the highest north-striking ridge to the east, where the canyon road turns sharply to the south and then east again around the ridge. From the roadside Sliderock outcrop, where it is overturned 55° to the west, we will walk along the overturned to recumbent west limb of a refolded syncline. From the road outcrop, follow the resistant Sliderock outcrops to the upper part of the north side of the canyon where the overturned beds are near horizontal. Farther east, this recumbent limb has been cross folded into two sets of antiformal synclines and synformal anticlines for 2,000 feet (600 m) east of the roadside outcrop. At road level, the micrites of the Rich Member of the Twin Creek display penetrative cleavage through the overturned fold limb.

The folds just viewed in South Eden Canyon represent shortening in front of and beneath the Laketown thrust sheet that formed as the thrust plane cut up section from a Pennsylvanian through Triassic decollement level to the decollement in the Gypsum Spring seen at Laketown (**Figure 18**).

Stop 16. Laketown thrust hanging wall and Laketown Dolomite at Old Laketown Canyon

From South Eden Canyon, retrace your route back to Laketown to view the stratigraphy and structure of the Laketown thrust sheet. The steeply east dipping section in Old Laketown Canyon lies on the east limb of Laketown anticline (Valenti, 1982, Plate 1). The Marathon #1-21 well, located 3.4 miles (5.5 km) south of Old Laketown Canyon, drilled the Ordovician and Cambrian section of the Laketown hanging wall before penetrating the thrust plane beneath the Cambrian Ute Formation (**Figure 18**). A thin interval of the Gypsum Spring was crossed immediately beneath the thrust, followed by a folded and imbricated Jurassic Nugget and Triassic Ankareh section to a total depth of 12,299 feet (3,727 m).

Old Laketown Canyon contains the type section of the Silurian Laketown Dolomite, which is not found in any of the thrust sheets to the east. Also observe mesoscopic structures in the Mississippian section.

Drive to Stop 17

The latitude of the Idaho-Utah border marks a fundamental change in the geomorphology and surface geology of the Wyoming-Idaho-Utah thrust belt. South of 42° N latitude the ranges of folded and faulted Paleozoic rocks we traveled through yesterday and this morning are replaced by broad plateaus of gently warped Maastrichtian through Eocene strata. The unconformities between the two rock packages developed diachronously across the area, depending on the position of the underlying thrust structures that controlled the loci of erosion and deposition from Maastrichtian through early Eocene time. The structural fronts and trailing ramps of the Hogsback, Absaroka, and Crawford thrusts were all the sites of uplift and erosion during late main phase movement on the easternmost thrust, the Hogsback thrust, during the early Eocene. The depositional basins between these uplifted areas were continuously translated eastward above the regional sole decollement by the Hogsback thrust. Basins formed on the hanging wall above an active decollement are called hanging-wall basins (Coogan, 1989) or, more colloquially, "piggyback" basins (Ori and Friend, 1984). The drive between Laketown and Fossil Butte National Monument skirts along the southern edge of one hanging-wall basin, preserved in Bear Lake Plateau, and transects a second and better known basin, Fossil Basin.

The large strip mine immediately to the northeast of Sage Creek Junction is Stauffer Chemical's Leefe phosphate mine, located in the hanging wall of the Crawford thrust sheet where it has been dropped down along the Bear River fault zone. The phosphate was stripped from the Phosphoria Formation where it was easily excavated in the trough of a shallow syncline. The prominent range viewed south-southwest of Sage, Wyoming is the Crawford Mountains, which are made up of Paleozoic through Triassic strata that define the leading edge of the Crawford thrust sheet.

East of Sage, Wyoming, the western margin of Fossil Basin is defined by homoclinally west dipping Mesozoic strata above the footwall ramp of the Absaroka thrust (Lamerson, 1982). A series of late normal faults can be recognized along the north side of the highway where hanging wall Tertiary strata are juxtaposed against footwall Mesozoic rocks. Immediately west of Fossil Basin, the Rock Creek normal fault is

well expressed by a long narrow strike valley. The conspicuous flatirons seen at the mouth of the valley are an overturned section of the Triassic Thaynes Formation in the fault footwall. The small hills at the base of the flatirons are early Eocene Wasatch and Green River formations that dip up to 45°E into the fault, typical of listric faults that shallow with depth. A drill hole through the fault plane (**Figure 19**) shows the Rock Creek fault soling into a thrust imbricate zone above the Absaroka thrust plane.

Stop 17. Fossil Butte National Monument

The early Eocene stratigraphy of Fossil Basin can be seen at a glance from the highway approach to Fossil Butte National Monument (**Figure 20**). Early Eocene strata are divided between the Wasatch Formation fluvial sequence and the intertonging Green River Formation lacustrine sequence (Oriel and Tracey, 1970). The lower member of the Wasatch Formation consists of gray claystone, variegated mudstone, and tan to red sandstone and conglomerate. The only outcrop of the lower member along the trip route is located 1.5 miles (2.4 km) east of Rock Creek, immediately past the railroad bridge, where sandstone ribs dip 10° to 15° into the basin center. At this location the lower member of the Wasatch is overidden to the west by a thrust fault that carries Triassic and Jurassic rocks in the hanging wall (**Figure 21**). The stratigraphy of the basin center is readily viewed to the northeast on this approach to Fossil Butte. The main body of the Wasatch Formation consists of red, purple, and yellow mudstone exposed in the foreground and on the lower slopes of Fossil Butte. A prominent vegetation band marks the contact between the Wasatch and Green River Formations. The Fossil Butte Member of the Green River Formation forms the tan cliffs immediately above this contact. The Fossil Butte Member is composed of mudstone, calcareous sandstone, siltstone, fissile shales, limestone, and oil shale. The main fossil fish bed is 50 feet (15 m) below the top of the member. The Angelo Member of the Green River Formation which caps Fossil Butte, consists of light colored limestone, marlstone, and mudstone.

We will stop briefly at Fossil Butte National Monument and visit the fossil fish museum and concession operated by Mr. Carl Ulrich and his family. Fossil Butte National Monument was established to preserve the fossil fish in situ. The fossil fish quarries operated by the Ulrich family are located on Fossil Ridge immediately south of Fossil Butte.

Drive to Kemmerer, Wyoming—eastern margin of Fossil Basin

On the drive east from Fossil Butte, note that the fine grained deposits of the Fossil Basin depocenter seen here contrast with the coarse-grained debris-flow deposits of the coeval and interfingering Tunp Member of the Wasatch Formation that ring the western, northern, and eastern peripheries of the basin (**Figure 22**). The Tunp Member is exposed north of the field trip route, where its source areas are correlated to areas of thrust-related uplift during deposition (Hurst and Steidtmann, 1986; Coogan, 1989). **Figure 20** shows the interfingering relationship between the Tunp and more basinal units.

The eastern margin of Fossil Basin displays a local angular unconformity between the early Eocene Wasatch Formation and the underlying Evanston Formation at Trail Creek, 12 miles (20 km) north of the field trip route (**Figure 22**). There, the Tunp Member of the Wasatch Formation dips gently into the Fossil Basin above Maastrichtian Evanston Formation beds that dip up to 60°W. The Tunp also angularly overlies the lower member of the Wasatch immediately to the west. In total, these relationships document the sequential development of the uplift at the Absaroka thrust front that sourced the coarse clastic deposits of the Tunp Member along the eastern margin of Fossil Basin. Since this uplift postdates slip along the Absaroka thrust plane, Hurst and Steidtmann (1986) proposed that early Eocene uplift of the Absaroka front was the result of footwall uplift due to slip across a ramp in the underlying Hogsback thrust (**Figure 19**). As illustrated in **Figure 23** however, the Absaroka thrust plane probably did experience early Eocene reactivated slip in its trailing ramp region along the western margin of the basin, where Absaroka-rooted thrusts cross-cut the Wasatch Formation.

The drive between Fossil Basin and Kemmerer, Wyoming transects the west dipping homocline of upper Cretaceous strata that are folded above the Hogsback footwall ramp (**Figure 19**). The coal mine immediately south of the highway is worked in the fluvio-deltaic, lower Campanian Adaville Formation, which was deposited concurrent with early Absaroka thrust motion to the west. The town of Kemmerer lies near the base of the lower Cretaceous, along the hogbacks of the Frontier Formation, source of the coal for the early coal mining operations that established the town.

Overnight at Kemmerer, Wyoming

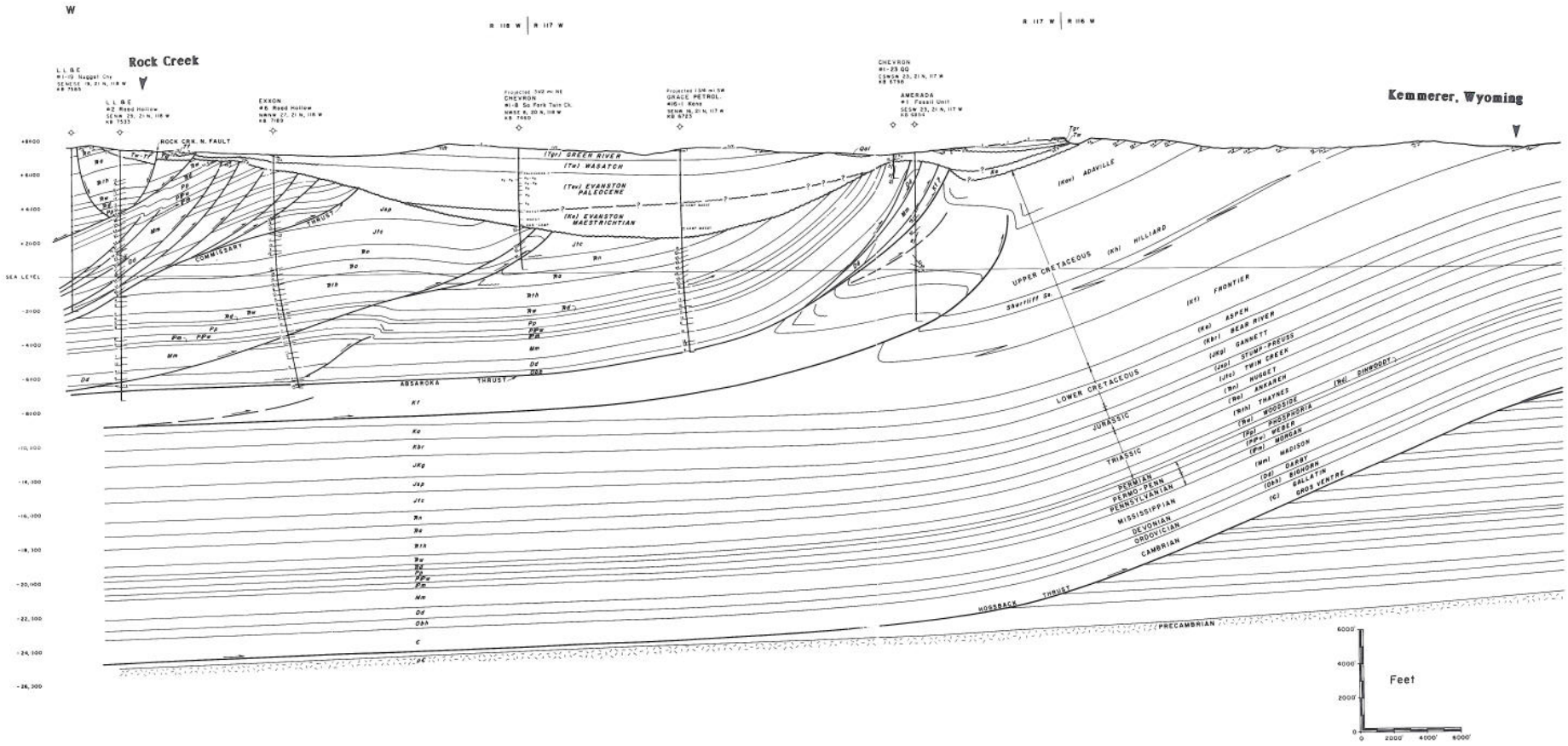

Figure 19. Cross section through northern Fossil Basin along field trip route (from Lamerson, 1982).

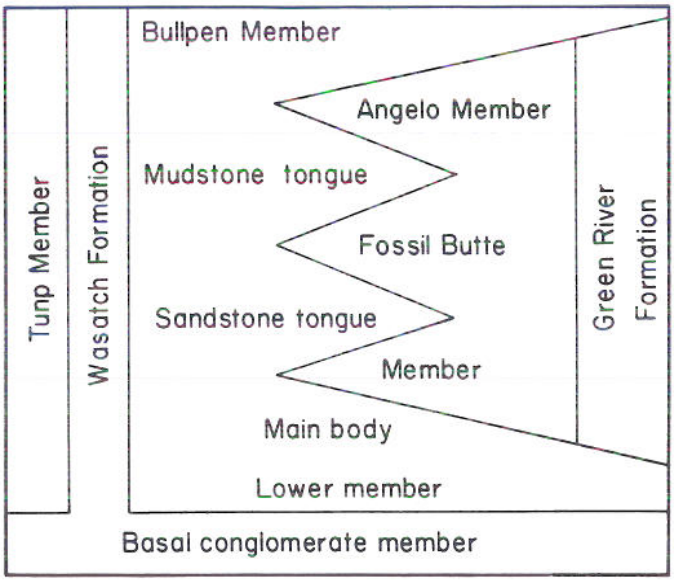

Figure 20. Correlation of early Eocene strata in Fossil Basin (modified from Oriel and Tracey, 1970).

Figure 21. Thrust fault on the west side of Fossil Basin. Ra= Triassic Ankareh, Jn = Jurassic Nugget, Twl = lower member of the Wasatch Formation.

Figure 22. View to the north of the eastern margin of Fossil Basin at Trail Creek. Foreground is underlain by the shallowly dipping Tunp Conglomerate Member of the Wasatch Formation (Twt), which angularly overlies steeply dipping Triassic (Ŕ) and Jurassic (J) strata of the Absaroka thrust hanging wall, and latest Cretaceous Evanston Formation (Ke). Onlap of the main body of the Wasatch (Tw) is seen to the upper left.

Field trip route and stop descriptions, day 3

Stop 18. Hams Fork Conglomerate, Absaroka thrust front, and Lazeart syncline northwest of Kemmerer

Boulder beds of the Hams Fork Conglomerate Member of the Evanston Formation are accessible where they underlie the Hams benchmark northwest of Kemmerer. The clast provenance of this conglomerate is of particular interest; the Hams Fork contains distinctive arkosic quartzite clasts that have a unique provenance in the Middle Cambrian through Proterozoic of the Willard and Paris thrust sheets located 45 miles (70 km) to the west. The presence of these clasts demonstrates that Fossil Basin was poorly developed in Maastrichtian time, allowing boulder-sized clasts to be transported across the basin from the west. The provenance of the quartzites also demonstrates that the hinterland source area was uplifted concurrent with slip on eastern thrusts (Schmitt, 1987), a point that will be reinforced at Stop 21.

The hilltop view from the benchmark also provides a view to the north of the Absaroka thrust hanging wall along Commissary Ridge and Lazeart syncline in Cretaceous rocks of the Absaroka footwall. Lazeart syncline is of particular interest since it has a two-phase history. The steeply dipping to overturned west limb developed as either a tip or drag fold during Absaroka thrust movement. The dip of the gentle east limb is the result of a footwall ramp in the underlying Hogsback thrust plane (**Figure 19**).

Drive to Stop 19

South from Kemmerer to Interstate 80, the field trip route follows a strike valley in the Upper Cretaceous Hilliard Shale. The Hilliard should be noted since it is the marine equivalent to the thick molasse sequence of the Echo Canyon Conglomerate seen at Stop 20. The hogbacks to the east are the Frontier Formation; the hills to the west mark the approximate location of the Absaroka thrust front beneath the Fossil Basin cover. The east-west trending Uinta Mountains are visible to the south, marking the southern boundary of the Wyoming salient of the Cordilleran thrust belt.

Figure 23 provides a cross sectional view of the field trip route along Interstate 80 to Evanston. The section illustrates the structural style of the oil and gas fields of the southern Absaroka thrust sheet. The folds that form structural traps in this area contrast with the highly imbricated structural style of the northern

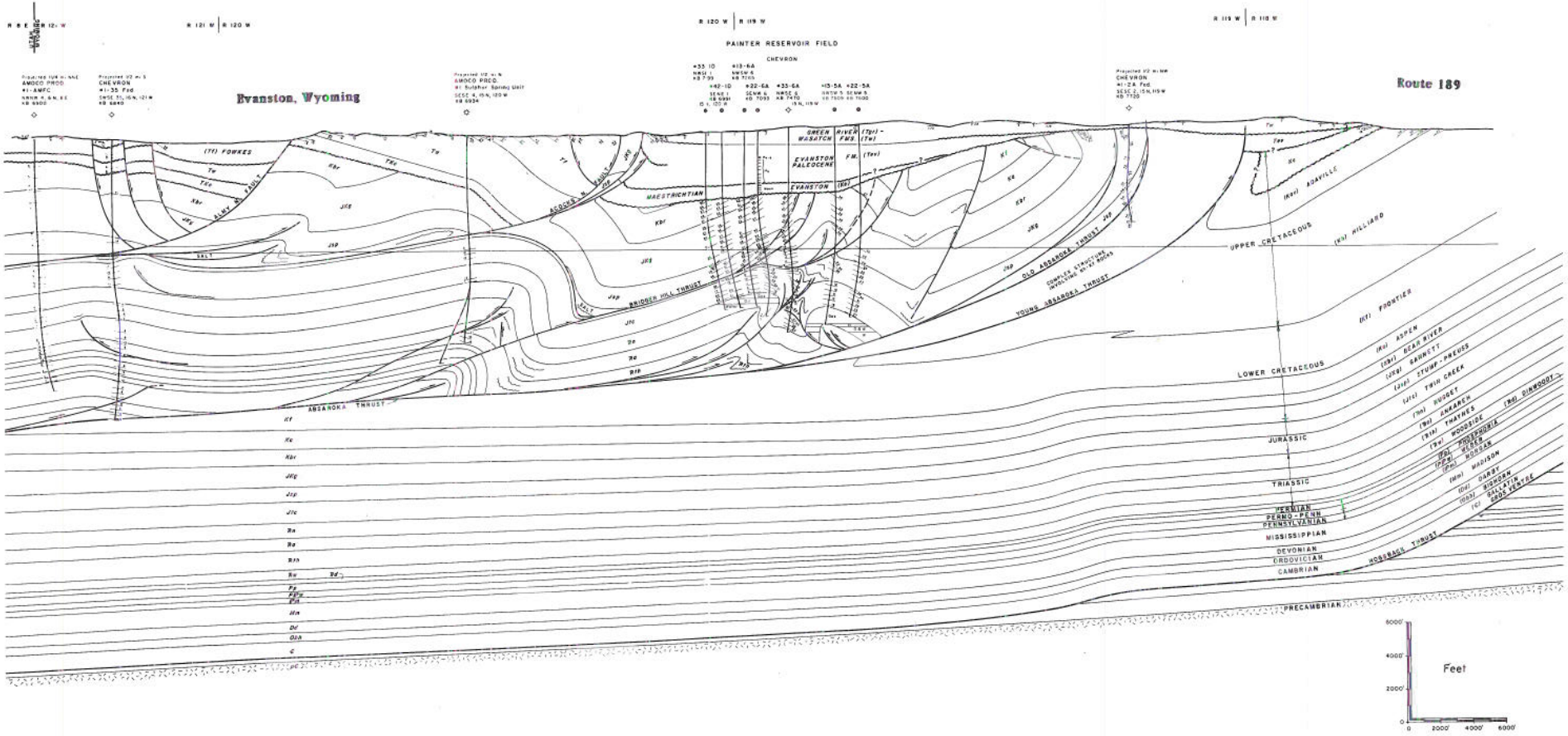

Figure 23. Cross section across southern Fossil Basin along field trip route (from Lamerson, 1982).

Absaroka sheet seen earlier at Alpine. The hanging-wall anticlinal traps were sourced from footwall Cretaceous marine shales, with hydrocarbon migration across the Absaroka thrust plane (Warner, 1982). The principal production in the Absaroka thrust is from two distinct trends of hanging-wall ramp anticlines. The eastern trend, represented in **Figure 23** by Painter Reservoir field, is the result of a hanging-wall ramp in the Triassic Thaynes Formation through Jurassic Twin Creek Limestone. The principal reservoir for the eastern trend is the Jurassic Nugget Sandstone, which generally produces sweet gas, oil, and condensate. In contrast, the western trend, represented in **Figure 23** by the Sulphur Spring well, is the result of a hanging-wall ramp through the Paleozoic section. The western trend produces from Paleozoic reservoirs, principally from the porous dolomites of the Mississippian Mission Canyon Limestone. The western trend production is limited to sour gas and condensate, with H_2S probably generated by thermocatalytic reaction of hydrocarbons with anhydrite in the Mission Canyon. The difference in hydrocarbon maturity from east to west is presumably the result of slight differences in burial history (Warner, 1982). In both cases, the migration path is thought to be through the hanging-wall cutoffs of the reservoir formations on the eastern limb of the anticlines (Lamerson, 1982). Note also that the Preuss salt decollement seen earlier at Salt River Pass is also an important feature in the southern thrust belt, having accommodated disharmonic folding above the producing structures.

Stop 19. View of Almy and Acocks normal faults, Evanston, Wyoming

This stop at the relay station above Evanston, Wyoming provides an overview of two Tertiary half grabens that form the east side of the valley of Bear River. Note that the Preuss salt decollement controlled both the late thrusting and later Basin and Range extension seen at this stop (**Figure 23**). The Medicine Butte thrust cuts the Evanston and Wasatch Formations, and represents thrusting well after main movement on the Absaroka thrust. The salt decollement of the Medicine Butte thrust also served to localize later extensional faults such as the Acocks and Almy normal faults. Once again, the listric shape of the normal faults is confirmed by drilling (**Figure 23**), and the characteristic rotation of Tertiary strata into the fault plane is well displayed in the 20° to 45°E dips of the Evanston through Fowkes formations in the Acocks fault hanging wall on the north side of Evanston.

Drive to stop 20

Conglomerates and mudstones of the Wasatch Formation are continuously exposed for 26 miles (42 km)

Figure 24. Angular unconformity between Evanston Formation (TKe) and Echo Canyon Conglomerate (Kec) along a tributary on the north side of Echo Canyon, Utah.

west of Evanston along Interstate 80. Farther west, two important angular unconformities, between the early Eocene Wasatch Formation and the underlying Maastrichtian-Paleocene Evanston Formation, and between the Evanston Formation and the underlying Coniacian-Santonian Echo Canyon Conglomerate (**Figure 24**), are exposed along the highway. Echo Canyon lies in Stevenson syncline, a fold formed on the backlimb of the Absaroka thrust above the Absaroka footwall ramp (**Figure 25**). Farther west along Echo Canyon, over 3,300 feet (1,000 m) of coarse boulder and cobble alluvial fan conglomerates are exposed along the canyon walls. Royse and others (1975) first proposed that the Echo Canyon Conglomerate was derived from uplift of the Crawford thrust sheet to the northwest. Recently, DeCelles (1988) interpreted the conglomerate clasts as having mixed provenance from both the Willard thrust hanging wall and the Paleozoic-Mesozoic section above the basement-cored anticlinorium east of Ogden and Salt Lake City (**Figure 25**). The Wasatch basement uplift is recognized as a ramp anticline that has been translated across the basal decollement shared by the Absaroka and Hogsback thrusts to the east (Royse and others, 1975). Essentially, the Wasatch uplift represents basement shortening that corresponds in timing and magnitude to the "thin skinned" shortening expressed by the thrusts to the east. Coogan (1987) noted that the Crawford thrust probably also shares the basal decollement with the basement uplift. Thus, the initial basement uplift recorded by the Echo Canyon provenance may indirectly correlate with movement on the Crawford thrust. Stop to view the angular unconformity above the Echo Canyon Conglomerate, and to take a closer look at the sedimentologic features of the conglomerate.

Stop 20. Echo Canyon Conglomerate at Echo

At Echo, Utah, the Coniacian-Santonian Echo Canyon Conglomerate records deposition in a proximal, coarse braided stream system. The individual gravel sets were mainly deposited as longitudinal bars (Crawford, 1979) that flowed to the southeast (Mann, 1974). At this location, upper Paleozoic through Jurassic clasts are readily identifiable. The next stop is along the eastern edge of the Wasatch basement uplift, where the Mesozoic and Paleozoic cover sequence is one probable source for the clasts found here at Echo.

Stop 21. Devils Slide, eastern edge of the Wasatch basement uplift

The Devils Slide is a series of topographic ridges and swales within the steeply east dipping Jurassic Twin Creek Limestone on the eastern flank of the Wasatch basement uplift. Poorly sorted boulder and cobble conglomerate angularly overlies the Twin Creek with a gentle east dip (**Figure 26**). Shales from the upper part of these conglomerates yield palynomorphs of Maastrichtian age (Jacobsen and Nichols, 1982). Thus, these conglomerates are correlative with the Evanston Formation, although DeCelles (1988) argued that the several intraformational unconformities in the middle and lower parts of the Devils Slide outcrop permits correlation of the lower outcrops to the Echo Canyon Conglomerate seen at the last stop. The angular clasts and poor sorting of the conglomerates clearly point to a proximal alluvial fan environment of deposition. The clasts came directly from the uplift to

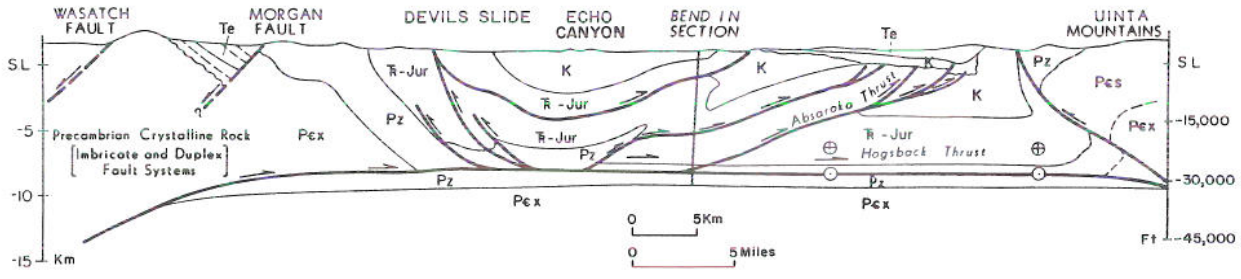

Figure 25. Cross section between the north flank of the Uinta Mountains and the Wasatch fault (from Bruhn and others, 1986).

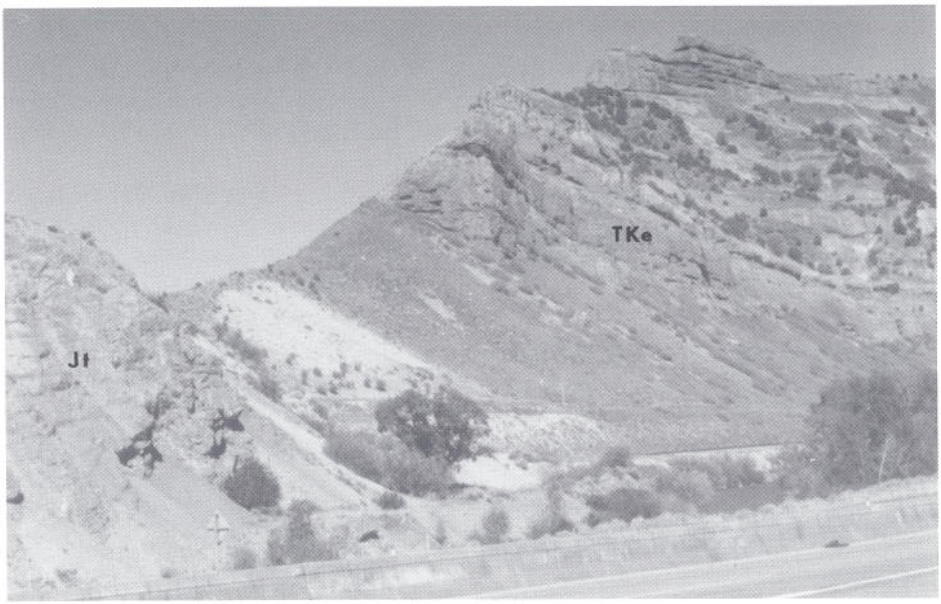

Figure 26. View of the Devils Slide area, showing shallowly dipping conglomerate of the Evanston Formation (TKe) above steeply dipping Twin Creek Limestone (Jt).

the west. Combined with the Echo Canyon Conglomerate seen at the last stop, the Maastrichtian Devils Slide alluvial fan deposits demonstrate a sequential uplift history for the basement ramp anticline that is contemporaneous with movement on the major thrusts to the east and northeast.

Stop 22. Devils Gate, Utah

Between Devils Slide and Devil's Gate, Utah, the basement uplift is cut by a Basin and Range normal fault at Morgan, Utah (**Figure 25**). In Morgan Valley, the Eocene to Oligocene volcaniclastic sequence of the graben is exposed with 15° to 50°E dips into the normal fault. The west side of Morgan Valley is bounded by Archean crystalline rocks of the basement uplift, which are well exposed along the Weber River at Devil's Gate. The migmatitic gneiss and amphibolite seen here underwent early granulite facies metamorphism about 2,600 m.y. ago, prior to amphibolite facies metamorphism about 1,790 m.y. ago (Hedge and others, 1983). Weber Canyon exposes numerous, low angle, greenschist-facies ductile shear zones that may be Mesozoic in age. At higher structural levels to the the north, cataclastic basement shear zones appear to have formed before major uplift of the basement but synchronous with emplacement of the overlying Willard thrust between 140 and 110 m. y. ago (Yonkee and others, 1989). Fission track ages from the Wasatch basement indicate that thrust uplift of the basement commenced about 85 m.y. ago, approximately during Crawford and early Absaroka thrust movement (Naeser and others, 1983).

Stop 23. Overview of Wasatch fault at the mouth of Ogden Canyon, Utah

This stop provides an overview of extensional faulting and sedimentation along the Wasatch Front between Ogden and Salt Lake City. Conspicuous faceted mountain front and numerous recent fault scarps are the main surface expressions of a system of normal fault segments that have accommodated at least 7 miles (11 km) of post-Oligocene uplift in the footwall immediately south of Salt Lake City, (Parry and Bruhn, 1987), with approximately 4 km at this location (Naeser and others, 1983). The topographic terraces along the mountain front are expressions of ancient shoreline levels of Pleistocene Lake Bonneville. The Pleistocene deltaic sequences along the mountain front were the sites of the pioneering descriptions of deltaic sedimentation by Gilbert (1890).

References cited

Allmendinger, R.W., and Jordan, T.E., 1981, Mesozoic evolution, hinterland of the Sevier orogenic belt: Geology, v. 9, p. 308-313.

Armstrong, F.C., and Oriel, S.S., 1965, Tectonic development of the Idaho-Wyoming thrust belt: American Association of Petroleum Geologists Bulletin, v. 49, p. 1847-1866.

Armstrong, R.L., 1982, Metamorphic core complexes: Annual Review of Earth and Planetary Science, v. 10, p. 129-154.

Blackstone, D.L., Jr., 1990, Precambrian basement map of Wyoming: outcrop and structural configuration: Geological Survey of Wyoming Map Series 27, scale 1:1,000,000.

Boyer, S.E., and Elliott, D., 1982, Thrust systems: American Association of Petroleum Geologists Bulletin, v. 66, no. 9, p. 1196-1230.

Bruhn, R.L., Picard, M.D., and Isby, J.S., 1986, Tectonics and sedimentology of Uinta arch, western Uinta Mountains, and Uinta basin: *in* Peterson, J.A., editor, Paleotectonics and sedimentation: American Association of Petroleum Geologists Memoir 41, p. 333-352.

Carr, T.R., and Paull, R.K., 1983, Early Triassic stratigraphy and paleogeography of the Cordilleran miogeocline, *in* Reynolds , M.W., and Dolly, E.D., editors, Rocky Mountain Paleogeography Symposium 2: Society of Economic Paleontologists and Mineralogists, p. 39-55.

Coogan, J.C., 1987, Thrust systematics and displacement transfer in the Wyoming-Idaho-Utah thrust belt: Geological Society of America Abstracts with Programs, v.19, no.7, p. 626.

Coogan, J.C., 1989, Distinguishing reactivated thrust slip vs. footwall uplift sedimentation patterns in hanging wall basins: Fossil Basin and Bear Lake Plateau, WY-ID-UT thrust belt: Geological Society of America Abstracts with Programs, v. 21, no. 6, p. 366.

Coogan, J.C., and Boyer, S.E., 1985, Variable shortening mechanisms in thrust belts and implications for balanced cross section construction; an example from the Idaho-Wyoming thrust belt: Geological Society of America Abstracts with Programs, v. 17, no.7, p. 552.

Coogan, J.C., and Yonkee, W.A., 1985, Salt detachments in the Jurassic Preuss Redbeds within the Meade and Crawford thrust systems, Idaho and Wyoming, *in* Kerns, G.J., and Kerns, R.L., editors, Orogenic patterns and stratigraphy of north-central Utah and southeastern Idaho: Utah Geological Association Publication 14, p. 75-82.

Crawford, K.A., 1979, Sedimentology and tectonic significance of the Late Cretaceous-Paleocene Echo Canyon and Evanston synorogenic conglomerate of the north-central Utah thrust belt: M.S. thesis, University of Wisconsin, Madison, 143 p.

Cressman, E.R., 1964, Geology of the Georgetown Canyon-Snowdrift Mountain area, southeastern Idaho: U.S. Geological Survey Bulletin 1153, 105 p.

DeCelles, P.G., 1988, Lithologic provenance modeling applied to the Late Cretaceous synorogenic Echo Canyon Conglomerate, Utah: a case of multiple source areas: Geology, v. 16, p. 1039-1043.

Dover, J.H., 1985, Geologic map and structure sections of the Logan 60' x 30' Quadrangle, Utah and Wyoming: U.S. Geological Survey Open File Report 85-216, 32 p.

Evans, J.P., and Craddock, J.P., 1985, Deformation history and displacement transfer between the Crawford and Meade thrust systems, Idaho-Wyoming overthrust belt, *in* Kerns, G.J., and R.L. Kerns, editors, Orogenic patterns and stratigraphy of north-central Utah and southeastern Idaho: Utah Geological Association Publication 14, p. 83-95.

Gilbert, G.K., 1890, Lake Bonneville: U.S. Geological Survey Monograph 1, 438 p.

Hedge, C.E., Stacey, J.S., and Bryant, B., 1983, Geochronology of the Farmington Canyon Complex, Wasatch Mountains, Utah, *in* Miller, D.M., Todd, V.R., and Howard, K.R., editors, Tectonic and stratigraphic studies in the eastern Great Basin: Geological Society of America Memoir 157, p. 37-44.

Hubbert, M.K., and Rubey, W.W., 1959, Role of fluid pressure in the mechanics of overthrust faulting: Geological Society of America Bulletin, v.70, p. 115-166.

Hunter, R.B., 1987, Timing and structural relations between the Gros Ventre foreland uplift, the Prospect thrust system, and the Granite Creek thrust, *in* Miller, W.R. editor, The thrust belt revisited: Wyoming Geological Association 38th Annual Field Conference Guidebook, p. 109-131.

Hurst, D.J., and Steidtmann, J.R., 1986, Stratigraphy and tectonic significance of the Tunp conglomerate in the Fossil Basin, southwest Wyoming: Mountain Geologist, v. 23, p. 6-13.

Jacobson, S.R., and Nichols, D.J., 1982, Palynological dating of syntectonic units in the Utah-Wyoming thrust belt, *in* R. B. Powers, editor, Geologic studies of the Cordilleran thrust belt: Rocky Mountain Association of Geologists, 735-750.

Jordan, T.E., and Douglass, R.C., 1980, Paleogeography and structural development of the late Pennsylvanian to early Permian Oquirrh Basin, northwestern Utah, *in* Fouch, T.D., and Magathan, E.R., editors: Rocky Mountain Paleogeography Symposium 1: Society of Economic Paleontologists and Mineralogists, p. 217-238.

Lamerson, P.R., 1982, The Fossil Basin and its relationship to the Absaroka thrust system, Wyoming and Utah, *in* Powers, R.B., editor, Geologic studies of the Cordilleran thrust belt: Rocky Mountain Association of Geologists, p. 279-340.

Lush, A.P, McGrew, A.J., Snoke, A.W., and Wright, J.E., 1988, Allochthonous Archean basement in the northern East Humboldt Range, Nevada: Geology, v. 16, p. 349-353.

Mann, D.C., 1974, Clastic Laramide sediments of the Wasatch hinterland, northeastern Utah: M.S. thesis, University of Utah, Salt Lake City, 112 p.

Mansfield, G.R., 1927, Geography, geology, and mineral resources of a part of southeastern Idaho: U.S. Geological Survey Professional Paper 152, 453 p.

Mitra, G., and Yonkee, W.A., 1985, Relationship of spaced cleavage to folds and thrusts in the Idaho-Utah-Wyoming thrust belt: Journal of Structural Geology, v. 7, 361-373.

Mitra, G., Hull, J.M., Yonkee, W.A., and Protzman, G.M., 1988, Comparison of mesoscopic and microscopic deformational styles in the Idaho-Wyoming thrust belt and the Rocky Mountain foreland, *in* Schmidt, C.J., and Perry, W.J., Jr., editors, Interaction of the Rocky Mountain foreland and the Cordilleran thrust belt: Geological Society of America Memoir 171, p. 119-141.

Naeser, C.W., Bryant, B., Crittenden, M.D., Jr., and Sorensen, M.L., 1983, Fission-track ages of apatite in the Wasatch Mountains, Utah, *in* Miller, D.M., Todd, V.R., and Howard, K.R., editors, Tectonic and stratigraphic studies in the eastern Great Basin: Geological Society of America Memoir 157, p. 29-36.

Olson, T.J., and Schmitt, J.G., 1987, Sedimentary evolution of the Miocene-Pliocene Camp Davis Basin, northwestern, Wyoming, *in* Miller, W.R., editor, The thrust belt revisited: Wyoming Geological Association 38th Annual Field Conference Guidebook, p. 225-243.

Ori, G. G., and Friend, P.F., 1984, Sedimentary basins formed and carried piggyback on active thrust sheets: Geology, v. 12, p. 475-478.

Oriel, S.S., 1986, The Idaho-Wyoming salient of the North American Cordilleran foreland thrust belt: Bull. Soc. geol. France, (8), t.II, no. 5, p.755-765.

Oriel, S.S. and Tracey, J.I., 1970, Uppermost Cretaceous and Tertiary stratigraphy of Fossil Basin, southwestern Wyoming: U.S. Geological Survey Professional Paper 635, 53 p.

Parry, W.T., and Bruhn, R.L., 1987, Fluid inclusion evidence for minimum 11 km vertical offset on the Wasatch fault, Utah: Geology, v. 15, p. 67-70.

Peale, A. C., 1879, Report on the geology of the Green River District: U.S.Geological and Geographic Survey of the Territories, Eleventh Annual Report, p.509-646.

Piety, L.A., Wood, C.A., Gilbert, J.D., Sullivan, J.T., and Anders, M.H., 1986, Seismotectonic study for the Palisades Dam and Reservoir: U.S. Bureau of Reclamation Seismotectonic Report 86-2, 198 p.

Protzmann, G.M., 1985, The emplacement and deformation history of the Meade thrust sheet, southeastern Idaho: M.S. thesis, University of Rochester, Rochester, N.Y., 117 p.

Royse, F., Jr., 1985, Geometry and timing of the Darby-Prospect-Hogsback thrust fault system, Wyoming: Geological Society of America Abstracts with Programs, v. 17, no. 4, p. 263.

Royse, F., Jr., Warner, M.A., and Reese, D.L., 1975, Thrust belt structural geometry and related stratigraphic problems, Wyoming-Idaho-northern Utah, *in* Bolyard, D.W., editor, Deep drilling frontiers of the central Rocky Mountains: Rocky Mountain Association of Geologists, p. 41-54.

Royse, F., Jr., and Lamerson, P., 1984, Field trip guide, northern Utah thrust belt and north Cottonwood uplift: American Association of Petroleum Geologists Structural Geology School, Park City, Utah.

Rubey, W.W., 1958, Geology of the Bedford quadrangle, Wyoming: U.S. Geological Survey Map GQ-109, scale 1:62,500.

Rubey, W.W., 1973, Geologic map of the Afton Quadrangle and part of the Big Piney Quadrangle, Lincoln and Sublette Counties, Wyoming: U.S. Geological Survey Miscellaneous Investigations Map I-686, scale 1:62,500.

Rubey, W.W., Oriel, S.S., and Tracey, J.I., Jr., 1975, Geology of the Sage and Kemmerer 15-minute Quadrangles: U.S. Geological Survey Professional Paper 855, 18 p. [Geological Survey of Wyoming Reprint 38]

Rubey, W.W., Oriel, S.S., and Tracey, J.I., Jr., 1980, Geologic map and structure sections of the Cokeville Quadrangle, Wyoming: U.S. Geological Survey Miscellaneous Field Investigations Map I-1129.

Schmitt, J.G., 1987, Origin of late Cretaceous to early Tertiary quartzite conglomerates — northwestern Wyoming, *in* Miller, W.R.,editor, The thrust belt revisited: Wyoming Geological Association 38th Annual Field Conference Guidebook, p.217-224.

Speed, R.C., and Sleep, N.H., 1982, Antler orogeny and foreland basin: a model: Geological Society of America Bulletin, v. 93, p. 815-828.

Valenti, G.L., 1982, Structure of the Laketown Quadrangle and petroleum exploration in the Bear Lake area, Rich County, Utah, *in* R. B. Powers, editor, Geologic studies of the Cordilleran thrust belt: Rocky Mountain Association of Geologists, p. 859-868.

Veatch, A.C., 1907, Geography and geology of a portion of southwestern Wyoming, with special reference to oil and coal: U.S. Geological Survey Professional Paper 56, 128 p.

Warner, M.A., 1982, Source and time of generation of hydrocarbons in the Fossil Basin, western Wyoming thrust belt, *in* Powers, R.B., editor, Geologic studies of the Cordilleran thrust belt: Rocky Mountain Association of Geologists, p. 805-815.

Wiltschko, D.V., and Dorr, J.A., 1983, Timing of deformation in the overthrust belt and foreland of Idaho, Wyoming, and Utah: American Association of Petroleum Geologists Bulletin, v. 67, 1304-1322.

Yonkee, W.A., 1983, Mineralogy and structural relationships of cleavage in the Twin Creek Formation within part of the Crawford thrust sheet in Wyoming: M.S. thesis, University of Wyoming, Laramie, 125 p.

Yonkee, W.A., Parry, W.T., Bruhn, R.L., and Cashman, P.H., 1989, Thermal models of thrust faulting: constraints from fluid-inclusion observations, Willard thrust sheet, Idaho-Utah-Wyoming thrust belt: Geological Society of America Bulletin, v. 101 p. 304-315.

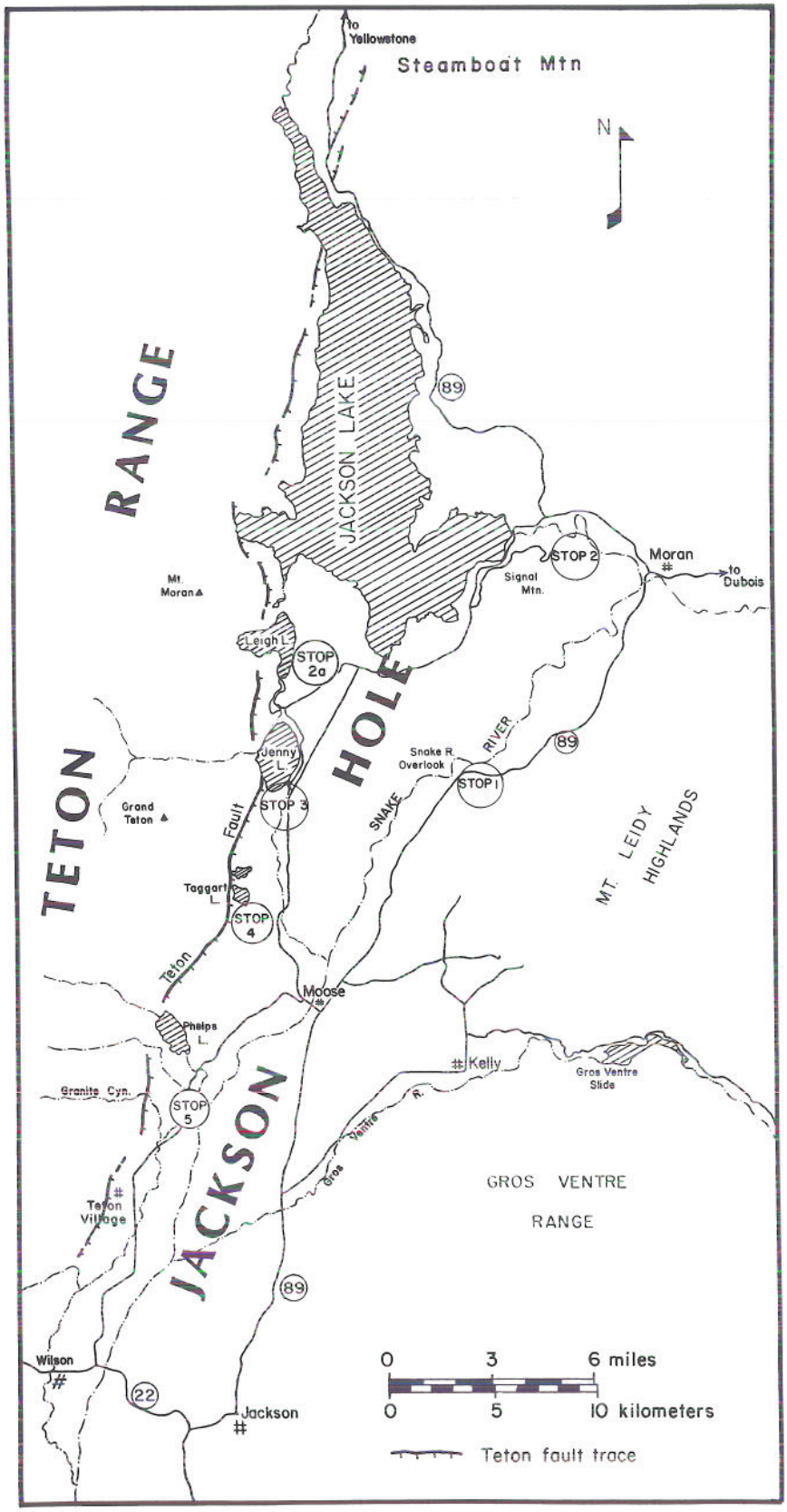

Figure 1. Trip route and stop locations, field trip no. 6. Map of Teton fault trace is taken from detailed mapping by Susong and others (1987) and data from the U.S. Bureau of Reclamation studies (Gilbert and others, 1983; Ostenaa, 1988).

Field trip no. 6

NEOTECTONICS AND STRUCTURAL EVOLUTION OF THE TETON FAULT

Robert B. Smith and John O.D. Byrd
Department of Geology and Geophysics
University of Utah
Salt Lake City, Utah 84112

and

David D. Susong[1]
U.S. Geological Survey
Cheyenne, Wyoming 82003

Trip Summary (see Figure 1)

Stop 1.	Snake River Overlook at Deadman Bar
Stop 2.	South Signal Mountain Overlook
2a.	Cathedral Group turnout
Stop 3.	Jenny Lake
Stop 4.	South Taggart Lake moraine (optional)
Stop 5.	Granite Canyon

Introduction

The Teton normal fault extends 44 miles (70 km) north-south along the east side of the Teton Range and is the principal structure responsible for the spectacular topographic relief of the range (**Figure 2**). The Teton fault has been mapped by previous workers: (1) at a regional scale (Love and Reed, 1971; Love and others, in press), and (2) in detail at several locations along the fault trace by Gilbert and others (1983) during an evaluation of the seismic safety of the Jackson Lake dam site. In 1987, a general earthquake hazard evaluation of the entire Teton fault zone (Smith, 1988) and surrounding region was initiated by the University of Utah that included detailed mapping and scarp profiling of the Teton fault by Susong and others (1987) and Smith (1988). In 1988 and 1989, additional components of the study were added: (1) a 14-mile-long (22.5-km) east-west 1st-order level line (Byrd and others, 1988) was established across the Teton fault to assess contemporary deformation, (2) a paleomagnetic evaluation of the Huckleberry Ridge Tuff was made to determine rotation about horizontal and vertical axes and related deformation associated with the Teton fault during the past 2 million years, and (3) a trench was excavated across the Teton fault to determine the age of faulting.

This field trip (**Figure 1**) will discuss the results from these studies and others of our colleagues with five stops that provide an overview of: (1) the geology of the Tetons and Jackson Hole as it relates to the Teton fault, (2) the extent and magnitude of Quaternary displacements on the Teton fault, (3) the regional earthquake setting and related earthquake hazards, (4) evidence of paleo-earthquake activity and neotectonic deformation, and (5) the recurrence times of large paleo-earthquakes on the fault.

The occurrence of two large historic earthquakes, the M_L 7.5, 1959, Hebgen Lake, Montana, and the M_s 7.3, 1983 Borah Peak, Idaho, events on large normal faults surrounding the Snake River Plain (**Figure 3**) has focused attention on the hypothesis that the Yellowstone hotspot, and its track, the Snake River Plain (SRP) volcanic system, has influenced the present-day

[1]Formerly at the University of Utah.

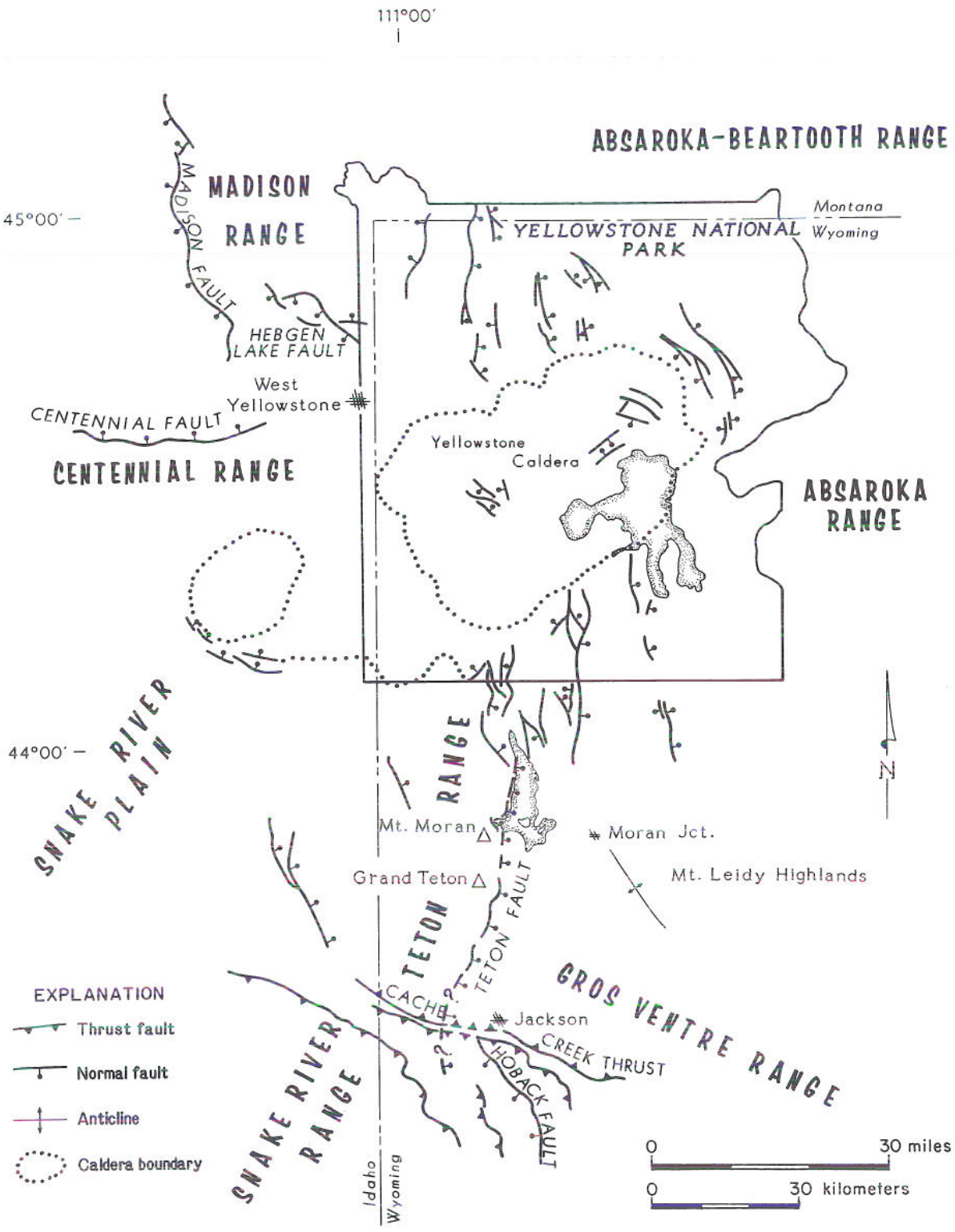

Figure 2. Regional tectonic index map of the Teton Range and Jackson Hole area.

seismotectonics of the central Intermountain seismic belt, including the Teton region (Smith, 1988). These earthquakes and several other large events of the Intermountain region and the Yellowstone Plateau (**Figure 4**) are part of a V-shaped pattern of epicenters surrounding the aseismic Snake River Plain (Smith and others, 1984). Lithospheric subsidence, both perpendicular and parallel to the Snake River Plain, suggests that thermal contraction and/or stress-field relaxation related to passage of the Yellowstone hotspot has strongly influenced the distribution of past events and the overall earthquake potential of the region (Smith and others, 1990).

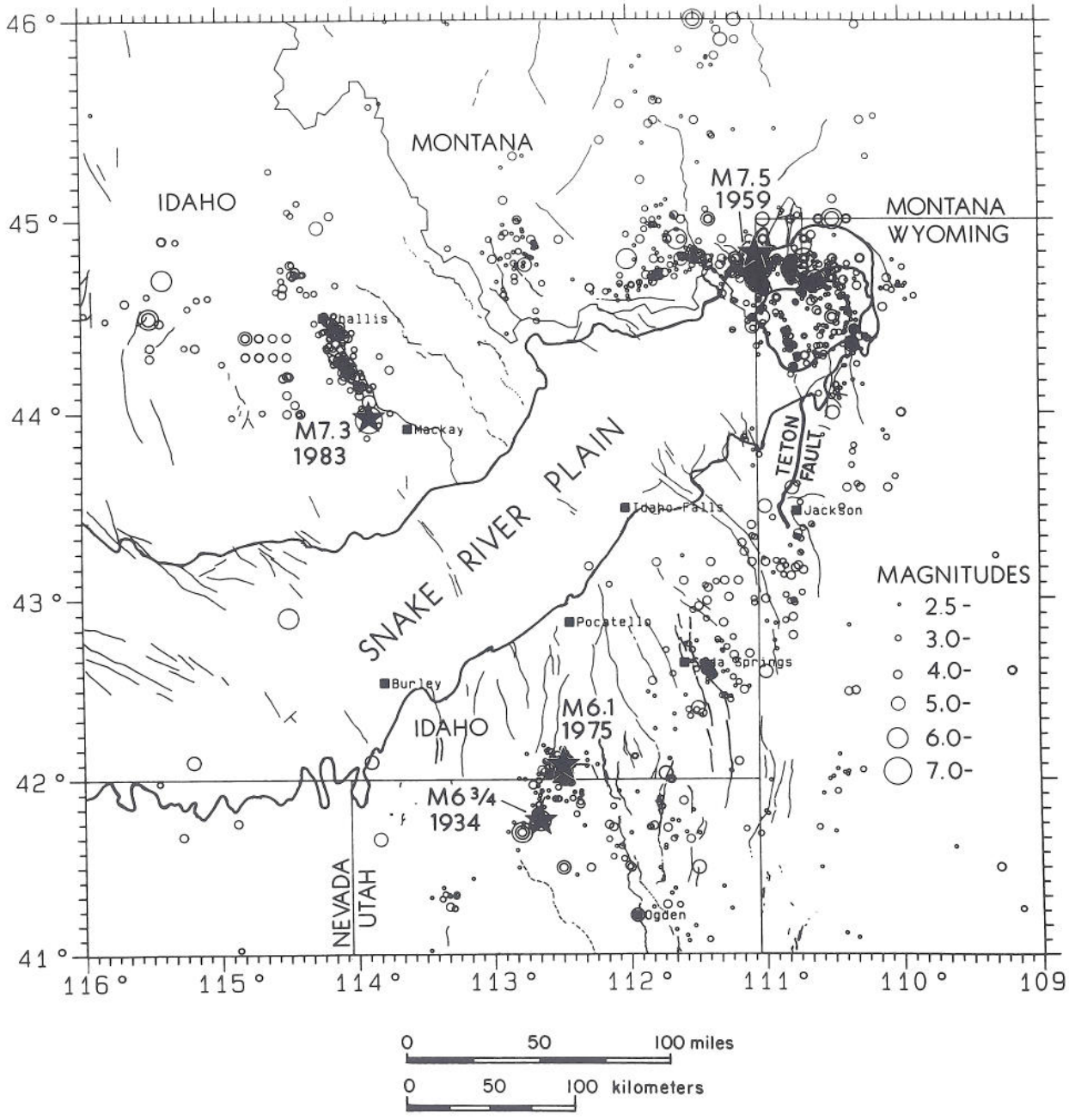

Figure 3. Seismicity map of the Snake River Plain, Yellowstone, and Teton region (map taken from Smith, 1988). Earthquake data are principally for the 1900 to 1985 period with a minimum magnitude cutoff of 3.5. Stars indicate the epicenters of the M_s 7.3, 1983 Borah Peak, Idaho, and the 1959, M_L 7.5 Hebgen Lake, Montana, earthquakes. The Yellowstone-Snake River Plain volcanic system is characterized by bimodal, basalt-rhyolite rocks. Blackened areas indicate numerous overlapping earthquakes.

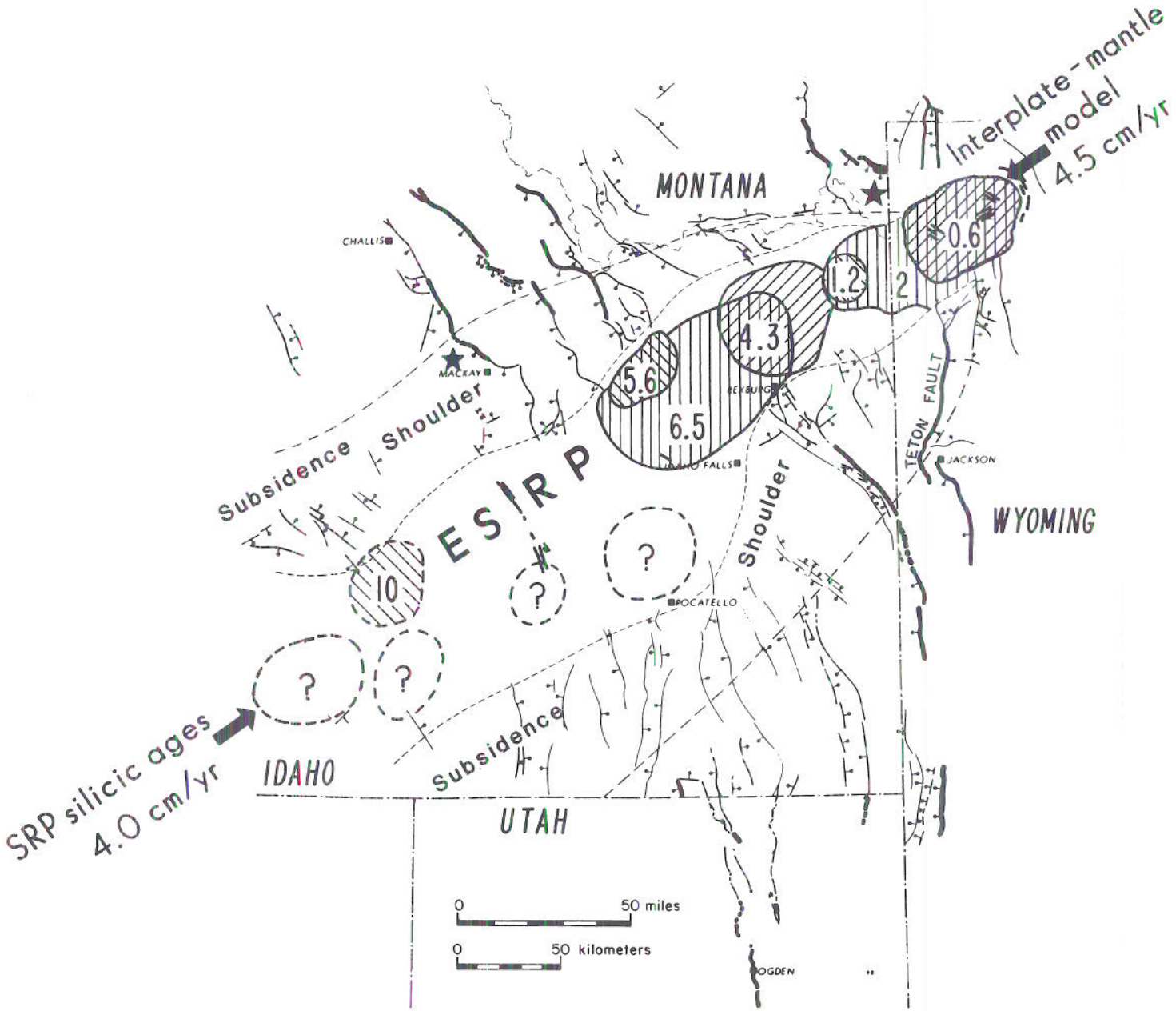

Figure 4. Distribution of late Cenozoic normal faults and boundary of hypothesized subsidence shoulder associated with Yellowstone hotspot lithospheric deformation (map modified from Smith and others, 1984). ESRP = eastern Snake River Plain. Arrow at Yellowstone is the direction of motion of the North American plate with respect to Yellowstone hotspot with a relative velocity of ~3.5 mm/yr. Fine-dashed line = boundary of Snake River Plain volcanic province and coarse-dashed line = boundary of hypothesized lithospheric subsidence shoulder. Stars indicate the epicenters of the M_s 7.3, 1983 Borah Peak, Idaho, and the 1959, M_L 7.5 Hebgen Lake, Montana, earthquakes. Heavy lines = normal faults with Holocene displacements, light lines = normal faults with Quaternary faulting, but lacking Holocene displacements. Caldera boundaries are indicated by vertical line pattern and heavy dashes. Outlines of calderas, with ages in millions of years, where known, are shown along the ESRP. Caldera locations and ages from Morgan and others (1984) and Mel Kuntz (personal communication, 1988).

The Teton fault zone is located on the southeastern edge of an active seismic zone in the Yellowstone area, and southeast of a seismically quiescent "shoulder" that trends subparallel to the aseismic Snake River Plain (**Figures 3** and **4**). The Teton area is also located southeast of an area of late Cenozoic normal faulting, where evidence of Holocene displacement is absent, and northwest of an area marked by Holocene faulting and surface rupture (Smith and others, 1990). These observations lead Smith and others (1984) to suggest that the thermal-mechanical effects of the Yellowstone hotspot may extend laterally away from the SRP in a roughly V-shaped pattern, parallel to the two major seismic zones surrounding the SRP, and may have influenced the earthquake potential of the Teton fault zone.

Stop descriptions

Stop 1. Snake River Overlook at Deadman Bar

Subsidence of the valley in the vicinity of Wilson, at the southern end of Jackson Hole, was first recognized by Love and Montagne (1956), who showed that two parallel tributaries at the base of the range were "lower in elevation than the Snake River in positions at right angles to the flow of the river." The important observation at the first stop on the field trip is to view (to the west) the westward tilt of the valley floor adjacent to the Teton fault. This area of subsidence, adjacent to the fault, has been measured by two detailed topographic profiles [measured by 1st-order leveling and electronic distance measuring (EDM)] that revealed up to 85 feet (26 m) of subsidence at Jenny Lake, over a zone 2.3 miles (3.7 km) wide east of the Teton fault, relative to the top of the uppermost terrace level west of the Snake River Overlook.

Stop 2. South Signal Mountain Overlook

This stop will emphasize the tectonics and regional geophysics of the area. Tectonically (**Figure 2**), the Teton Range is located at the northeastern side of the Basin-Range province, east of the Snake River Plain volcanic province, south of the Quaternary Yellowstone volcanic plateau, and on the northern margin of the Wyoming-Idaho Overthrust Belt. The Teton range is a westward tilted, Precambrian-cored fault block composed of intensely deformed and metamorphosed Precambrian gneiss, diabase, and quartz monzonite (Reed, 1973). West dipping Paleozoic sedimentary and Quaternary volcanic rocks cover the core of the range and extend across its northern and southern ends (Love and others, in press; Lageson, 1987). The structural evolution of the Teton Range has been influenced by four major post-Paleozoic events:

(1) Mesozoic to early Tertiary, east-west compression accompanying development of the Wyoming-Idaho Overthrust Belt province; several Laramide structures, such as the Spread Creek anticline, are visible east of Signal Mountain, and the northern edge of the Overthrust Belt, the Cache Creek and Jackson thrusts, can be seen on the horizon to the south;

(2) The late Tertiary Basin-Range epeirogeny and crustal extension that produced the Teton fault with its subsequent 3.7 to 6.9 miles (6 to 11 km) of stratigraphic displacement and the resultant topography of Jackson Hole;

(3) Late Cenozoic volcanism and crustal deformation associated with the nearby Snake River Plain volcanic system during passage of the Yellowstone hotspot with subordinate silicic volcanism found throughout the area north of Jackson Hole; and

(4) Extensive silicic volcanism associated with the Quaternary Huckleberry Ridge tuff of the Yellowstone volcanic plateau that caps the north end of the Teton Range and is seen in scattered outcrops throughout the northern end of the valley.

From the south Signal Mountain Overlook, one can view the spectacular topography of the Teton Range that attains a maximum relief of 7,200 feet (2.2 km) adjacent to the 13,770-foot-high (4,197-m) peak of the Grand Teton. The precipitous topographic relief on the east side of the range was produced principally by movement on the Teton fault (**Figure 2**) and is the focus of the field trip.

It is interesting to note that the area of highest relief along the Teton Range does not coincide with the north-south trending drainage boundary, in the middle of the range, but is located approximately 2.5 miles (4 km) east of the drainage boundary, where it is marked by a line connecting the high peaks at the front of the range. This pattern is suggestive of a high uplift rate,

eg. a rapid westward tilt rate, of the footwall block of the Teton fault that exceeds the normal rate of erosion and weathering of the mountain front.

The Teton fault zone is marked by an estimated 3.7 to 6.9 miles (6 to 11 km) of total stratigraphic displacement (Byrd and others, 1988) that has taken place over the past 7 to 9 million years (Love and Reed, 1971). Quaternary fault scarps, up to 157 feet (48 m) high, are present along 34 miles (55 km) of the 44-mile-length (70-km) of the Teton fault and are well preserved in Pinedale aged (~15,000 years old) moraines, younger fluvial deposits, and alluvial material. Components of left-lateral offset are also evident in the south-central part of the fault zone.

Based upon 17 EDM profiles and topographic surveys of the Teton fault scarp and extensive detailed geologic mapping (**Figure 5**), Quaternary surface offsets across the fault are shown to increase from an average of 33 feet (10 m) at the northern and southern ends of the fault to a maximum of 98 feet (30 m) in the central portion of the fault zone, defining, in part, three fault segments; the south, central, and north (Susong and others, 1987; Smith, 1988). Ostenaa (1988) evaluated segmentation of the Teton fault on the basis of Bureau of Reclamation studies and suggested two segments; one including the southern and central segments and a northern segment the same as Susong and others (1987) and Smith (1988). The lateral variation in surface offset along the fault also coincides with the changes in topographic relief (highest in the central segment) along the mountain front, suggesting a causal relationship between the areas of highest topography and the areas of greatest fault activity.

The southern end of the Teton fault appears to terminate near its intersection with older Overthrust Belt structures at the Cache Creek and Jackson thrusts (**Figure 2**). The fault may extend south of Wilson, although no Quaternary scarps are preserved there. The boundary between the southern and central segments is postulated to coincide with a 23° counterclockwise change in strike of the fault south of Taggart Lake. This segment boundary is also marked by an increase in average surface offset (greater in the central segment) and evidence for a left lateral component of offset on the central segment that is not seen to the south.

The boundary between the northern and central segments (**Figure 1**) is postulated to occur near Moran Bay, where the middle segment of the Teton fault terminates and may splay into a zone of highly fractured and jointed Precambrian bedrock north of Moran Canyon. The northern segment of the fault appears to begin 1.25 miles (2 km) east, on the north side of Moran Bay, and extend north to Wilcox Point where it may separate into multiple faults. One of these northernmost faults appears to extend northward beneath Jackson Lake and has been identified in the Steamboat Mountain area on the east side of the lake. Other branches of the fault may extend northward along the Snake River to the area near the boundary of Yellowstone National Park.

However, local earthquake data collected by nearby seismograph networks suggest a pronounced zone of small background earthquakes that extends northward from the Teton fault beneath the Pitchstone Plateau of Yellowstone National Park and may reflect activity on the ancient Teton fault, now covered by the Quaternary Yellowstone volcanics. Offset segments of the Teton fault are thought to step right (eastward) across the area north of Jackson Lake and several other normal faults appear to take up the displacement northeastward into the Yellowstone Plateau.

Deformation in the hanging wall of the northern part of the Teton fault is also suggested by the 10° to 20° westward tilt of Tertiary-Quaternary tuffs that are exposed at Signal Mountain. However, it is important to note that a significant portion of the deformation of the Signal Mountain block may be due, in part, to its location in the footwall of an unexposed normal fault on the east side of the mountain.

Paleomagnetic survey

In 1988 and 1989, personnel from the University of Utah and the University of New Mexico collected paleomagnetic samples at 67 sites in the Huckleberry Ridge Tuff throughout the footwall and hanging wall blocks of the Teton fault to evaluate the magnitude and extent of post 2 million year rotations about vertical and horizontal axes associated with the deformation along the structure. The sampling campaigns included collection at closely spaced sites along an east-west traverse extending from the western flank of the Tetons, across the northern end of the range, and continuing across the northern Jackson Hole region including Signal Mountain.

Seismic reflection survey of Jackson Lake

Seismic reflection surveys of Jackson Lake were made by the University of Utah in 1974 (Smith and others, in preparation). The reflection profiles show a pronounced Quaternary basin, with up to 660 feet (200 m) of lacustrine deposits, associated with the main north-south lake basin. This basin was associated with

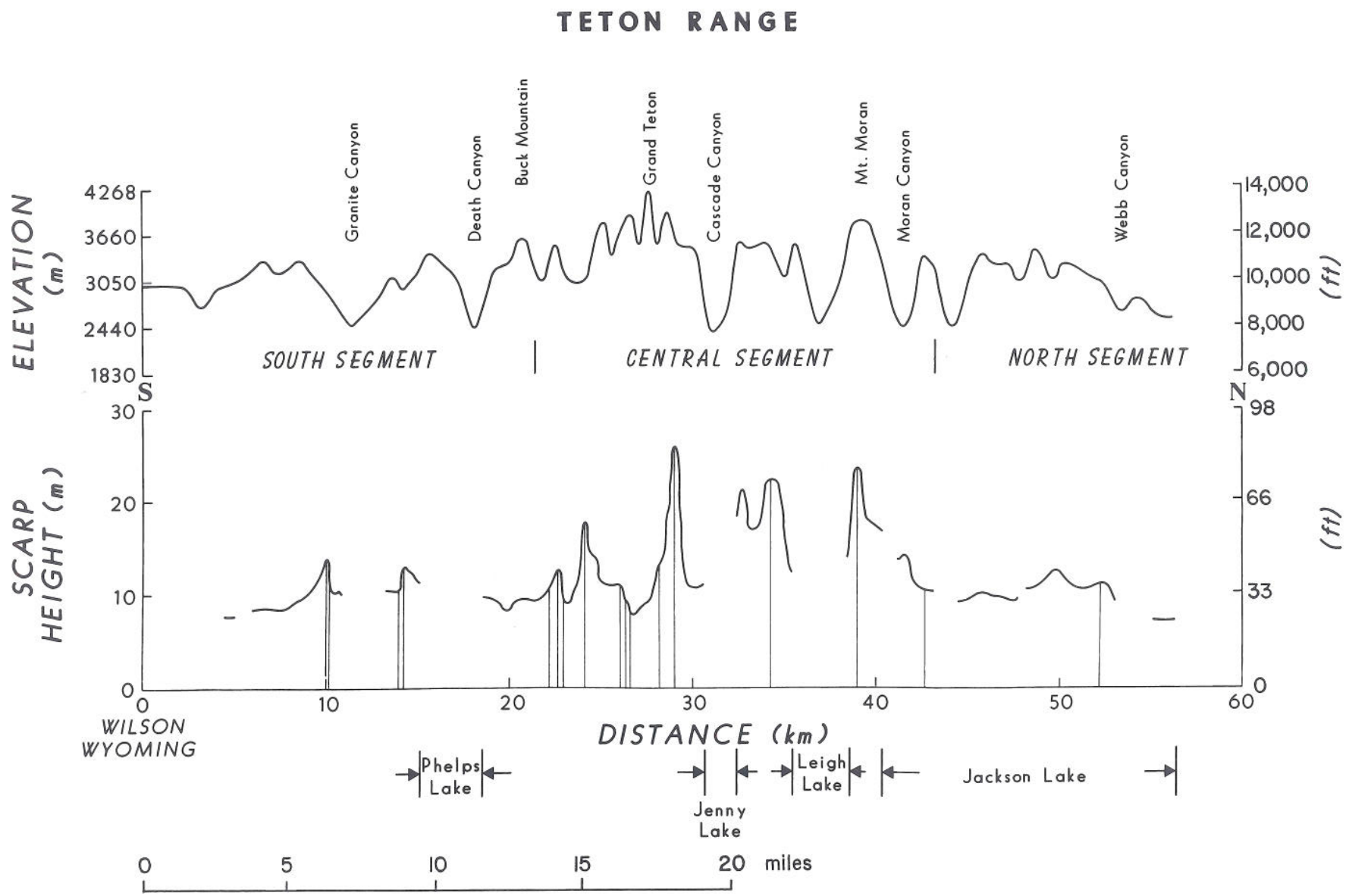

Figure 5. Topographic relief of the footwall block and Quaternary surface offsets across the Teton fault. Fault offsets were measured by EDM profiles at locations marked by vertical lines. Segment boundaries are discussed in text.

the ancestral Jackson Lake, which probably filled a glacially scoured depression adjacent to the Teton fault at the base of the range. Notably, no evidence of faulting or related tectonic deformation of the Quaternary sediments was seen on the seismic profiles. However, several episodes of sedimentation and subaerial exposure can be interpreted from the seismic profiles in the flat-lying main lake basin sediments.

In contrast, a more complex pattern of variable east-to-west dipping Quaternary lake sediments can be seen on the profiles in Jackson Lake west of Signal Mountain. These patterns are probably sedimentary features that result from scouring and deposition due to the advance and retreat of glaciers in and around Signal Mountain, as interpreted by Ken Pierce of the U.S. Geological Survey (personal communication).

Seismicity

Historic earthquake data (**Figures 3** and **6**) show that the the Teton fault zone is in a state of relative seismic quiescence and is surrounded by a dispersed earthquake activity associated with the Intermountain seismic belt. Local earthquake surveys by the University of Utah and the U.S. Bureau of Reclamation show a diffuse pattern of background seismicity in the Mt. Leidy Highlands, the area east of Moran, the southern Teton Range, and the Gros Ventre Range. However, the evidence for extensive Quaternary displacements and the contemporary seismic quiescence of the Teton fault led Smith (1988) to postulate a seismic gap for the Teton fault (**Figure 6**). If this hypothesis is true, the fault may be locked and the seismicity gap may be expected to "fill in" with a large earthquake in the future to accommodate the regional crustal deformation. Alternate explanations for the seismic quiescence of the Teton fault include: (1) the general seismicity of the area may be migrating eastward into the Gros Ventre and surrounding mountains, (2) the period of historical observation may not be sufficient to make a reasonable estimate of the long-term seismicity rate, and (3) the area surrounding the fault zone may not now be storing potential energy for some unknown reason.

By comparison, the region surrounding the Teton region has experienced some of the largest earthquakes in historic time, including the magnitude M_L 7.5, 1959 Hebgen Lake earthquake (the largest historic earthquake in the Rocky Mountains) 56 miles (90 km) from the Teton fault, and earthquakes as large as M_s 6.1 and extensive swarms associated with the Yellowstone caldera that begin just 6.2 miles (10 km) north of the Teton fault. In addition, the M_s 7.3, 1983 Borah Peak, Idaho, earthquake occurred on the Lost River fault on the west side of the Snake River Plain in a tectonic setting similar to that of the Teton area. These two M > 7 events are considered as hypothetical working models for the type and style of large earthquakes that one could expect in the Jackson Hole area. Similar ground deformation, ground accelerations, and surface rupture properties for these events could be postulated for the Teton fault. These analogues are useful to assess the expected hazards, ground deformation, and effects on structures and facilities in the Jackson Hole area during a major earthquake.

Stop 2a. Cathedral Group Turnout

From this location (**Figure 1**), a view to the west of one of the largest Quaternary fault scarps of the Teton fault is seen on the west side of String Lake. Here, a 112-foot (34-m) fault scarp in glacial debris and alluvial material marks the fault trace. Note the scalloped shape of the fault scarp above String Lake that is suggestive of a large landslide. At this location the scarp is on strike and is contiguous with the main fault trace. We believe that most of the scarp height is due to displacement on the fault, but there may be some additional displacement amplification by slumping and landslides.

Another notable feature seen at this stop is the subsidence of a north-south trending area, extending 2.3 miles (3.7 km) east from String Lake. On the basis of EDM profiling, we have documented 95 feet (29 m) of subsidence relative to the crest of the Jackson Lake glacial outwash. This zone of subsidence parallels the range front and confines the streams and lakes to the pronounced southward drainage direction from Leigh Lake to String Lake to Jenny Lake. This area at the south end of Leigh Lake marks the northernmost extent of regional subsidence adjacent to the Teton fault.

Stop 3. Jenny Lake

On the west side of Cottonwood Creek, at the outlet of Jenny Lake, a bench mark of a 1st-order level line established and surveyed in 1988 by the University of Utah and the University of California, Santa Barbara can be seen. Fifty bench marks were established and surveyed to assess contemporary deformation that may be associated with pre-, co-, and post-seismic movement of the Teton fault. This east-west profile of accurately measured bench marks extends 14 miles (22.5 km) from within the footwall of the Teton fault (in the center of the Teton Range) eastward at approximately 1,640 ft (500 m) intervals, crossing the Teton fault west of Jenny Lake, around the north end of

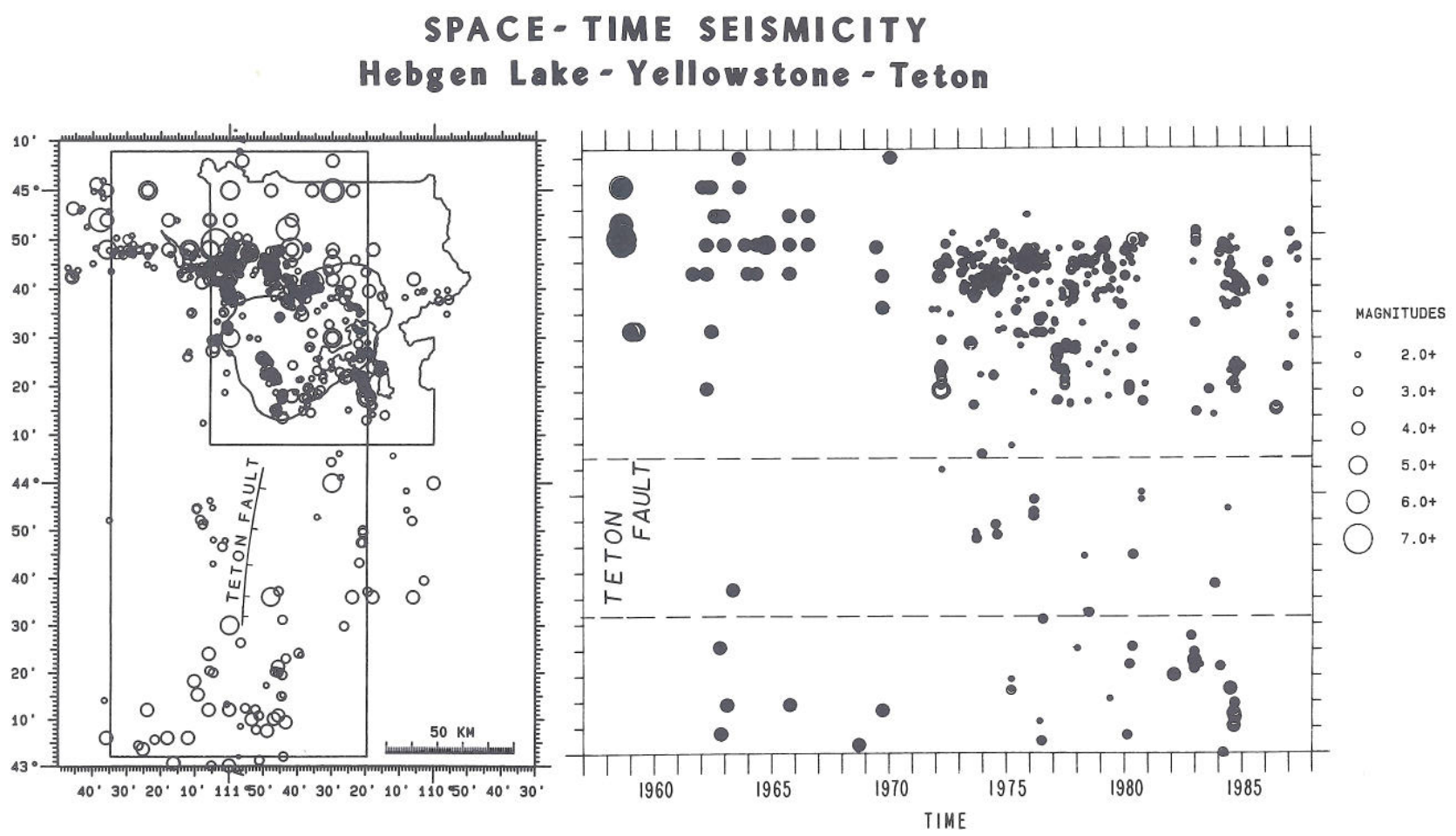

Figure 6. Time-space plot of seismicity surrounding the Teton fault zone for the period 1959 to 1987, showing the general seismic quiescence of the Teton fault at the M > 3 level. Figure taken from Smith (1988). Blackened areas indicate numerous overlapping earthquakes.

Timbered Island to the Snake River near Deadman Bar, well into the hanging wall. Preliminary results from the 1989 initial re-leveling survey show that the footwall block, the Teton Range, subsided 1.27×10^{-4} inches $\pm 1.78 \times 10^{-5}$ inches (5 mm $\pm$ 0.7 mm) relative to the valley floor, the hanging wall—notably in the opposite directions of the expected pre-seismic deformation for a normal fault.

In addition, three of the leveling benchmarks were observed by Global Satellite Positioning (GPS) instruments in 1989 and tied to the regional Yellowstone GPS network. This newly developed method, useful to assess contemporary tectonics, will provide a tie for determining vertical and lateral deformation within a global framework, and can be used to determine the regional extensional strain rates of the Jackson Hole region with respect to the North American plate.

Walk westward 1.25 miles (2 km) from the west side of Cottonwood Creek (Stop 3), along the upper horse trail, to observe the Teton fault south of Jenny Lake where it crosses the top of the south Jenny Lake moraine. At this site, approximately 82 feet (25 m) of vertical displacement along the north-south trending Teton fault, with several meters of displacement along a westward facing antithetic fault, can be seen in the Pinedale-age moraine. In addition, there is a suggestion here for a component of left-lateral offset across the main fault, similar to that observed in the lateral moraine on the south side of Taggart Lake, 6.2 miles (10 km) to the south; however the complex pattern of moraine terminations and the oblique offset due to the faulting make this interpretation somewhat equivocal. At Jenny Lake, the fault extends northward along a steep escarpment and then continues beneath the west side of the lake. To the south, the fault is exposed at the base of a steep slope west of the Moose Ponds. It continues 1.25 miles (2 km) southward, crossing a large alluvial fan above Lupine Meadows, and splays into two or possibly three strands within the fan, where a total of 98 feet (30 m) of fault offset has been measured.

The close association of the scarp with the Moose Ponds suggests that back-tilt along the fault may play a role in damming intermittent streams and forming a sag pond. Young debris flows from the Lupine Meadows alluvial fan are also deposited near the front of the pond, suggesting that they too contribute to the obstruction of stream flow and formation of the ponds.

Fault modeling

Jenny Lake is a good place to review the data and possible reasons for the subsidence and range-front capture of southward flowing streams adjacent to the Teton fault. Westward back-tilting of the valley floor due to Quaternary displacement on the Teton fault is a possible explanation for the observed subsidence and stream flow pattern. Other explanations suggest that the apparent westward tilt of the valley may be a result of westward flow along pre-exisiting drainages exiting from the terminal moraines in the vicinity of Jackson Lake, and/or aggradation of sediments deposited by the Snake and Gros Ventre rivers. However, we believe that the juxtaposition of the westward tilted valley against the active Teton normal fault is a natural consequence of slip and hanging-wall subsidence associated with displacement on the fault. Similar patterns of hanging-wall deformation, subsidence, and tilting have been observed in association with several large normal faulting earthquakes in the western U.S., eg. the M_L 7.5, 1959, Hebgen Lake, Montana, event; the M_s 7.3, 1983, Borah Peak, Idaho, event; and the M_L 7.1, 1954, Dixie Valley, Nevada, earthquake.

Using analytic models of subsurface faulting and accompanying surface deformation of the Teton fault, Byrd and others (1988) evaluated the role of hypothetical prehistoric earthquakes and their effects on deformation of the valley floor, incorporating the topographic profile along the 1st-order level line from Jenny Lake to the Snake River. Models of surface deformation resulting from displacement due to normal-faulting earthquakes nucleating at depths of 9.4 miles (15 km) on a variety of plausible subsurface fault geometries, with dips of 45° to 60°, were constructed. The results suggest that the present westward tilt of the valley may be due to as many as five $M > 7$ earthquakes with a total surface offset of 131 feet (40 m) in the last 15,000 years (since Pinedale glaciation) on the Teton fault.

Stop 4. South Taggart Lake Moraine (optional)

An excellent exposure of the Quaternary scarp of the Teton fault with a major left-lateral component of slip can be seen by hiking west for 1.5 miles (2.4 km) from the National Park Service Beaver Creek housing area, along the main trail and westward up and onto the south Taggart Lake moraine at the base of the range front. Here the Teton fault offsets glacial morainal material with up to 105 feet (32 m) of vertical displacement with evidence of an apparent 85 feet (26 m) of left-lateral offset. A 6.6-foot (2-m) antithetic fault scarp marks the west side of a back-tilted graben that extends for some 100s of meters north-south at this location.

Stop 5. Granite Canyon

Beginning at the main Granite Canyon trail head, on the Moose-Wilson road, an excellent exposure of the Teton fault can be seen by walking 1.75 miles (2.6 km) along the trail to the mouth of Granite Canyon. In this area, the southern segment of the Teton fault cuts Pinedale moraine, till, glacial outwash, younger debris-flow material, and fluvial deposits. Scarp heights range from 10 to 49 feet (3 to 15 m) north and south of the mouth of the canyon, with 3- to 6.6-foot-high (1- to 2-m) antithetic fault scarps east of the main fault that mark the eastern limit of a well-developed back-tilted graben structure.

The larger and older scarps, north and south of the canyon mouth, range from 26 to 49 feet (8 to 15 m) high, and are exposed in the Pinedale moraine and outwash deposits. Erosion by the modern stream channel has destroyed the antithetic scarps in the younger deposits and has modified the strike of the larger scarps. The youngest fault scarps within the modern outwash plain range from 6.6 to 10 feet (2 to 3 m) high and offset fluvial outwash, debris flow, and channel deposits.

Four Pinedale-age and younger alluvial surfaces are offset by the fault in the vicinity of the mouth of Granite Canyon. These surfaces have been identified on the basis of their geometric relationships to small recessional moraines nested within the larger Granite Canyon moraine complex, as perched or hanging stream channels cut by the fault, as debris flow levees or fluvial terraces, and as an active outwash plain.

Trenching results

A 10-foot (3-m) fault scarp was excavated in 1989 at the mouth of Granite Canyon to evaluate the displacement and age of faulting on the Teton fault. The trench exposed a 13.5-foot (4.1-m), down to the east, single-event displacement on an 85°E dipping fault. Back tilting of surfaces in the hanging wall block is approximately 3°, with a 2° depositional slope in the footwall, resulting in a net vertical displacement of 13 feet (4 m).

The faulting juxtaposed a fluvial deposit capped by a paleosol horizon against fluvial and debris flow units overlying a Pinedale age (approximately 15,000 years old) glacial till. Colluvial materials and alluvial fan deposits derived from the fault scarp have buried the down-thrown fluvial and paleosol units exposed in the trench. Charcoal fragments were observed and collected from the base of and within the paleosol horizon. Carbon dating by Beta Analytic Inc., using conventional methods and extended counting of two charcoal samples recovered from the base of the colluvial wedge and the base of the paleosol, yielded ages of 7,150 ± 120 years, and 7,240 ± 190 years, respectively.

Comparison of the displacement event recorded in Granite Canyon trench with the surface displacements associated with other earthquakes of the western U.S. Cordillera suggests that the displacement was produced by a $7.1 < M_s < 7.4$ earthquake. This is the first quantitative estimate of the expected size for large and damaging earthquakes that could occur on the Teton fault in the future. If this event is a characteristic earthquake for this area, the larger scarps immediately north and south of the trench site may be the product of three or four earthquakes of similar magnitude during the past 15,000 years.

References cited

Byrd, J.O.D., Geissman, J. Wm,.and Smith, R.B.,1988, Seismotectonics of the Teton fault and possible relationship to the Yellowstone hotspot: Eos, Transactions of the American Geophysical Union, v. 69, no. 44, p. 1419.

Gilbert, J.D., Ostenaa, D., and Wood, C., 1983, Seismotectonic study; Jackson Lake Dam and Reservoir, Minidoka Project, Idaho-Wyoming: U.S. Bureau of Reclamation Seismotectonic Report 83-8, 123 p.

Lageson, D.R., 1987, Laramide uplift of the Gros Ventre Range and implications for the origin of the Teton fault, Wyoming: Wyoming Geological Association 38th Annual Field Conference Guidebook, p. 78-89.

Love, J.D., and Montagne, J., 1956, Pleistocene and recent tilting of Jackson Hole, Teton County, Wyoming: Wyoming Geological Association 11th Annual Field Conference Guidebook, p. 169-178.

Love, J.D., and Reed, J.C., Jr., 1971, Creation of the Teton landscape: Grand Teton Natural History Association, 120 p.

Love, J.D., Reed, J.C., Jr., and Christiansen, A.C., in press, Geologic map of Grand Teton National Park: U.S. Geological Survey Miscellaneous Investigations Map I-2031, scale 1:62,500.

Morgan, L. A., Doherty, D.J., and Leeman, W.P., 1984, Ignimbrites of the eastern Snake River Plain: evidence for major caldera-forming eruptions: Journal of Geophysical Research, v. 89, p. 8665-8678.

Ostenaa, D.A., 1988, Late Quaternary behavior of the Teton fault, Wyoming: Geological Society of America Abstracts with Programs, v. 20, no. 7, p. A14.

Reed, J.C., 1973, Geologic map of the Precambrian rocks of the Teton Range, Wyoming: U.S. Geological Survey Open File Report 73-230, scale 1:62,500.

Smith, R.B., 1988, Seismicity and earthquake hazards of the Borah Peak-Hebgen Lake-Yellowstone-Teton region—implications for earthquakes in extensional and active volcanic regimes: Geological Society of America Abstracts with Programs, v. 20, no. 7, p. A12.

Smith, R.B., Nagy, W. C., and Doser, D. I., 1990, The Borah Peak earthquake sequence: regional seismicity, fault kinematics, stress field inversion, and relationship to the Snake River Plain: Bulletin of the Seismological Society of America (in press).

Smith, R.B., Richins, W. D., and Doser, D. I., 1984, The Borah Peak earthquake: seismicity, faulting kinematics and tectonic mechanism, *in* Workshop XXVIII on The Borah Peak Earthquake: U.S. Geological Survey Open File Report 85-290, p. 236-263.

Susong, D.D., Smith, R.B., and Bruhn, R.L., 1987, Quaternary faulting and segmentation of the Teton fault zone, Grand Teton National Park, Wyoming: Eos, Transactions of the American Geophysical Union, v. 68, p. 1452.

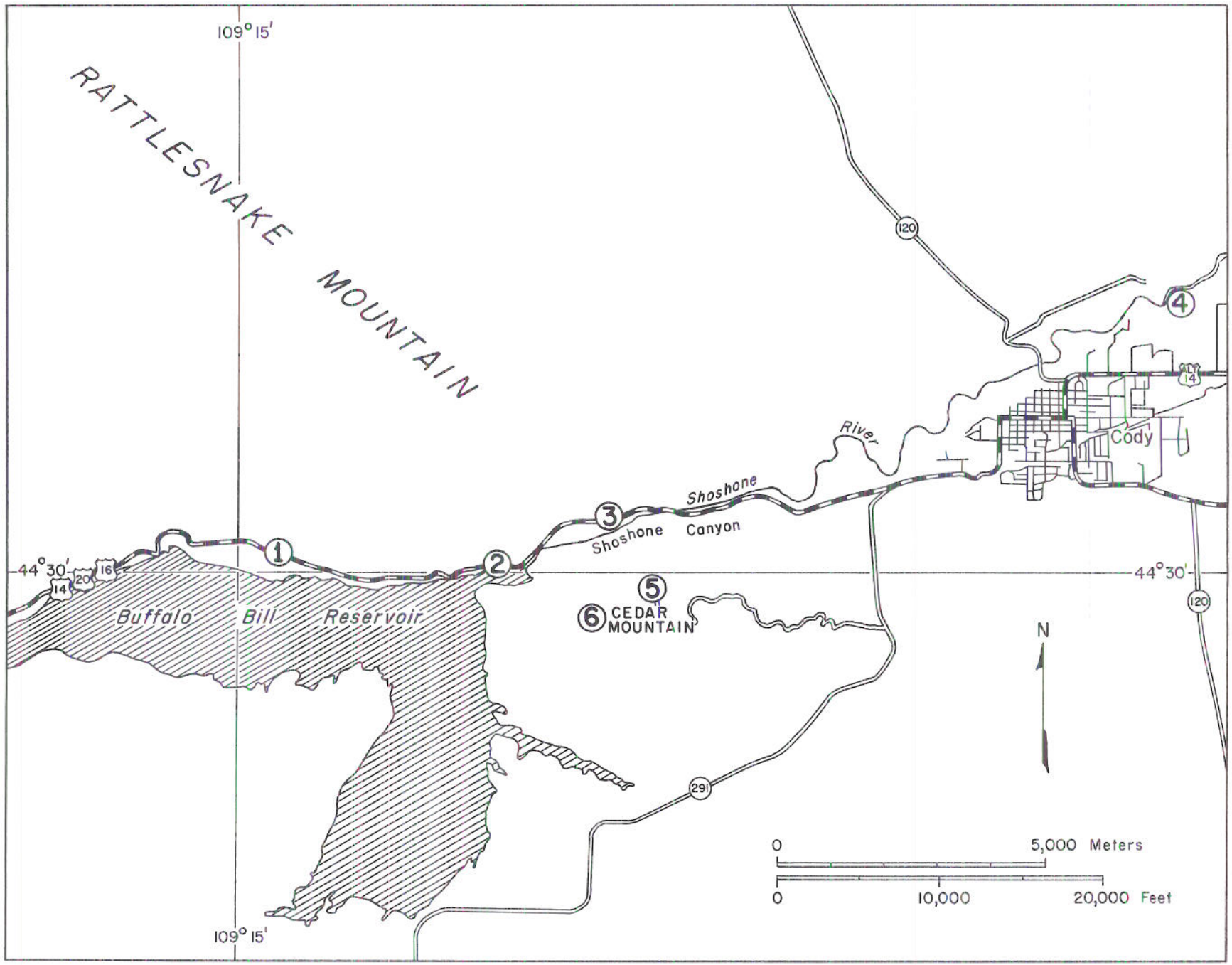

Figure 1. Trip route and stops, field trip no. 7, part 1.

Field trip no. 7, part 1

HETEROGENEOUS LARAMIDE DEFORMATION IN THE RATTLESNAKE MOUNTAIN ANTICLINE, CODY, WYOMING

Eric A. Erslev
Department of Earth Resources
Colorado State University
Fort Collins, Colorado 80523

Trip summary (see Figure 1)

Stop 1. Overview at the entrance to Buffalo Bill State Park
Stop 2. Southwest limb of Rattlesnake Mountain anticline
Stop 3. Precambrian-Cambrian contact, back limb of Rattlesnake Mountain anticline
Stop 4. (optional) Symmetric folding of Frontier Formation northeast of Cody
Stop 5. Eastern summit of Cedar Mountain
Stop 6. Western summit of Cedar Mountain

Introduction

The Rattlesnake Mountain anticline, a classic Rocky Mountain structure featured in many structural geology textbooks, owes its fame to the excellent exposures in Shoshone Canyon west of Cody, Wyoming. This field trip will view and discuss this classic profile through the deeper structural levels of a Laramide foreland uplift. While there is much to be gleaned from these classic exposures, the three-dimensional geometry and the strong influence of pre-existing basement weaknesses make the Rattlesnake Mountain anticline in Shoshone Canyon a questionable choice for an archetypal Rocky Mountain foreland structure.

Published structural models of Rattlesnake Mountain anticline offer a great variety of structural mechanisms, including passive drape folding over normal-faulted basement blocks (Johnson, 1934; Pierce, 1966; Stearns, 1971); passive folding over thrust blocks (Erslev, 1986); fold-thrust models involving extensive basement folding (Brown, 1984; Blackstone, 1986); and fault propagation folding over thick zones of reverse fault splays (Schmidt and Garihan, 1983) or cataclastic material (Cook, 1983, 1988). Shoshone Canyon's 3,600 feet (1 km) of local relief was used by Stearns (1971, 1978) as a basis for a significant portion of his vertical uplift model for Laramide basement-cored uplifts. Subsequent interpretations of the Rattlesnake Mountain anticline by Schmidt and Garihan (1983), Cook (1983, 1988), Brown (1984), Stone (1984, after Blackstone, 1940), and Erslev (1986) based their cross sections on Stearns' surface data and the original 15-minute geological quadrangles by Pierce (1966) and Pierce and Nelson (1968). Excellent reviews of this debate are contained in Stone (1984) and Blackstone (1986), who documented the three-dimensional nature of thrust faulting in this northwestern margin of the Bighorn Basin.

This study of the Rattlesnake Mountain anticline and surrounding structures was based on the recognition that these hypotheses should be testable using field and subsurface data. Despite the excellent exposures and volume of material written on Rattlesnake Mountain, very little detailed structural data has been collected. The lack of detailed constraints compromises the validity of methods of Rocky Mountain cross-section balancing (Brown, 1984; Erslev, 1986; Cook, 1988; Narr and Suppe, 1989) based on the poorly defined geometry of Rattlesnake Mountain anticline. For instance, Brittenham and Tadewald (1985) showed that all of the proposed models for the anticline (except that of Blackstone, 1986) conflict with the depth to basement in the footwall documented by well and seismic data.

This field trip will view the exposures at Shoshone Canyon and Cedar Mountain (directly to the southwest) (**Figures 1** and **2**) and present the initial results of detailed geological studies currently underway at Colorado State University. Diverse deformation styles and intensities will be viewed, showing the highly heterogeneous nature of foreland strain.

Acknowledgments

I would like to acknowledge previous contributors to the Rattlesnake Mountain debate, whose work is often overly simplified and inadequately represented in subsequent literature. Donald Fairchild of the Bureau of Reclamation provided access to construction areas and freely shared his geological observations. I would also like to thank Robbie Gries for her encouragement and access to industry data and James Rogers, Donald Stone, and Donald L. Blackstone, Jr. for many stimulating discussions concerning the Rattlesnake Mountain anticline. Acknowledgment is made to the Donors of the Petroleum Research fund, administered by the American Chemical Society, for the support of this research.

Stop descriptions

Stop 1. Overview at the entrance to Buffalo Bill State Park

This stop is 5 miles west of Buffalo Bill Dam at the western end of Shoshone Canyon. To the east, Shoshone Canyon, carved by the Shoshone River, separates Rattlesnake Mountain to the northeast from Cedar Mountain (Stops 5 and 6) to the southeast. The linear crest of Rattlesnake Mountain defines the anticlinal crest in the Mississippian Madison Limestone. The

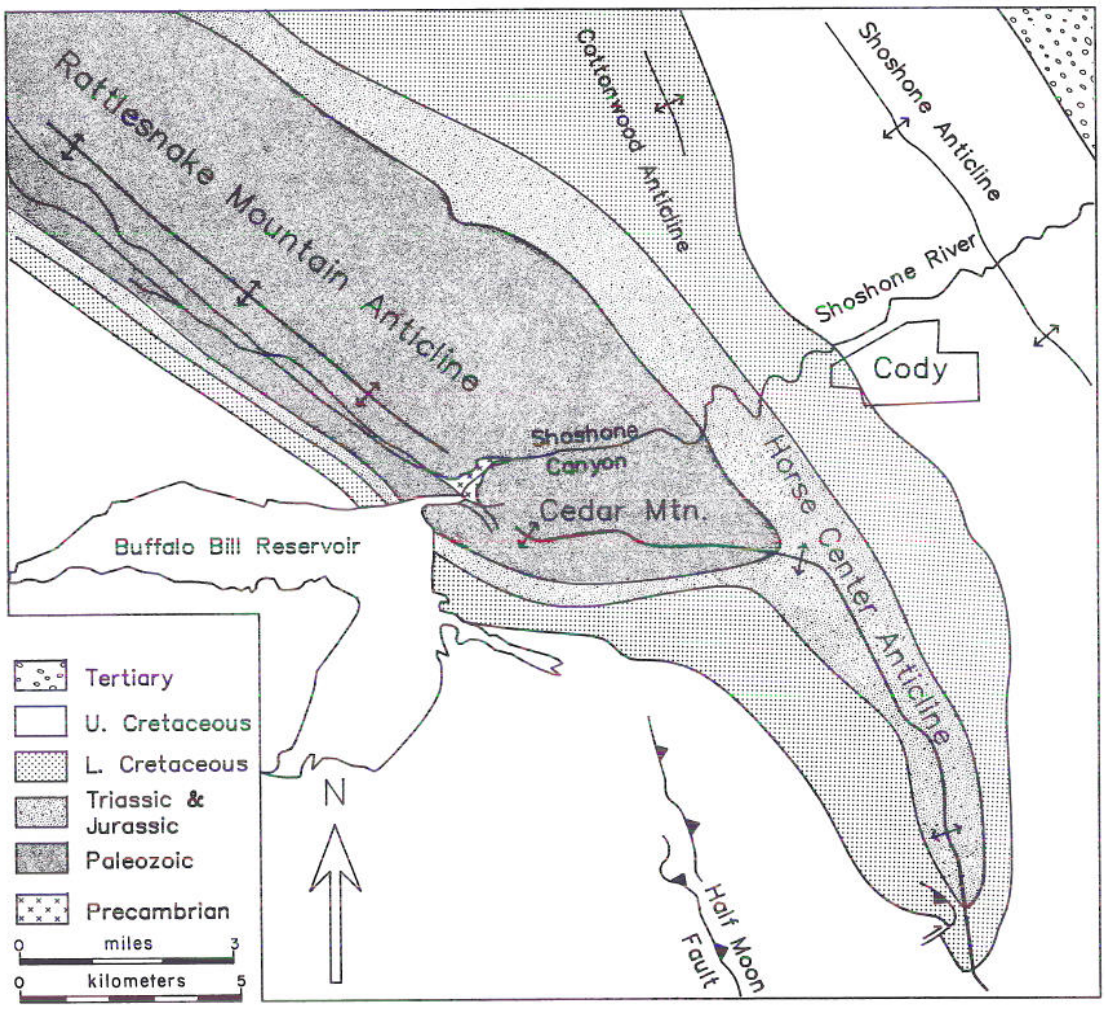

Figure 2. Geologic map of the Rattlesnake Mountain area, simplified from Pierce (1966, 1970) and Pierce and Nelson (1968).

steep southwestern limb of the anticline is characterized by near-vertical to recumbent Paleozoic strata forming spectacular palisades. Mapping by Pierce and Nelson (1968) documented some sections with vertical beds and some with overturned strata dipping as little as 42°NE.

Cedar Mountain (**Figure 3**) forms a conical termination of the Rattlesnake Mountain structure, with the Pennsylvanian Tensleep Formation dipping up to 35° due south along the southern side of the mountain. The last stops of this field trip will use Cedar Mountain for an up-plunge view of the profile through the anticline on the north wall of Shoshone Canyon.

Stop 2. Southwest limb of Rattlesnake Mountain anticline

Traverse through the southwest limb of Rattlesnake Mountain anticline to the fault contact with Precambrian basement. (Park on north side of road, 1/3 mile west of tunnel entrance at Buffalo Bill Dam).

Road cuts and natural outcrops of Paleozoic rocks along the north shore of Buffalo Bill Reservoir provide an intriguing profile through the steep, southeastern limb of the Rattlesnake Mountain anticline (**Figure 4**). Tensleep Sandstone, Amsden Formation, Madison Limestone, Three Forks-Jefferson Formation and upper Bighorn Dolomite show their lowest inclinations of the entire mountain front, with upright strata dipping 40° to 50°SW. These units appear to be minimally deformed, maintaining their original thicknesses (Stearns, 1971).

The lower part of the Ordovician Bighorn Dolomite and the shales of the Cambrian Snowy Range Formation, exposed immediately adjacent to the fault-bounded Precambrian granitic gneiss, are more highly inclined (40° to 80° SW) and faulted. The presence of conjugate faults, both symmetric to and at a high angle to bedding, suggests that these faults result from layer stretching, not imbricate faulting rooted in the master fault bounding the Precambrian rocks. This layer extension caused mega-boudinage of lower sedimentary units (Cambrian Pilgrim Limestone, Gros Ventre Formation, and Flathead Sandstone), which are omitted in this exposure of the steep forelimb of the anticline.

Across the reservoir to the southeast (**Figure 3**), a very different geometry is exposed. Here, the Bighorn Dolomite is imbricated on a series of back thrusts bringing southwest over northeast. The Pilgrim Limestone is exposed near the waterline and adjacent to the

Figure 3. View of Cedar Mountain from the southeast corner of Rattlesnake Mountain. The highest peak, capped by Tensleep Sandstone, will be used as a vantage point for Stop 6.

fault. Enhanced normalized Fry stain analysis (Erslev, 1988) of oolitic limestones in the Pilgrim Limestone show minimal internal strains with ellipticities (X/Y) not exceeding 1.05. Mega-boudinage of the Flathead and Gros Ventre formations results in major thinning and local omission of these strata adjacent to the 30-foot-thick (10-m) cataclastic fault.

The Precambrian rocks adjacent to the highly deformed Cambrian section are remarkably undeformed. Precambrian diabase occurs in the fault plane on both sides of the reservoir and in foliated dikes paralleling the fault. This suggests that the exposed fault was localized by a pre-existing Precambrian mafic dike. Thus, the orientation of the basement-bounding normal fault, which dips 82° to 84° SW (by triangulation), is not representative of the Laramide stress field. This normal faulting cannot be solely responsible for the basement deformation because its orientation indicates basement extension incompatible with the shortening clearly indicated by the folded sedimentary strata.

Stop 3. Precambrian-Cambrian contact, back limb of Rattlesnake Mountain anticline

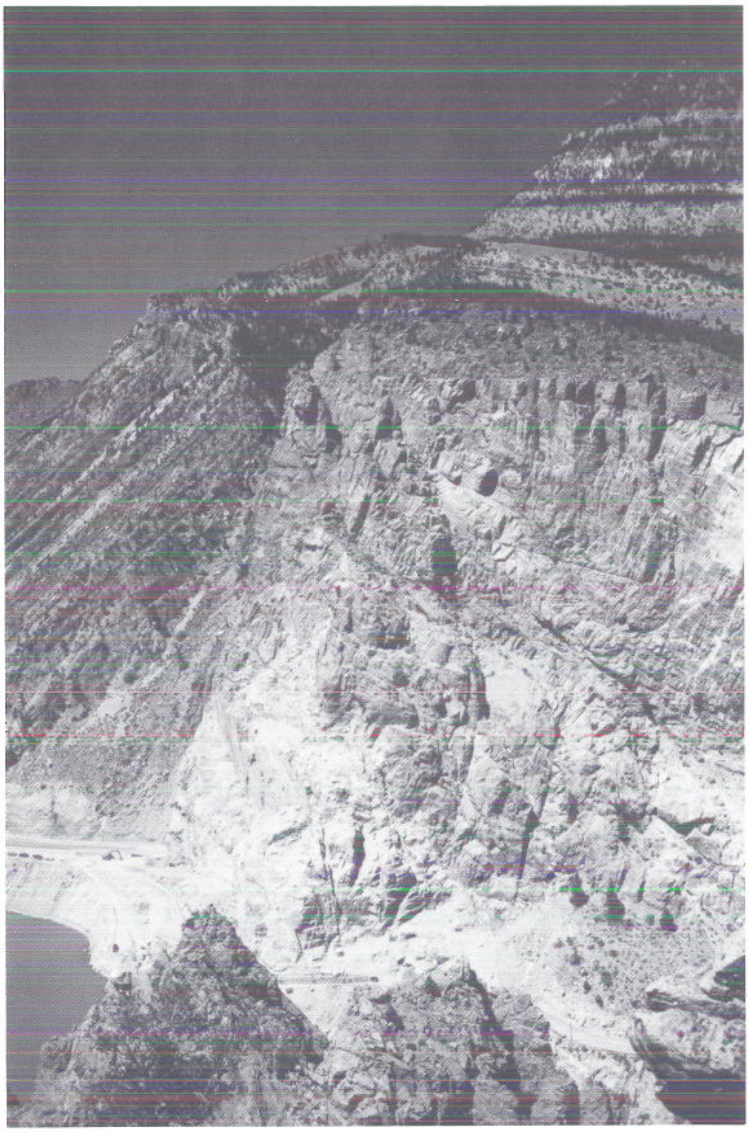

Figure 4. View to the north of the normal fault between the coherent basement block and folded Paleozoic strata at Stop 2. This photograph was taken from the Paleozoic unconformity south of the Shoshone River.

Park in the turn out east of the easternmost tunnel. The spectacular exposure of the Flathead unconformity in the rock wall behind the new power plant shows the minimal deformation characteristic of the back limb near the basement-cover interface. Faulting in this area parallels a large, east-west striking diabase dike exposed in the river bottom and in the notch between tunnels on the road. This fault is nearly vertical, with approximately 30 feet (10 m) of south-down, dip-slip motion. This is the largest fault within the basement exposures. Its parallelism to a mafic dike again shows the importance of preexisting weaknesses to fault localization. It is possible that the east-west faults at the southern flank of Cedar Mountain and along the front of the east-west Pat O'Hara anticline to the north were localized by parallel mafic dikes.

The old Yellowstone road in the bottom of Shoshone Canyon provides excellent access to nearly continuous basement exposures. Over 300 orientations of fault and joint planes were measured in basement and Flathead Sandstone exposures adjacent to the road and along the rim of the inner canyon. **Figure 5A** shows that the fault planes and slickenside lineations are highly variable in orientation, with maxima parallel to the two mafic dike orientations discussed above. These faults are primarily dip-slip normal faults, although some east-west strike-slip faulting of both right- and left-lateral shear sense occurs in the basement. These strike-slip displacements may be Precambrian.

Figures 4, 5b and 6 show that joints and faults measured along the old Yellowstone

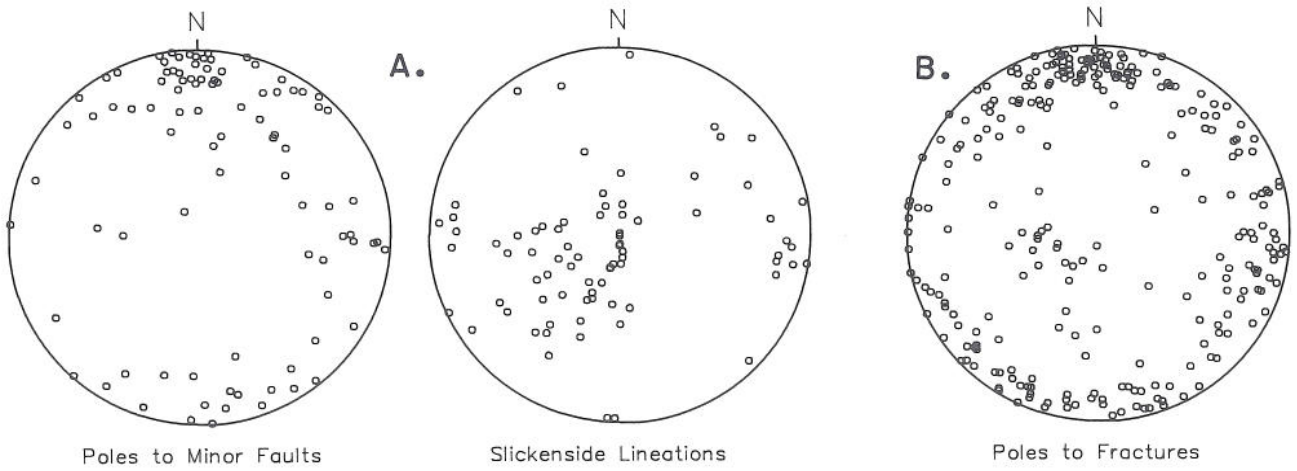

Figure 5. (A) Fault plane and slickenside orientations in the up-thrown Precambrian basement and Flathead Sandstone in Shoshone Canyon. (B) Joint and fault plane orientations collected in nearly continuous basement exposures along the old Yellowstone road in the bottom of Shoshone Canyon.

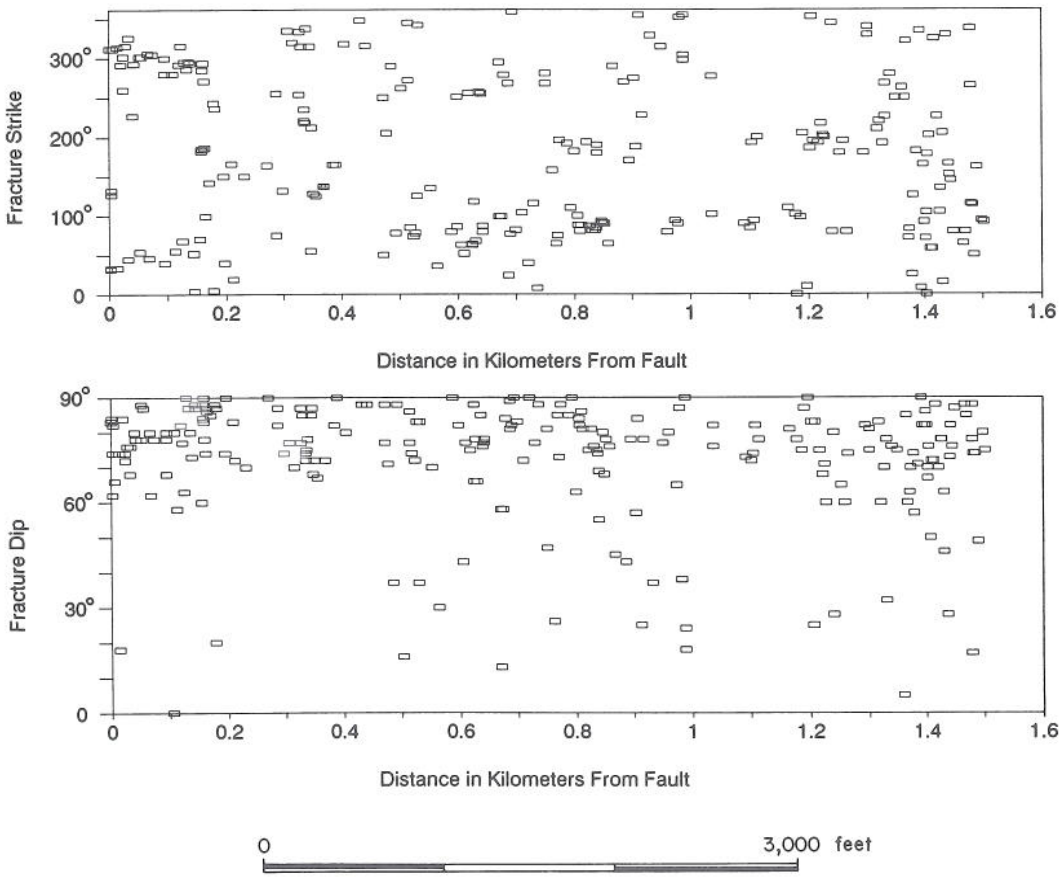

Figure 6. Fracture traverse through basement, Rattlesnake Mountain. Joint and fault plane orientations from Figure 5B, plotted versus distance from the fault to examine the spatial distribution of fracturing relative to the fault plane.

road are predominantly high angle and do not show major changes in orientation or frequency as the fault is approached. This supports the hypothesis of coherent basement blocks in Laramide uplifts. In addition, there is no perceptible change in the orientation of the Flathead Sandstone as the fault is approached. Oolites in the overlying Pilgrim Limestone also show no perceptible deformation, suggesting that the sedimentary strata overlying the basement block are largely undeformed.

Stop 4. (optional) Symmetric folding of the Frontier Formation 2 miles northeast of Cody.

In sharp contrast to the large-wavelength, asymmetrical Rattlesnake Mountain anticline, smaller symmetric anticlines and synclines mark the eastern extent of the Rattlesnake Mountain block. Seismic profiles (Lowell, 1983) and drilling (Pierce, 1966; unpublished Texaco drilling) indicate that these structures are thin-skinned fault-bend folds or buckle folds, which occur above the major, northeast-directed, Line Creek-Oregon Basin thrust system. In 1985, Texaco drilled Sheets #1 just north of this area, penetrating the basement overhang of a northeast-directed blind thrust and then entering basement a second time. Thus, these folds probably result from the transfer of thrust shortening from the blind thrust system to surface folds.

Stop 5. Eastern summit of Cedar Mountain

This stop on the top of the Tensleep Sandstone is an excellent place to see the relationship between structures in the Cody area. **Figure 7** shows a computer-generated plunge projection of contacts in the north wall of Shoshone Canyon. This profile was combined with subsurface data and balancing methods detailed by Erslev (1986) to constrain a regional cross section

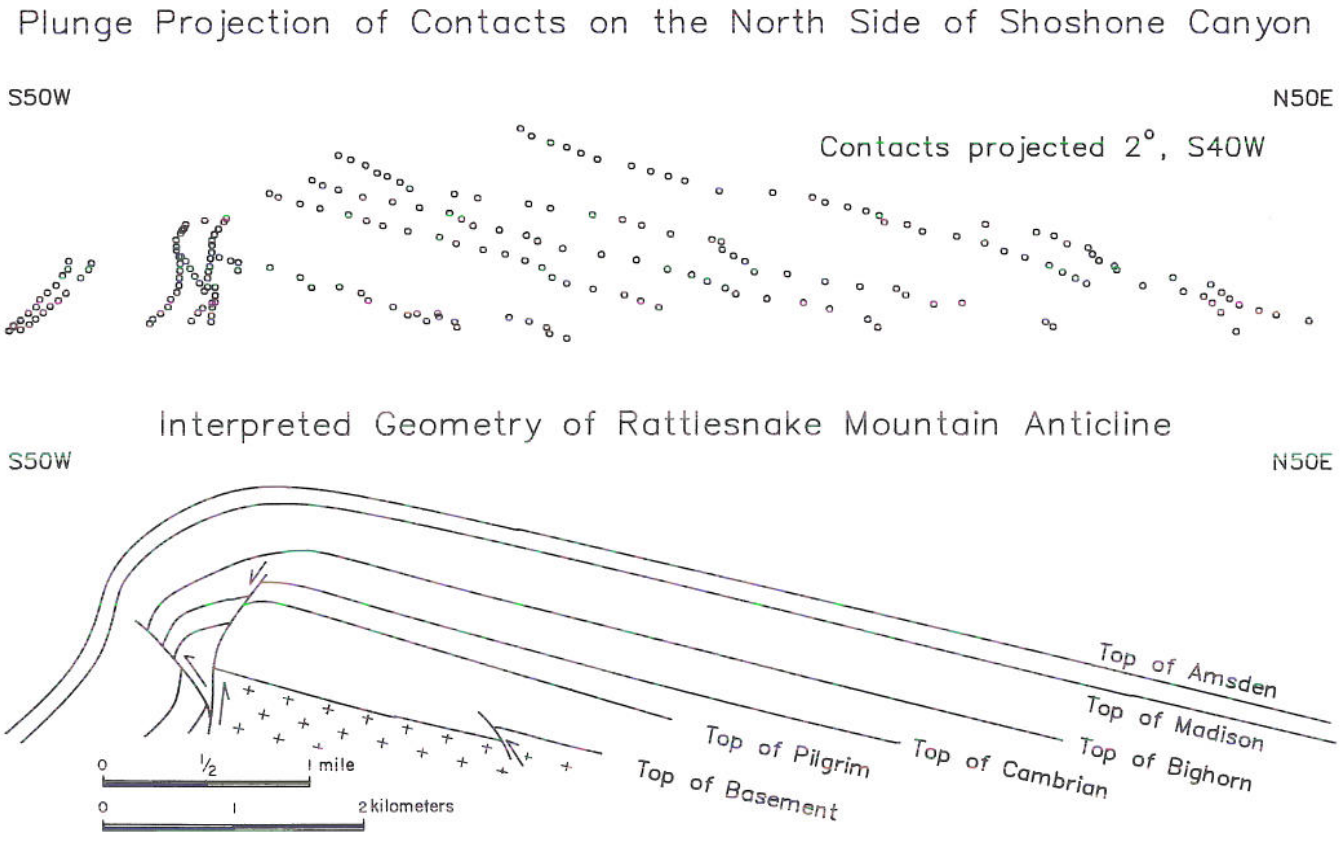

Figure 7. Up-plunge projection of unit contacts mapped by Erslev (unpublished) and Pierce (1966) in the north wall of Shoshone Canyon. The apparent variability of unit thickness in the back limb of the anticline is due to concealed and slumped contacts and variations in structural plunge within the canyon.

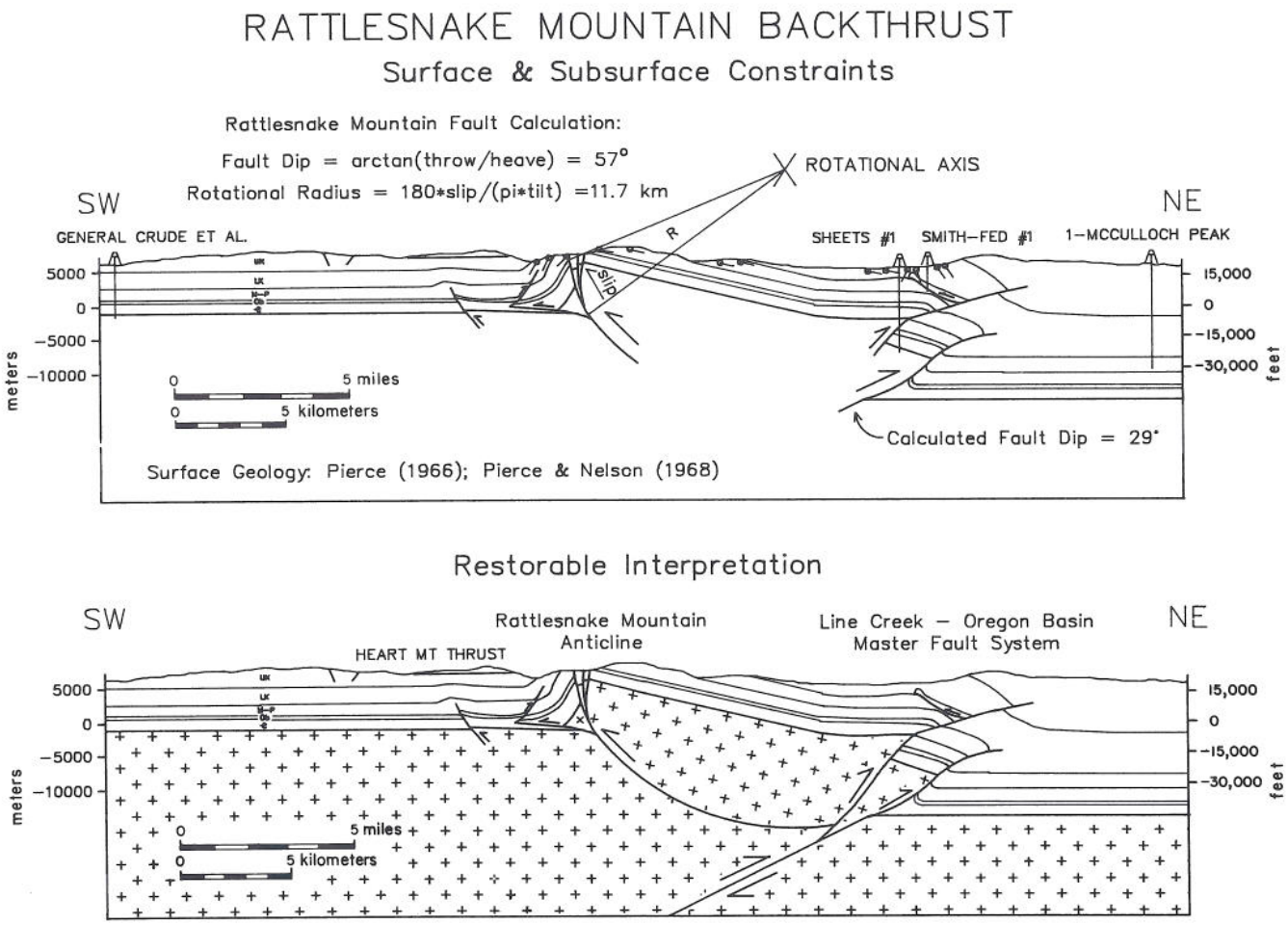

Figure 8. Regional cross section trending N50°E through wells General Crude et al. (SW1/4, SE1/4 sec. 11, T.52N, R.105W) and Sheets #1 (SW1/4, SW1/4 sec. 21, T.54N, R.102W), showing data used to calculate the restorable interpretation. The cross section goes through the crest of Rattlesnake Mountain anticline 6.5 miles (10.5 km) northwest of the Shoshone River in Shoshone Canyon.

through Rattlesnake Mountain (**Figure 8**). This section balances by both bed length and basement block geometry, which restore to a nearly continuous mosaic. Narrow basement fault zones are indicated throughout, consistent with field observations and in sharp contrast with models by Cook (1983, 1988) and Brown (1984). The shortening and vertical displacement of the asymmetrical Rattlesnake Mountain anticline indicates that the dip of the fault equivalent to the fold (Erslev, 1986) is 57° NE at the level of the Madison Limestone. Calculated fault curvature based on the relative tilt between the hanging wall and footwall brings the Rattlesnake Mountain fault around into concordance with the basin-boundary fault system penetrated by Texaco well Sheets #1. This interpretation clearly shows that the Rattlesnake Mountain structure is a back thrust off the blind basin boundary fault system, [the Line Creek and Oregon Basin faults of Blackstone (1986)] responsible for the uplift of Oregon Basin to the south and the Beartooth Mountains to the northwest.

Stop 6. Western summit of Cedar Mountain

From this excellent vantage point (pictured in **Figure 3**), the geometry of the crest of Rattlesnake Mountain anticline is clearly seen. The major fault at road level between the Cambrian and Precambrian strata bifurcates upward into two fault splays (**Figure 7**). The eastern splay remains a normal fault, throwing the tip of the structure down. The western splay curves outward, taking up progressively more slip as a major thrust.

The reason for the dominance of the high-angle fault at Buffalo Bill Dam is apparent from the three-dimensional geometry of the uplift. South of Cedar Mountain, the anticline curves sharply eastward before continuing southeasterly as the partially thin-skinned Horse Center anticline. This left the southwestern tip of the Rattlesnake Mountain structure relatively unsupported and the corner broke off. The corner is presently lodged under the sedimentary strata, allowing significantly shallower dips in the frontal limb of the anticline at this corner.

This geometry also explains why the basement rocks are so anomalously undeformed in Shoshone Canyon. In many equivalent structures (e.g, Forellen fault of the Teton Range and Milner Mountain anticline of the northeast Front Range), slumping of the basement tip bends the hanging wall downward. At Rattlesnake Mountain, the eastern fault splay propagates north out of the canyon where it allows the tip of the hanging wall to bend in this manner. However, in Shoshone Canyon, the tip of the basement has already fallen off, leaving behind a thick, coherent basement block with little reason to fold.

Summary

Two-dimensional balancing of a regional cross section shows that Rattlesnake Mountain anticline is cored by a back-thrust basement chip off the main basin-boundary faults to the east. The three-dimensional geometry of the anticline indicates that Shoshone Canyon cuts through the conical tip of the structure. The resulting out-of-the plane motion adds to complexities due to fault localization on pre-existing basement weaknesses. These characteristics make the Rattlesnake Mountain anticline a non-ideal type locality for Rocky Mountain foreland structures. The diversity of foreland structures suggests, however, that no single structure can portray the full range of foreland responses to Laramide compression.

Strain in the basement rocks and sedimentary strata during the development of basement-cored anticlines is highly heterogeneous. Field observations at Rattlesnake Mountain and numerous other localities show the following characteristics:

1. Basement deformation occurs due to cataclasis in narrow shear zones (30 ft/10 m thick at Rattlesnake Mountain), which opportunistically exploit pre-existing weaknesses, yet give overall basement shortening.

2. The lowest sedimentary strata are commonly highly extended and rotated toward the master fault orientation.

3. Upper sedimentary strata either show no elongation or shortening or are shortened by thrusting and/or folding.

This highly anisotropic strain pattern can be modeled as a triangular shear zone with constant slip (**Figure 9**). At deeper levels in the uplift, the shear zone is narrow, resulting in high shear strain, which causes elongation of the lower strata (e.g., Stop 2). Higher in the structure, the shear zone is thicker, causing a lower shear strain, which causes bed shortening by thrust faulting and symmetric folding (e.g., Stop 4). This model is currently being tested with field, experimental, and theoretical (computer) data. Triangular shear zones may provide a valid kinematic model for the development of fault-propagation folds.

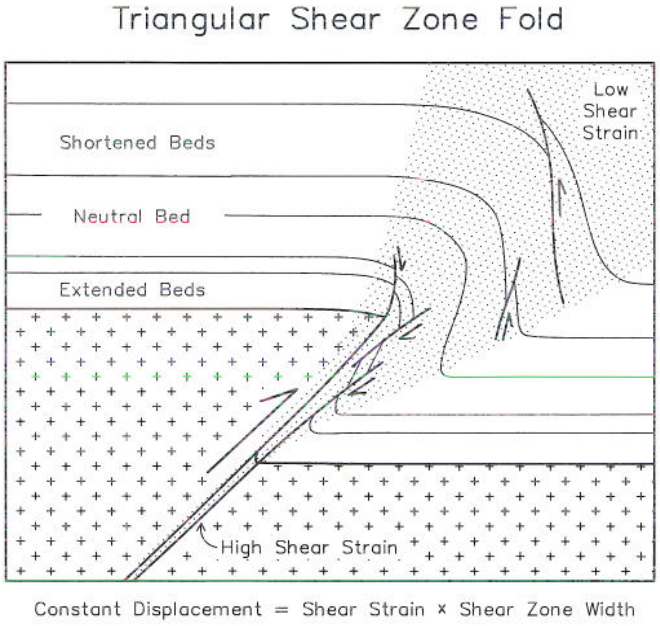

Figure 9. Triangular shear zone model for basement-cored fault-propagation folds.

References cited

Blackstone, D.L., Jr., 1940, Structure of the Pryor Mountains, Montana: Journal of Geology, v. 48, p. 590-618.

Blackstone, D.L., Jr., 1986, Structural geology—northwest margin, Bighorn Basin: Park County, Wyoming and Carbon County, Montana, *in* Garrison, P.B., editor, Geology of the Beartooth uplift and adjacent basins: Montana Geological Society and Yellowstone-Bighorn Research Association Joint Field Conference and Symposium, p. 125-136.

Brittenham, M.D., and Taldewald, B.H., 1985, Detachment and basement involved structure beneath the Absaroka Range volcanics, *in* Gries, R.R., and Dyer, R.C., editors, Seismic exploration of the Rocky Mountain region: Rocky Mountain Association of Geologists and Denver Geophysical Society, p. 31-43.

Brown, W.G., 1984, A reverse fault interpretation of Rattlesnake Mountain anticline, Wyoming: Mountain Geologist, v. 21, p. 31-35.

Cook, D.G., 1983, The northern Franklin Mountains, Northwest Territories, Canada—a scale model of the Wyoming province, *in* Lowell, J.D., editor, Conference on Rocky Mountain foreland basins and uplifts: Rocky Mountain Association of Geologists, p. 315-338.

Cook, D.G., 1988, Balancing basement-cored folds of the Rocky Mountain foreland, *in* Schmidt, C.J., and Perry, W.J., Jr., editors, Interaction of the Rocky Mountain foreland and the Cordilleran thrust belt: Geological Society of America Memoir 171, p. 53-64.

Erslev, E.A., 1986, Basement balancing of Rocky Mountain foreland uplifts: Geology, v. 14, p. 259-262.

Erslev, E.A., 1988, Normalized center-to-center strain analysis of packed aggregates: Journal of Structural Geology, v. 8, p. 201-209.

Johnson, G.D., 1934, Geology of the mountain uplift transected by the Shoshone Canyon, Wyoming: Journal of Geology, v. 42, p. 809-838.

Lowell, J.D., 1983, Foreland deformation, *in* Lowell, J.D., editor, Conference on Rocky Mountain foreland basins and uplifts: Rocky Mountain Association of Geologists, p. 1-8.

Narr, W., and Suppe, J., 1989, Kinematics of low-temperature, basement-involved compressive structures: Geological Society of America Abstracts with Programs, v. 21, p. A137.

Pierce, W.G. , 1966, Geologic map of the Cody Quadrangle, Park County, Wyoming: U.S. Geological Survey Geologic Quadrangle Map GQ-542, scale 1:64,500.

Pierce, W.G., 1970, Geologic map of the Devils Tooth Quadrangle, Park County, Wyoming: U.S. Geological Survey Geologic Quadrangle Map GQ-817, scale 1:64,500.

Pierce, W.G., and Nelson, W.H., 1968, Geologic map of the Pat O'Hara Mountain Quadrangle: U.S. Geological Survey Geologic Quadrangle Map GQ-755, scale 1:64,500.

Schmidt, C.J., and Garihan, J.M., 1983, Laramide tectonic development of the Rocky Mountain foreland of southwestern Montana, *in* Lowell, J.D. editor, Conference on Rocky Mountain foreland basins and uplifts: Rocky Mountain Association of Geologists, p. 271-294.

Stearns, D.W., 1971, Mechanisms of drape folding in the Wyoming province: Wyoming Geological Association 23rd Annual Field Conference Guidebook, p. 125-143.

Stearns, D.W., 1978, Faulting and forced folding in the Rocky Mountain foreland, in Matthews, V., II, editor, Laramide folding associated with basement block faulting in the western United States: Geological Society of America Memoir 151, p. 1-37.

Stone, D.S., 1984, The Rattlesnake Mountain, Wyoming, debate: a review and critique of models: Mountain Geologist, v. 22, p. 37-46.

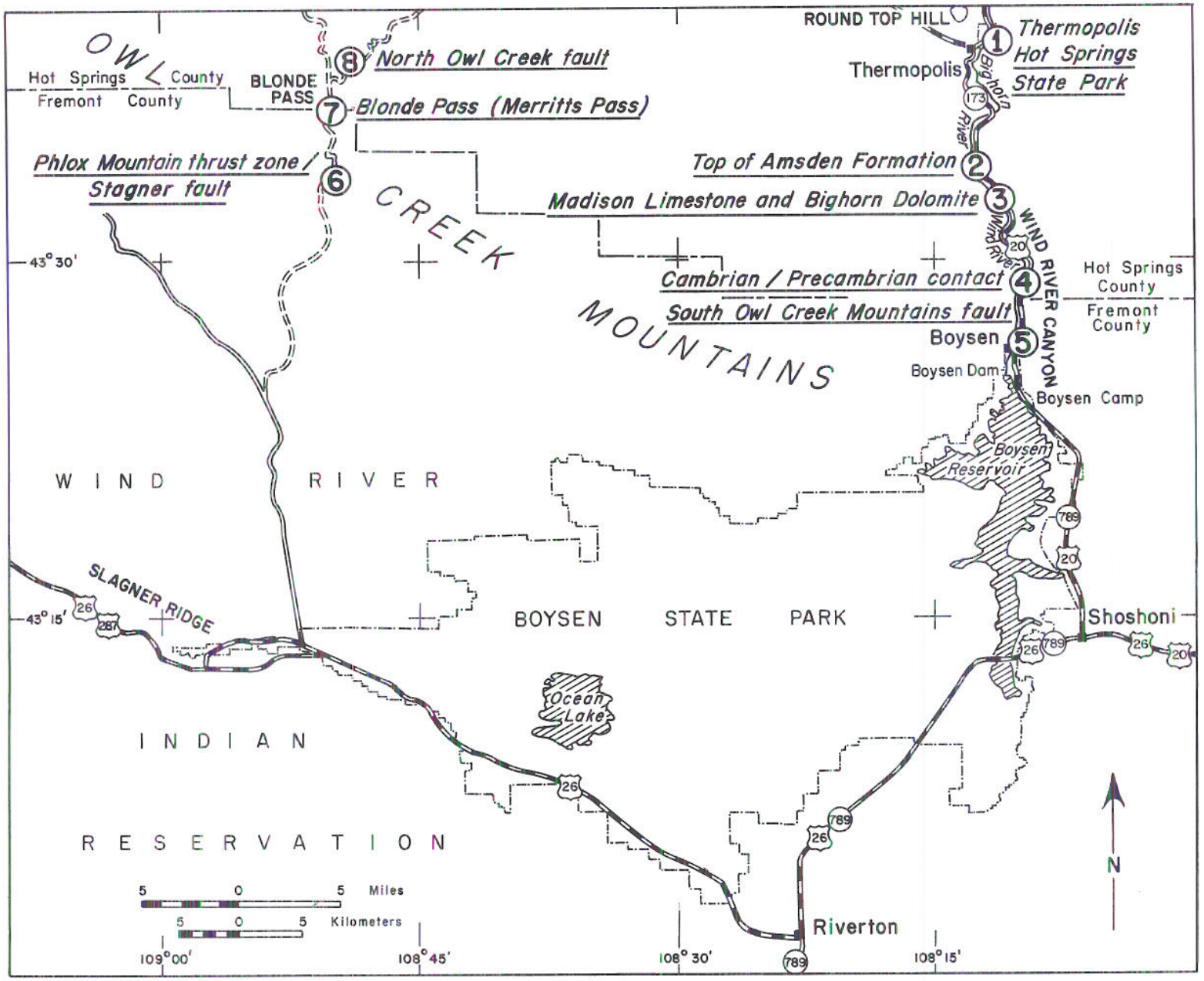

Figure 1. Trip route and stop locations, field trip no. 7, part 2.

Field trip no. 7, part 2

STRATIGRAPHIC AND STRUCTURAL OVERVIEW OF THE OWL CREEK MOUNTAINS AREA, WYOMING

Earnest D. Paylor, II[1] and Harold R. Lang

Jet Propulsion Laboratory
4800 Oak Grove Drive
Pasadena, California 91109

[1]also with Department of Earth and Space Sciences
University of California, Los Angeles
Los Angeles, California 90024

Trip summary (see Figure 1)

Stop 1. Thermopolis; Hot Springs State Park
Stop 2. Top of Amsden Formation in Wind River Canyon
Stop 3. Madison Limestone and Bighorn Dolomite in Wind River Canyon
Stop 4. Cambrian/Precambrian contact in Wind River Canyon
Stop 5. Boysen State Park, South Owl Creek Mountains fault
Stop 6. Intersection of Phlox Mountain thrust zone and Stagner fault
Stop 7. Blonde Pass (Merritts Pass)
Stop 8. North Owl Creek fault

Introduction

This guide provides a stratigraphic and structural overview of the Owl Creek Mountains and adjacent Wind River and Bighorn basins. Stops on a one-day field trip are described. The trip is separated into two segments: (1) an examination of the Paleozoic sequence and basement contact exposed in the Wind River Canyon and (2) an examination of Late Cretaceous through Eocene structures related to contractional and strike-slip faulting in the western Owl Creek Mountains.

This guide benefited substantially from information contained in previously published guides including: Wyoming Geological Association (1964), Sundell (1985), Maughn (1987), and Love (1989). Relevant geologic maps that cover the area include those by Tourtelot and Thompson (1948), Masursky (1952), Troyer and Keefer (1955), Murphy and others (1956), Keefer and Troyer (1964), McGrevy and others (1969), Keefer (1970), Maughn (1972), and Love and Christiansen (1985).

Keefer (1965a, 1965b), Thomas (1965), and Love (1960, 1970) described the stratigraphic and structural evolution of the region. Mills (1956), Gower (1978), and Love and others (1987) tabulated applicable stratigraphic nomenclature. Revisions of Eocene nomenclature and chronology were provided by Stucky (1984a, 1984b), Korth (1982), and Krishtalka and others (1987). Milek (1986) documented local history, folklore, and culture.

Acknowledgments

This paper includes results of one phase of research conducted as part of the Multispectral Analysis of Sedimentary Basins Project, carried out at the Jet Propulsion Laboratory, California Institute of Technology, under contract with the National Aeronautics

and Space Administration. It also includes preliminary results from Ph.D. research being conducted by the senior author at the University of California, Los Angeles. The field trip and research was made possible by the generosity of the Joint Shoshone and Arapaho Business Council providing access to the Wind River Indian Reservation; specifically, we thank John Washakie, Burton Hutchinson, and David Ferris for their time and assistance.

Critical reviews by J.D. Love and J.A. Lillegraven improved the text and are greatly appreciated.

Descriptive summary

Location and access

The Owl Creek Mountains (**Figure 2**), an east-west trending uplift, forms the topographic and structural boundary between the Wind River and Bighorn basins. The range can be traced west from the juncture of the southern Bighorn Mountains/Casper arch, near Badwater (T.39N, R.88W), to the southern end of the Washakie Range and the southern end of the Absaroka Volcanic Plateau (approximately T.7N, R.3W), north of Burris. Highway 20 from Thermopolis to Shoshoni traverses the central portion of the range through the spectacular Wind River Canyon, cut by superposition of the north flowing Wind River through the range. The western portion of the range is traversed on the Wind River Indian Reservation by a dirt road (Blonde Pass/ Merritts Pass Road) that runs from approximately Bargee Reservoir on the south to Anchor Reservoir on the north. Access to the reservation is allowed only by special permit from the Joint Shoshone and Arapaho Business Council. Numerous other dirt roads (shown on the Thermopolis, Nowater Creek, and Arminto 1:100,000 U.S. Geological Survey topographic maps) provide additional access to the range. The road from Blonde Pass north is rough and rocky and suitable only for 4-wheel drive vehicles.

Geologic significance of the region

Wind River Canyon is one of the best localities for viewing the Paleozoic miogeoclinal sequence of western North America. Geological features include excellent exposures of Precambrian through Mesozoic rocks and structures related to Laramide-style (basement-involved contractional deformation from Late Cretaceous through Eocene) and post-Laramide tectonics. Cenozoic rocks are also exposed at the south end of the canyon and in the adjacent Wind River Basin. In addition, the Owl Creek Mountains and adjacent areas host a variety of natural resources, including mineral deposits of economic importance (copper, gold, iron, tungsten, beryllium, lithium, and uranium) (Hausel and others, 1985), geothermal fluids (e.g., Hinckley and others, 1982), and oil and gas (Wyoming Geological Association, 1989).

Stratigraphic setting

The stratigraphic succession exposed in the Owl Creek Mountains area is summarized in **Figure 3**. The oldest rocks are an Archean metavolcanic sequence consisting of dark gray to green hornblende amphibolites, gneisses, and quartz-biotite schists (Condie, 1967). The protoliths are thought to have been largely volcanogenic supracrustal rocks including tholeiitic basalts, basaltic andesites, dacites, and possibly minor fine-grained sedimentary rocks. They yield U-Pb zircon ages of approximately 2,900 Ma, and Rb-Sr ages of approximately 2,700 Ma, which is interpreted to be the age of metamorphism (Condie, 1967; Mueller and others, 1985). These rocks are intruded by potassic granites and pegmatites (approximately 2,700 Ma), and by mafic and felsic dikes (approximately 2,100 Ma) (Hausel and others, 1985; Blundell, 1988).

During most of the Paleozoic and Mesozoic, central Wyoming was part of a vast stable continental shelf located east of the Cordilleran geocline. During this time, the shelf experienced cycles of regional upward and downward movements but the principal geologic activity was subsidence and accumulation of shelf sediments (**Figure 2**) in tropical, shallow seas (e.g., Keefer, 1965a; Thomas, 1965).

The base of the Cambrian System is composed of arkosic to micaceous sandstones and conglomerates of the Flathead Sandstone. The Gros Ventre Formation, conformably overlying the Flathead, consists of greenish gray, micaceous and glauconitic mudstones and shales, which are often poorly exposed. The Gros Ventre grades into the Gallatin Limestone, which contains calcareous claystones and thin-bedded cliff-forming limestones that are typically oolitic and contain flat-pebble conglomerates near the top.

(FROM LOVE AND CHRISTIANSEN, 1985)

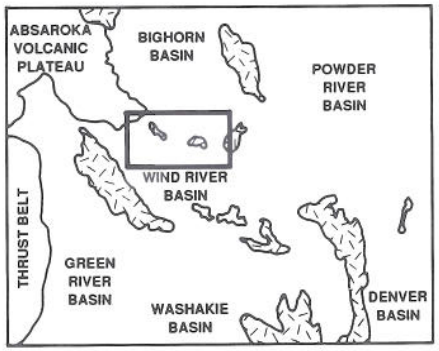

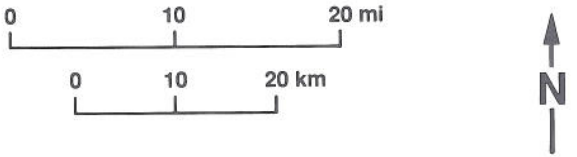

Figure 2. Map showing the location of the Owl Creek Mountains in central Wyoming. Geology is from the *Geologic map of Wyoming* (Love and Christiansen, 1985). Numbers indicate locations of field trip stops.

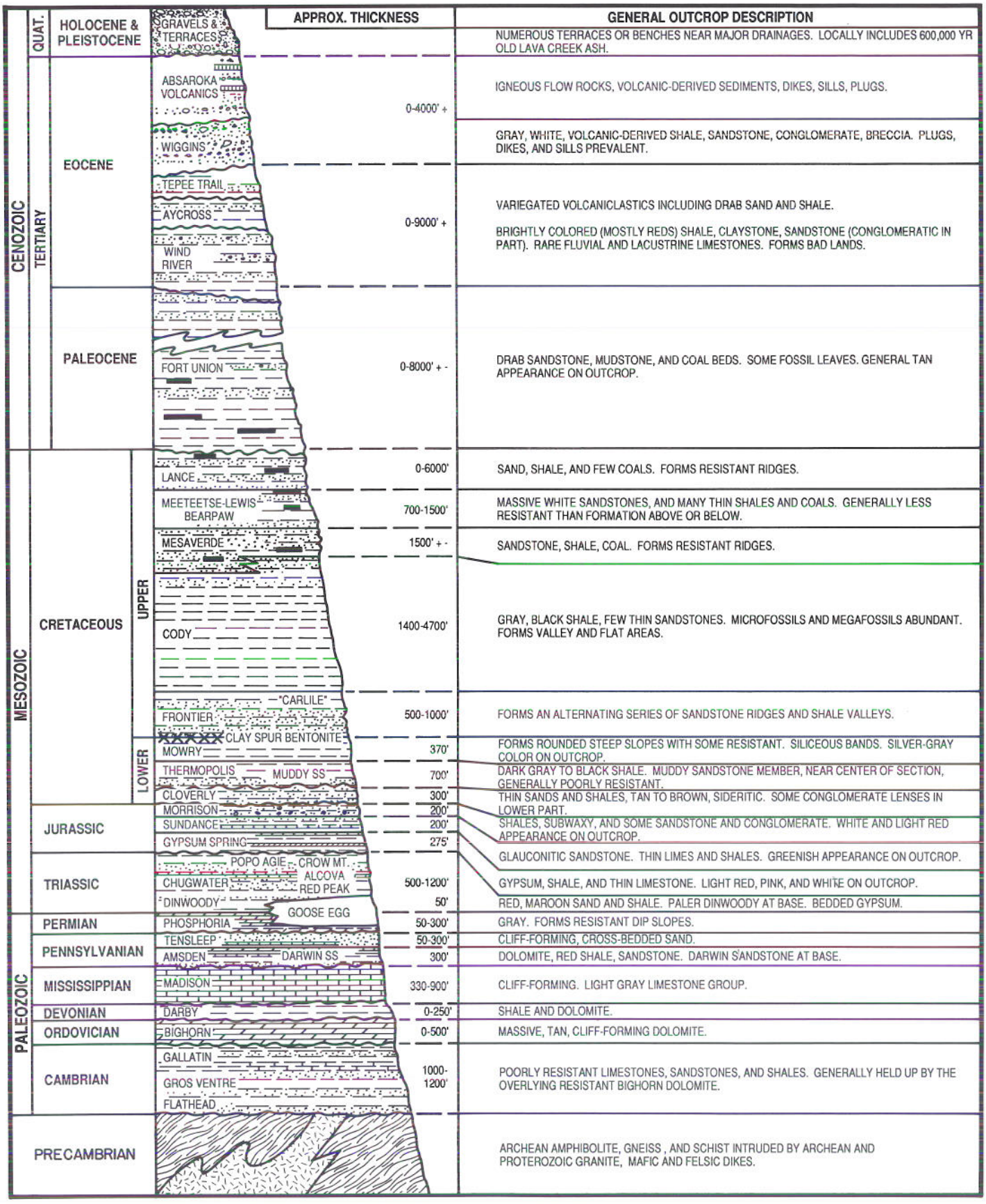

Figure 3. Generalized stratigraphic column for the Owl Creek Mountains area, central Wyoming (modified from Sundell, 1985, p. 81).

The Ordovician and Mississippian systems are represented by the cliff-forming Bighorn Dolomite and Madison Limestone. Only present locally, shales of the Devonian Darby Formation form a very subtle ledge in the carbonate cliff in the Wind River Canyon, and thicken to the west and north. The final phases of miogeoclinal sedimentation are recorded by basal red shales of the Pennsylvanian and Mississippian Amsden Formation, which grade upward into carbonates and eolian sandstones of the Tensleep Sandstone.

Permian and Triassic strata include thin-bedded, fossiliferous dolostones of the Phosphoria Formation, and bedded gypsum and mudstones of the Dinwoody Formation and the partially-equivalent, more gypsiferous, Goose Egg Formation. These strata interfinger with red mudstones of the basal member of the Chugwater Formation, the Red Peak. The overlying, thin (1 to 20 feet thick) algal limestone of the Alcova Member is a prominent ledge-forming marker bed that caps Red Peak cliffs throughout much of central Wyoming. Triassic sedimentation was completed with deposition of fluvial red sandstones, siltstones, shales, and mudstones of the highest Chugwater members, the Crow Mountain Sandstone and Popo Agie.

Jurassic strata, deposited on the margin of the Sundance Sea, include bedded gypsum of the Gypsum Spring Formation; green, shallow-marine coquinoid limestones, oolitic beach sandstones, and eolian sandstones of the Sundance Formation; and terrestrial, dinosaur-fossil-bearing variegated sandstones, mudstones, and minor carbonates of the Morrison Formation.

Cretaceous strata record cyclical marine invasions of the North American Western Interior (Kauffman, 1969). Siliciclastic strata deposited on the western margin of epeiric seaways include beach, estuarine, deltaic, and continental sandstones (Cloverly, Frontier, Mesaverde, Meeteetse, and Lance formations and Muddy Sandstone Member of the Thermopolis Shale) and marine/paludal shales (Thermopolis, Mowry, Cody, Lewis) (Hogle and Jones, in press). The source terrain was dominantly the rising Sevier highlands to the west and early Laramide-style uplifts within the foreland region.

Marine sedimentation ceased before Tertiary time. Foreland deformation (Late Cretaceous through Eocene) created uplifts that segregated central Wyoming into smaller intermontane basins. During and after maximum deformation, basins were largely filled with fluvial clastic debris shed from foreland uplifts and volcaniclastic material originating from volcanic centers to the west (e.g., Keefer, 1965b; Seeland, 1978). This phase of sedimentation is recorded by rocks of the Fort Union Formation through the Absaroka Volcanic Supergroup (**Figure 3**). Lacustrine deposits intertongue locally with these clastic deposits. Development of the present physiographic configuration began in the late Pliocene following regional upwarping of several thousand feet (Love, 1970). Quaternary-Holocene re-excavation of the basins is expressed by a complex sequence of stream terraces in basin interiors (Morris and others, 1959; Richmond, 1976).

Structural setting

Principal structural elements in the Owl Creek Mountains record Laramide-style and post-Laramide-style tectonics. In general, the range is an east-west trending, asymmetric antiform cored by Precambrian basement rocks. The geometry of the range is typical of many Laramide-style Wyoming foreland uplifts, as summarized by Brown (1988). However, the western portion of the range, west of Mexican Pass (T.6N, R.4E) (**Figure 2**), differs dramatically in style, particularly the geometry and kinematics of faulting. Based on unconformable stratigraphic relations, deformation may have begun in Late Cretaceous, but major uplift and folding of the Owl Creek Mountains probably did not occur until Paleocene to Eocene time, as evidenced by boulder clasts in syntectonic conglomerates in the Indian Meadows and equivalent formations (e.g., Keefer, 1965a; 1965b).

Precambrian basement rocks of the eastern Owl Creek Mountains have been uplifted and now override the northern edge of the Wind River Basin along the east-striking South Owl Creek Mountains fault (Keefer, 1970), creating approximately 30,000 feet of structural relief on the basement surface (**Figure 4**). Unfortunately, the fault is not exposed at the surface because it is covered by Tertiary deposits. Kinematic data are therefore unavailable for the fault plane, resulting in assumption of transport direction perpendicular to the range-bounding South Owl Creek Mountains fault (e.g., Gries, 1983; Kanter and others, 1981). Based on seismic reflection data, the fault is interpreted to dip gently to the north with approximately 10 miles of basement overhang (e.g., Gries, 1983), and to merge with the northeast dipping, low-angle Casper arch thrust (e.g., Skeen and Ray, 1983). The tip of the thrust plate has been penetrated by boreholes at Madden Deep field near its eastern end, and by the CIG exploration well approximately 4 miles southeast of Boysen Dam. Near the surface, the southern tip of the thrust plate is a complex fault zone resulting from basinward isostatic collapse of the uplifted hanging wall (e.g., Sales, 1983). In this collapse zone, east striking normal faults displace and rotate Paleozoic

and Mesozoic rocks thousands of feet toward the Wind River Basin (Fanshawe, 1939; Wise, 1963).

Unlike the eastern portion of the range, the western Owl Creek Mountains are composed of three northwest trending, west-southwest vergent, basement-cored, en echelon, anticlinal uplifts: Phlox Mountain, Sheep Ridge, and Jenkins Mountain (**Figure 5**). Well-exposed, northeast dipping, low-angle fault zones bound the steep to overturned southwest limbs of the uplifts.

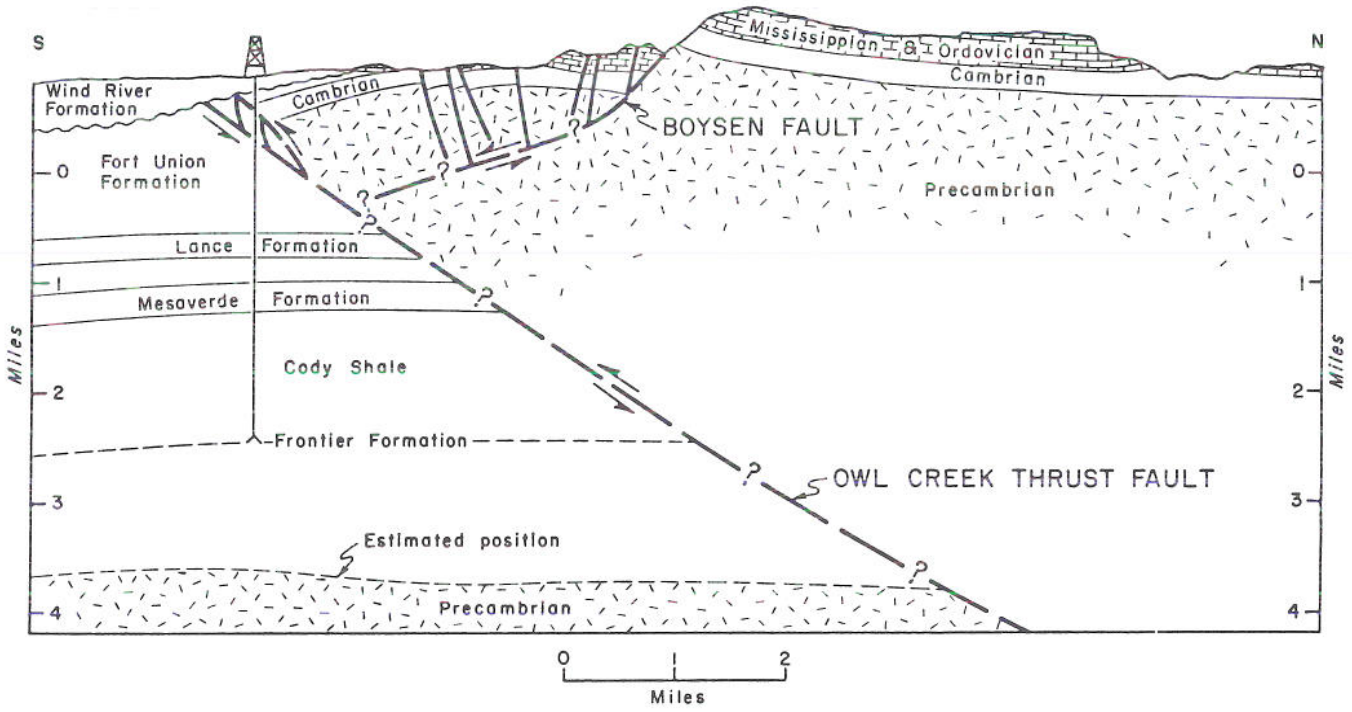

Figure 4. Generalized north-south structural cross section of the Owl Creek Mountains antiform near Wind River Canyon (after Blackstone, 1988).

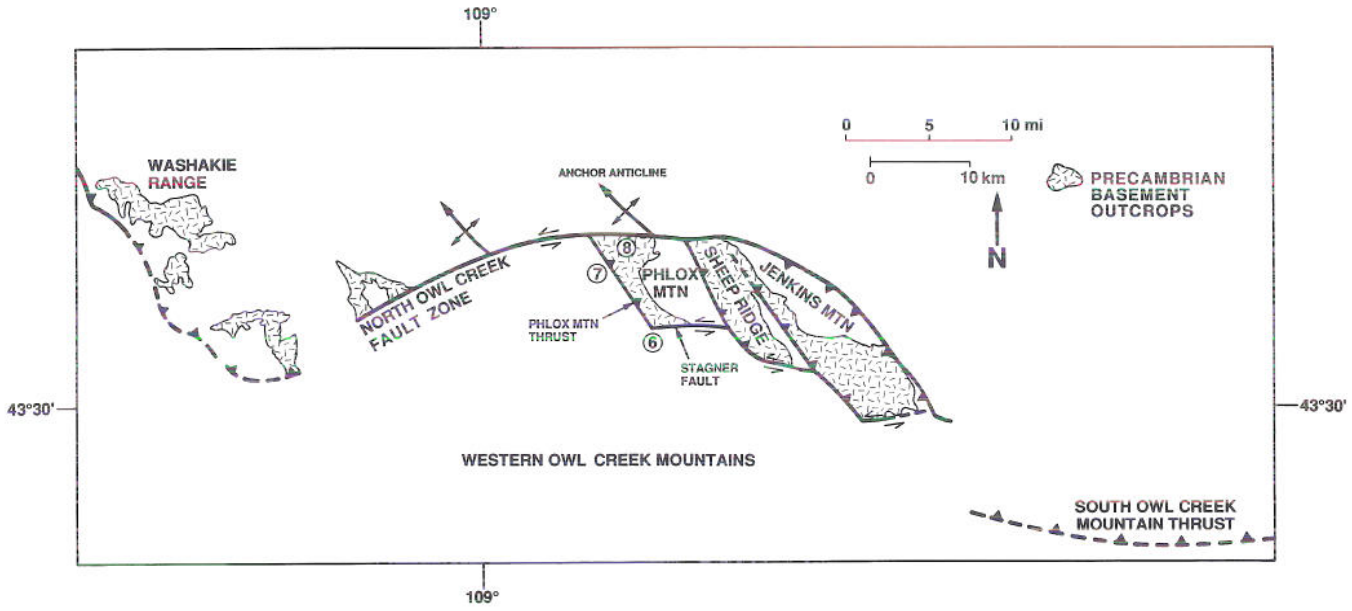

Figure 5. Location map of western Owl Creek Mountains, showing major faults bounding uplifted Precambrian basement rocks of Phlox Mountain, Sheep Ridge, and Jenkins Mountain anticlines. Field trip Stops 6, 7, and 8 are located.

These fault zones are terminated by well-exposed, east-west striking, high-angle faults that form the north and south boundaries of the basement uplifts. Stratigraphic separation along the low-angle fault zones appears to decrease toward the northwest, suggesting a clockwise rotation of hanging walls during faulting (Blundell, 1988; Paylor, 1989). Mesoscopic-scale kinematic indicators yield an overall west-southwest transport direction on both high-angle and low-angle fault zones (Paylor, 1989; Paylor, in press). Approximately 6.5 miles of west-southwest crustal shortening is attributable to the three uplifts. Unfortunately, no subsurface data are available for this portion of the range.

Road log and stop descriptions

Thermopolis to Diversion Dam Road

0.0 miles Holiday Inn parking lot; Thermopolis, Wyoming; turn right out of the parking lot.

0.1 Turn left at stop sign toward Hot Springs State Park.

Stop 1. Thermopolis; Hot Springs State Park

0.5 Park in the parking area and walk to the main Hot Springs pool. The purpose of this stop is to discuss and examine the Thermopolis hydrothermal system and the associated Thermopolis anticline. The system is on the thrust-faulted, steep southern limb of the Thermopolis anticline, southern Bighorn Basin. Near the main pool, a sign describes the geology, chemistry, and history of the park. Walk to the rim pools and overview of the Bighorn River. Extensive travertine deposits are associated with the modern pools. From the overlook of the adjacent Bighorn River, older travertine deposits can be seen unconformably capping the Red Peak Member of the Chugwater Formation on Round Top Hill and T-Hill, as much as 600 feet above the modern river level. According to Hinckley and others (1982) the system produces nearly 3,000 gallons/minute of 130°F (54°C) water from Paleozoic aquifers (Phosphoria, Tensleep, Madison, and Flathead formations). Water flows under artesian pressure from the Owl Creek Mountains recharge area to the Thermopolis anticline through an intervening syncline, where it is probably heated by conduction in the deepest parts of the syncline. Faults on the southern flank of Thermopolis anticline act as conduits to return the heated water to the surface at the park. Some residents in the immediate vicinity benefit from the resource by using the heated water for residential space heating.

Leave the park the same way you entered, proceeding past the Holiday Inn.

1.1 Turn left at the intersection onto Park Street (Highway 20-789). Straight ahead in the foreground is Round Top Hill and T Hill, capped by old travertine deposits that unconformably overlie the Triassic Red Peak Member of the Chugwater Formation.

1.7 Intersection of Highway 20-789 and Highway 120; continue straight toward Wind River Canyon and Shoshoni.

Stops 2 through 4 provide a stratigraphic sequence in Wind River Canyon. This leg of the field trip examines the Cretaceous through Precambrian sequence exposed in the southern Bighorn Basin and Wind River Canyon (**Figure 3**). Maughn's (1972) geologic map and accompanying descriptive materials are an important source of stratigraphic information for the canyon. Photographs showing some of the rocks exposed in the canyon are included in **Figure 6**. The drive from Stop 1 to Stop 2 traverses the stratigraphic sequence from the Thermopolis Shale to the Tensleep Sandstone. The Phosphoria dip slope (treeless), forming the gentle north dipping limb of the east Owl Creek Mountains antiform, is seen south of the road (**Figure 6a**). The Phosphoria is exposed at the entrance of Wind River Canyon. The road proceeds down section to Stop 2, where the Tensleep (**Figure 6b**) and Amsden formations will be examined.

Stop 3 examines the Madison Limestone (**Figure 6c**) and Bighorn Dolomite. The canyon road continues down section through the Gallatin and Gros Ventre formations to Stop 4, at the Cambrian Flathead Sandstone contact with the Precambrian crystalline basement complex (**Figure 6d**) that forms the core of the Owl Creek Mountains. The contact is an unconformity, below which are several feet of weathered granitic basement.

2.7 Excellent view of the Owl Creek Mountains dip slope and incised Wind River Canyon, caused by superposition of the Bighorn River on the mountain range (**Figure 6a**).

3.8 Intersection with Buffalo Creek Highway to the east. View east across the river of lower Cretaceous

a.

b.

Figure 6. Photographs of rock units exposed at Stops 2, 3, and 4 in the Wind River Canyon. (a) View south at mile 5.1, where the gentle Phosphoria Formation dip slope, cut by Wind River Canyon, is clearly visible. The light colored band on the lower west (right) canyon wall is the Tensleep Sandstone. (b) Exposure of large-scale, eolian crossbedded orthoquartzites of the Tensleep Sandstone on the east side of Wind River Canyon near mile 6.9.

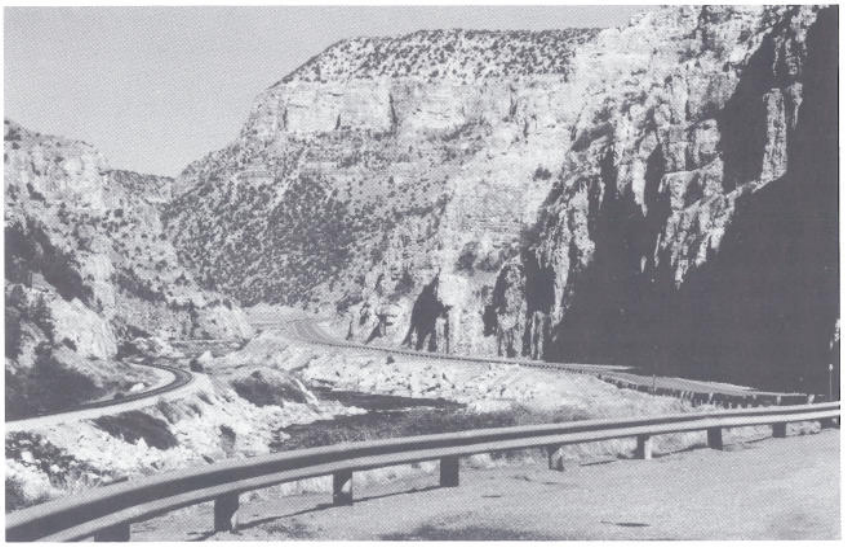

c.

d.

Figure 6, continued. (c) View south near mile 10.2 (Stop 3) showing dolostones of the Madison Limestone in the foreground. In the distance is the cliff-forming Tensleep Sandstone, capped by the Phosphoria Formation. Less resistant rocks below the Tensleep Sandstone are in the Amsden Formation. (d) Exposure of Cambrian Flathead Sandstone and Archean granite basement at Stop 4. Clearly visible is the weathered granite regolith, an unconformity exhibiting considerable relief, below well-bedded, marine, arkosic sandstone and pebble conglomerate.

Cloverly Sandstone (pine-covered rim on skyline). Below the Cloverly is the gastrolith-bearing Upper Jurassic Morrison Formation (poorly exposed varicolored shale). Below the Morrison, is the Upper Jurassic Sundance Formation, which is mostly green glauconitic sandstones with some thin fossiliferous limestones (belemnoids, oysters, and pelecypods) and oolitic sandstones. Below the Sundance are pink and white banded beds of the middle Jurassic Gypsum Spring Formation. The dark red to purplish shale below the Gypsum Spring Formation is the Red Peak Member of the Chugwater Formation.

5.1 Road cut exposing the Red Peak Member of the Chugwater Formation. Buffalo Creek drainage is to the east. The treeless Phosphoria dip slope forming the north flank of the Owl Creeks Mountains is visible to the south (**Figure 6a**).

6.4 Top of the Triassic Dinwoody Formation. The Dinwoody Formation is mostly gray-green shales and dolomitic shales and is approximately 60 feet thick at this location. Gypsum beds, generally found at the top of the unit, thicken substantially east of Wind River Canyon.

6.5 Top of the Permian Phosphoria Formation. The Phosphoria Formation is mostly dolostone and limestone and is approximately 220 feet thick in this area. Phosphate nodules are common locally. Brachiopods and bryozoa are common fossils here.

6.7 Roadside table. A glassed-in sign on the west side of the road, showing a stratigraphic section and a geologic cross section of the Owl Creek Mountains, provides a good explanation of the geology of the Wind River Canyon. The name of the river changes from Bighorn River to Wind River (south of this location).

6.9 Top of the Pennsylvanian Tensleep Sandstone (**Figure 6b**), dipping 7°N. The top is better exposed on the west side of the river. Here, the Tensleep is mostly orthoquartzite. There are a few dolostone beds in the upper Tensleep and more at the base. The Tensleep is approximately 375 feet thick in the Wind River Canyon, and is a major oil producing formation in the region.

Stop 2. Top of Pennsylvanian/Mississippian Amsden Formation

7.7 The top of the Amsden Formation is picked at the first occurrence of green shale stringers in the dolostones. Buff and rusty weathering sandstone are exposed on the west side of the canyon.

8.3 Top of the Mississippian Madison Limestone. Here, the Madison Limestone is approximately 475 feet thick. Most of the basal 300 feet is dolostone and the remaining 175 feet is largely limestone. The top of the Madison is a vugular and cavernous surface due to karst topography, which developed after deposition. Brachiopods and bryozoa are common. The Madison is an important hydrocarbon reservoir in the Bighorn and Wind River basins.

9.8 Top of the Ordovician Bighorn Dolomite. The Bighorn is approximately 140 feet thick in the Wind River Canyon. Locally, between the Madison and Bighorn, there is a three- or four-foot-thick unit, the Devonian Darby Formation, which appears to be channel fill. It is composed of yellow, slightly dolomitic mudstone and green shale.

Stop 3. Madison Limestone (Figure 6c) and Bighorn Dolomite

10.2 Turn right at the memorial for William Barrow Pugh. Examine the Madison Limestone and Bighorn Dolomite contact, which is difficult to locate here.

10.8 Top of the Cambrian Gallatin Formation. The abrupt decrease in slope at the base of the Bighorn Dolomite marks the approximate top of the Gallatin Formation. The Gallatin Formation is about 450 feet thick. It is composed of gray and greenish shales at the base, a middle cliff-forming limestone member (about 80 feet thick) overlain by greenish shales (largely covered), and an upper varicolored limestone characterized by flat-pebble limestone conglomerate.

13.8 Approximate top of the Cambrian Gros Ventre Formation. The Gros Ventre Formation is approximately 400 feet thick and consists mostly of gray to brown siltstones and shales, and red to brown sandstones, part of which are turbidites. Exposures of the Gros Ventre are characteristically poor and they often exhibit a hummocky topography due to slumping.

16.1 Top of the Cambrian Flathead Sandstone. The Flathead is about 250 feet thick and is composed mostly of arkosic sandstones and quartzite. Crossbedding, worm burrows, and ripple marks can be found in the outcrop.

Stop 4. Cambrian/Precambrian contact (Figure 6d)

16.4 Turn right at the intersection and park. Cross the highway to examine the Cambrian Flathead Sand-

stone and the top of the Precambrian basement complex.

16.6 Top of the Precambrian basement. The weathered zone on top of the basement can be seen (**Figure 6d**). The basement lithology here is granitic.

16.8 Precambrian metamorphic complex. Lithologies exposed here include dark colored phyllite schist and gneiss intruded by pink, white, and gray granite and pegmatites. Metamorphic foliations and cleavages dip gently to the south here but steepen near the range front (i.e., near the complexly normal faulted toe of the Owl Creek thrust).

18.0 Three tunnels cut into the basement complex. Note the steep south dips of the metamorphic foliations and cleavages.

18.2 Here, the road crosses the Boysen normal fault, which exhibits over 1,500 feet of displacement. The fault plane dips 65°S and juxtaposes upper Cambrian shales against the Precambrian on the north side of the fault. The south block is a graben. This is the north margin of the Wind River Basin.

Stop 5. Boysen State Park

18.9 Turn right into the Upper Wind River Canyon Campground of Boysen State Park and park. The purpose of this stop is to examine structures associated with the hanging wall of the South Owl Creek Mountains fault (**Figure 4**). Detailed mapping of the area is found in Fanshawe (1939), Tourtelot and Thompson (1948), and Wise (1963). Of particular interest here is normal faulting, interpreted to result from collapse of the range front. Two types of normal faults are exposed: (1) east-west striking, high-angle faults that are generally down-to-the-south and (2) low-angle faults, probably gravity-driven detachments. The high-angle faults exhibit up to 2,500 feet of structural relief and are well exposed from approximately 2 miles north of Boysen Dam (at the Boysen fault) to the north edge of the Wind River Basin. This zone is typified by "a seeming confusion of normal faults, small horsts, graben, and tilted blocks" involving Paleozoic strata (Wise, 1963,p. 586). Low-angle faults affect the Madison Limestone and Bighorn Dolomite in upper plates that detached from the uplifted mountain front and slid southward over the northern edge of the Wind River Basin.

Turn right leaving the parking lot and proceed toward Shoshoni.

20.2 Cambrian strata dip south across from access road to Boysen Dam.

20.4 Boysen Dam.

21.3 Road to Bureau of Reclamation Boysen Camp. On west side of road, Chugwater redbeds overlain by Sundance sandstone dip southwest approximately 55°.

22.0 Variegated Eocene Wind River Formation can be seen lapping unconformably onto Phosphoria and Chugwater strata on the north side of the road.

24.1 Large resistant, yellow/orange sand body on the right side of the road is a paleodrainage channel fill (thalweg) in the Eocene Wind River Formation.

29.2 Thalweg on the right side of the road.

34.6 Junction of Highways 20-789 and 26-789 at Shoshoni; turn right onto Highway 26-789 to Riverton.

56.6 Intersection of Highways 26-789 and 26 in downtown Riverton; turn west (right) on Highway 26 and continue 34 miles to Diversion Dam Road, where the second segment of the field trip begins. Reset odometer.

Diversion Dam Road to North Owl Creek fault

0.0 Intersection of Highway 26-287 and Diversion Dam Road; turn north onto Diversion Dam Road. In the distance to the south, the Tertiary Fort Union Formation rests with angular discordance on the Cretaceous Cody Shale. Notice also that the Cody Shale is more tightly folded than the Fort Union, suggesting contemporaneous or episodic deformation before and after deposition of the Fort Union strata.

1.3 Intersection of Diversion Dam Road and Maverick Springs Road; turn north onto Maverick Springs Road. The road is on Eocene Wind River Formation and traverses Mexican Draw.

12.8 Flat-lying Wind River Formation rests unconformably on the steeply dipping Cretaceous Mesaverde Formation.

14.1 Intersection of Maverick Springs Road and Mail Camp road; turn north onto Mail Camp Road.

15.4 Southeast plunging nose of Maverick Springs Dome is visible on west side of road.

16.7 Northern limb of Little Dome is visible on the east side of the road. Dip slopes of the Mowry Shale are exposed.

19.4 Northeast limb of Maverick Springs Dome is visible on the west side of the road. The Frontier Formation sandstones form cuestas.

21.3 Tightly folded Antelope Ridge can be viewed to the west. Antelope ridge and the anticline immediately to the north of it are accommodation folds caused by volumetric adjustments in the sedimentary sequence. They are in the core of a larger anticline south-southeast of the road (mile 24.6). Because of their tightly folded geometry, these accommodation folds, are probably detached from the lowermost Paleozoic and Precambrian rocks, and probably from the units immediately above (Cretaceous Cody and Mesaverde formations). Folds such as these are common in the southern Bighorn and northwest Wind River basins.

23.9 Intersection; continue straight on the main road.

24.6 Resistant Mesaverde sandstone forming the escarpment on the east side of the road is the northeast limb of an anticline; the Cody Shale is exposed below the Mesaverde.

25.4 Intersection of main road and dirt road; turn north onto a dirt road.

26.4 Bear north onto Mail Camp Road.

Stop 6. Intersection of Phlox Mountain thrust zone and Stagner fault

27.0 Park and walk east approximately 165 feet to the top of a terrace. The purpose of this stop is to discuss and examine complex structural relations associated with the intersection of the low-angle Phlox Mountain thrust zone and the high-angle Stagner fault (**Figure 7**). The low-angle fault zone contains slivers of overturned and brecciated Paleozoic carbonates, bounded by low-angle faults. Orientations of slicken-

Figure 7. Photograph viewing northeast at the location where the Phlox Mountain thrust zone and the Stagner fault merge. Structures and rock units are labelled: Pe = Precambrian rocks; Pz = Paleozoic rocks; Mz = Mesozoic rocks; barbed line = approximate location of Phlox Mountain thrust fault zone; fault with T/A represents Stagner fault (T = motion toward viewer, A = motion away from viewer).

side lineations (**Figure 8**), fault-zone tension gashes, and mesoscopic-scale fold axes indicate that the dominant direction of motion on the low-angle fault zone, top-to-the-WSW, was overprinted by top-to-the-NNW/SSE motion thought to be associated with volumetric adjustments in the fault zone (**Figure 8**). Precambrian basement rocks occur in the hanging wall, and the youngest rock unit in the foot wall is the Permian Phosphoria Formation. Slickenside lineations indicate that motion on the high-angle Stagner fault was left-lateral oblique (**Figure 8**). North of Stagner fault, approximately 1.25 miles of west-southwest shortening is associated with the uplift along the low-angle thrust zone. South of Stagner fault, the amplitude of folding decreases dramatically and shortening is considerably less. Stagner fault is the southern boundary of uplifted basement at Phlox Mountain; the northern boundary is the high-angle North Owl Creek fault as described at Stop 8 (**Figure 7**).

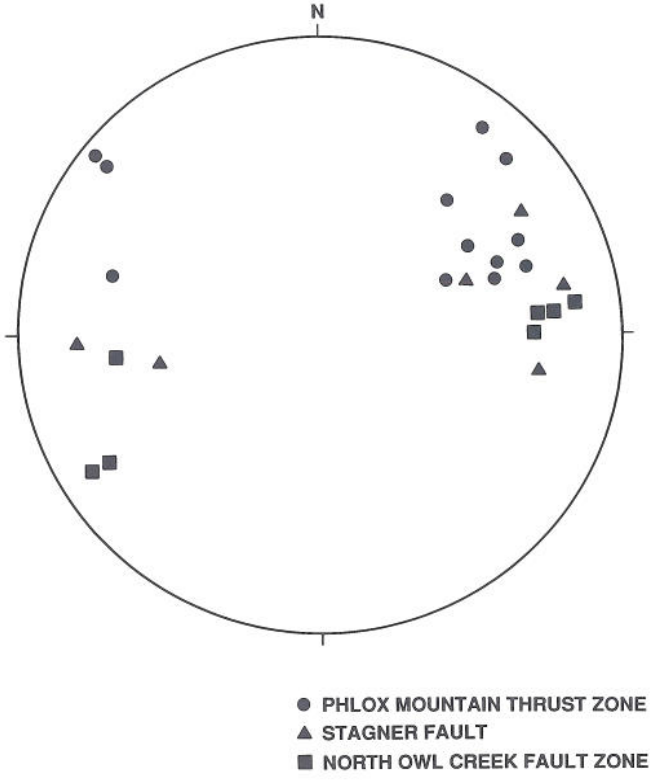

Figure 8. Lower hemisphere equal-area plot of slickenside lineations measured on the Phlox Mountain thrust zone (dots), Stagner fault (triangles), and the North Owl Creek fault zone (squares). All data are kinematically consistent and yield an overall transport direction of west-southwest for this portion of the western Owl Creek Mountains. The three dots in the northwest quadrant represent a second phase of strike-slip motion thought to be associated with volumetric adjustments along the Phlox Mountain thrust zone only.

27.4 Intersection of Mail Camp and Stagner Roads; continue straight on Mail Camp Road.

28.5 Intersection of Mail Camp and Blonde Pass Roads; turn north onto Blonde Pass Road, which is cut on terrace material overlying the Triassic Chugwater Formation.

29.7 Notice the Precambrian basement complex in thrust contact with an overturned sliver of Madison, Amsden, Tensleep, and Phosphoria formations on the east side of the road.

30.8 Contact between the Triassic Dinwoody and Permian Phosphoria formations.

32.1 Excellent view southeast along Phlox Mountain thrust zone.

32.4 Mississippian Madison Limestone outcrop crosses the road.

Stop 7. Blonde Pass (also referred to as Merritts Pass)

33.2 At Blonde Pass, the Cambrian Gallatin Formation is well exposed in the footwall of the Phlox Mountain thrust zone. Note flat-pebble conglomerates in the Gallatin. The thrust zone, only poorly exposed here, places Precambrian granitic rocks on the Cambrian Gros Ventre Formation. Exposures of the Madison Limestone at this location demonstrate the highly fractured nature of rocks near the thrust zone.

Stop 8. North Owl Creek fault.

34.9 Park on the north side of the road. The high-angle North Owl Creek fault zone (**Figure 9**), associated fault breccias and Tertiary volcanic rocks(?) found along the fault, and a northwest-trending Precambrian mylonitic shear zone truncated by the fault are exposed here. The southern Bighorn Basin (from Thermopolis to Anchor anticline) and the southern end of the Absaroka Range can also be viewed. The North Owl Creek fault zone here is a system of interconnecting faults and fault-bound slivers of Paleozoic rocks, bound by two east-west striking main faults (**Figure 10**). To the east, the fault zone dips approximately 80°S, changing to approximately 70°N toward the west. Orientations of slickenside lineations (**Figure 8**) on the main faults and the geometry of folds associated with the faults indicate left-lateral oblique motion (i.e., WSW transport) along the fault zone. As illustrated in **Figure 8**, this transport direction is consistent with

that determined for the Phlox Mountain thrust zone and Stagner fault.

Turn around and drive back down Blonde (Merritts) Pass.

Figure 9. Photograph viewing north-northeast at the North Owl Creek fault zone from Stop 8. Blonde Pass/Merritts Pass road is located by a double line (see also Figure 10). P€ = Precambrian basement rocks. The light colored rock in the fault zone is Madison Limestone.

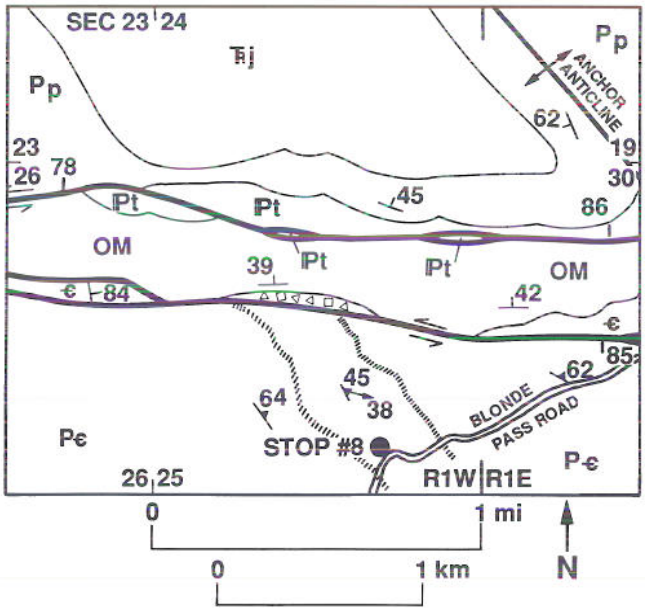

Figure 10. Sketch map of the North Owl Creek fault zone near Stop 8, showing rock units, major faults, brecciated zone, and Precambrian mylonite zone. Blonde Pass (Merritts Pass) road and Stop 8 are also located. P€ = Precambrian, OM = Ordovician-Mississippian, PPt = Tensleep Sandstone, Pp = Phosphoria Formation, TrJ = Triassic-Jurrassic.

References cited

Blackstone, D. L., Jr., 1988, Traveler's guide to the geology of Wyoming: Geological Survey of Wyoming Bulletin 67, 130 p.

Blundell, J. S., 1988, Structural trends of Precambrian rocks, Sheep Ridge anticline, western Owl Creek Mountains, Wyoming: M.S. thesis, University of Wyoming, Laramie, 81 p.

Brown, W. G., 1988, Deformation styles of Laramide uplifts in the Wyoming foreland, *in*, Schmidt, C. J., and Perry, W. J., editors, Interactions of the Rocky Mountain foreland and the Cordilleran thrust belt: Geological Society of America Memoir 171, p. 1-26.

Condie, K. C., 1967, Petrologic reconnaissance of the Precambrian rocks in the Wind River Canyon, central Owl Creek Mountains, Wyoming: University of Wyoming Contributions to Geology, v. 6, p. 123-129.

Fanshawe J. R., 1939, Structural geology of Wind River Canyon area, Wyoming: American Association of Petroleum Geologists Bulletin, v. 23, p. 1439-1492.

Gower, M. A., 1978, Catalogue of Paleozoic, Mesozoic, and Cenozoic rock names for the Wind River Basin, *in* Boyd, R. G., editor, Resources of the Wind River Basin: Wyoming Geological Association 30th Annual Field Conference Guidebook, p. 39-45.

Gries, R. R., 1983, North south compression of Rocky Mountain foreland structures, *in*, Lowell, J. D., editor, Rocky Mountain foreland basins and uplifts: Rocky Mountain Association of Geologists, p. 9-32.

Hausel, W. D., Graff, P. J., and Albert, K. J., 1985, Economic geology of the Copper Mountain supracrustal belt, Owl Creek Mountains, Fremont County, Wyoming: Geological Survey of Wyoming Report of Investigations 28, 33 p.

Hinckley, B. S., Heasler, H. P., and King, J. K., 1982, The Thermopolis hydrothermal system, with an analysis of Hot Springs State Park: Geological Survey of Wyoming Preliminary Report 20, 42 p.

Hogle, D. G., and Jones, R. W., in press, The Wind River basin: subsurface and beyond: The Mountain Geologist.

Kanter, L. R., Dyer, R., and Dohmen, T. E., 1981, Laramide crustal shortening in the northern Wyoming Province: University of Wyoming Contributions to Geology, v. 19, p. 135-142.

Kauffman, E. G., 1969, Cretaceous marine cycles of the Western Interior: The Mountain Geologist, v. 6, p. 227-245.

Keefer, W. R., 1965a, Geologic history of the Wind River Basin: American Association of Petroleum Geologists Bulletin, v. 49, p. 1878-1892.

Keefer, W. R., 1965b, Stratigraphy and geologic history of the uppermost Cretaceous, Paleocene, and Eocene rocks in the Wind River basin, Wyoming: U.S. Geological Survey Professional Paper 495-A, 77 p.

Keefer, W. R., 1970, Structural geology of the Wind River Basin, Wyoming: U.S. Geological Survey Professional Paper 495-D, 60 p.

Keefer, W. R., and Troyer, M. C., 1964, Geology of the Shotgun Butte area, Fremont County, Wyoming: U.S. Geological Survey Bulletin 1157, 123 p., 3 plates.

Korth, W. R., 1982, Revision of the Wind River faunas, early Eocene of central Wyoming, part 2, Geological setting: Carnegie Museum of Natural History, Annals of Carnegie Museum, v. 51, p. 57-78.

Krishtalka, L., West, R. M., Black, C.C., Dawson, M. R., Flynn, J. J., Turnbull, W. D., Stucky, R. K., McKenna, M. C., Bown, T. M., Golz, D. J., Lillegraven, J. A., 1987, Eocene (Wasatchian through Duchesnean) biochronology of North America, *in*, Woodburne, M. O., editor, Cenozoic biochronology of North America: University of California Press, Berkeley, p. 77-117.

Love, J. D., 1960, Cenozoic sedimentation and crustal movement in Wyoming: American Journal of Science, v. 258 A, p. 204-214.

Love, J. D., 1970, Cenozoic geology of the Granite Mountains area, central Wyoming: U.S. Geological Survey Professional Paper 495-C, 154 p.

Love, J. D., 1989, Yellowstone and Grand Teton National Parks and the Middle Rocky Mountains, *in*,

Sedimentation and tectonics of western North America: 28th International Geological Congress field trip guidebook, American Geophysical Union, T328:1-T328:93.

Love, J. D., and Christiansen, 1985, Geologic map of Wyoming: U. S. Geological Survey, scale 1:500,000.

Love, J. D., Christiansen, A. C., and VerPloeg, A. J., 1987, Proposed stratigraphic nomenclature chart for the state of Wyoming (first draft): Geological Survey of Wyoming, chart.

Masursky, H., 1952, Geology of the western Owl Creek Mountains: Wyoming Geological Association 7th Annual Field Conference Guidebook, 1 plate.

Maughn, E. K., 1972, Geologic map of the Wedding of the Waters Quadrangle, Hot Springs County, Wyoming: U. S. Geological Survey Geologic Quadrangle Map GQ-1042, scale 1:24,000.

Maughn, E. K., 1987, Wind River Canyon, Wyoming, in, Bens, S. S., editor, Geological Society of America Centennial Field Guide: Geological Society of America Rocky Mountain Section, p. 191-196.

McGrevy, L. J., Hodson, W. G., and Rucker, S. J., IV, 1969, Ground water resources of the Wind River Indian Reservation, Wyoming: U.S. Geological Survey Water-Supply Paper 1576-I, 145 p.

Milek, D. B., 1986, Hot Springs: a Wyoming county history: Basin, Wyoming, Saddlebag Books, 346 p.

Mills, N. K., 1956, Subsurface stratigraphy of the pre-Niobrara formations in the Bighorn Basin, Wyoming, *in* Nomenclature Committee, Wyoming Geological Association, Wyoming stratigraphy, subsurface stratigraphy of the pre-Niobrara formations in Wyoming: Wyoming Geological Association, Casper, Wyoming, p. 9-21.

Morris, D. A., Hackett, O. M., Vanlier, K. E., and Moulder, E. A., 1959, Ground water resources of Riverton Irrigation Project area, Wyoming: U.S. Geological Survey Water Supply Paper 1375, 205 p.

Mueller, P. A., Peterman, Z. E., and Granath, J. W., 1985, A bimodal Archean volcanic series, Owl Creek Mountains, Wyoming: Journal of Geology, v. 93, p. 701-712.

Murphy, J.F., Privrasky, N.C., and Morlein, G.A., 1956, Geology of Sheldon-Little Dome area, Fremont County, Wyoming: U.S. Geological Survey Oil and Gas Investigations Map OM-181, scale 1:48,000.

Paylor, E. D., 1989, Fault kinematics, western Owl Creek Mountains, Wyoming: evidence for a possible transfer zone linking the Bighorn and Wind River thrust systems: Geological Society of America Abstracts with Programs, v. 21, p. A135-A135.

Paylor, E. D., in press, East-west transport of Rocky Mountain foreland uplifts, evidence from the western Owl Creek Mountains, Wyoming: The Mountain Geologist.

Richmond, G. M., 1976, Pleistocene stratigraphy and chronology in the mountains of western Wyoming, *in,* Mahaney, W. C., editor, Quaternary stratigraphy of North America: Dowden, Hutchinson, and Ross, Stroudsburg, Pennsylvania, 353-379 p.

Sales, J. K., 1983, Collapse of Rocky Mountain basement uplifts, *in*, Lowell, J. D., editor, Rocky Mountain foreland basins and uplifts: Rocky Mountain Association of Geologists, p. 79-97.

Seeland, D. A., 1978, Eocene fluvial drainage patterns and their implications for uranium and hydrocarbon exploration in the Wind River Basin, Wyoming: U. S. Geological Survey Bulletin 1446, 21 p.

Skeen, R. C., and Ray, R. R., 1983, Seismic models and interpretation of the Casper Arch thrust: application to Rocky Mountain foreland structure, *in*, Lowell, J. D., editor, Rocky Mountain foreland basins and uplifts: Rocky Mountain Association of Geologists, p. 99-124.

Stucky, R. K., 1984a, Revision of the Wind River faunas, early Eocene of central Wyoming, part 5, Geology and biostratigraphy of the upper part of the Wind River Formation, northeastern Wind River Basin: Carnegie Museum of Natural History, Annals of Carnegie Museum, v. 53, Article 9, p. 231-293.

Stucky, R. K., 1984b, Revision of the Wind River faunas, early Eocene of central Wyoming, part 6, Stratigraphic sections and locality descriptions, upper part of the Wind River Formation: Carnegie Museum of Natural History, Annals of Carnegie Museum, v. 53, Article 10, p. 295-325.

Sundell, K. A., 1985, Field trip #5, Casper to Cody, Wyoming: Wyoming Geological Association Earth Science Bulletin, v. 19, p.79-116.

Thomas, L. E., 1965, Sedimentation and structural development of the Bighorn Basin: American Association of Petroleum Geologists Bulletin, v. 49, p. 1867-1877.

Troyer, M. C., and Keefer, W. R., 1955, Geology of the Shotgun Butte area, Fremont County, Wyoming: U.S. Geological Survey Oil and Gas Investigations Map OM-172, scale 1:48,000.

Tourtelot, H. A., and Thompson, R. M., 1948, Geology of the Boysen area, central Wyoming: U.S. Geological Survey Oil and Gas Investigations Preliminary Map 91, 2 sheets, scale 1:48,000.

Wise, D. 1963, Keystone faulting and gravity sliding driven by basement uplift of Owl Creek Mountains, Wyoming: American Association of Petroleum Geologists Bulletin, v. 47, p. 586-598.

Wyoming Geological Association, 1964, Highway geology of Wyoming: Wyoming Geological Association, Casper, 361 p.

Wyoming Geological Association, 1989, Wyoming oil and gas fields, Bighorn and Wind River Basins: Wyoming Geological Association, 555 p.

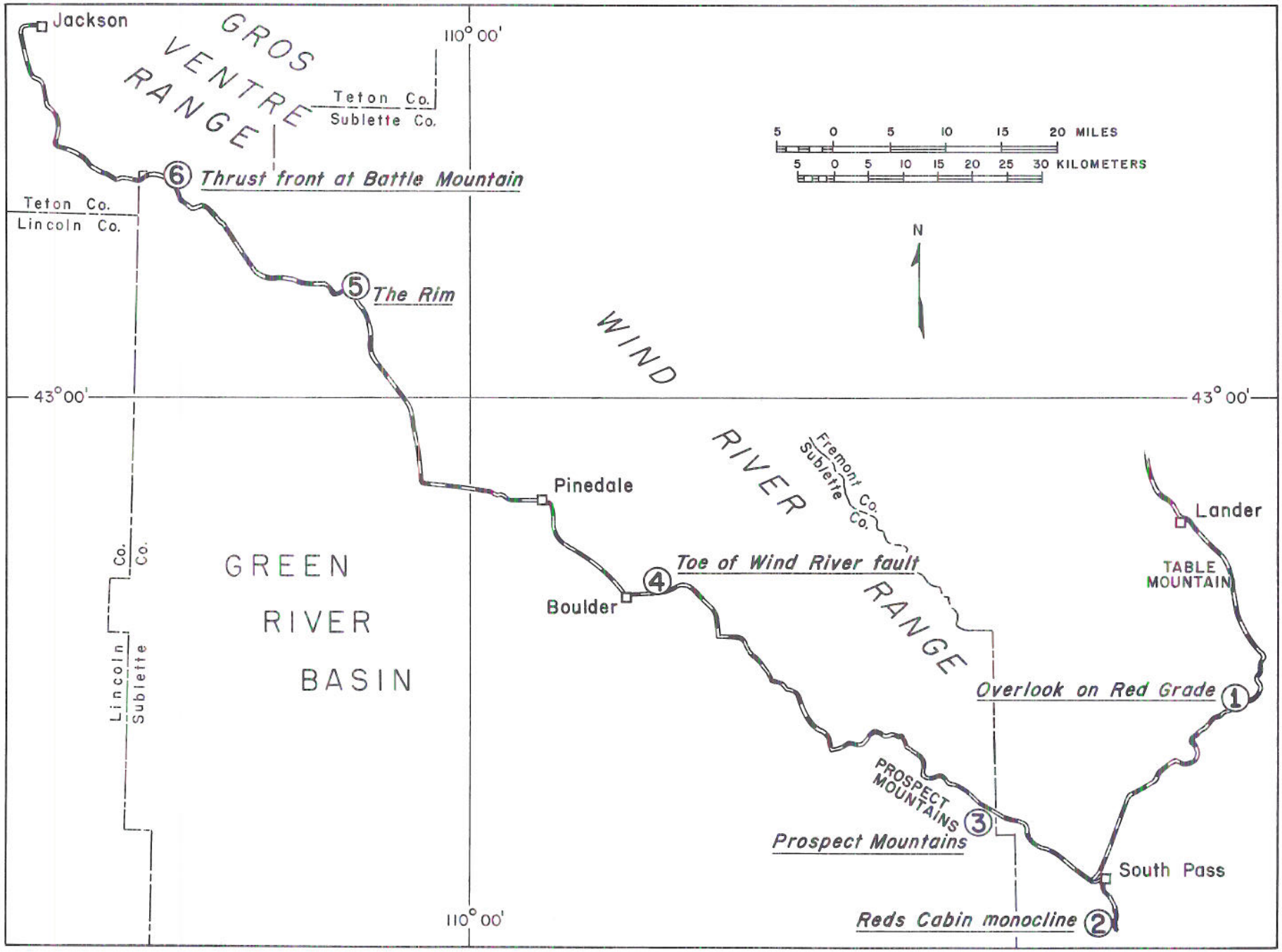

Figure 1. Trip route and stop locations, field trip no. 7, part 3.

Field trip no. 7, part 3

LARAMIDE AND POST–LARAMIDE STRUCTURAL HISTORY OF THE WIND RIVER RANGE

James R. Steidtmann
Department of Geology and Geophysics
The University of Wyoming
Laramie, Wyoming 82071

Trip summary (see Figure 1)

Stop 1. Overlook on Red Grade
Stop 2. Reds Cabin monocline
Stop 3. Prospect Mountains
Stop 4. Toe of the Wind River fault
Stop 5. The Rim (optional)
Stop 6. Thrust front at Battle Mountain (optional)

Introduction

The Wind River Range is the largest basement-cored uplift in the broken foreland of Wyoming, exposing Precambrian crystalline rocks over an area 110 mi long and 30 mi wide in central-western Wyoming (**Figure 2**). The trace of the Wind River fault underlies the topographic Green River Basin as much as 25 mi west of the present crest of the range. Only at Reds Cabin monocline (**Figures 2 and 3**) and about 3 mi east of the town of Boulder (**Figure 1**) is there surface expression of the fault. Vertical separation on the Wind River thrust is 8.5 mi (Smithson and others, 1979) and present structural relief on Precambrian basement between the crest of the range and the adjacent Green River Basin is nearly 9.8 mi.

The topography of the range consists of a crestal ridge bounded on the northeast by dip slopes on Paleozoic and Mesozoic strata and on the southwest by two relatively flat surfaces (**Figure 4**). The crestal ridge includes 47 of the 50 named peaks in the Wyoming foreland that are 13,000 ft. or higher. Immediately west of this ridge, a distinct topographic break separates the crest from a relatively flat surface called the Wind River peneplain by Westgate and Branson (1913).

The objectives of this trip are to observe the structural, sedimentologic and geomorphic character of the Wind River Range and adjacent Green River Basin and to discuss the significance of this information in terms of the uplift history of the range.

Geological setting

Tectogenic sedimentary rocks

Sedimentary rocks generally associated with uplift and subsequent collapse of the Wind River mountains range in age from Late Cretaceous through Tertiary but only those of early Eocene age and younger are exposed at the surface along the southwestern margin of the range (**Figure 5**). Steidtmann and others (1986) showed that tectogenic sediments shed by the Wind River uplift are of three general types and that each can be related to a specific structural setting. (1) The Lance Formation (Late Cretaceous), Fort Union Formation (Paleocene), and main body of the Wasatch Formation (early Eocene) make up a subregional clastic apron and were generated by uplift of the entire range on the Wind River fault. These deposits consist mainly of

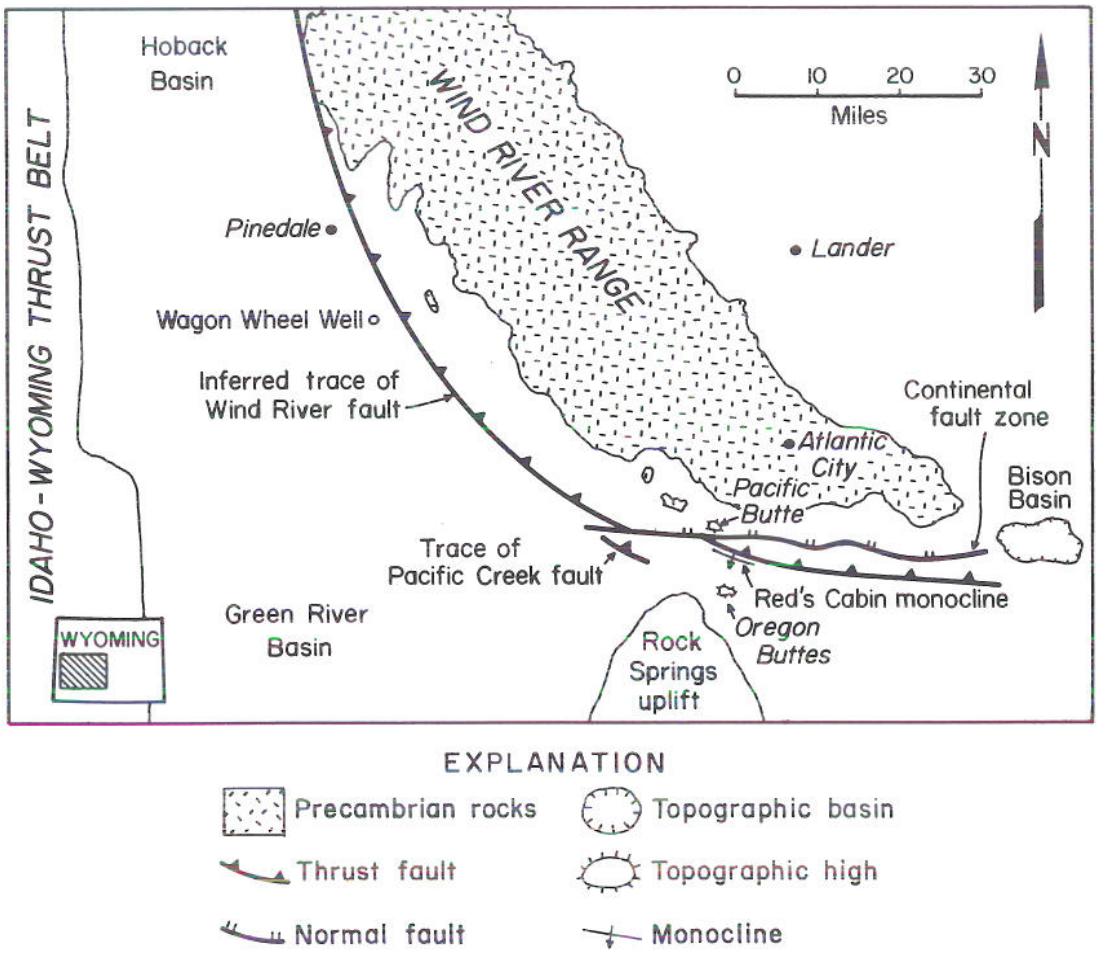

Figure 2. Index map showing the location of the Wind River Range in western Wyoming, the traces of the Wind River and Continental faults, and the location of Reds Cabin monocline.

Figure 3. Photograph of Reds Cabin monocline, a fold over the toe of the Wind River fault along the southwest flank of the range. Youngest folded beds (foreground) belong to the Cathedral Bluffs Tongue of the Wasatch Formation (latest early Eocene). These are overlain by undeformed sediments of the Green River Formation (arrow). (Location shown in Figure 2.)

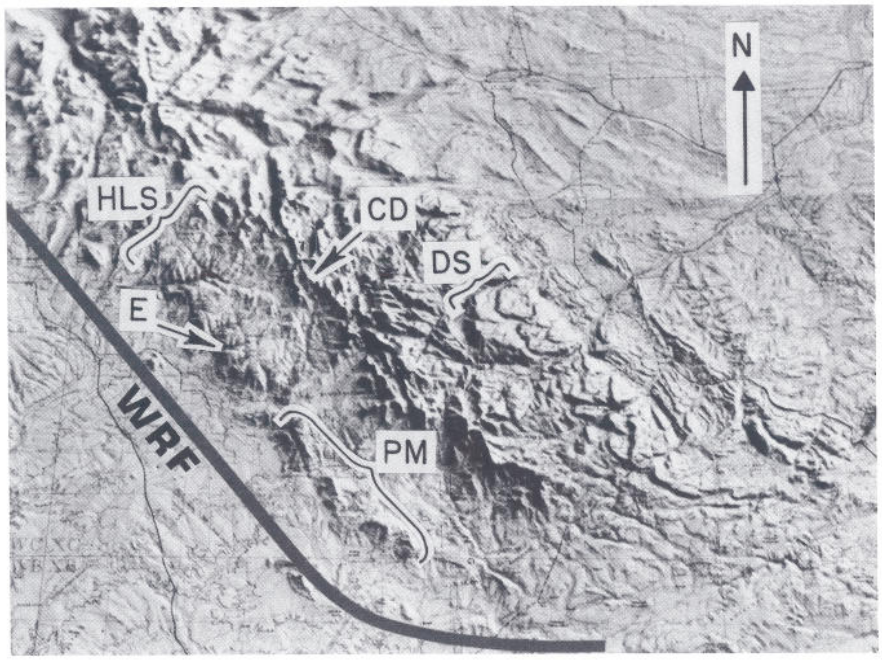

Figure 4. View of plastic relief map (two sheets) of the southern Wind River Range. Trace of Wind River fault is shown (WRF). High-level erosion surface (HLS) is bounded on the west by an escarpment (E) and on the east by high peaks of the Continental Divide (CD). Dip slopes of Paleozoic and Mesozoic sedimentary rocks flank the east side of the range (DS). PM designates Prospect Mountains.

siltstone, sandstone, and pebble beds. (2) The South Pass Formation (late Oligocene), and conglomerates in the White River Formation (Oligocene) and at the base of the Arikaree Formation (late Oligocene) are intramontane alluvial deposits related to faulting in the core of the range. (3) Fault–scarp clastic wedges in the Cathedral Bluffs Tongue of the Wasatch Formation (early Eocene), Circle Bar beds (mid Miocene), and Leckie beds (post-South Pass) document local topographic highs.

Structure

Before Berg's (1961) work using industry seismic information, structural relations between the Wind River Range and the adjacent Green River Basin

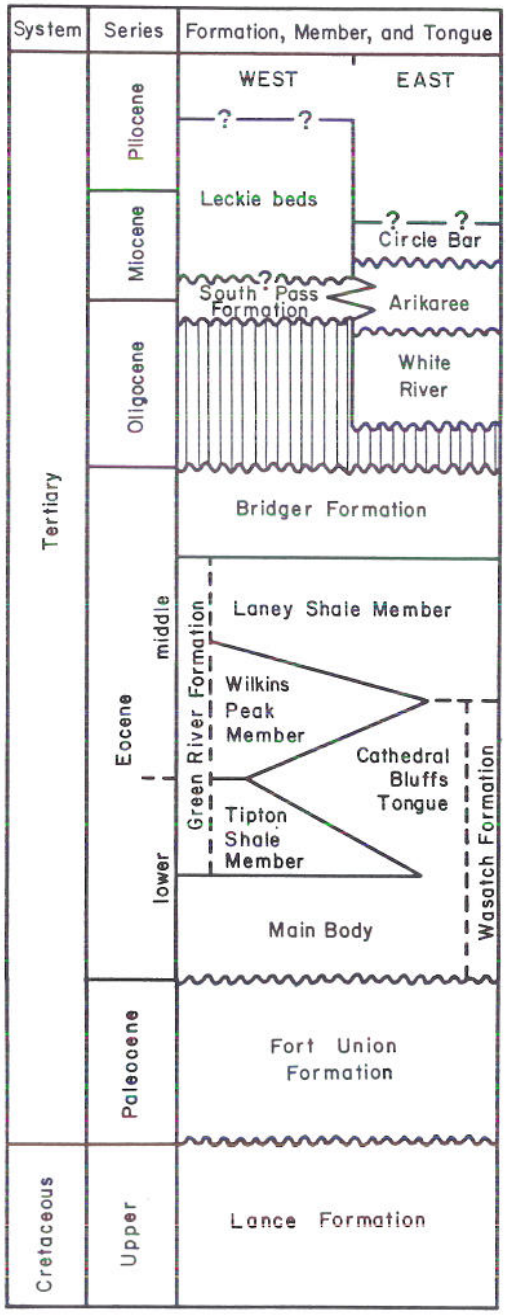

Figure 5. Simplified stratigraphic column of Tertiary rocks exposed along the southwest flank of the Wind River Range (adapted from Steidtmann and Middleton, 1986).

remained obscure because the range-bounding faults are, for the most part, covered by tectogenic sediments shed during uplift of the range. However, Berg's work, together with interpretations of the COCORP Wind River seismic data (Smithson and others, 1979; Lynn and others, 1983; Sharry and others, 1986), has now clarified these range-basin relationships. In contrast, structural relationships in the core of the range remain relatively unknown because of inaccessibility and the complexities of mapping crystalline rocks of varying lithologies and with multiple episodes of deformation. Only recently have the map compilation of Worl and others (1986) and the detailed structural analysis of Mitra and Frost (1981) and Mitra (1984) dealt with the complex geology of the crystalline core.

The most complete information about the dip-section geometry of the Wind River fault at depth comes from interpretations of the COCORP Wind River profile (**Figure 6**). Smithson and others (1978,1979) showed that the Wind River fault generates a continuous reflection from near the surface to a depth of about 15 mi and that the thrust appears as a complex zone of faults. The thrust has 9 mi of vertical separation and 16 mi of horizontal separation. In contrast, Lynn and others (1983) showed the Wind River fault to be a complex zone that splays and flattens with depth in such a way as to explain the tilting of the range northeastward into the Wind River basin. Sharry and others (1986) reprocessed the same data in an attempt to correct for problems arising from crooked-line geometry and line orientations. Their migrated section shows that the Wind River thrust dips at 30 degrees from the surface to 4 mi depth, where the dip begins to flatten, soling out at about 13.5 mi. Furthermore, they interpret the crust below the fault to be thrust into lens-shaped packages that give rise to a duplex structure at 10.5 to 16 mi depth.

Juxtaposed Tertiary beds of different age are the main surface indication of the Continental fault system (**Figure 2**). These beds were originally mapped by Nace (1939) and later by Berman (1955), Hummel (1958), and McGrew (1959) and are part of a trend across central Wyoming, where late Tertiary collapse has downdropped previously uplifted blocks, preserving much of the late Tertiary sedimentary record.

Mapping in the core of the range (Link, 1976; Mitra and Frost, 1981; Worl and others, 1986) has identified both Precambrian and Cenozoic faults. Other workers have suggested that faults in the core of the range bound the high-level erosion surface on the northeast and southwest. Couples and Stearns (1978) interpreted the high-level surface to be the result of downdropping of the shattered lobe in their rigid block rotation model and Erslev (1986) predicted normal faulting in this region based on basement-balancing procedures. Sediment provenance and fission-track data (Steidtmann and others, 1989) have indicated Tertiary faulting in the core of the range. The escarpment that bounds the southwest side of the high-level erosion surface is controlled by a fault in the hanging wall of the Wind River thrust and the sharp topo-

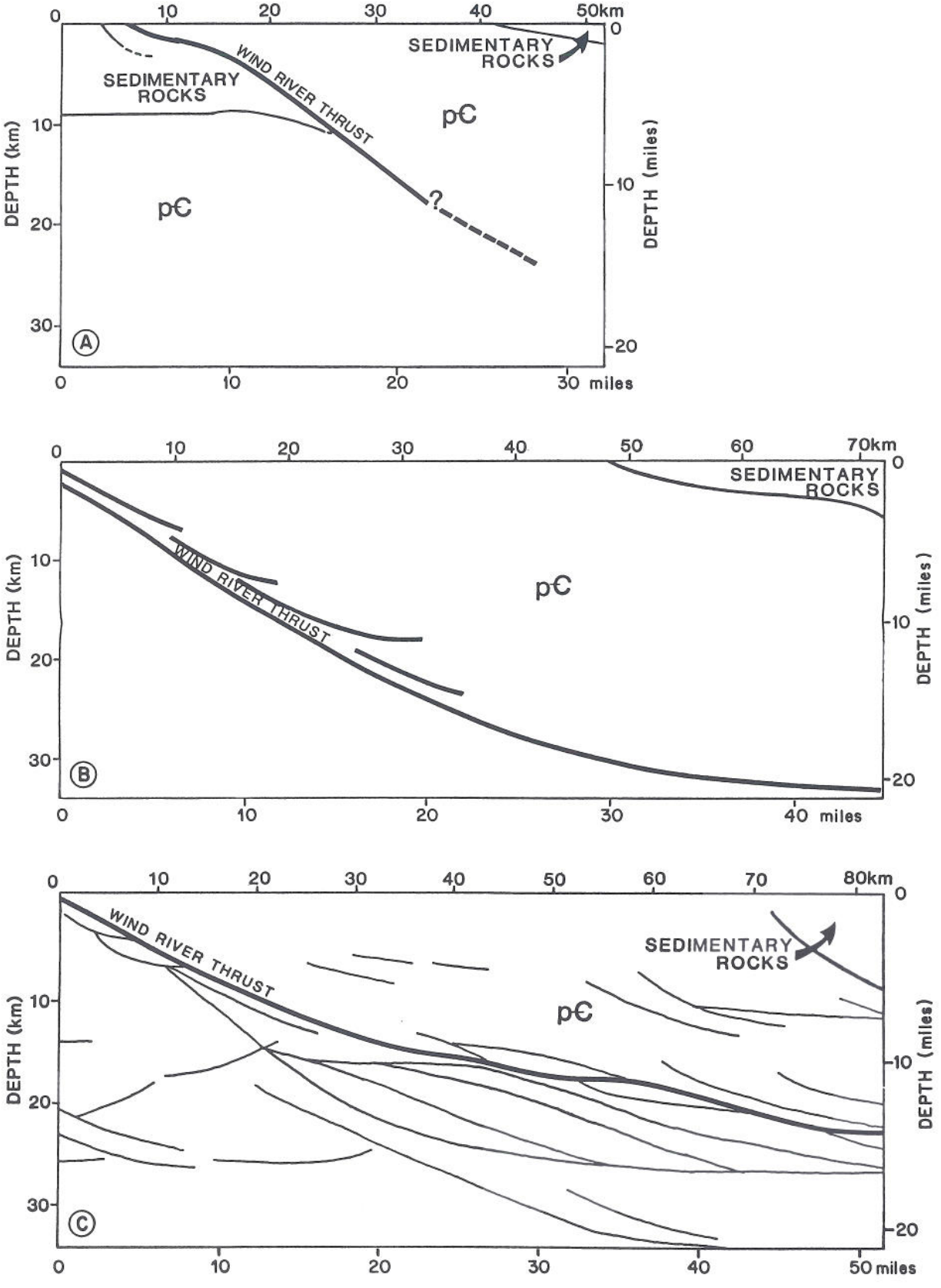

Figure 6. Line drawing depicting interpretations of the COCORP Wind River Seismic line by (A) Smithson and others (1979), (B) Lynn and others (1983), and (C) Sharry and others (1986). (See text for discussion.)

graphic break where the range crest rises abruptly above the erosion surface was formed by reactivation of Precambrian shear zones.

Summary of structural events

The time of formation of some of the structures mentioned above can be determined or constrained (with varying degrees of certainty) by structural control of depositional patterns, overlapping and crosscutting relations, paleocurrent and provenance data, and the dating of ash beds in locally derived tectogenic sediments. The timing of these events is summarized below.

1. The Wind River area was a topographic high at least as early as late Albian time, when it controlled regional drainage development (Dolson, 1988). Initial motion of the Wind River fault may have begun during the Turonian, when the Green River Basin began to subside very rapidly (Shuster and Steidtmann, 1988). By the Paleocene, the Wind River uplift had, at least in part, been stripped to its Precambrian core and feldspathic sediments were being shed. Motion on the Wind River fault ceased at the end of the early Eocene or the beginning of the middle Eocene.

2. Formation of imbricates in the hanging wall of the Wind River thrust occurred just prior to final motion on the Wind River fault. This was an extremely rapid event, which uplifted the eroded core of the range and formed a fault scarp and associated coarse clastic wedge in the Cathedral Bluffs Tongue of the Wasatch Formation.

3. The tip of the Wind River thrust sagged into the basin sometime between the middle Eocene and the end of the Oligocene, when middle Eocene sediments on the hanging wall were tilted basinward.

4. The crest of the range was uplifted by reactivation of Precambrian shear zones during late Oligocene or earliest Miocene time. Sediment sources in the core of the range were rejuvenated, shedding coarse clastics across the toe of the Wind River fault.

5. The southern end of the range began to collapse along the Continental normal fault during middle Miocene time and local fault-scarp clastic wedges were shed by the high-standing blocks.

Stop descriptions

Stop 1. Overlook on Red Grade

North-northwest from Red Grade Overlook, a cross section of the northeast flank of the Wind River Range is exposed. The entire Paleozoic and Mesozoic stratigraphic section is present on this side of the range and from this point we can see Permian through Jurassic rocks in the foreground and a tightly folded anticline in the Permian Phosphoria Formation. In the distance, is the distinct angular unconformity on Table Mountain. The age of the overlying unit there is not certain but in the immediate vicinity of the stop it appears that the same unconformity is overlain by Oligocene White River beds. The almost perfect horizontality of this unconformity indicates that this part of the range could not have been tilted after erosion cut the surface. This constraint indicates that the latest Oligocene-earliest Miocene uplift in the range must have been limited to its core.

Stop 2. Reds Cabin monocline

Reds Cabin monocline is actually a 2 mile-long asymmetrical anticline over the toe of the Wind River fault. At the surface, folding involves rocks of the Eocene Wasatch and Green River formations and fold amplitude dies out gradually to the northwest. The local stratigraphy and overlapping and crosscutting relations in the fold indicate that latest motion on the Wind River fault initially controlled the position of the shoreline of Lake Gosiute, folded the tectogenic deltaic and fluvial sediments, and ceased in latest early Eocene or earliest middle Eocene. The limited extent of this fold along the trace of the Wind River fault suggests that the fault is a zone consisting of related but separate segments that moved somewhat independently.

Stop 3. Prospect Mountains

The Prospect Mountains are horsts left standing when the south end of the range collapsed along the Continental fault zone and imbricate fault zone in the hanging wall of the Wind River fault. Small bouldery alluvial fans were (and still are) shed from these blocks and cover the South Pass Formation in this area. The fans have not been dated but sediments shed from high-standing blocks along the Continental fault zone have been dated as middle Miocene. To the southwest, tilted beds of the middle Eocene Bridger Formation are overlain by latest Oligocene-earliest Miocene South Pass conglomerate beds, indicating that the toe of the Wind River fault sagged into the sediments of the Green River Basin sometime between deposition of these two units.

The South Pass conglomerate is the most obvious evidence for uplift in the core of the Wind River Range during latest Oligocene or earliest Pliocene. The paucity of locally derived coarse clasts in sediments deposited after motion on the Wind River fault ceased and the transport of Absaroka volcanic clasts southward across what is now the crest of the range indicate that by the end of the early Eocene there was little topographic relief on the range. Uplift of the crest of the range in latest Oligocene once again created a local sediment source, which supplied clasts to the South Pass Conglomerate.

Stop 4. Toe of the Wind River fault

Stop just east of the town of Boulder to see steeply dipping Cambrian and Ordovician sedimentary rocks over the toe of the Wind River fault. This is the only other area, in addition to Reds Cabin monocline, where there is good surface evidence for the location of the thrust. The position of the thrust relative to the crest of the range and the step-like topography of the range have been interpreted as evidence for imbricate faulting in the hanging wall in the Wind River fault, which uplifted the high-level erosion surface to its present relative elevation.

Stop 5. The Rim (optional)

The Rim is a drainage divide that separates the Green River Basin to the south from the Hoback Basin to the north. Road cuts here expose distal alluvial fan deposits and pressure-marked metaquartzite clast conglomerates of the early Eocene Pass Peak Formation, which were shed southward from the Jackson Hole-Gros Ventre Range area. It is not clear whether this fan was the result of reworking of the lithologically similar Pinyon Conglomerate to the north, during a time of uplift there, or whether it represents a younger, more distal (southern) progradation of the same episode of conglomerate deposition.

Pressure marks and related fractures are ubiquitous on clasts throughout both the Pinyon and the Pass Peak formations, rendering them impossible to transport without breaking. This implies that burial deep enough to generate pressure fracturing must have occurred in both the Pinyon and the Pass Peak after the early Eocene. Fractured clasts are present in the Pass Peak to an elevation of 10,000 ft, suggesting that this part of the basin was filled to a much greater depth than today.

From this stop, the front of the western U.S. fold-thrust belt can be seen to the west.

Stop 6. Thrust front and Battle Mountain (optional)

Directly north from this stop, the Jurassic Nugget Sandstone overlies the Paleocene Hoback Formation at Battle Mountain. This classic thrust locality has had an interesting history of interpretation. Until industry seismic information became available, this thrust (called the Jackson, Cliff Creek, or Prospect thrust depending on the reference) was considered to be the frontal fault of the fold-thrust belt in this area and all sediments to the east of the fault were dated as Tertiary. Early seismic showed that a back fault (Game Hill fault) brought up Late Cretaceous beds and repeated the Tertiary section to the east. Recently, field mapping and seismic interpretation have shown that the fault we are viewing on Battle Mountain is in the hanging wall of the frontal thrust system and not the frontal thrust itself.

References cited

Berg, R.R., 1961, Laramide tectonics of the Wind River Mountains: Wyoming Geological Association 16th Annual Field Conference Guidebook, p. 70-80.

Berman, J.E., 1955, Geology of Elk Mountain and Tabernacle Butte area, Sublette County, Wyoming: M.A. thesis, University of Wyoming, Laramie, 639 p.

Couples, G., and Stearns, D.W., 1978, Analytical solutions applied to structures of the Rocky Mountain foreland on local and regional scales, *in* Matthews, V., III, editor, Laramide folding associated with basement block faulting in the western United States: Geological Society of America Memoir 151, p. 313-336.

Dolson, J., 1988, Lower Cretaceous Muddy Formation valley fills and paleo hills, *in* Rocky Mountain Section, Society of Economic Paleontologists and Mineralogists Field Guide (unpublished, unpaginated).

Erslev, E.A., 1986, Basement balancing of Rocky Mountain foreland uplifts: Geology, v. 14, p. 259-262.

Hummel, J.M., 1958, Geology of the Pacific Creek area, Sublette and Fremont Counties, Wyoming: M.S. thesis, University of Wyoming, Laramie, 76 p.

Link, P.K., 1976, The geology of the Wind River Mountains, Wyoming with emphasis on fluid inclusions from high grade metamorphic rocks, Paradise Basin Quadrangle: Senior thesis, Yale University, New Haven, Connecticut, 103 p.

Lynn, H.B., Quam, S., and Thompson, G.A., 1983, Depth migration and interpretation of the COCORP Wind River, Wyoming, seismic reflection data: Geology, v. 11, p. 462-469.

McGrew, P.O., 1959, The geology and paleontology of the Elk Mountain and Tabernacle Butte area: Bulletin of the American Museum of Natural History, v. 117, p. 117-176.

Mitra, G., 1984, Brittle to ductile transition due to large strains along the White Rock thrust, Wind River mountains, Wyoming: Journal of Structural Geology, v. 6, p. 51-61.

Mitra, G., and Frost, B.R., 1981, Mechanisms of deformation within Laramide and Precambrian deformation zones in basement rocks of the Wind River Mountains: University of Wyoming Contributions to Geology, v. 19, p. 161-174.

Nace, R.L., 1939, Geology of the northwest part of the Red Desert, Sweetwater and Fremont counties, Wyoming: Wyoming Geological Survey Bulletin 27, 51 p.

Sharry, J., Langen, R.T., Jovanovich, D.B., Jones, G.M., Hill N.R., and Guidish, T.M., 1986, Enhanced imaging of the COCORP seismic line, Wind River Mountains, *in* Barazingi, M., and Brown, L., editors, Reflection seismology; a global perspective: American Geophysical Union Geodynamics Series, v. 13, p. 223-236.

Shuster, M.W., and Steidtmann, J.R., 1988, Tectonic and sedimentary evolution of the northern Green River basin, western Wyoming, *in* Schmidt, C.J., and Perry, W.J., editors, Interaction of the Rocky Mountain foreland and the Cordilleran thrust belt: Geological Society of America Memoir 171, p. 515-530.

Smithson, S.B., Brewer, J.A., Kaufman, S., Oliver, J.E., and Hurich, C.A., 1978, Nature of the Wind River thrust, Wyoming, from COCORP deep-reflection data and from gravity data: Geology, v. 6, p. 648-652.

Smithson, S.B., Brewer, J.A., Kaufman, S., Oliver, J.E., and Hurich, C.A., 1979, Structure of the Laramide Wind River uplift, Wyoming, from COCORP deep reflection data and gravity data: Journal of Geophysical Research, v. 84, p. 5955-5972.

Steidtmann, J.R., and Middleton, L.T., 1986, Eocene–Pliocene stratigraphy along the southern margin of the Wind River Range, Wyoming: revisions and implications from field and fission-track studies: Mountain Geologist, v. 23, p. 19-25.

Steidtmann, J.R., Middleton, L.T., Bottjer, R.J., Jackson, K.E. McGee., L.C., Southwell, E.H., and Lieblang, S., 1986, Geometry, distribution and provenance of tectogenic conglomerates along the southern margin of the Wind River Range,

Wyoming, *in* Peterson J.A., editor, Paleotectonics and sedimentation in the Rocky Mountain region: American Association of Petroleum Geologists Memoir 41, p. 321-332.

Steidtmann, J.R., Middleton, L.T., and Shuster, M.W., 1989, Post-Laramide (Oligocene) uplift in the Wind River Range, Wyoming: Geology, v. 17, p. 38-41.

Westgate, L.G., and Branson, E.B., 1913, The later Cenozoic history of the Wind River mountains, Wyoming: Journal of Geology, v. 11, p. 142-159.

Worl, R.G., Koesterer, M.E., and Hulsebosch, T.P., 1986, Geologic map of the Bridger wilderness and the Green–Sweetwater roadless area, Sublette and Fremont counties, Wyoming: United States Geological Survey Miscellaneous Field Studies Map MF-1636-B.

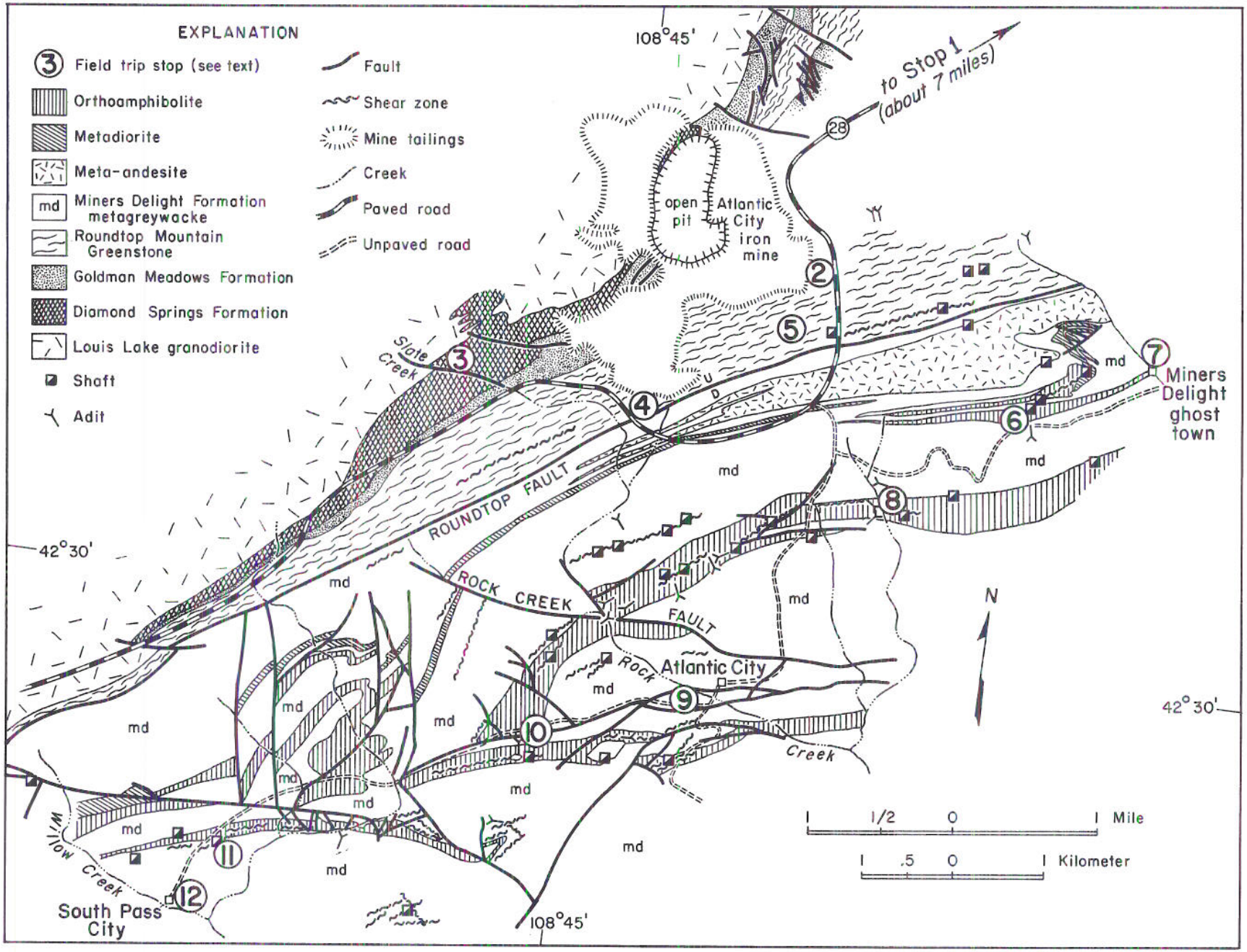

Figure 1. Generalized geologic map of the South Pass-Atlantic City district (modified from Hausel, 1990), showing trip route and stop locations, field trip no. 8.

Field trip no. 8

GUIDE TO GOLD MINERALIZATION AND ARCHEAN GEOLOGY OF THE SOUTH PASS GREENSTONE BELT, WIND RIVER RANGE, WYOMING

W. Dan Hausel
Geological Survey of Wyoming
Laramie, Wyoming 82071

and

Joseph Hull
Department of Mineralogy and Petrology
Uppsala University
Uppsala, Sweden

Trip summary (see Figure 1)

Stop 1.	Overlook of Red Canyon
Stop 2.	Overlook of the Atlantic City iron mine
Stop 3.	Diamond Springs Formation and Goldman Meadows Formation west of the Atlantic City mine entrance.
Stop 4.	Roundtop Mountain deformation zone and adjacent rocks south of the Atlantic City iron mine.
Stop 5.	Roundtop Mountain Greenstone
Stop 6.	Peabody Ridge overlook and rocks.
Stop 7.	Miners Delight ghost town (optional)
Stop 8.	Snowbird mine
Stop 9.	Overlook of Atlantic City and Rock Creek
Stop 10.	Duncan mine area
Stop 11.	Carissa mine (optional)
Stop 12.	South Pass City historic site

Introduction

The South Pass greenstone belt has been Wyoming's most prolific source of gold and iron ore, and recent sampling in the region has identified numerous gold, chromium, copper, silver and tungsten anomalies, as well as some tin anomalies (Hausel, 1987b, 1990). Work by Prinz (1974) identified several arsenic soil-geochemical anomalies that may be redolent of gold mineralization, based on the association of gold with arsenopyrite at some mines in the belt

Total iron ore production from the greenstone belt is more than 90 million tons, but the total amount of gold produced is unknown because few records were kept and preserved. Gold production estimates range from a conservative low of 70,000 ounces (Koschmann and Bergendahl, 1968) to optimistic estimates of more than 327,000 ounces (Hausel, 1987a) for the South Pass-Atlantic City district. The Lewiston district near the southeastern edge of the greenstone belt has not produced any iron ore, and no gold production estimates have been made for the district; it appears the amount of precious metals recovered from the Lewiston district was considerably less than from the South Pass-Atlantic City district.

Several authors have interpreted this belt to represent a partially exposed and fragmented Archean greenstone terrane (Bayley and others, 1973; Condie, 1967, 1981; Hausel, 1987a; Houston and Karlstrom, 1979; Hull, 1988; and Karlstrom and others, 1981). The exposed metamorphic terrane crops out over 150 to 250 square miles and forms a synclinorium of steeply dipping sedimentary, volcanic, and plutonic rocks that has been metamorphosed to amphibolite facies with a small island of greenschist-facies rocks found along the north. Bedding and several structural elements (such as foliation, isoclinal fold axes, and auriferous shear zones) parallel the axis of the basin.

The northwestern and southeastern flanks of the greenstone belt are in fault contact and/or intruded by granodiorite plutons. These plutons represent a major Late Archean cratonization event that was followed by the intrusion of small domical granite stocks emplaced along the western margin of the greenstone belt. These granitic masses, as well as movement along some Archean structures, produced local refolding.

The northeastern and southern flanks of the greenstone belt are buried by Phanerozoic rocks. In the northeast, the Archean supracrustal rocks underlie a relatively complete Phanerozoic section, at the base of which are fluvial quartzites of the Flathead Formation (Cambrian). Preliminary paleocurrent studies on the quartzites indicate paleoflow directions were into the greenstone belt from the adjacent granite-gneiss terrane (Tom J. Mitko, personal communication, 1986), which may account for a paucity of gold deposits in the Flathead Formation. To the south, the supracrustals are covered by Tertiary sedimentary rock, eluvium, and alluvium that progressively thicken southward to the Continental fault (a boundary fault of the Wind River Range). The Continental fault projects downward to the toe of the Wind River thrust.

Because of the past economic importance and the potential significance of the South Pass region to Wyoming, this greenstone belt has been the subject of several investigations. In the early 1980s, interest in this Archean terrane was renewed when the Metals and Precious Stones Division of the Geological Survey of Wyoming commenced investigations aimed at assisting the mining industry and gold prospectors in the search for commercial mineralization. In addition to studying aspects of the structure, geochemistry, stratigraphy, petrology, and economic and mining geology, the Division mapped the entire greenstone belt on a scale of 1:24,000 and 24 historic mines on a scale of 1:240, and produced a regional 1:48,000-scale map (Hausel, 1990).

Acknowledgments

Without the willingness of many property owners and claimants, we would be unable to conduct this field excursion. Our appreciation is expressed to Jim Niggemeyer and Robert Klinger of Universal Equipment Company for access to the Atlantic City mine. We also wish to thank Steve Gyorvary, Bob Johnson, and Dave Geible for providing unlimited access to their properties. Bart Rea and Bruce Ward gave permission to examine and collect samples at the Duncan mine, but requested we use extreme caution around the historic buildings and mine portals. I also thank Consolidated McKinney Resources and Grif Williams for access to the Carissa mine during the mapping of the greenstone belt. I also thank the employees of the Wyoming Recreation Commission at the South Pass historic site for their willingness to show reconstructed South Pass City. I am also indebted to Jim Case, of the Geological Survey of Wyoming, and Rich Weiland, of the University of Wyoming Geology Department, for eliminating some of the bureaucratic headaches that go along with running a field trip. This field trip was initially run for the International Geological Congress in July, 1989 (Snyder and others, 1989).

Geography and history

The South Pass region forms a gradual sloping pediment at the base of the high snowy peaks of the Wind River Range. The highest peak in the range, and the highest point in Wyoming, is Gannett Peak (elevation 13,804 feet). The South Pass pediment is considerably lower, at 8,500 feet near the base of the rugged peaks to 7,200 feet along the banks of the Sweetwater River.

The greenstone belt received its name from historic South Pass, which lies a few miles south of the belt, where the Oregon Trail crossed the Continental Divide. The pass was first used in 1812, and its easy grade made it the prominent route for thousands of emigrants on their way west in covered wagons and on horse back.

Gold was discovered in the South Pass region as early as 1842, but because of Indian hostilities, no serious gold mining endeavors were pursued until H.S. Reedall discovered gold in bedrock on June 8, 1867, near the present site of South Pass City. During the following winter, a hundful of miners worked what became known as the Carissa lode by crushing quartz in a hand mortar and extracting more than 400 ounces of gold by panning (Spencer, 1916). When news of the discovery reached the outside world, a gold rush ensued. South Pass City was organized adjacent to the Carissa mine and within a short time the town became the home of more than 2,000 people. Four miles to the east on Rock Creek, a second town, known as Atlantic City, became the home of more than 500 people. Today, South Pass City and Atlantic City have only a few dozen residents each, and Miners Delight, a third boom town constructed 4 miles northeast of Atlantic City, has been abandoned since 1907.

Within five or six years after the initial Carissa discovery, the gold rush activities subsided and many mines and claims were abandoned. In 1879, twelve years after the Carissa discovery, another gold discovery, 12 miles southeast of Atlantic City, led to the establishment of Lewiston (originally known as Lewis Town) and the Lewiston district in the vicinity of Strawberry Creek. Very little historic information was recorded about the district and today little remains of the historic townsite.

Because of the remoteness and poor accessibility of the historic South Pass region, only bits and pieces of its early mining history were recorded. Since 1879, gold mining activities appear to have been sporadic, with a peak from 1933 to 1941, when several placers were dredged resulting in the recovery of a minimum of 11,500 ounces of gold (Hausel, 1987b). Calculations based on the average grade and the volume of gravel mined suggest that more than three times this amount was actually recovered.

During the late 1950s, mining interest in the South Pass region shifted from gold to iron ore, and the structurally thickened banded iron formation along the northern margin of the greenstone belt was outlined for open-pit mining (Bayley, 1963). From 1962 to 1983, more than 90 million tons of iron ore were recovered from the Atlantic City mine before operations were suspended.

Regional geology and Archean stratigraphy

The Wind River Range, which hosts the South Pass greenstone belt, is a Precambrian-cored Laramide uplift bounded by thrust faults with Phanerozoic sedimentary rocks draped over its flanks. The core of the uplift contains 2.8 to 3.2 Ga amphibolite-facies orthogneiss intruded by 2.5 to 2.8 Ga granite and granodiorite (Aleinikoff and others, 1987; Stuckless and others, 1985). The South Pass greenstone belt lies at the southern toe of the Wind River Range and is formed of a tripartite succession of metamorphosed sedimentary, volcanic, and plutonic rocks. These rocks have been metamorphosed to amphibole and greenschist facies and subjected to a minimum of three episodes of deformation.

The Miners Delight Formation, youngest of the Archean supracrustal successions, has yielded a Rb-Sr whole-rock isochron of 2.8 Ga (Z.E. Peterman, personal communication to Stuckless and others, 1985). The Miners Delight Formation is a relatively thick unit dominated by metagreywacke with other metasedimentary rocks and three suites of metaigneous rocks. Bayley and others (1973) estimated the Miners Delight Formation to be about 5,000 feet thick but, due to transposition of bedding, the actual thickness may not be determinable.

The great majority of gold mines in the greenstone belt occur within the Miners Delight Formation. The mines are organized into two principal mining districts, the South Pass-Atlantic City and Lewiston districts, located on opposing limbs of the South Pass synclinorium. Two other important gold-bearing areas lie outside the greenstone belt in Tertiary boulder conglomerates eroded from the greenstone belt; Tertiary paleoplacers also occur within the greenstone terrane. Essentially all of the lode mines in the Lewiston district were developed in shear zones in metagreywacke. The shears occur along the limb of a district-wide fold and exhibit narrow zones of hematite-chlorite-quartz alteration. In the South Pass-Atlantic City district, many of the lode mines occur in shear zones spatially associated with a prominent belt of mafic hornblende-plagioclase amphibolites. This orthoamphibolite belt is a complex mixture of foliated amphibolite, metadiabase, and metabasalt with dominant tholeiitic chemistries (**Figure 2**).

A less prominent belt of ultramafic amphibolite lies structurally above (but stratigraphically below according to Bayley and others, 1973) the mafic amphibolite belt. These rocks include actinolite schist and tremolite/actinolite-talc-chlorite schist, some of which

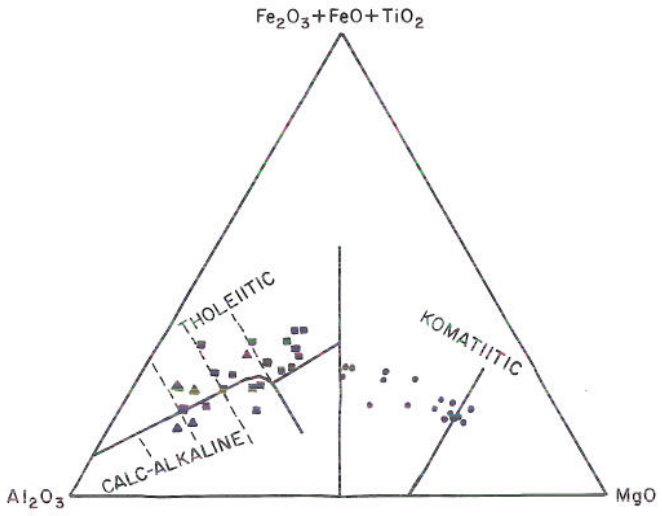

Figure 2. Jensen plot of Miners Delight Formation metaigneous rocks (data from Bayley and others, 1973; Bow, 1986; and Hausel, 1990). Dots represent tremolite/actinolite-talc-chlorite and actinolite schists, squares are hornblende-plagioclase amphibolites, triangles are meta-andesites and metadiorite porphyries.

are carbonate or calc-silicate altered and have chemistries similar to komatiite (Bow, 1986; Hausel, 1987b). Between these two amphibolite belts is a mixed member of metagreywacke, massive metabasalt, vesicular metabasalt, chlorite schist, metaconglomerate, and meta-agglomerate. The amphibolites are commonly flanked by a thin graphitic schist member.

The extreme competency contrasts between these rock types resulted in a favorable environment for the development of shear zones during regional deformation. Shears are believed to have developed preferentially during folding at sites of rock competency contrast (Bayley and others, 1973). Bow (1986) also suggested a genetic link between the auriferous shears and ultramafic (komatiitic) amphibolites. Although the ultramafic rocks may have contributed to the total gold budget of the greenstone belt, it is highly unlikely they were the sole source.

Wallrock alteration is not pervasive but is expressed by weak potassium metasomatized zones (sericite, biotite) with quartz, cherty quartz, carbonate (calcite), and chlorite with less extensive and restricted zones of iron sulfide (pyrite, pyrrhotite), and/or arsenopyrite overprinting the amphibolite facies rocks. Microscopically, secondary sericite, biotite, quartz, and carbonate may be present with accessory tourmaline and chlorite.

Metagreywacke and greywacke schist, the most common rock types found in the Miners Delight Formation, often host gold-bearing shears. The metagreywacke is commonly fine grained, poorly sorted, massive, grey to black, with bedding overprinted by foliation. Mineralogically, most metagreywackes consist of angular to subangular quartz, plagioclase (oligoclase), and rock fragments in a recrystallized matrix of biotite, untwinned plagioclase, and quartz with or without garnet, chlorite, and sericite. Locally, some greywackes are spotted with porphyroblasts of altered cordierite (and andalusite ?) replaced by a mixture of quartz, sericite, and biotite. Lithic fragments of chert, quartzite, and phyllite are common, but igneous fragments are rare. Chemically, these rocks are dominated by quartz diorite to granodiorite compositions (Condie, 1967) and lesser mafic compositions (Hausel, 1987b) (**Figure 3**).

In addition to metagreywacke and amphibolite, the Miners Delight Formation contains some thin units of meta-andesite, cherty metagreywacke, metaconglomerate, quartzite, metatuff, and tuffaceous quartzite. These rocks are well exposed on Peabody Ridge near the northern edge of the greenstone belt.

The Miners Delight Formation is separated from the underlying Roundtop Mountain Greenstone by the Roundtop fault, located along the northwestern margin of the greenstone belt (Bayley and others, 1973). Locally, the Roundtop fault includes a relatively broad mylonitic and brecciated zone termed the Roundtop Mountain deformation zone by Hull (1988).

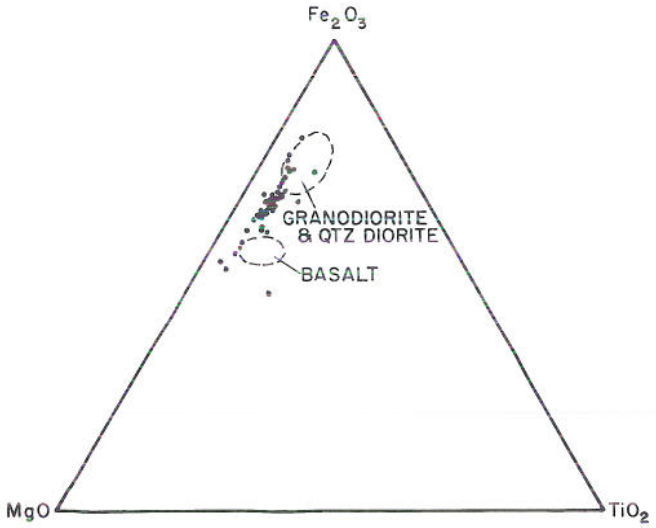

Figure 3. Fe_2O_3-MgO-TiO_2 plot of metagreywacke compositions of the Miners Delight Formation (data from Condie, 1967; and Hausel, 1987b,1990).

The Roundtop Mountain Greenstone occurs in both limbs of the South Pass synclinorium. Better outcrops occur along the northern margin of the belt at Roundtop Mountain, where the formation is about 1,000 feet thick. Here, the unit consists of greenstones, greenschists, metadiabase, pillow metabasalt, and minor actinolite and chlorite schist metamorphosed to greenschist facies at Roundtop Mountain and grading into amphibolite facies to the northeast and southwest (Bayley and others, 1973). On the eastern edge of the greenstone belt, the Roundtop Mountain Greenstone includes amphibolite, mica schist, metabasalt, and minor grunerite schist. Chemically, these rocks are dominated by metatholeiites that have Ti:V ratios generally greater than 20 (Harper, 1985; Hausel, 1987b).

Minor outcrops of actinolite schist have similar chemistries to basaltic komatiite (**Figure 4**). Possible spinifex-textured rock was reported by Harper on Roundtop Mountain, but no true spinifex textures were recognized by the authors. Some (secondary) pseudospinifex-textured metatholeiite of unknown origin occurs on Roundtop Mountain (Hausel, 1990). Gold deposits are not as common in the Roundtop Mountain Greenstone as in the Miners Delight Formation, although anomalous gold and silver occur with copper sulfides in milky quartz at some localities, and anomalous gold has been discovered in discrete veins (Hausel, 1990).

Underlying and grading into the greenstones is a dominantly metasedimentary unit known as the Goldman Meadows Formation (Bayley and others, 1973). This formation includes amphibolite, quartzite, mica schist, porphyroblastic mica schist, and banded iron formation. Both para- and ortho- amphibolites are present. The quartzites include orthoquartzites and fuchsitic quartzites; mica schists include biotite and muscovite schists with common andalusite porphyroblasts; and banded iron formation is formed of alternating bands of quartz-rich and magnetite-rich layers with amphibole and selvages of chlorite schist. Locally, the iron formation contains stratiform and crosscutting bands of pyrite and accessory chalcopyrite. Gold has not been recovered from the iron formation although some anomalies (up to 1.37 ppm Au) were recently detected (Hausel, 1987b).

The lowermost supracrustal unit, named the Diamond Springs Formation, consists of amphibolite, metadiabase, metabasalt, serpentinite, and tremolite/actinolite-talc-chlorite schist (Hausel, 1987b). Where exposed, the unit forms a conformable contact with the overlying Goldman Meadows Formation and has some intercalated augen and migmatitic gneiss on the belt's northwestern flank (Talpey, 1984). Along the southeastern margin, rocks of the Diamond Springs Formation lie in fault contact with granodiorite. To the extreme northwest, these rocks and the Goldman Meadows Formation and Roundtop Mountain Greenstone are absent. The major-element chemistry of amphibolites and schists of the Diamond Springs Formation are suggestive of high-magnesian tholeiites and basaltic and ultramafic komatiites (**Figure 5**). The "immobile" trace-element chemistry (Ti, Zr, Y, V, Cr, Ni) is also consistent with mafic and ultramafic precursors (Hausel, 1987b, 1990).

The structure of the greenstone belt is complex; Hull (1988) defined folds and associated minor struc-

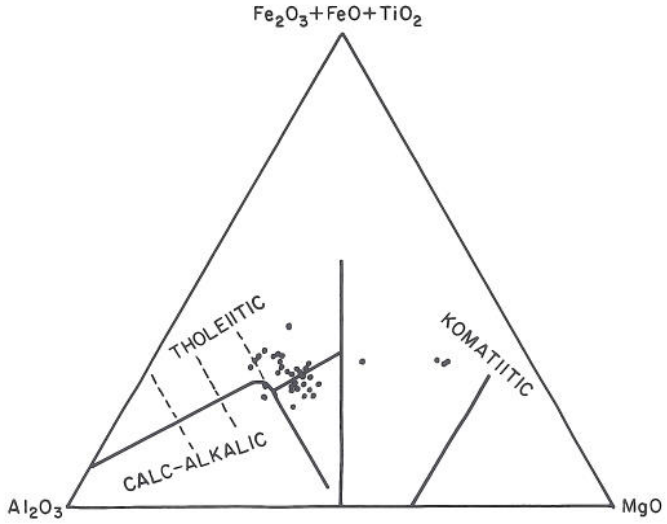

Figure 4. Jensen plot of Roundtop Mountain Greenstone rocks (data from Harper, 1985; and Hausel, 1990).

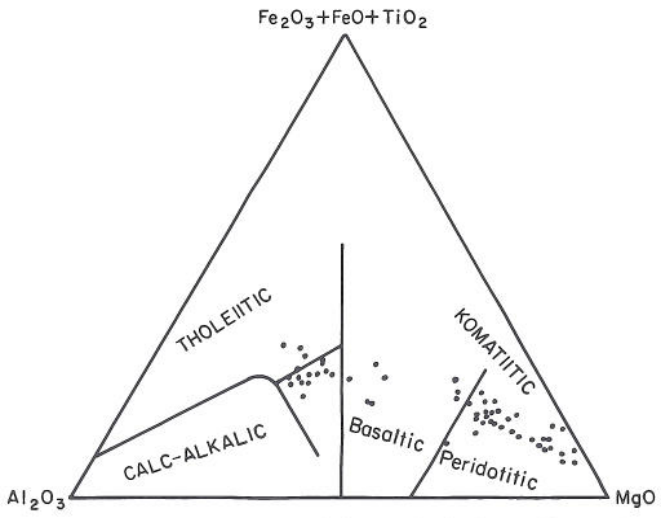

Figure 5. Jensen plot of Diamond Springs Formation metaigneous rocks (data from Hausel, 1987b,1990).

tures based on morphology. The initial layer-parallel shortening of the Miners Delight Formation produced isoclinal to tight, shallow-plunging folds (F1) with an upright cleavage and rare eggbasket crossfolds (F2). Flattening and rotation of early buckle folds produced steeply plunging upright F3 isoclines with mylonitic schistosity. F4 buckle folds and crenulation cleavage adjacent to the Roundtop Mountain deformation zone are common (Hull, 1988).

Gold deposits

Much of the gold mined from the South Pass greenstone belt was recovered from placers and narrow (± 5 feet) shear zones parallel or closely parallel to regional foliation. These shears are continuous over distances of several yards to more than a mile and commonly pinch and swell along trend. The continuation of the shears downdip has never been fully tested since the deepest gold mine in the greenstone belt is only 400 feet deep (the Carissa mine), and the deepest known drilling is only 550 to 600 feet deep. At these depths, the auriferous shears are still persistent.

Megascopically, the shears are permeable zones of cataclastics containing discontinuous quartz boudins and sheared and brecciated quartz lenses and pods. Sulfides (arsenopyrite, pyrrhotite, and pyrite) generally occur in accessory amounts and seldom occur in quantities greater than 5 percent. Gold is found as free gold filling fractures in quartz and has also been identified in pyrite and arsenopyrite.

The tenor of the mineralized shears is not well established. However, historic reports indicate the Carissa ore averaged 10.29 ppm (0.3 oz/ton) Au and the Mary Ellen mine averaged 13.72 ppm (0.4 oz/ton) Au (Beeler, 1908). Recent sampling in some mines showed the ore in site at the Alpine mine averaged 7.55 ppm (0.22 oz/ton), the Diana mine averaged 4.46 ppm (0.13 oz/ton), and the Tabor Grand mine averaged 7.89 ppm (0.23 oz/ton) Au (Hausel, 1989). At best, the shear zones appear to possess trace to weakly anomalous gold along much of their strike lengths with sporadic high-grade ore shoots, some of which include rare lenses of specimen-grade ore. For example some specimen-grade ore recovered from the Hidden Hand mine in the 1930s assayed 10 percent (3,100 oz/ton) Au.

Ore shoots are structurally controlled and occur at pinches and swells, at intersections of lodes (shear structures and veins) (Armstrong, 1948), at intersections of Archean shear zones with Laramide (?) faults, and in fold closures (Hausel, 1990). The control of shoots by Laramide structures is not well understood, but may be the the result of supergene enrichment due to increased permeability imparted by the Laramide structure. Fold closures can be found enclosing ore shoots at a number of mines in the South Pass-Atlantic City district. Possibly the best documented example is where enhanced gold values occur within a tight drag fold in the Duncan shear zone (Hausel, 1990).

Mineralization extends beyond some shears into the adjacent fractured wallrock, forming an envelope of low-grade mineralization. This is the case at the Carissa mine where a 5-foot to 15-foot-wide shear is enclosed by a 100- to 300-foot zone of rehealed fractured country rock possessing a low-grade gold tenor of a trace to 82.3 ppm (2.4 oz/ton) and averaging 0.69 to 1.72 ppm (0.02 to 0.05 oz/ton) (Beeler, 1908).

Stop descriptions

Stop 1. Overlook of Red Canyon

Park at the turnout; the view is to the north of the highway. The prominent redbed forming the eastern (right) canyon wall is Chugwater Formation sandstones, shales, and siltstones (Triassic), which are overlain by buff to tan aeolian crossbeds of the Nugget Sandstone (Jurassic). The dip slope on the left is formed of a resistant cherty unit of the Phosphoria Formation (Permian). In the far distance, Table Mountain is capped by the basal boulder conglomerate unit of the Wind River Formation (Eocene), which forms a prominent angular unconformity with the underlying sedimentary rocks (Blackstone, 1988).

During the late 1800s to early 1900s, Oligocene conglomerates of the White River Formation exposed in small areas in the southern canyon wall were worked for gold using hydraulic mining techniques (Antweiler and others, 1980). The quantity of gold recovered from this area was estimated by Jamison (1911) to have been about 1,050 ounces. This paleoplacer, known as the Twin Creek paleoplacer, continues to the east and is estimated to include more than a billion cubic yards of gravel (Antweiler and others, 1980).

Stop 2. Overlook of the Atlantic City iron mine

The open pit was developed in banded iron formation of the Goldman Meadows Formation. The rock is a banded schist with alternating quartz-rich and magnetite-rich layers with amphibole, accessory chlorite, and local sulfides. The iron formation is generally less than 100 feet thick but was structurally thickened at the mine site by internal folding and plication, and by repetition along faults and slippage along foliation.

U.S.Steel Corporation operated the mine from 1962 to 1983, and recovered more than 90 million tons of taconite before selling the mine to Universal Equipment Company, the current owners. At full capacity, 5.5 million tons of taconite were mined each year. The taconite was mined and pelletized at the mine site and then shipped by rail to the Geneva Steel Works near Provo, Utah. Mapping by Bayley (1963), indicates a huge unmined iron resource remains.

Stop 3. Diamond Springs Formation and Goldman Meadows Formation west of the Atlantic City mine entrance

Examine rocks of the lowermost Archean supracrustal unit (the Diamond Springs Formation), which consist of mafic to ultramafic schists, and some samples of banded iron formation and mica schist of the overlying Goldman Meadows Formation.

Walk about 100 yards west from the Pacific Power and Light substation to an outcrop of cumulate-textured serpentinite. This is a relatively fine-grained, conformable serpentinite that becomes increasing chlorite rich to the south. Based on its chemistry and fine-grained texture, the serpentinite is interpreted as a metamorphosed peridotite flow (Hull, 1988; Hausel, 1990). The whole-rock chemistry for serpentinites of the Diamond Springs Formation shows an affinity for ultramafic komatiite with MgO contents of 38.1 to 26.6%, Cr contents of 10,100 ppm to 1,700 ppm, and Ni contents of 2,570 ppm to 860 ppm. A sample of serpentinite from this locality yielded 30.6% MgO, 2,700 ppm Cr, and 1,200 ppm Ni (**Table 1**, no. 23D). The $CaO:Al_2O_3$ ratio is low, possibly because of CaO depletion during serpentinization.

Several serpentinites in this area contain cross-fiber asbestos. Another serpentinite to the northeast, on the northern highwall of the Atlantic City mine, was mined for asbestos before 1921.

Table 1. Whole-rock and trace-element analyses for some representative rocks from South Pass.

Sample number	23D	1G	38D	21R	21M	95M	44M	53M
SiO_2	37.80	56.10	44.70	52.79	64.40	58.16	44.18	41.52
Al_2O_3	4.18	0.23	6.27	13.77	14.30	17.44	8.45	10.50
TiO_2	0.40	<0.03	0.71	1.01	0.60	1.16	0.79	0.66
Fe_2O_3	14.60	33.40	12.60	12.96	5.89	1.22	10.55	10.58
FeO	-	7.55	-	-	-	4.31	-	-
MnO	0.17	0.19	0.16	0.20	0.09	0.11	0.17	0.19
MgO	30.60	0.76	21.20	6.69	3.08	3.01	20.84	20.49
CaO	2.56	1.50	7.09	10.31	2.88	5.81	7.17	7.74
Na_2O	0.03	<0.20	0.18	1.90	3.28	4.17	0.66	0.30
K_2O	0.03	<0.03	<0.03	0.04	2.46	1.70	<0.03	0.17
P_2O_5	0.34	0.10	0.29	0.28	0.31	0.46	0.42	0.20
CO_2	-	0.02	-	-	-	0.40	-	-
LOI	8.80	0.27	4.70	1.70	0.60	1.59	4.8	4.6
TOTAL	99.69	100.12	99.60	101.65	97.98	99.58	98.19	96.95
CaO/Al_2O_3	0.61	-	1.06	0.75	-	-	0.8	0.7
Ti /V	-	-	-	24	-	-	-	-
Ag (ppm)	<5	<2	<5	<0.1	-	-	<5	-
As (ppm)	2	10	3	-	29	-	2	80
Au (ppb)	6	<8	<5	<5	13	-	<5	20
Cr (ppm)	2,700	11	3,100	200	217	-	1,400	2,047
Ni (ppm)	1,200	14	1,200	48	43	-	630	409
Pd (ppb)	6	-	2	-	-	-	<2	-
Pt (ppb)	20	-	15	-	-	-	<15	-
V (ppm)	-	16	-	244	-	-	-	-

23D= cumulate serpentinite from Diamond Springs Formation near Atlantic City mine entrance.
1G= banded oxide facies magnetite-quartz-amphibole iron formation from Goldman Meadows Formation near Lewiston Lakes.
38D= talc-chlorite-tremolite schist from Diamond Springs Formation north of sample 23D.
21R= greenstone (metabasalt).
21M= metagreywacke from Lewiston district.
95M= meta-andesite (average of 3 analyses from Peabody Ridge) (Bayley and others,1973).
44M= actinolite schist.
53M= tremolite schist (Bow, 1986).

Gold contents of the serpentinites are low, from less than 0.005 ppm to 0.016 ppm (Hausel, 1990). However, this is considerably higher than the average ultramafic rock, which contains only 0.0008 ppm gold (Kerrich, 1983).

From the serpentinite, walk west to Slate Creek to examine (out of place) banded iron formation bank-fill boulders. These boulders were mined from the Atlantic City open pit and dumped here to support the creek banks during flash floods. The boulders are representative of the iron formation member of the Goldman Meadows Formation, which lies above the Diamond Springs Formation. The iron formation consists of banded magnetite-metachert with varying amounts of amphibole and chlorite in a microhornfelsic texture. Isoclinal folds are often recognizable, and foliation-conformable quartz veins and veinlets are often boud-

inaged. Sulfides (pyrite and uncommon chalcopyrite) occur in some samples along foliation, suggesting they are syngenetic. The average iron content of the iron formation is approximately 33.0% (Bayley, 1963). The gold content is poorly known; a few samples were collected for gold analyses that ranged from less than 0.005 ppm to 1.1 ppm, indicating the iron formation is a viable exploration target. A typical analysis of banded iron formation is listed in **Table 1** (sample no. 1G).

Walk north along Slate Creek and cross the former railroad of the Atlantic City mine. Some fill on the north side of the railroad bed consists of metapelite of the Goldman Meadows Formation transported here from the open pit. Many of these schists are porphyroblastic. The most common porphyroblasts are andalusite and almandine. A few schists display tight to isoclinal folds and prominent cleavage. Continue up the slope across tholeiitic metagabbro, metadiabase, metabasalt, felsic gneiss, and talc-chlorite schist.

The gneiss is an S-type gneiss believed to have been tectonically emplaced into the greenstone belt (Talpey, 1984). The talc-chlorite-tremolite schist is chemically equivalent to a peridotitic komatiite (**Table 1**, no. 38D), and is interpreted to be a metamorphosed komatiite or subvolcanic equivalent. Nearby, a metabasalt displays an ellipsoidal fracture suggestive of a pillow structure (Greg Harper, personal communication, 1986). This unit is tightly folded; fold limbs are crenulated.

Stop 4. Roundtop Mountain deformation zone and adjacent rocks south of the Atlantic City iron mine

A road cut on Highway 28 exposes the Roundtop Mountain deformation zone. Examine the Roundtop Mountain deformation zone (RMDZ) and adjacent rocks in the northern road cut along Wyoming Highway 28 south of the iron mine. The RMDZ is an important Archean terrane boundary at South Pass, separating the Miners Delight terrane to the southeast from the Roundtop Mountain and other terranes to the northwest. The RMDZ juxtaposes two sequences that differ greatly in paleoenvironment, provenance, lithologies, geochemistry, and metamorphic grade.

The road cut exposes about 1,120 feet of dipping, strongly foliated to phyllonitic, Roundtop Mountain Greenstone cut by dikes and/or sills of metadiabase to metagabbro. The anastomosing greenstone foliation is often buckled into chevrons or kinks, especially near the RMDZ. Carbonaceous phyllites and metasiltstones and plutonogenic metasandstones that overlie the greenstones are found adjacent to the RMDZ in an outcrop-scale duplex about 160 feet thick. The greenstone-metasediment sequence is repeated four times in this duplex. Nearby, pillows in the greenstones and graded bedding in the metasandstones indicate the top lies to the south, that is, towards the RMDZ.

On the southeast side of the RMDZ, the road cut exposed about 190 feet of Miners Delight metasandstones (quartzose, lithic, and calcareous varieties), metaconglomerate, and perhaps some metavolcanic rocks. Though intense deformation and amphibolite-facies metamorphism has obscured most primary textures, metasandstones in the road cuts can be identified by characteristic elliptical biotite clots and occasional quartz sand grains. Primary textures and structures are well preserved just south of Highway 28 on the ridge east of Rock Creek. Fining-upward cycles of volcanogenic conglomerates, greywackes, and siltstones are interstratified with relatively thick porphyritic flows. Graded bedding indicates the Miners Delight rocks are younger to the north. Thus, the two terranes face each other across the RMDZ.

The highest grade tectonites forming the RMDZ itself are 150 feet of strongly schistose and laminated, black amphibolitic mylonites and ultramylonites. Forty feet of these mylonites were probably derived from prograde metamorphism of the greenstones; the rest were derived from the Miners Delight terrane. Similar mylonites and ultramylonites can be found in relatively narrow (less than 1 inch to a few inches) zones in both terranes. Foliation is uniform and essentially vertical in the RMDZ mylonites, with a mineral lineation raking slightly east of the down-dip line. Schistosity on both sides of the RMDZ steepens slightly as the mylonite zone is approached, suggesting a component of simple-shear deformation with the north side (Roundtop Mountain terrane) down relative to the south. This interpretation of the sense of shear is supported by asymmetric boudinage of both foliation and deformed quartz veins, and small oblique shear zones extending the mylonitic foliation (i.e. shear bands). Microscopic kinematic indicators are rare in the thoroughly recrystallized mylonites.

The mylonites and adjacent rocks are cut by a complex sequence of retrograde deformation zones that show a variety of movement directions and senses. Narrow (inches to a few feet) chlorite-rich zones of quasiplastic mylonites (gold-bearing elsewhere) to brittle dilatant microbreccias are usually subparallel to the higher temperature fabric. Chlorite- and quartz-coated slickensides, often with subhorizontal slickenlines, are also found on many foliation surfaces. In the

greenstones, especially along lithologic contacts, chlorite rich "button schists" form shear zones up to 6 feet thick; subhorizontal lineations are typical of these zones as well. Laramide fault zones, containing calcite-cemented breccia and gouge are the most conspicuous in the road cuts; these faults are often bounded by striated sliding surfaces.

At least two "end member" scenarios can be envisioned to explain the geometry and kinematics of the Roundtop Mountain deformation zone. In the first model, the Miners Delight terrane was thrust over the greenstones of the Roundtop Mountain terrane and metamorphic inversion led to a limited amount of prograde metamorphism in the footwall. Thrusting was presumably toward the foreland or arc-ward (towards the northwest). With continued collision and subhorizontal shortening, this thrust was rotated and steepened to its present near-vertical orientation. Rotation may have been related to underthrusting and underplating, analogous to modern accretionary prisms. On a regional scale, structural elements fan across the South Pass orogen.

Alternatively, the RMDZ may have formed as a normal or extensional fault in the latter half of the deformation history. Syn- to late-orogenic extension faulting is now being recognized in many fold and thrust belts, including the Canadian Cordillera, the Scandinavian Caledonides, and the Alps. Extensional faulting may be related to gravitational collapse of an overthickened lithosphere, to dynamic processes in orogenic wedges (the "critical taper" model), or to some other cause. At South Pass, lower grade rocks of the Roundtop Mountain terrane were dropped down against the higher grade rocks in the footwall. In other orogens, early thrusts are often reactivated as later normal or extension faults; reactivation might explain some of the kinematic complexities along the RMDZ (Hull, 1988).

Stop 5. Roundtop Mountain Greenstone

Drive past the Highway Department substation, continue north on the dirt road, and stop at the topographic saddle near the base of the hill. The saddle marks the trend of the Roundtop Mountain deformation zone. Continue up the slope across greenstones and cross a weakly foliated metaleucodacite porphyry sill with narrow joint-controlled, foliation-parallel quartz veinlets that has been prospected at several points along trend. Phenocrysts of oligoclase and quartz occur in a dense sericitized groundmass with some disseminated arsenopyrite. The sill was emplaced along a shear in the greenstones. It yields weak gold anomalies; Bayley and others (1973) reported a sample from the sill gave 0.34 ppm (0.01 oz/ton) Au and 0.34 ppm Ag. Metaleucodacite and metatonalite sills and plugs are relatively uncommon in the greenstone belt, but where found they generally yield elevated gold contents. At the Mary Ellen stock south of Atlantic City, for example, conjugate quartz veins hosted by the metatonalite porphyry possess enriched gold values. Historic reports suggest the vein averaged 14.4 ppm (0.42 oz/ton) gold.

The top of the hill provides an excellent opportunity (weather permitting) for photographing the Atlantic City mine. Walk east to the cliffs near the powerline. Here are some well-preserved deformed pillow lavas. **No hammers please!** Although the pillows are stretched parallel to foliation, the cusp shapes provide the same top solution, i.e., the top of the Roundtop Mountain Greenstone lies to the south (Bayley, 1965). The greenstones are metatholeiites with Ti:V ratios averaging 25 (**Table 1**, no. 21R). Mineralogically, these rocks are composed of chlorite, actinolite, epidote, and minor apatite. The original plagioclase has been entirely sausseritized. Along trend to the northeast and to the southwest, the greenstones and greenschists grade into amphibolites.

Stop 6. Peabody Ridge overlook and rocks

Peabody Ridge overlooks the Gold Dollar mine. The Gold Dollar adit, located downhill in the valley to the south, was driven 1,350 feet across regional foliation with the intention of intersecting the westernmost extent of the Miners Delight shear zone. The Miners Delight shear is traceable from the Gold Dollar shaft 3,000 feet east to the Miners Delight mine before it disappears under eluvial cover. At the Miners Delight mine, the shear is folded and forms an ore shoot. Although the Gold Dollar shaft lies on the western extent of this structure, there is no evidence of an ore shoot at this site.

On the skyline to the south, the northern flanks of Oregon Butte and Continental Peak mark the approximate trace of the Continental fault. Immediately south of the fault scarp lies the Oregon Buttes paleoplacer. This is an Eocene boulder conglomerate facies of the Wasatch Formation eroded from the South Pass granite-greenstone terrane. The boulders in the conglomerate are typical of a granite-gneiss terrane, although some Miners Delight metagreywacke boulders and pebbles are found locally. The conglomerate is extensive, covering a surface area of nearly 10 square miles.

Samples collected by Love and others (1978) yielded an average gold content of 0.00185 oz/yd^3. However, the eastern lobe of the conglomerate east of the Dickie Springs placer has a higher average gold content (0.0027 oz/yd^3). This lobe has a stratigraphic thickness of 1,300 feet and an areal extent of 8 square miles and possibly possesses a gold resource of more than 28.5 million ounces (Love and others, 1978).

You are standing on the southern slope of Peabody Ridge. This ridge has a variety of rock types including mafic amphibolite, meta-andesite porphyry, cherty metagreywacke, metatuff, and metagreywacke. The metagreywacke is a proximal facies formed of subangular quartz and feldspar (oligoclase) grains in a matrix of biotite, quartz, and feldspar. Rock fragments include metachert, quartzite, and phyllite; igneous fragments are uncommon in the greywackes. Primary sedimentary features commonly found include crossbeds, graded beds, and channels. No other place in the greenstone belt contains better preserved greywacke. Whole-rock compositions range from granitic to basaltic, averaging granodioritic to quartz dioritic (Condie, 1967; Hausel, 1987b, 1990) (**Table 1**, no. 21M). Several beds of cherty metagreywacke crop out along the slope as resistant low ridges. The rock produces a conchoidal to hackly fracture and rings when struck with a hammer (John Nold, personal communication, 1987). Microscopically, these rocks possess fine-grained mosaics of quartz with minor chlorite and muscovite in a preferred orientation, although portions have ultramylonitic texture. Chemically, the rock has 74 to 75 percent SiO_2 (about 8 to 10 percent greater silica than the average metagreywacke).

The mafic amphibolite (metagabbro) occurs as a foliated, medium-grained, hornblende-plagioclase amphibolite with tholeiitic affinity. Meta-andesite on Peabody Ridge includes massive, trachytic porphyry and vesicular flows primarily of calc-alkaline affinity (**Table 1**, no. 95M). These rocks contain oligoclase and hornblende phenocrysts in a dense microlitic groundmass of biotite and hornblende and a fine-grained residue, possibly of feldspar and quartz (Bayley and others, 1973).

Stop 7. Miners Delight (Cummins City) ghost town (optional)

Miners Delight ghost town is protected by the U. S. Bureau of Land Management. The town was established sometime in 1868, after the discovery of the Miners Delight lode, located 1/2 mile upstream (west) of the town. According to Jamison (1911), the Miners Delight mine was one of the two greatest producers in the district and may have yielded 60,000 ounces of gold during its short lifetime before it underwent litigation.

Stop 8. Snowbird mine

The Snowbird mine is unique in the greenstone belt, but similar undeveloped veins have been mapped a short distance downstream from the adit and south of the Mary Ellen mine near Atlantic City. Two different lodes were developed. The northern lode is a massive breccia vein; it has two generations of quartz, with common massive calcite and abundant sulfides (pyrite and traces of chalcopyrite). Breccia clasts are country rock fragments. The host for the vein includes metagreywacke and metabasalt.

Bayley and others (1973) determined a model lead date of 2.8 Ga for the deposit, but the Snowbird has two different vein systems and it is unknown from which lode the sample was taken. One vein is the sulfide-rich breccia vein described above and the second vein system is a sulfide-poor carbonated mylonite and shear 320 feet to the south.

Jamison (1911) estimated 375 ounces of gold were recovered from the mine and Prinz (1974) recovered a calcite-quartz sample from the mine dump that assayed 4.5 ppm (0.13 oz/ton) Au with 30 ppm As. It is not known which of the two veins this sample was from. Samples taken every 10 feet in the mine indicate the northern breccia vein has a paucity of gold; samples ranged from no detectable gold and silver to only 0.37 ppm (0.01 oz/ton) Au, 0.5 ppm (0.015 oz/ton) Ag, with 197 ppm Cu (Hausel, 1990). The vein seems more suited as a smelter flux than a primary gold deposit.

Stop 9. Overlook of Atlantic City and Rock Creek

Atlantic City was established during the early gold rush and may have housed more than 500 people by about 1870. The town was well known for having one of the best "French Quarters" in the Rocky Mountain region, and the first brewery in Wyoming was located in Atlantic City, but the brand name of the beer has been lost to time. (Some people in the area suggest "Miners Delight" would have made an excellent label.)

Rock Creek runs through Atlantic City and was dredged along a 6-mile stretch from 1933 to 1941. Dredge tailings are visible along the stream banks. The placer gravels were reported to average (0.012 oz/yd^3) and in the first year of operation nuggets up to 3.4 ounces were recovered (Ross and Gardner, 1935).

Stop 10. Duncan mine area

Stop along Little Beaver Creek north of the Duncan mine. The road cut exposes actinolite schist. Chemically, this unit is equivalent to ultramafic komatiite (MgO = 20.84%, Cr = 1,400 ppm, and Ni = 630 ppm) (**Table 1**, no. 44M), although the rare-earth element content is elevated and more typical of basaltic komatiite.

Bow (1986) recognized an important relationship between some actinolite schists and elevated gold contents in adjacent shear zones, and suggested these rocks were the source of the gold in the greenstone terrane. However, there are many auriferous shears in the belt that are spatially isolated from these schists, and gold-bearing shears occur in a variety of rock types, the most common being metagreywacke, followed by hornblendic amphibolite. Some recent stable-isotope and fluid-inclusion studies suggest the most likely gold source was the metagreywackes (Spry and McGowan, 1989).

Walk south across metagreywacke to the Exchange shear exposed in a short adit. This shear is hosted by hornblendic amphibolite near the amphibolite-metagreywacke contact. Note the isoclinal fold in the wallrock adjacent to the shear. Wallrock silicification includes boudinaged quartz in the shear and two generations of cherty quartz in the south wall of the shear. Visible gold can be found here. Samples taken over a 40-foot width in the adjacent wallrock exhibited evidence of silica flooding and potassium enrichment that declines rapidly away from the shear zone. This enrichment is petrographically manifested in increased amounts of quartz and sericite that decline rapidly away from the shear zone.

Continue south to a small metatonalite plug west of the Duncan shaft. The metatonalite consists of quartz and oligoclase phenocrysts in a recrystallized matrix of sericite, quartz, and feldspar. The plug exhibits an east-west trending foliation inherited from a Duncan shear zone it intruded.

Walk east to the Duncan glory hole. The trend of the shear exposed in the glory hole is oblique to the principal shears at the Exchange prospect, and to the east at the Mary Ellen mine. However, this is the same shear found near the Mary Ellen mine and at the metatonalite plug to the west and it has been modified by a steeply plunging, northerly trending drag fold. The fold encloses an ore shoot that yielded 33 ppm (0.96 oz/ton) Au from a 2-foot channel sample. The adjacent wallrock is also fractured and mineralized over a width of nearly 40 feet. Samples taken in the wallrock yielded values of 6.6 ppm to 0.53 ppm Au (0.19 to 0.015 oz/ton) (Hausel, 1989).

Stop 11. Carissa mine (optional)

The Carissa mine has been one of the two most productive gold mines in the district. According to Jamison (1911), early production was 50,000 ounces of gold. However, some production figures reported by the *Wyoming Industrial Journal* for 1899 to 1902 indicated 179,024 ounces of gold were recovered over the 4-year period. This is probably too much, as indicated by the extent of the mine workings and reported average ore grade. The mine is 400 feet deep with five levels and has more than 2,400 feet of drifts, although this does not include stopes. The average ore grade was reported at 10.3 ppm (0.3 oz/ton) with a tenor ranging from a trace to 8,900 ppm (260 oz/ton) Au.

The shear zone ranges from 6 to 50 feet wide and includes more than one generation of quartz. Quartz boudins parallel the penetrative shear fabric, folded veins trend perpendicular to the shear trend, and quartz breccia veins also cut the shear fabric. Some stope-scale ore shoots are controlled by folds (Bow, 1986).

The wallrock is fractured and rehealed over a 200- to 300-foot width. Interfolial veins and veinlets are common in the wallrock. Composite chip samples taken in the wallrock over a 97-foot width yielded an average gold value of 0.8 ppm (0.02 oz/ton). Thirty-seven feet of the northern wallrock averaged 1.43 ppm (0.04 oz/ton) Au. Another 30-foot composite chip sample within this zone averaged 2.4 ppm (0.07 oz/ton) Au (Hausel, 1989).

Carbonated tremolite/actinolite-talc-chlorite schist adjacent to the shafthouse,has similar chemistry to peridotitic komatiite (**Table 1**, no. 53M).

Stop 12. South Pass City historic site

The historic site is a partial reconstruction of historic South Pass City. Possibly as many as 2,000 or more people lived here during the height of the gold rush.

References

Aleinikoff, J.N., Compston, W., Stuckless, J.S., and Worl, R.C., 1987, Conventional and ion microprobe U-Pb ages of Archean rocks from the Wind River Range, Wyoming: Geological Society of America Abstracts With Programs, v. 19, no. 7, p.569.

Antweiler, J.C., Love, J.D., Mosier, E.L., and Campbell, W.L., 1980, Oligocene gold-bearing conglomerate, southeast margin of Wind River Range, Wyoming: Wyoming Geological Association 32nd Annual Field Conference Guidebook, p. 223-237.

Armstrong, F.C., 1948, Preliminary report of the geology of the Atlantic City-South Pass mining district, Wyoming: U.S. Geological Survey Open File Report, 64 p.

Blackstone, D.L., 1988, Traveler's guide to the geology of Wyoming: Geological Survey of Wyoming Bulletin 67, 130 p.

Bayley, R.W., 1963, Preliminary report on the Precambrian iron deposits near Atlantic City, Wyoming: U.S. Geological Survey Bulletin 20, 23 p.

Bayley, R.W., 1965, Geologic map of the Miners Delight Quadrangle, Fremont County, Wyoming: U.S. Geological Survey Map GQ-773, scale 1:24,000.

Bayley, R.W., 1968, Ore deposits of the Alantic City district, Fremont County, Wyoming, *in* Ridge, J.D., editor, Ore deposits of the United States 1933-1967: American Institute of Mining Engineers, p. 598-604.

Bayley, R.W., Procter, P.D., and Condie, K.C., 1973, Geology of the South Pass area, Fremont County, Wyoming: U.S. Geological Survey Professional Paper 793, 39 p.

Beeler, H.C., 1908, A brief review on the South Pass gold district, Fremont County, Wyoming: Office of the State Geologist, miscellaneous printed report, Cheyenne, 23 p.

Bow, C.S., 1986, Structural and lithologic controls on Archean greywacke-hosted gold mineralization in the Sweetwater district, Wyoming, USA, *in* Keppie, J.D., Boyle, R.W., and Hanes, S.J., editors, Turbidite-hosted gold deposits: Geological Association of Canada Special Paper 32, p. 107-118.

Condie, K.C., 1967, Geochemistry of Early Precambrian greywackes from Wyoming: Geochimica Cosmochimica Acta, v. 31, p. 2135-2149.

Condie, K.C., 1981, Archean greenstone belts: Elsevier, Amsterdam, The Netherlands, 434 p.

Harper, G.D., 1985, Dismembered Archean ophiolite, Wind River Range, Wyoming (USA): Ofioliti, v. 10, p. 297-306.

Hausel, W.D., 1987a, Structural control of Archean gold mineralization within the South Pass greenstone terrain, Wyoming (USA), *in* Hurst, R.W., Davis, T.E., and Augustithis, S.S., editors, The practical applications of trace elements and isotopes to mineral resources evaluation: Theophrastus Publications, Athens, Greece, p. 199-216.

Hausel, W.D., 1987b, Preliminary report on the gold mineralization, petrology, and geochemistry of the South Pass granite-greenstone belt, Wind River Range, Wyoming, *in* Miller, W.R., editor, Wyoming Geological Association 38th Annual Field Conference Guidebook, p. 287-304.

Hausel, W.D., 1989, The geology of Wyoming's precious metal lode and placer deposits: Geological Survey of Wyoming Bulletin 68, 248 p.

Hausel, W.D., 1990, Economic geology of the South Pass granite-greenstone belt, Wind River Range, western Wyoming: Geological Survey of Wyoming Report of Investigations 44, in press.

Houston, R.S., and Karlstrom, K.E., 1979, Uranium-bearing quartz-pebble conglomerates—exploration model and United States resource potential: U.S. Department of Energy Open File Report GJBX-1(80), 510 p.

Hull, J.M., 1988, Structural and tectonic evolution of Archean supracrustals, southern Wind River Range, Wyoming: PhD dissertation, University of Rochester, New York, 280 p.

Jamison, C.E., 1911, Geology and mineral resources of a portion of Fremont County, Wyoming: Office of the State Geologist, Bulletin 2, Series B, Cheyenne, 90 p.

Karlstrom, K.E., Houston, R.S., Flurkey, A.J., Cooldge, C.M., Kratochvil, A.L., and Sever, C.K., 1981, A summary of the geology and uranium potential of Precambrian conglomerates in southeastern Wyoming, v. 1: U.S. Department of Energy Open File Report GJBX-139(81), 541 p.

Kerrich, R., 1983, Geochemistry of gold deposits in the Abitibi greenstone belt: Canadian Institute of Mining and Metallurgy Special Volume 27, 75 p.

Koschmann, A.H., and Bergendahl, M.H., 1968, Principal gold producing districts of the United States: U.S. Geological Survey Professional Paper 610, 283 p.

Love, J.D., Antweiler, J.C., and Mosier, E.L., 1978, A new look at the origin and volume of the Dickie Springs-Oregon Gulch placer gold at the south end of the Wind River Range: Wyoming Geological Association 30th Annual Field Conference Guidebook, p.379-391.

Prinz, W.C., 1974, Map showing geochemical data for the Atlantic City gold district, Fremont County, Wyoming: U.S. Geological Survey Miscellaneous Investigations Map I-865, scale 1:24,000.

Ross, C.L., and Gardner, E.D., 1935, Placer methods of the E.T. Fisher Company, Atlantic City, Wyoming: U.S. Bureau of Mines Information Circular IC-6846, 11 p.

Snyder, G.L., Hausel, W.D., Klein, T.L., Houston, R.S., and Graff, P.J., 1989, Precambrian rocks and mineralization, Wyoming Province: 28th International Geological Congress, Guide to Field Trip T-332, 48 p.

Spencer, A.C., 1916, The Atlantic gold district and the north Laramie Mountains: U.S.Geological Survey Bulletin 626, 85 p.

Spry, P.G., and McGowan, K.I., 1989, Origin of Archean lode gold mineralization at Atlantic City-South Pass, Wyoming: fluid inclusion and stable isotope study [abstract]: 1989 International Geological Congress, Washington, D.C., p.163.

Stuckless, J.S., Hedge, C.E., Worl, R.G., Simmons, K.R., Nkomo, I.T., and Wenner, D.B., 1985, Isotopic studies of the Late Archean plutonic rocks of the Wind River Range, Wyoming: Geological Society of America Bulletin, v. 96, p. 850-860.

Talpey, J.G., 1984, Geochemical and structural evolution of Archean gneisses at South Pass, Wyoming: M.S. thesis, University of Rochester, New York, 102 p.

Wyoming Recreation Commission, 1976, Wyoming, a guide to historic sites: Big Horn Publishers, Basin, Wyoming, 327 p.

Common abbreviations used in the field trip guides:

Time

ka	=	thousand years
Ma	=	million years
Ga	=	billion years

Geologic time divisions (where not otherwise noted)

Pe or PЄ	=	Precambrian
Є	=	Cambrian
O	=	Ordovician
D	=	Devonian
IP	=	Pennsylvanian
P	=	Permian
Ŧ	=	Triassic
J	=	Jurassic
K	=	Cretaceous

Temperature

°F	=	degrees fahrenheit
°C	=	degrees celsius

Distance

mi	=	mile
ft	=	feet
in	=	inch
km	=	kilometer
m	=	meter
cm	=	centimeter
mm	=	millimeter

Earthquake measurement

M_L	=	Local magnitude
M_s	=	Surface-wave magnitude

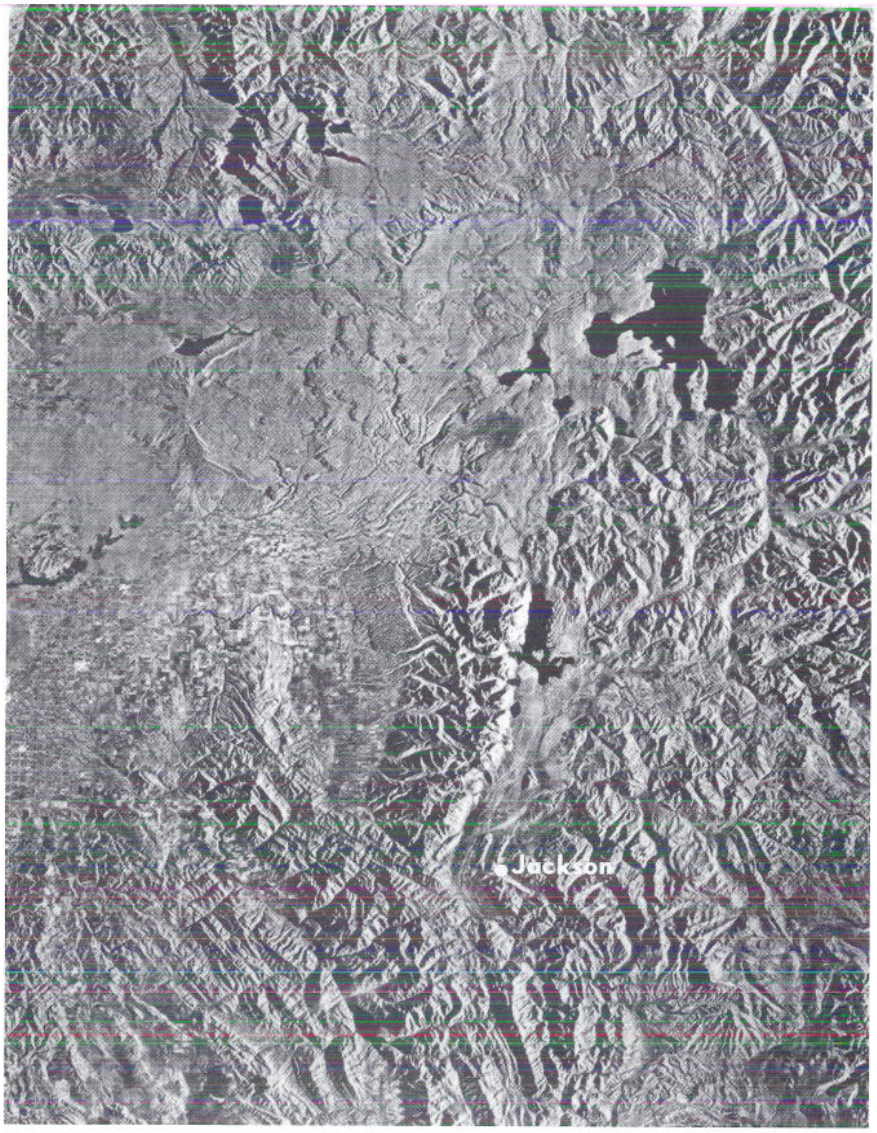

STATE OF WYOMING
1933
GEOLOGICAL SURVEY

Geology -- Interpreting the past to provide for the future